Name: Sophie Douglas Oxford College: Worcester College

Title: Regulation of CRAC channels and agonist-induced Ca^{2+} signals

Thesis submitted for the degree of Doctor of Philosophy

Submission term: Michaelmas 2012

Abstract

Calcium ions (Ca^{2+}) are extremely important intracellular messengers, activating a plethora of cellular processes. Growing evidence now points to a major role for the local Ca^{2+} signal in driving specific cellular responses. The simplest and most fundamental local Ca^{2+} signal is the Ca^{2+} microdomain, which rapidly forms when Ca^{2+} permeable ion channels open. In non-excitable cells the dominant Ca^{2+} entry channels are store-operated Ca^{2+} channels (SOCCs). The best characterised is the Ca^{2+} release activated Ca^{2+} (CRAC) channel. How local Ca^{2+} entry through CRAC channels impacts on channel function however is unclear. I have investigated the interaction between the Ca^{2+} binding protein calmodulin and CRAC channel activity and subsequent agonist-induced Ca^{2+} signals. Furthermore, I have investigated a role for mitofusin 2 (a protein that is known to tether the ER and mitochondria) on these Ca^{2+} signals.

Using three different calmodulin mutant constructs with alterations to their Ca^{2+} binding sensitivities, I have shown that calmodulin facilitates CRAC channel dependent Ca^{2+} entry and maintains agonist-induced cytosolic Ca^{2+} oscillations in a lobe-specific manner. Calmodulin has four Ca^{2+} binding sites, two on the N-lobe and two on the C-lobe. I found a dominant negative calmodulin mutant (CAM4M, where all four binding sites had been mutated), or one where the C-lobe could not bind Ca^{2+} (CAM2C), impaired both Ca^{2+} influx through CRAC channels and maintenance of cytosolic Ca^{2+} oscillations. In contrast, a Ca^{2+}-insensitive N-lobe mutant had little effect, (CAM2N). Knockdown of the mitochondrial Ca^{2+} uniporter regulator (MICU1) or mitochondrial membrane depolarization had similar effects to those seen with CAM4M or CAM2C, suggesting that at least in part, the action of calmodulin was through regulation of mitochondrial Ca^{2+} dynamics. This was confirmed by directly measuring the mitochondrial matrix Ca^{2+} concentration in intact RBL-1 cells using the mitochondrial targeted, fluorescent protein, pericam. Both CAM4M and disruption of mitochondrial Ca^{2+} buffering impaired agonist-induced mitochondrial Ca^{2+} uptake, suggesting that the modulation of CRAC channels occurred through Ca^{2+}-calmodulin facilitation of mitochondrial Ca^{2+} uptake. Using a mutant Orai1 (A73E) that cannot bind calmodulin, I have shown that calmodulin tethered to the CRAC channel provides a major source of calmodulin for effective mitochondrial Ca^{2+} uptake. Physiological relevance of my proposed pathway was provided from experiments where I showed knockdown of MICU1 impaired agonist-induced CRAC channel dependent NFAT-1-driven gene expression. In addition, I establish a crucial role for mitochondrial MFN2 and presumably its ability to properly link the mitochondria and ER in the control of CRAC channels and agonist-induced Ca^{2+} signals.

Acknowledgements

There are a number of people I would like to thank that have provided both the academic and personal support that has enabled me to complete this thesis. Firstly, I would like to express my deepest gratitude to my supervisor, Professor Anant Parekh, for making this project possible. I am very thankful to him for giving me the opportunity to undertake this project in such an exciting area of science. He has provided me with unrivalled knowledge in the calcium field, and taught me to become a competent experimental scientist. Even more so, Anant has inspired and guided me throughout my DPhil and his patience and support have always kept me on track. In addition, more practically he has enabled me to gain patch clamp data which otherwise would not have been possible. I am extremely appreciative to him for all the time, feedback, advice, knowledge and personal support he has given me at all times.

I would like to extend this gratitude to other scientists within my department that have helped me achieve my goals: Dr. Joseph Di Capite, Dr. Daniel Bakowski, Dr. Pulak Kar, Dr. Siaw-Wei Ng and a special appreciation goes to Ms Charmaine Nelson who helped me obtain the fluorescence microscopy images in Chapter 5 of this thesis. I would also like to thank other members of our group who have assisted me at various times: Dr. Krishna Samanta and Miss Helen Batchelor.

Throughout my three years of studying at the University of Oxford for my DPhil I have been provided with all the support and equipment I have needed to carry out my research project. I must therefore thank Worcester College and the Department of Physiology, Anatomy and Genetics for such an opportunity and all the resources that have been at my disposal. I extend a particular thank you to my college personal tutor Dr. John Parrington, who has remained supportive and has offered me wise advice throughout this entire process. I am very grateful to him for all the help, guidance and motivation he has provided.

Funding from the Medical Research Council (MRC) has enabled this project to take place. Therefore I would like to kindly thank this funding body for all the financial aid.

In addition to my work colleagues and available academic facilities this thesis would not have been possible without the love, support and patience of my dearest family. Both my parents and brother have unconditionally provided me with constant encouragement and motivation throughout my entire life, always inspiring me to achieve my goals. I am indebted to my parents for all they have helped me to achieve and for the constant guidance they have provided and determination they have instilled in me. They have never let me down and been there for me every single day no matter what. I would especially like to thank my biggest supporter, my Mother, for all the emotional support she has given me.

My warmest appreciation also extends to my wonderful, supportive friends, who have cheered me up continuously and always listened to my difficulties and provided me with positive thoughts.

Contents

Chapter 1. General Introduction p1

1.1 The importance of Ca^{2+} as a second messenger p2

1.2 Ca^{2+} entry mechanisms p5

1.3 The pattern/ shape of the Ca^{2+} signal p6

  1.3.1 *Temporal changes in Ca^{2+}* p6

  1.3.2 *Spatial changes in Ca^{2+}* p14

1.4 Functional consequences of local Ca^{2+} entry through SOCCs p20

1.5 Ca^{2+} sensors p24

1.6 Store-operated CRAC channels p27

  1.6.1 *Key features of I_{CRAC}* p28

  1.6.2 *CRAC channel pore size and single channel conductance* p30

  1.6.3 *Pharmacology of CRAC channels* p31

  1.6.4 *CRAC channel activation and the identification of the molecular determinants of the channel* p32

  1.6.5 *Model of CRAC channel activation* p39

  1.6.6 *Regulation of CRAC channel activity* p41

1.7 Calmodulin p42

1.7.1 *Structure and targets of calmodulin* p42

1.7.2 *Regulation of ion channels by calmodulin* p43

1.7.3 *Regulation of CRAC channels by calmodulin* p50

1.7.4 *Calmodulin as a local Ca^{2+} sensor* p51

1.8 Mitochondria p52

1.8.1 *Mitochondria are not simply sinks for Ca^{2+}* p52

1.8.2 *Structure and biophysical properties of mitochondria* p55

1.8.2.1 *Electrochemical gradient for driving mitochondrial Ca^{2+} uptake* p55

1.8.2.2 *Characteristics and molecular determination of the mitochondrial Ca^{2+} uniporter* p57

1.8.2.3 *Mitochondria efficiently buffer Ca^{2+} when close to sources of high Ca^{2+}* p60

1.8.2.4 *Physical tethering between mitochondria and the ER* p64

1.8.3 *Mitofusin Proteins* p67

1.8.4 *Regulation of the mitochondrial Ca^{2+} uniporter, MCU* p72

1.8.5 *Mitochondrial control of CRAC channels* p75

1.9 Aims of thesis p82

Chapter 2. Materials and Methods p84

2.1 Cell culture p85

2.2 Materials p85

2.3 Cytosolic Ca^{2+} imaging p92

2.4 Mitochondrial matrix Ca^{2+} imaging p93

2.5 Cell transfection p94

2.6 Gene reporter assay p95

2.7 Patch clamp experiments of I$_{CRAC}$ undertaken together with my supervisor (Professor Anant Parekh) p95

2.8 Fluorescence microscopy carried out with a lab colleague (Ms. Charmaine Nelson) p96

2.9 Statistical significance p97

Chapter 3. Lobe-specific modulation of CRAC channels by calmodulin p98

3.1 Introduction p99

3.2 Results p105

- **a .**Calmodulin Constructs p105
- **b.** Calmodulin facilitates CRAC channel activity in a Ca^{2+}-dependent manner p105
- **c.** Ca^{2+}-calmodulin modulates CRAC channels in a lobe-specific manner p110

d. Calmodulin facilitates I_{CRAC} in a lobe-specific manner p112

e. Calmodulin modulates CRAC channels through a Ca^{2+}-dependent step p114

f. Calmodulin is required to maintain physiologically-induced cytosolic Ca^{2+} oscillations p117

g. The modulation of LTC_4-induced cytosolic Ca^{2+} oscillations by calmodulin does not involve CAM kinase II p120

h. Calmodulin modulates the maintenance of LTC_4-induced Ca^{2+} oscillations in a lobe-specific manner p122

i. Ca^{2+} influx through CRAC channels sustains cytosolic Ca^{2+} oscillations p124

j. Calmodulin also impacts on IP_3 receptor-driven Ca^{2+} release p127

k. Mitochondrial involvement in LTC_4-induced Ca^{2+} oscillations p130

l. Addressing the mechanism underlying the increase in the first Ca^{2+} release spike induced by LTC_4 in the presence of the calmodulin mutants p139

3.3 Discussion p143

Chapter 4. Regulation of mitochondrial Ca^{2+} uptake by calmodulin p151

4.1 Introduction p152

4.2 Results p157

a. A rise in mitochondrial matrix [Ca^{2+}] is evoked following ER Ca^{2+} depletion p157

b. Evidence supporting pericam is targeted to the mitochondrial matrix p160

1. No change in the pericam signal is detected when the inner mitochondrial membrane is depolarized p160

2. No change in the pericam signal is detected when the mitochondrial Ca^{2+} uniporter regulator (MICU1) is knocked down p162

3. No change in the pericam signal is detected when cells are bathed in zero Ca^{2+} external solution and stimulated with thapsigargin p164

c. Calmodulin facilitates mitochondrial Ca^{2+} uptake p167

d. Calmodulin is not essential to induce a mitochondrial matrix Ca^{2+} rise if cytosolic Ca^{2+} is very high p170

e. Calmodulin tethered to Orai1 is a major source of calmodulin for facilitating mitochondrial Ca^{2+} uptake p174

f. The facilitation of mitochondrial Ca^{2+} uptake by calmodulin tethered to Orai1 cannot be explained by differences in the initial rate of CRAC channel dependent Ca^{2+} entry p182

g. Mitochondrial Ca^{2+} uptake facilitates NFAT-1-dependent gene expression p186

4.3 Discussion p189

Chapter 5. The role of MFN2 in the modulation of CRAC channels and agonist-induced Ca^{2+} signals p198

5.1 Introduction p199

5.2 Results p204

a. MFN2 modulates CRAC channel dependent Ca^{2+} entry p204

b. MFN2 helps to maintain agonist-induced cytosolic Ca^{2+} signals p212

c. MFN2 facilitates mitochondrial Ca^{2+} uptake of IP_3-induced Ca^{2+} release p217

d. MFN2 impacts on IP_3R-driven Ca^{2+} release p227

5.3 Discussion p230

Chapter 6. General Discussion p237

6.1 General discussion p238

Chapter 7. References p250

7.1 References p251

List of Figures and Tables

Chapter 1. Introduction

Figure 1. Modes of Ca^{2+} transport involved in increasing or lowering cytosolic Ca^{2+} concentration [Ca^{2+}]. p4

Figure 2. The cytosolic Ca^{2+} oscillation pattern observed when a single RBL-1 cell is stimulated with a low concentration of agonist. p7

Figure 3. Cycle of events involved in the generation of IP_3-induced cytosolic Ca^{2+} oscillations upon agonist stimulation. p8

Figure 4. The Ca^{2+} microdomain rapidly formed when Ca^{2+} permeable ion channels open. p16

Figure 5. A microdomain formed by a single Ca^{2+} permeable ion channel versus one formed by a cluster of Ca^{2+} permeable ion channels. p17

Figure 6. Exposure of Ca^{2+} to targets which vary in distance from the channel pore. p18

Figure 7. Functional consequences of SOCC dependent Ca^{2+} microdomains. p24

Figure 8. The activation of CREB-dependent gene expression by local Ca^{2+} entry through L-type voltage-operated Ca^{2+} channels by calmodulin. p25

Figure 9. The activation of two temporally separate pathways by the CRAC channel dependent Ca^{2+} microdomain and closely positioned Syk. p26

Figure 10. Activation of CRAC channels upon agonist stimulation. p28

Figure 11. Current-voltage relationship of I_{CRAC}. p29

Figure 12. Time-course of I_{CRAC}. p30

Figure 13. Structure and functional domains of STIM1. p34

Figure 14. Structure of Orai1. p38

Figure 15. Predicted structure of the CRAC channel. p39

Figure 16. The formation of endoplasmic reticulum-plasma membrane junctions upon ER store depletion. p40

Figure 17. Structure of calmodulin. p42

Figure 18. Structure and key Ca^{2+} transporters of a mitochondrion. p55

Figure 19. ER-mitochondrial physical tethering. p67

Figure 20. Structure and important domains of Mitofusin 2. p68

Figure 21. The arrangement of the outer mitochondrial (OMM), inner mitochondrial (IMM) and ER/SR membrane as proposed by García-Pérez et al 2011. p71

Figure 22. Mitochondrial regulation of the CRAC channel. p81

Chapter 2. Material and Methods

Table 1. cDNA constructs p86-88

Table 2. RNAi constructs p88

Table 3. Solutions used p89

Table 4. Drugs applied p90-92

Chapter 3. Lobe-specific modulation of CRAC channels by calmodulin

Figure 1. Calmodulin facilitates CRAC channel driven Ca^{2+} entry in a Ca^{2+}-dependent manner. p108-109

Figure 2. Calmodulin modulates CRAC channels in a lobe-specific manner. p111

Figure 3. Whole-cell patch clamp recordings reveal a lobe-specific modulation of I_{CRAC} by calmodulin. p113

Figure 4. Calmodulin modulates I_{CRAC} through a Ca^{2+}-dependent step. p116

Figure 5. Calmodulin maintains physiologically-induced cytosolic Ca^{2+} oscillations. p119

Figure 6. LTC_4-induced cytosolic Ca^{2+} oscillations are maintained in the presence of CAM kinase II blockade. p121

Figure 7. Calmodulin modulates LTC_4-induced Ca^{2+} oscillations in a lobe-specific manner.p123

Figure 8. CRAC channel dependent Ca^{2+} entry is required to maintain LTC_4-induced Ca^{2+} oscillations. p126

Figure 9. The effect of calmodulin on IP_3-mediated Ca^{2+} release p129

Figure 10. FCCP impairs the maintenance of LTC_4-induced Ca^{2+} oscillations. p133

Figure 11. Knockdown of MICU1 impairs CRAC channel dependent Ca^{2+} entry and maintenance of LTC_4-induced Ca^{2+} oscillations. p136

Figure 12. FCCP impairs the maintenance of LTC_4-induced Ca^{2+} oscillations even in the absence of external Ca^{2+} and presence of La^{3+}. p138

Chapter 4. Regulation of mitochondrial Ca^{2+} uptake by calmodulin

Figure 1. Ca^{2+} release from the ER induces a rise in mitochondrial matrix [Ca^{2+}]. p159

Figure 2. No measureable change is detected in the pericam signal when the IMM is depolarized. p161

Figure 3. No detectable rise in matrix Ca^{2+} occurs when MICU1 has been knocked down. p163

Figure 4. No detectable change in the pericam signal is observed when cells are bathed in zero Ca^{2+} and stimulated with thapsigargin. p166

Figure 5. Calmodulin facilitates mitochondrial Ca^{2+} uptake. p169

Figure 6. The mitochondrial matrix Ca^{2+} rise does not require calmodulin if cytosolic Ca^{2+} is very high. p173

Figure 7. Calmodulin tethered to Orai1 sustains mitochondrial Ca^{2+} uptake. p177

Figure 8. Calmodulin tethered to Orai1 facilitates mitochondrial Ca^{2+} uptake. p180-181

Figure 9. The effect of calmodulin tethered to Orai1 on CRAC channel activity. p185

Figure 10. Mitochondrial Ca^{2+} uptake facilitates NFAT-1-dependent gene expression. p188

Chapter 5. The role of MFN2 in the modulation of CRAC channels and agonist-induced Ca^{2+} signals.

Figure 1. Knockdown of MFN2 by transfecting cells with MFN2 RNAi increases CRAC channel dependent Ca^{2+} entry. p206

Figure 2. Expression of MFN2 ActA increases CRAC channel dependent Ca^{2+} entry. p209

Figure 3. Overexpressing MFN2 reduces CRAC channel dependent Ca^{2+} entry in HEK 293 cells. p211

Figure 4. Knockdown of MFN2 impairs the maintenance of physiologically-induced Ca^{2+} oscillations. p214

Figure 5. Expression of MFN2 ActA cDNA impairs the maintenance of cytosolic Ca^{2+} oscillations. p216

Figure 6. MFN2 facilitates mitochondrial Ca^{2+} uptake of IP_3-induced Ca^{2+} release. p219

Figure 7. Mitochondrial MFN2 facilitates mitochondrial Ca^{2+} uptake. p221

Figure 8. Transfection with 1.6 µg MFN2 ActA cDNA fails to significantly affect mitochondrial Ca^{2+} buffering. p223

Figure 9. Expression of MFN2 IYFFT cDNA impairs mitochondrial Ca^{2+} buffering. p226

Figure 10. MFN2 modulates IP_3R-driven Ca^{2+} release. p229

List of Cartoon models: created to illustrate key findings and enable one to visualize the build up of the proposed mechanism of this thesis, by which cytoplasmic Ca^{2+} modulates CRAC channel activity.

Cartoon model 1. Ca^{2+}-calmodulin dependent facilitation of CRAC channels. p107

Cartoon model 2. Modulation of CRAC channels by Ca^{2+}-calmodulin involves a Ca^{2+}-dependent step. p115

Cartoon model 3. Mitochondrial Ca^{2+} buffering facilitates CRAC channel activity. p135

Cartoon model 4. Summary of the results of Chapter 3 for the modulation of CRAC channels by cytoplasmic Ca^{2+}. p150

Cartoon model 5. Ca^{2+}-calmodulin dependent facilitation of mitochondrial Ca^{2+} uptake. p168

Cartoon model 6. Consideration of the position of the major source of calmodulin for the facilitation of mitochondrial Ca^{2+} uptake. p172

Cartoon model 7. Calmodulin tethered to Orai1 is a major source of calmodulin for Ca^{2+}-calmodulin dependent facilitation of mitochondrial Ca^{2+} uptake. p179

Cartoon model 8. The proposed mechanism of this thesis (summating the findings of Chapter's 3 and 4, cartoon models 1-7) for the modulation of CRAC channels by cytoplasmic Ca^{2+}. p183, 194 & 245

Abbreviations

VOCC	Voltage-operated Ca^{2+} channel
SOCC	Store-operated Ca^{2+} channel
CRAC	Ca^{2+} release activated calcium channel
TRP	Transient receptor potential channels
I_{CRAC}	Current directly flowing through CRAC channel
STIM1	Stromal interaction molecule 1
CAD	CRAC channel activation domain
SAM	Sterile α-motif domain
WT	Represents control cell/cells for respective experiment
RBL-1	Rat Basophilic Leukaemia-1
HEK 293	Human Embryonic Kidney
Ca^{2+}	Calcium ion
$[Ca^{2+}]$	Calcium ion concentration
CDI	Ca^{2+}-dependent inactivation
CDF	Ca^{2+}-dependent facilitation
Gd^{3+}	Gadolinium ion
La^{3+}	Lanthanum ion
Na^{+}	Sodium ion
Ba^{2+}	Barium Ion
Mn^{2+}	Manganese ion
MCU	Mitochondrial Ca^{2+} Uniporter
MICU1	Mitochondrial Ca^{2+} Uniporter/Uptake 1 (Regulator)
IMM	Inner mitochondrial membrane
OMM	Outer mitochondrial membrane
NCX	Na^{+}/Ca^{2+} exchanger
PMCA	Plasma membrane Ca^{2+} ATPase
PM	Plasma membrane
ER	Endoplasmic reticulum
SERCA	Sarcoplasmic reticulum calcium ATPase

MFN	Mitofusin
MFN1	Mitofusin 1
MFN2	Mitofusin 2
MFN2 ActA	MFN2 mutant targeted to the mitochondria
MFN2 IYFFT	MFN2 mutant targeted to the ER
MAM	Mitochondria-associated membrane
CAM	Normal calmodulin
CAM4M	Dominant negative calmodulin mutant (completely Ca^{2+}-insensitive)
CAM2C	Calmodulin mutant where the C-lobe is Ca^{2+}-insensitive
CAM2N	Calmodulin mutant where the N-lobe is Ca^{2+}-insensitive
NFAT-1	Nuclear factor of activated T cells
Thap	Thapsigargin
LTC_4	Leukotriene C_4
ATP	Adenosine triphosphate
2-APB	2-Aminoethoxy diphenyl borate
Synta	(3-fluoropyridine-4-carboxylic acid (2’,5’-dimethoxybiphenyl-4-yl)amide), CRAC channel blocker.
BAPTA	1,2-bis(2-aminophenoxy)ethane-*N,N,N′,N′*-tetraacetic acid
EGTA	Ethylene glycol tetraacetic acid
FCCP	Carbonyl cyanide 4-(trifluoromethoxy)phenylhydrazone
MAPK/MEK	Mitogen-Activated Protein Kinase/ ERK kinase
ERK	Extracellular signal-regulated kinase
PBS	Phosphate-buffered saline
GFP/CFP/YFP	Green/Cyan/Yellow fluorescent protein
PLC	Phospholipase C
IP_3	Inositol 1,4,5 trisphosphate
IP_3R	Inositol 1,4,5 trisphosphate Receptor
DAG	Diacylglycerol
PKC	Protein kinase C
Syk	Spleen tryosine kinase

STAT	Signal transducers and activators of transcription
RNAi	RNA interference
cDNA	Complementary DNA
5-LOX	5-Lipoxygenase
$cPLA_2$	Phospholipase A_2
PIP_2	Phosphatidylinositol 4,5 bisphosphate
FRET	Fluorescence resonance energy transfer
MEF	Mouse embryonic fibroblast
TIRF	Total internal reflection fluorescence
CMTIIa	Charcot-Marie-Tooth neuropathy type IIa
CAM KII	Ca^{2+}-calmodulin-dependent protein kinase II (CAM KII).
TM	Transmembrane
NADPH	Nicotinamide adenine dinucleotide phosphate (reduced)
$FADH_2$	Flavin adenine dinucleotide (reduced)

Chapter 1.
General Introduction

1. General Introduction

1.1 The importance of Ca^{2+} as a second messenger

Cells need to respond to changes in their environment. This ability is essential for the life, development and survival of every organism. Cells can detect hundreds of stimuli (for example hormones, neurotransmitters and growth factors), which act on the cell surface to activate cellular responses via a much smaller number of intracellular second messengers. These second messengers (which include cAMP, cGMP, IP_3 (inositol 1,4,5 trisphosphate), DAG (diacylglycerol) and Ca^{2+}) serve to amplify the primary external signal, such that activation of a single extracellular receptor is transduced into the generation of numerous second messengers.

Calcium was not identified as a key signalling ion until 1883 (Carafoli 2003). The landmark experiment which revealed that Ca^{2+} was essential for the contraction of the heart was reported by Sydney Ringer. He discovered that an isolated rat heart failed to contract when bathed in distilled water, yet rhythmically contracted in London tap water (which contained high amounts of Ca^{2+}) or in distilled water where Ca^{2+} had been added. Following this, several important, subsequent discoveries helped to confirm the importance of Ca^{2+} as a signalling messenger. Heilbrunn 1940 showed that Ca^{2+} only caused contraction of frog heart muscle fibres when applied to the cut ends of such fibres, not to their surface. Bailey 1942 revealed that Ca^{2+} stimulated myosin ATPase activity and Weber 1959 showed that this was by direct binding and activation of actomyosin. Additionally, muscle relaxation was found to be induced by chelating Ca^{2+} (Bolzer 1954). Furthermore, in the 1960s, the ability of Ca^{2+} to cross intracellular membranes was revealed from evidence that Ca^{2+} was accumulated by both the mitochondria (Vasington and Murphy 1962, De Luca and Engstorm 1961) and the sarcoplasmic reticulum (Ebashi and Lipmann 1962). All these studies led to an explosion of research into the calcium field.

Calcium is now well established as an extremely important intracellular messenger, in nearly every cell type. It is considered the signal for life because it drives sperm motility and egg fertilisation. Calcium can also induce death (necrosis and apoptosis) (Rizzuto et al 2003, Parekh and Putney 2005), leading to the view that calcium is a life or death signal. In addition to these extremes, a rise in cytoplasmic Ca^{2+} activates a plethora of temporally distinct cellular responses, ranging from exocytosis (Neher 1998, Berridge 1997), muscle contraction (Berridge 1997, Berridge et al 2000) and enzyme activity (Bautista and Lewis 2004, Fagan et al 1998) (which occur within milliseconds to seconds), to gene transcription (Deisseroth et al 1996, Dolmetsch et al 2001, Kornhauser et al 2002), cell growth (Greka et al 2003, Wang and Poo 2005, Li et al 2005) and proliferation (occurring over several hours to days) (Berridge et al 2000, 2003, Carafoli 2002). Cytosolic Ca^{2+} levels must therefore be tightly regulated. Increases in intracellular Ca^{2+} occur via the entry of Ca^{2+} across the plasma membrane or release of Ca^{2+} from the intracellular Ca^{2+} stores, (such as the endoplasmic reticulum (ER)), via Ca^{2+} permeable ion channels. In addition, Ca^{2+}can be released slowly from the mitochondria predominantly in most cells via the $3Na^{+}/Ca^{2+}$ exchanger (NCX) (Palty et al 2010, 2012) but some is also released via H^{+}/Ca^{2+} exchangers (Jiang et al 2009). On the other hand, cytosolic Ca^{2+} levels can be lowered by 1) extrusion of Ca^{2+} across the plasma membrane via the plasma membrane Ca^{2+} ATPase (PMCA) pump and exchangers (such as the $3Na^{+}/Ca^{2+}$ exchanger, NCX), 2) the binding of Ca^{2+} by Ca^{2+} protein buffers (for example calbindin and calmodulin), and 3) the sequestration of Ca^{2+} into organelles such as the ER (via SERCA, the sarcoplasmic reticulum Ca^{2+} ATPase pump) and mitochondria (by the Ca^{2+} uniporter). Figure 1 illustrates transporters involved in increasing or lowering cytosolic Ca^{2+}. The resulting steady state Ca^{2+} concentration that arises reflects the balance between Ca^{2+} entry and removal mechanisms. The intracellular Ca^{2+} concentration of resting cells is normally around 100-200 nM. This is measured using fluorescent Ca^{2+}-sensing indicators that are loaded into cells (Tsien and Tsien 1990). Ca^{2+} stores have a limited capacity (due to their finite size) and so raise Ca^{2+} only transiently. Therefore it is Ca^{2+} influx that drives most of the cellular responses.

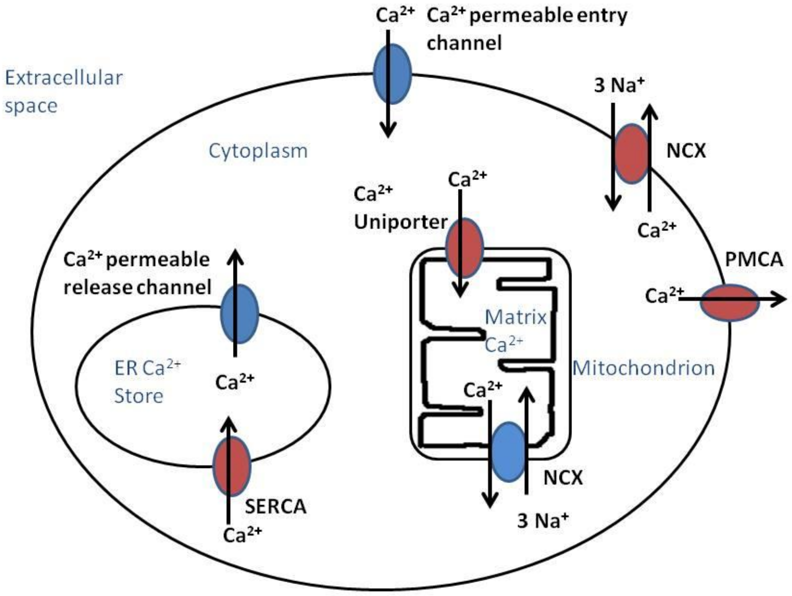
Ca2+
Ca2+ permeable entry channel
Extracellular space
3 Na+
NCX
Cytoplasm
Ca2+
Ca2+ Uniporter
Ca2+
Ca2+
PMCA
Ca2+ permeable release channel
Ca2+
Matrix Ca2+
ER Ca2+ Store
Ca2+
Mitochondrion
Ca2+
NCX
SERCA
Ca2+
3 Na+

Figure 1 shows modes of Ca^{2+} transport involved in increasing (blue) or lowering (pink) cytosolic Ca^{2+} concentration $[Ca^{2+}]$. Cytosolic Ca^{2+} levels can be elevated by 1) Ca^{2+} entry into the cell across the plasma membrane via Ca^{2+} permeable ion channels, 2) through the release from the endoplasmic reticulum (ER) (via Ca^{2+} release channels for example IP_3(inositol 1,4,5 trisphosphate)-induced receptors (IP_3R)) or 3) slowly from the mitochondria mainly via the $3Na^+/Ca^{2+}$ exchanger (NCX). Intracellular $[Ca^{2+}]$ can be reduced by the uptake of Ca^{2+} into the ER via the sarcoplasmic reticulum Ca^{2+} ATPase pump (SERCA), or uptake by the mitochondria via the Ca^{2+} uniporter, although these organelles have limited storage capacity. Ca^{2+} is also extruded via the plasma membrane Ca^{2+} ATPase pump (PMCA) or $3Na^+/ Ca^{2+}$ exchanger (NCX). (Note under certain conditions the NCX can also operate in the reverse mode, where it acts to cause Ca^{2+} influx).

1.2 Ca^{2+} entry mechanisms

A 10,000 fold concentration difference between the extracellular fluid (1 mM Ca^{2+}) and cytosol (100 nM Ca^{2+}) (maintained by the plasma membrane ATPases and Na^+/Ca^{2+} exchangers) and a negative resting membrane potential (around -80 mV), means that a huge electrochemical gradient exists across the plasma membrane for driving Ca^{2+} influx where free Ca^{2+} levels are low at rest (Parekh and Putney 2005). Resting cells have a low permeability to Ca^{2+}, but the opening of even a small number of Ca^{2+} permeable ion channels upon cell stimulation, can cause a dramatic rise in cytosolic Ca^{2+} concentration to high levels. This is a result of the strong driving force for Ca^{2+} entry. Numerous Ca^{2+} channels are known to exist, ranging from stretch activated channels (SAC), receptor-operated cation channels (ROCC), second messenger-operated channels (SMOC), voltage-operated Ca^{2+} channels (VOCC) and store-operated Ca^{2+} channels (SOCC) (Parekh and Putney 2005).

The two main types of cell surface Ca^{2+} channels are the VOCC and store-operated Ca^{2+} channels. VOCCs are activated upon depolarization of the plasma membrane, for example after an action potential. They are almost exclusively found in excitable cells, where they are the dominant Ca^{2+} channel for neurons and muscle. VOCCs are divided into three families, Cav1 (L-type), Cav2 (N-, P-, Q-, R-type) and Cav3 (T-type). The best characterised and targeted by drugs is the L-type channel. SOCCs on the other hand are widespread, being found in both excitable and non-excitable cells. They represent the dominant class of Ca^{2+} channels in non-excitable cells, such as those which make up the immune system. These channels are activated voltage-independently, by the depletion of Ca^{2+} in the intracellular stores, a concept first proposed by Putney 1986 and known as ‘capacitative calcium entry’. The existence of

SOCCs was directly demonstrated by Hoth and Penner 1992, with their discovery of CRAC channels in mast cells. CRAC channels (Ca^{2+} release activated Ca^{2+} channels) remain the best characterised example of a SOCC.

1.3 The pattern/ shape of the Ca^{2+} signal

Ca^{2+} entry through VOCCs and SOCCs is known to activate a plethora of cellular responses. However, this poses the problem of specificity. How can a promiscuous messenger like Ca^{2+} induce certain Ca^{2+}-dependent responses and not others? The answer lies in the pattern/ shape of the Ca^{2+} signal (Berridge et al 2000). Information is encoded in both the amplitude of the Ca^{2+} signal as well as its spatial (Neher 1998, Chang et al 2008) and temporal profile (Dolmetsch et al 1998).

Specificity is initially provided by the size of the Ca^{2+} signal. Small increases in intracellular Ca^{2+} will only activate high affinity processes, whilst lower affinity processes will only be stimulated by large increases in intracellular Ca^{2+} (this is known as the affinity-based model). However, large Ca^{2+} rises will also stimulate high and moderate affinity processes. Therefore the simple affinity-based model cannot be the sole mechanism for specificity. A substantial body of evidence now supports the concept that the temporal (kinetics) and the spatial nature (where the Ca^{2+} rises) of the Ca^{2+} signal is crucial in establishing which Ca^{2+}-dependent responses are activated, and when (Berridge et al 2000, Neher 1998, Rizzuto et al 2006).

1.3.1 *Temporal changes in* Ca^{2+}

Temporal changes in Ca^{2+} can be viewed in virtually all cell types in the form of Ca^{2+} oscillations, which are seen upon stimulation with low levels of agonist (Di Capite et al 2009a). Oscillations are characterised by repetitive rises in cytosolic Ca^{2+} concentration, rather than a sustained plateau (Thomas et al 1996, Di Capite et al 2009a). Figure 2 illustrates the cytosolic Ca^{2+} oscillation pattern in a single RBL-1 cell, following stimulation with a submaximal dose of agonist. Notice the repetitive, transient increases and subsequent rapid decreases in cytosolic Ca^{2+} concentration. With each Ca^{2+} oscillation some Ca^{2+} is lost from the cell, reducing the Ca^{2+} available for subsequent Ca^{2+} release. This results in the inevitable rundown of the oscillations over time, which can be seen in figure 2 below.

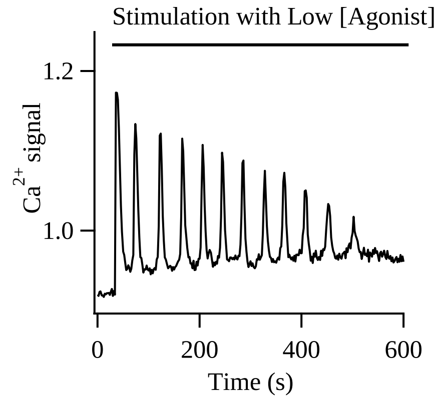

Figure 2 illustrates the cytosolic Ca^{2+} oscillation pattern when a single RBL-1 cell is stimulated with a low concentration of agonist, (for example 160 nM leukotriene C_4). Cells are loaded with the fluorescent Ca^{2+} indicator, Fura 2-AM, to observe the dynamic changes in intracellular calcium concentration in real-time. The Ca^{2+} signal transiently rises and falls and the oscillations decay over time.

Ca^{2+} oscillations arise from the periodic opening and closing of Ca^{2+} permeable ion channels. In excitable cells, membrane potential changes vary the activity of voltage-operated Ca^{2+} channels. This can evoke cytosolic Ca^{2+} oscillations, either from the repetitive opening and closing of the plasma membrane channels themselves, or by the induction of Ca^{2+}-induced Ca^{2+} release via the ryanodine receptors positioned on the SR membrane (Parekh 2011). Most cytosolic Ca^{2+} oscillations however, are a result of low level agonist stimulation of plasma membrane G-protein coupled receptors that generate IP_3 production via coupling to the enzyme phospholipase C (PLC), (see figure 3, which illustrates the cycle of events involved). Upon activation, phospholipase C cleaves PIP_2 (phosphatidylyinositol 4, 5 bisphosphate), to form DAG (diacylglycerol) and IP_3 (inositol 1,4,5 trisphosphate). IP_3 subsequently binds to and activates IP_3Rs on the ER membrane, which open and release Ca^{2+} from the intracellular stores.

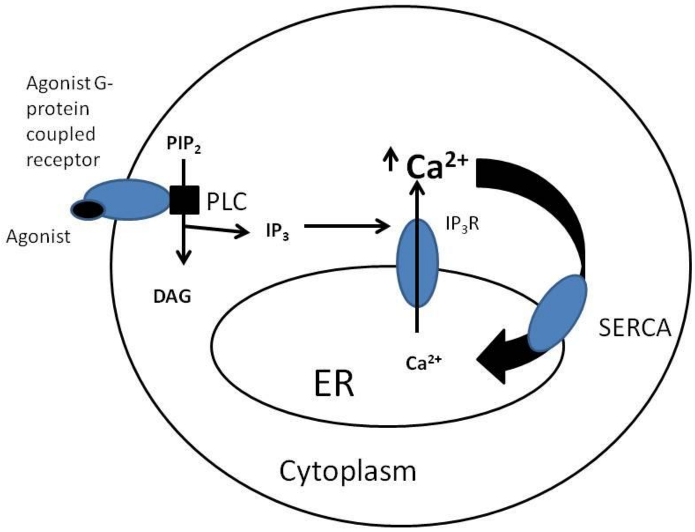

Figure 3 describes the generation of IP_3-induced cytosolic Ca^{2+} oscillations upon agonist stimulation, for example by submaximal concentrations of LTC_4. An agonist such as histamine or leukotriene C_4, binds to its specific cell surface receptor (a seven transmembrane, G-protein coupled receptor) coupled to phospholipase C (PLC), which subsequently cleaves PIP_2 (phosphatidylyinositol 4, 5 bisphosphate) to generate DAG (diacylglycerol) and IP_3 (inositol 1, 4, 5, trisphosphate). The latter acts on IP_3Rs to activate and open them to cause Ca^{2+} release. The repetitive opening and closing of the IP_3R evokes cytosolic Ca^{2+} oscillations. Some of the Ca^{2+} released is pumped back into the ER via SERCA pumps for subsequent Ca^{2+} release.

How IP_3Rs evoke oscillatory Ca^{2+} signals is not completely clear. There may well be cell- and/or agonist-specific mechanisms involved (Parekh 2011). Two separate hypotheses exist to explain the mechanism by which IP_3 can induce cytosolic Ca^{2+}

oscillations. Kabawata et al 1996 and Hirose et al 1999 support the view that IP_3 levels oscillate to drive the periodic opening and closing of the IP_3R, where increases in IP_3 open the channels and decreases in IP_3 close the channels. IP_3-induced Ca^{2+} oscillations are thought to arise via feedback pathways, which regulate PLC activity, independent of the status of the receptor linked to PLC. Hirose et al 1999 monitored the translocation of a GFP tagged domain of PLC (pleckstin homology domain-PH-GFP) and found it oscillated synchronously with cytosolic Ca^{2+} oscillations in epithelial cells, stimulated with ATP. Since they provided evidence that the translocation of PH-GFP is secondary to increases in IP_3 concentration, they explained that the oscillations in the translocation of PH-GFP that occurred simultaneously with cytosolic Ca^{2+} oscillations, reflected oscillations in intracellular IP_3. Kabawata et al 1996 provided good evidence for a role for PKC (protein kinase C) phosphorylation of G-protein coupled receptors, in producing cytosolic Ca^{2+} oscillations in HEK cells (transfected with a glutamate-receptor subtype). On the other hand, Wakui et al 1989 and Adkins et al 1999 support a view that IP_3 levels remain elevated and cytosolic Ca^{2+} oscillations are a consequence of Ca^{2+}-dependent feedback on the activity of the IP_3R. Small rises of Ca^{2+} would promote release facilitating the IP_3R, whilst the build up of higher levels of cytosolic Ca^{2+} upon further release would feedback to inactivate the channel (Finch et al 1991, Bezprozvanny et al 1991). Wakui et al 1989 found that injection of an IP_3 analogue, insensitive to metabolism (IPS_3) (to exclude the possibility of IP_3 being phosphorylated or degraded) into mouse pancreatic, acinar cells evoked pulses of Ca^{2+}activated Cl^- current that were similar to those induced by ACh. Different mechanisms may therefore underlie the induction of cytosolic Ca^{2+} oscillations in different cell types or more than one mechanism maybe involved.

What is clear however is that Ca^{2+} release via the IP_3R is sufficient alone to cause IP_3-induced Ca^{2+} oscillations. Di Capite et al 2009a showed that submaximal concentrations of agonist leukotriene C_4 induced Ca^{2+} oscillations which could last for a few minutes in mast cells bathed in Ca^{2+}-free external solution. Leukotriene C_4 (LTC_4) is an important proinflammatory lipid mediator (Boyce 2007, Peters-Golden et al 2006), which activates plasma membrane cysteinyl leukotriene type I receptors coupled to PLC. In contrast, sustained cytosolic Ca^{2+} oscillations ensued in the presence of 2 mM external Ca^{2+}. This leads to the finding that Ca^{2+} entry through store-operated Ca^{2+} channels is required to maintain cytosolic Ca^{2+} oscillations. In the absence of Ca^{2+}, no Ca^{2+} enters the cell but released Ca^{2+} is still extruded via the plasma membrane Ca^{2+} ATPase (PMCA) (Moreau et al 2005). Therefore after each Ca^{2+} release event some Ca^{2+} is lost from the cell, leaving less Ca^{2+} for store refilling. Over time, the Ca^{2+} available for subsequent oscillations is lost and the oscillations completely run down. In the presence of external Ca^{2+}, depletion of the stores opens SOCCs and causes Ca^{2+} to enter the cell. This provides an effective source of Ca^{2+} to replenish the ER stores and supplies the Ca^{2+} needed for subsequent Ca^{2+} release events. Consistent with this view, continuous oscillations can be achieved in cells bathed in zero Ca^{2+} and 1 mM La^{3+} (Di Capite et al 2009a), which blocks the PMCA, (preventing Ca^{2+} clearance). Under such conditions, no Ca^{2+} is lost from the cell. Therefore more Ca^{2+} recycles back into the ER for the subsequent cycle of Ca^{2+} release.

Cytosolic Ca^{2+} oscillations occur in most cells. This implies that they encode a universal signalling mechanism (Thomas et al 1996). Such oscillations drive a range of specific Ca^{2+}-dependent responses such as exocytosis (Tse et al 1993), mitochondrial metabolism (Hajnóczky et al 1995) and gene expression (Dolmetsch et al 1998, Li et al 1998). Hajnóczky et al 1995 simultaneously measured cytosolic Ca^{2+} oscillations (using the Ca^{2+}-sensitive fluorescent indicator Fura 2) and NADPH and $FADH_2$ fluorescence in single hepatocyte cells. They showed that each vasopressin-induced cytosolic Ca^{2+} oscillation in hepatocytes resulted in a transient rise in mitochondrial metabolism. This was revealed from the finding that NADPH and $FADH_2$ levels (taken as a measure of Ca^{2+}-dependent enzyme activity which determine the rate of mitochondrial metabolism) rose with each IP_3-dependent cytosolic Ca^{2+} oscillation. In pituitary gonadotrophes, single secretion events have been recorded following each cytosolic Ca^{2+} oscillation (Tse et al 1993).

Cytosolic Ca^{2+} oscillations encode information in their amplitude (Tse et al 1993), frequency (Dolmetsch et al 1998) and subcellular spatial profile (Di Capite et al 2009a), to impart specificity to Ca^{2+} and drive specific responses. Oscillations of different amplitude activate specific targets based on the affinity of the target to bind Ca^{2+} at one or more site. Targets with a low affinity are only activated by high amplitude Ca^{2+} oscillations. Some targets have a number of Ca^{2+} binding sites which further induces specificity between different Ca^{2+} sensors. Ca^{2+} sensors with different numbers of Ca^{2+} binding sites will be selectively activated by different amplitude oscillations. A target with a single Ca^{2+} binding site can be effectively activated by concentrations of Ca^{2+} that would be ineffective at activating a target with multiple

Ca^{2+} binding sites of the same affinity (Parekh 2011). It will take more Ca^{2+} to activate a target with four Ca^{2+} binding sites compared to a target with a single Ca^{2+} binding site despite all sites having the same affinity for Ca^{2+}, (please see Parekh 2011, figure 2, for an illustration of this concept). An example of amplitude coding by cytosolic oscillations can be illustrated by consideration of Ca^{2+}-induced exocytosis in excitable cells. Tse et al 1993 showed in pituitary gonadotrophes that application of gonadotropin releasing hormone induced a cytosolic IP_3-dependent Ca^{2+} oscillation and rhythmic exocytosis. Through simultaneously measuring cytosolic Ca^{2+} elevations with each secretion event using high temporal resolution capacitance measurements, they revealed that each Ca^{2+}i (intracellular Ca^{2+}) rise was accompanied with a corresponding burst of exocytosis. This exocytotic event was sensitive to the amplitude of the cytosolic Ca^{2+} elevation. Brief depolarisation steps to open VOCCs caused Ca^{2+} transients < 100 nM in size and failed to cause vesicle secretion, whilst Ca^{2+}i transients raised to 100 nM were capable of causing a resultant exocytotic event in chromaffin cells. Therefore to trigger vesicle secretion a threshold Ca^{2+} concentration was required to activate exocytosis, based on the affinity of the target to bind Ca^{2+}.

Information can also be encoded in the frequency (kinetics) of the Ca^{2+} oscillations. Targets which rapidly bind Ca^{2+} (fast on-rate) preferentially respond to transient signals whereas targets with a slow Ca^{2+} binding rate (slow on-rate) require a sustained Ca^{2+} response. Certain Ca^{2+} activated enzymes have been identified to be sensitive to the kinetic properties of Ca^{2+} oscillations such as protein kinase C (PKC), Ca^{2+}/calmodulin-dependent protein kinase II (CAMKII) and calcineurin. Dolmetsch et al 1998 demonstrated that the frequency or kinetics of the Ca^{2+} signal induced specificity to the activation of transcription factors. Jurkat T cells, pre-stimulated with thapsigargin to deplete the stores and open CRAC channels were alternately exposed to external solutions of either 0 mM Ca^{2+} or 1.5 mM Ca^{2+}, using a Ca^{2+}-clamp technique. Such an approach was used to enable them to evoke Ca^{2+} signals of variable kinetics. They found that the Ca^{2+}-dependent transcription factor NFAT was preferentially activated by transient Ca^{2+} signals compared with a sustained Ca^{2+} rise, despite similar elevations in bulk cytosolic Ca^{2+}. This revealed that the transcription factor was sensitive to the time-course (kinetics) of the Ca^{2+} signal. Furthermore, oscillations with different amplitudes but the same frequency or those with different frequencies but the same amplitude could be evoked in T cells, using this Ca^{2+}-clamp approach. Such an approach was used to investigate whether different transcription factors were sensitive to different Ca^{2+} oscillation patterns. Whilst changes in amplitude of the oscillations alone (in the face of a constant frequency) activated all three transcription factors (NF-κB, Oct/OAP and NFAT) similarly, changes in frequency alone (when amplitude was kept constant) specifically activated certain transcription factors and not others. Low frequency oscillations only activated NF-κB, whilst high frequency oscillations were required to activate all three factors. This demonstrates that different Ca^{2+}-dependent transcription factors can be distinctly activated in response to the frequency or kinetics of the cytosolic Ca^{2+} oscillations. Such an effect was carried through to impact on the expression of their resultant genes. Expression of the genes secondary to each transcription factor was also sensitive to the frequency of the cytosolic Ca^{2+} oscillations.

Although information is encoded in the amplitude and frequency of cytosolic Ca^{2+} oscillations, there are limitations to the level of specificity that these two variables can induce. High frequency oscillations would activate targets sensitive to both low and high frequencies. Increasing evidence now reveals that oscillations also encode information with regards to their subcellular location. This was demonstrated by Di Capite et al 2009a, who showed that only IP_3-induced Ca^{2+} oscillations accompanied by Ca^{2+} entry through CRAC channels activated c-fos gene expression (an important component of chemokine regulation; Lee et al 2004) in mast cells. This illustrated the importance of the spatial profile of Ca^{2+} oscillations. They evoked cytosolic Ca^{2+} oscillations by application of low concentrations of LTC_4 in the presence or absence of external Ca^{2+}. LTC_4 evoked continuous cytosolic Ca^{2+} oscillations in the presence or absence of external Ca^{2+} (latter occurred only if PMCA was blocked by La^{3+}) that were similar in size and duration. However, only in the presence of external Ca^{2+} were subsequent CRAC channel dependent Ca^{2+} entry and a subplasmalemmal Ca^{2+} rise induced. Since the gene c-fos (important for regulating immune cell function; Lee et al 2004) was only expressed in mast cells exposed to external Ca^{2+}, it demonstrated that the expression of c-fos was sensitive to the spatial location of the Ca^{2+} rise. Therefore research is now focusing on the importance of the spatial profile of Ca^{2+} signals in driving Ca^{2+} specific cellular actions.

1.3.2 *Spatial changes in Ca^{2+}*

Upon cell stimulation, Ca^{2+} channels open and the Ca^{2+} that permeates the channels reaches very high concentrations locally surrounding the channel pore; such signals are called Ca^{2+} microdomains. These signals are of major importance to allow Ca^{2+} to elicit specificity (Neher 1998, Parekh 2008a). Within 100 nm of the channel, Ca^{2+} levels can reach very high concentrations (>100 µM) within hundreds of microseconds. This is too fast to be captured by cytosolic Ca^{2+} buffers. Further away from the channel (>100 nm) the lower Ca^{2+} concentrations are potently suppressed by buffers (Neher 1998). This establishes steep spatial Ca^{2+} gradients within the cell. Microdomains are dynamic signals and different Ca^{2+} permeable channels establish microdomains of variable size (see figure 4). How high and how far Ca^{2+} spreads is regulated by many factors. These include Ca^{2+} selectivity of the channel, channel conductance, membrane potential, extracellular Ca^{2+} concentration and the nature and amount of intracellular buffers (Rizzuto et al 2006, Parekh 2008a). However, most notably the size of a microdomain is determined by the single channel flux (Rizzuto et al 2006, Parekh 2008a). The larger the flux of Ca^{2+} through a Ca^{2+} permeable ion channel, the larger is the microdomain that develops. The single channel flux depends on both the electrochemical gradient for Ca^{2+} entry and the single channel conductance. Channels with a low single channel conductance will produce small microdomains, whereas channels with a larger conductance will establish much larger microdomains (where Ca^{2+} spreads further into the cell). This is clearly shown in figure 4.

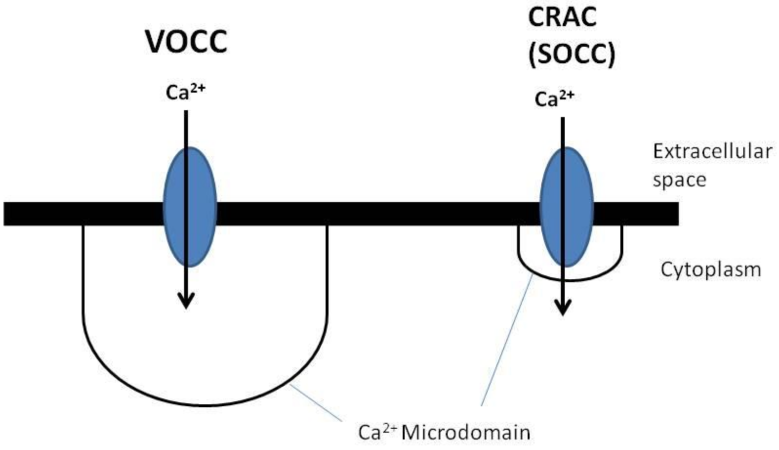

Figure 4 demonstrates the Ca^{2+} microdomain rapidly formed when Ca^{2+} permeable ion channels open. How high and how far the microdomain spreads is strongly dependent on the single channel flux. The L-type voltage-operated Ca^{2+} channel (VOCC), which has a single channel conductance of around 24 pS, generates a much larger microdomain upon activation than the Ca^{2+} release activated Ca^{2+} channel (CRAC, a type of store-operated Ca^{2+} channel (SOCC)), which has a tiny single channel conductance of < 1 pS. As one can see the microdomain that forms when Ca^{2+} enters through the VOCC spreads much deeper into the cell, occupying a much larger area.

Microdomains are brief in duration, rapidly building up and collapsing within hundreds of microseconds (Parekh 2011, Neher 1998). Their temporal nature is influenced by the open probability of the channel. Furthermore, microdomains are dependent on the number of ion channels that form them. Microdomains can be a result of the opening of a single Ca^{2+} channel or a cluster of channels, as shown by figure 5. In the case of a cluster of channels, neighbouring single channel microdomains will summate together to increase the size and spread of the microdomain (Parekh 2011, Lewis 2007).

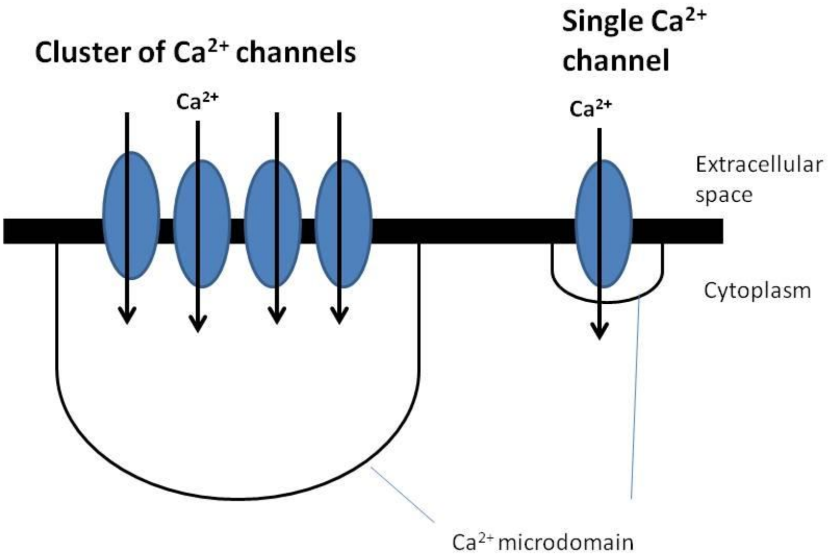
Cluster of Ca2+ channels
Ca2+
Single Ca2+ channel
Ca2+
Extracellular space
Cytoplasm
Ca2+ microdomain

Figure 5 reveals the difference in the size of a microdomain formed by the opening of a single Ca^{2+} permeable ion channel, versus the microdomain formed by the opening of a cluster of the same Ca^{2+} permeable ion channels. Clusters of channels form a much larger Ca^{2+} microdomain that diffuses deeper into the cell, as a result of the summation of the individual single channel microdomains.

The consequence of microdomains is that targets with a low affinity for Ca^{2+} are activated rapidly and with high fidelity when positioned within close proximity of the microdomain, whereas the same targets >100 nm away would be activated much more slowly and weakly, if at all (Neher 1998; this is demonstrated in figure 6). The position of Ca^{2+} targets relative to a microdomain is very important in establishing the speed and extent of activation.

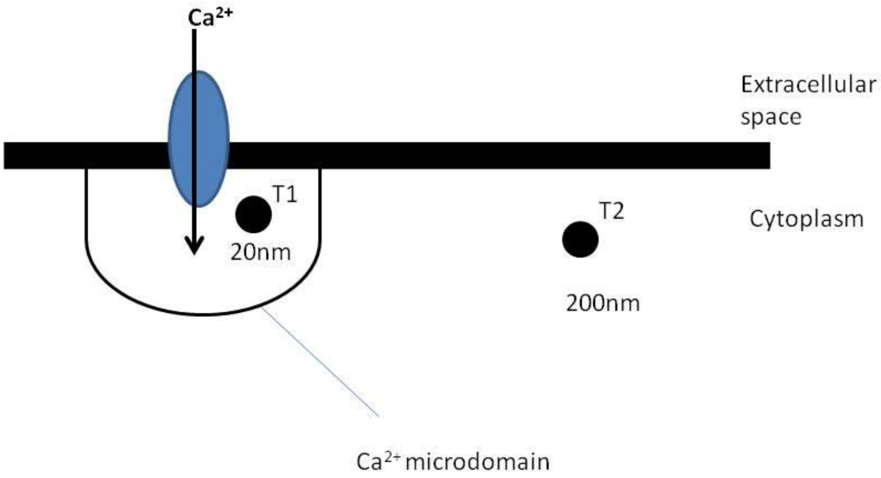

Figure 6 (adapted from Neher 1998) illustrates the exposure of Ca^{2+} to targets which vary in distance from the channel pore. Target 1 (T1), is 20 nm from the channel pore and positioned within the microdomain (this exact distance is dependent on channel type). Here it is always exposed to high, local Ca^{2+} concentrations ≈100 µM. The microdomain area is independent of cytoplasmic Ca^{2+} buffers. Target 2 (T2) positioned 200 nm from the channel pore (outside of the microdomain) is exposed to much lower Ca^{2+} concentrations (≈5-10 µM), due to suppression of the signal by cytosolic Ca^{2+} buffers. Given that both targets have the same affinity to bind Ca^{2+}, T1 would be rapidly activated with high fidelity, whereas activation of T2 would be slower, with a much lower probability.

Microdomains are short-lived (occurring over microseconds), developing immediately on channel opening and disappearing upon channel closure (Parekh 2011). The Ca^{2+}-sensitive photoprotein aequorin (Llinas et al 1992 in squid giant axons, Marsault et al 1997 in smooth muscle cells, Nakahashi et al 1997 in HEK cells) and green fluorescent protein-based Ca^{2+} probes (cameleons) localised to the plasma membrane have been used to detect such hotspots (Isshiki et al 2002, Nagai et al 2004).

It is important to point out that the term Ca^{2+} microdomain is not always used to describe the local, small volumes of Ca^{2+} that arise upon the opening of Ca^{2+} permeable ions channels. In the literature, the term is also used to describe Ca^{2+}

signals restricted to a specific subcellular domain. Such microdomains extend over a much larger area (hundreds of nanometers to micrometers) compared to the small channel dependent microdomains that extend over small distances (within 100 nm of the channel pore). For example, steep Ca^{2+} gradients have been identified between the secretory and basal pole of pancreatic acinar cells (Thorn et al 1993a, b), which result from a belt of mitochondria that separate the two domains. This belt buffers cytosolic Ca^{2+}, preventing the diffusion of Ca^{2+} from one pole to the other (Tinel et al 1999). In this thesis, I will concentrate on the importance of Ca^{2+} microdomains arising through the opening of Ca^{2+} permeable ion channels (CRAC channels), their regulation and subsequent functional consequences.

A striking example of the versatility of Ca^{2+} and the importance of its spatial profile is identified in smooth muscle. A global rise in cytosolic Ca^{2+} (arising from the opening of VOCCs and subsequent Ca^{2+}-induced Ca^{2+} release by the ryanodine receptors), is known to induce muscle contraction (Berridge 1997). On the other hand, the local Ca^{2+} release from the IP_3R positioned close to the plasma membrane activates potassium channels. This hyperpolarizes the membrane and therefore induces relaxation of the muscle (Berridge 1997, Nelson et al 1995, Petkov et al 2001). Where a Ca^{2+} rise occurs and how far it spreads is therefore of great importance in determining what type of response is induced.

The importance of high, local Ca^{2+} signals that arise from intracellular Ca^{2+} release events is illustrated by Rizzuto et al 1993, 1998 and Hajnóczky et al 1995. Rizzuto et al 1998 revealed that the close apposition between the ER and mitochondria enable the efficient transfer of Ca^{2+} from IP_3R to the mitochondrial matrix. Furthermore, Hajnóczky et al showed that the efficient transmission of Ca^{2+} into the matrix in response to IP_3R-driven Ca^{2+} release helped determine the rate of mitochondrial metabolism and consequential availability of ATP.

1.4 Functional consequences of local Ca^{2+} entry through SOCCs

Local entry of calcium through SOCCs has been shown to drive many important functional responses (summarized in figure 7). The first to be identified was the regulation of Ca^{2+}-sensitive adenylate cyclases (Fagan et al 1998, Gu and Cooper 2000, Martin and Cooper, 2006). Local Ca^{2+} influx through SOCCs is also known to be important for the production of nitric oxide (NO) in smooth muscle or endothelia (Isshiki et al 2004). An additional example of the close coupling between local Ca^{2+} entry through SOCCs and the activation of an enzyme positioned in the plasma membrane close to the SOCC is provided by Bautista and Lewis 2004. They reveal the importance of CRAC channel dependent Ca^{2+} entry (a well characterised SOCC) in the regulation of the plasma membrane Ca^{2+}ATPase pump (PMCA), in Jurkat T cells. Increasing the local entry through CRAC channels by increasing extracellular Ca^{2+} concentrations from 2 to 20 mM had no effect on the bulk cytosolic $[Ca^{2+}]$, yet markedly enhanced PMCA activity. Furthermore, low concentrations (5 µM) of 2-APB (known to enhance CRAC channel activity several fold) or hyperpolarization (from +30 to -70 mV) of the plasma membrane, enhanced CRAC channel activity and PMCA activity. Under such conditions minimal effects on global intracellular Ca^{2+} were observed. Therefore CRAC channel dependent Ca^{2+} microdomains were controlling PMCA activity. The local rise in Ca^{2+} following CRAC channel dependent Ca^{2+} entry was found to increase the activity rate of the pump to clear Ca^{2+}. Such modulation arose from the close physical coupling between the channel and pump and the exposure of high local Ca^{2+} signals to the pump directly.

Evidence also exists to demonstrate that local entry through CRAC channels is involved in the specific activation of targets located within the cytoplasm (some distance away from the influx channel). In RBL cells, Chang et al 2004, 2006 showed that CRAC channel dependent Ca^{2+} influx following thapsigargin stimulation in 2 mM Ca^{2+} drove the production of an important intracellular signalling molecule, arachidonic acid (aa) and the secretion of a potent intercellular proinflammatory signal, leukotriene C_4 (LTC_4; Boyce 2007). This involved the activation of two cytosolic Ca^{2+}-dependent enzymes, phospholipase A_2 ($cPLA_2$) and 5-lipoxygenase (5-LOX). These enzymes are not anchored next to the CRAC channel in this case but are positioned some distance away. They showed that the thapsigargin-induced rise in arachidonic acid and LTC_4 generation was blocked in the presence of CRAC channel blockers 2-APB (at high concentrations, 20 µM) and 10 µM Gd^{3+}. This showed that CRAC channels were driving the response. Secondly, they established that it was the local Ca^{2+} entry through these CRAC channels that was crucial. The ability of thapsigargin to activate these cytosolic enzymes and produce and release arachidonic acid and LTC_4 is abolished in zero Ca^{2+}, despite a rise in bulk cytosolic [Ca^{2+}] still being observed. Confirmation that local Ca^{2+} entry and not a bulk cytosolic Ca^{2+} rise was preferentially activating arachidonic acid and LTC_4 synthesis was provided by Chang et al 2008. They showed that in the presence of 1 mM La^{3+} to block the PMCA in Ca^{2+}-free solution, LTC_4 secretion was less effectively stimulated compared to that in 2 mM Ca^{2+} following thapsigargin application. This was despite both conditions producing a rise in bulk cytosolic Ca^{2+} of similar amplitude and time-course. Consistent with this, partial block of CRAC channels with 100 nM La^{3+} in 2 mM Ca^{2+}, which established a larger CRAC channel dependent Ca^{2+} microdomain than cells bathed in 0.25 mM Ca^{2+}, caused a larger increase in LTC_4 secretion following thapsigargin stimulation compared to 0.25 mM Ca^{2+}. This was in spite of both conditions evoking a similar rise in bulk cytosolic Ca^{2+}. Furthermore, the fast Ca^{2+} chelator, BAPTA (capable of buffering local CRAC channel dependent Ca^{2+} entry) but not the slow Ca^{2+} chelator, EGTA (which is incapable of buffering local Ca^{2+} signals) suppressed arachidonic acid and LTC_4 secretion. Collectively, the experiments demonstrate that the local entry through CRAC channels and not a bulk cytosolic Ca^{2+} rise is crucial for activating these cytosolic enzymes (positioned some distance away from the CRAC channel). The activation pathway, which involves a Ca^{2+} sensor, Syk, to convey the Ca^{2+} signal, is described and illustrated in figure 9, section **1.5**.

Local entry through CRAC channels has also been linked to the activation of Ca^{2+}-dependent transcription factors and nuclear gene expression. These include c-fos expression (Ng et al 2009 in RBL cells), NFAT-1 (nuclear factor of activated T cells) activation and nuclear migration in HEK cells, and NFAT-1-driven gene expression in RBL cells (Kar et al 2011). Ng et al showed that thapsigargin failed to activate c-fos expression in zero Ca^{2+} or zero Ca^{2+} and La^{3+} .The prominent thapsigargin-dependent c-fos expression observed in 2 mM Ca^{2+} was substantially reduced following depolarization of the plasma membrane by TEA^{+}/Cs^{+} or lowering external Ca^{2+} to 0.5 mM concentration. All three conditions impaired CRAC channel dependent Ca^{2+} entry, yet had minimal effects on the bulk cytosolic rise in Ca^{2+}. Kar et al 2011 used an eGFP-NFAT-1 (green fluorescent protein tagged NFAT1) construct and single cell live imaging to monitor NFAT-1 movement in HEK cells. Whilst thapsigargin induced the activation and movement of NFAT-1 to the nucleus in 2 mM Ca^{2+}, such an effect was blocked in zero Ca^{2+} or following the inhibition of CRAC channel influx with Synta (a potent CRAC channel blocker, Ng et al 2008). Furthermore, cytoplasmic EGTA, a Ca^{2+} chelator which buffered bulk cytosolic Ca^{2+} rises but left the CRAC channel dependent Ca^{2+} microdomain intact, failed to affect NFAT-1 movement. NFAT-1 movement was however significantly impaired when external Ca^{2+} was lowered to 0.5 mM Ca^{2+}. Such a condition reduced CRAC channel dependent Ca^{2+} entry, yet evoked a bulk cytosolic Ca^{2+} concentration similar to that found with thapsigargin stimulation in 2 mM Ca^{2+}. Therefore it is the local Ca^{2+} entry signal which is driving NFAT-1 activation and its movement to the nucleus. In addition to their experiments on HEK cells, Kar et al 2011 showed that agonist-induced CRAC channel dependent Ca^{2+} entry increased NFAT-1-dependent gene expression in RBL cells by transfecting cells with an eGFP plasmid driven by an NFAT-1 promoter. This effect was blocked by Synta. Local entry through CRAC channels is essential in activating downstream functional consequences such as nuclear gene expression. Investigating the regulation of CRAC channels is therefore important in order to establish how CRAC channels drive downstream cellular responses and impact upon cell physiology.

It is easy to understand how local Ca^{2+} entry can directly, rapidly and robustly activate targets even with low affinities for Ca^{2+}, if the latter are positioned close to or are associated with the Ca^{2+} channel. However, how local Ca^{2+} influx activates targets some distance away, such as nuclear gene expression or cytoplasmic enzyme activation is not so simple. This involves an additional signalling component to sense the local signal and convey it to the distant target.

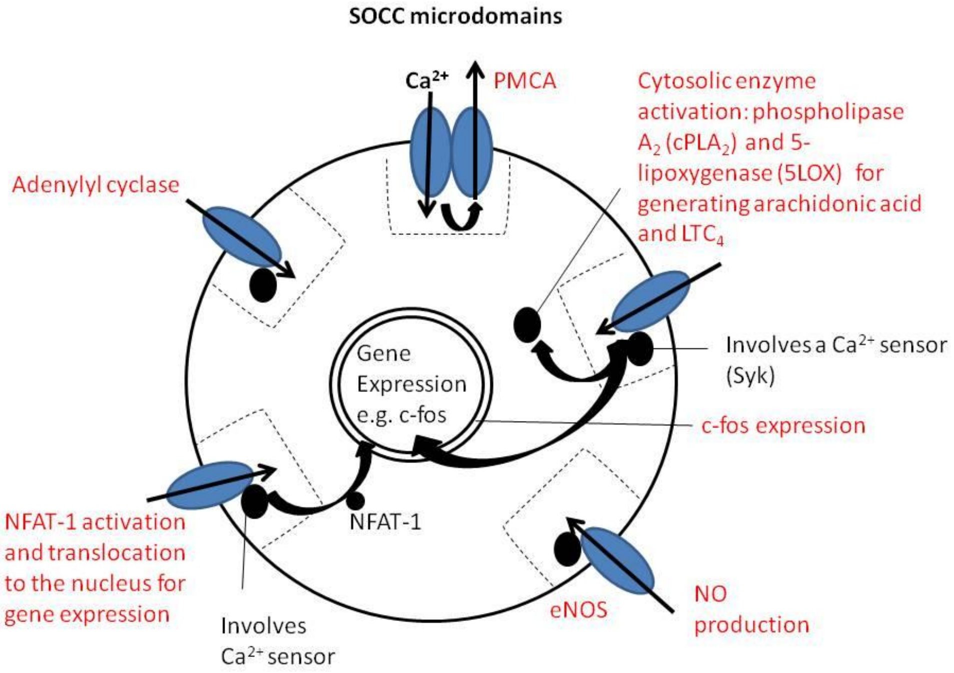
SOCC microdomains
Ca2+
PMCA
Cytosolic enzyme activation: phospholipase A2 (cPLA2) and 5-lipoxygenase (5LOX) for generating arachidonic acid and LTC4
Adenylyl cyclase
Involves a Ca2+ sensor (Syk)
Gene Expression e.g. c-fos
c-fos expression
NFAT-1 activation and translocation to the nucleus for gene expression
NFAT-1
Involves Ca2+ sensor
eNOS
NO production

Figure 7 (adapted from Parekh 2008a) summarizes the functional consequences of SOCC dependent Ca^{2+} microdomains, (such as the well characterised, CRAC channel). Local Ca^{2+} entry through CRAC channels can drive short-ranging (such as plasma membrane Ca^{2+} ATPase activity (PMCA)) and long-range signalling events (including c-fos expression and NFAT-1-driven gene expression).

1.5 Ca^{2+} sensors

Local Ca^{2+} influx through Ca^{2+} channels can be detected by a range of proteins, which are found attached to or positioned within the sphere of the Ca^{2+} microdomain of the channel. Some of these Ca^{2+} sensors are capable of transmitting local Ca^{2+} signals over relatively long distances. Two important Ca^{2+} sensors that have been identified to transduce local Ca^{2+} entry into distant functional consequences are calmodulin and Syk.

Dolmetsch et al 2001 showed in neurons that calmodulin tethered to the IQ domain of L-type Ca^{2+} channels, relayed local Ca^{2+} entry to the nucleus for CREB-dependent gene expression (such a pathway is shown in figure 8). They found that expression of L-type Ca^{2+} channel constructs with point mutations in their IQ domain (rendering them unable to bind calmodulin), impaired CREB-dependent gene expression in neurons. This was despite no effect on bulk intracellular Ca^{2+}. Furthermore, expression of a calmodulin mutant unable to bind Ca^{2+} also inhibited this CREB-dependent signalling pathway. Similar effects were found in the MEF-2-dependent signalling pathway, which provided evidence that in order for L-type channels to activate nuclear gene expression, calmodulin was required to relay the signal from the plasma membrane to the nucleus.

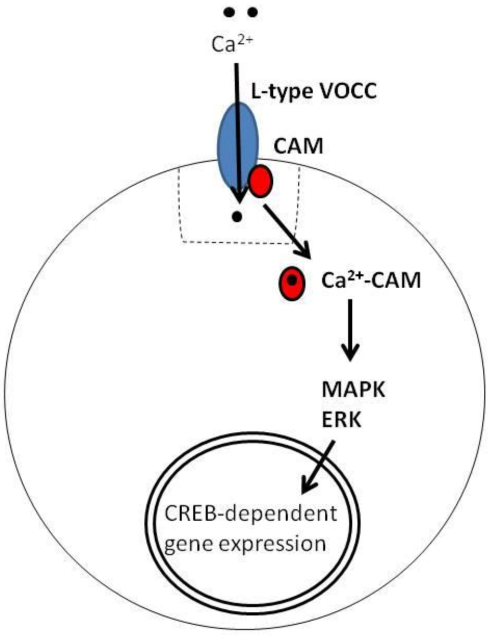

Figure 8 summarizes the activation of CREB-dependent gene expression by local Ca^{2+} entry through L-type voltage-operated Ca^{2+} channels, by calmodulin (CAM). Upon opening of L-type channels the local Ca^{2+} entry binds to calmodulin tethered to the channel. The resultant Ca^{2+}-calmodulin (Ca^{2+}-CAM) complex, dissociates from the channel and activates CREB-dependent gene expression via the cytosolic ERK/MAPK enzyme signalling pathway.

Another important Ca^{2+} sensor, Syk, was identified by Ng et al 2009 in mast cells. This non-receptor tyrosine kinase was shown to couple local Ca^{2+} entry through CRAC channels to both ERK activation (the signalling pathway involved in LTC_4 secretion) and gene expression, two processes which occurred over very different time scales. Figure 9 shows the sequence of events involved in each of these Syk-dependent pathways. Knockdown of the endogenous function of Syk, by transfecting RBL-1 cells with Syk RNAi, significantly impairs both c-fos expression and ERK phosphorylation. This work demonstrates that the same local Ca^{2+} signal, arising from open CRAC channels, can activate two temporally distinct cellular processes, via the Ca^{2+} sensor Syk.

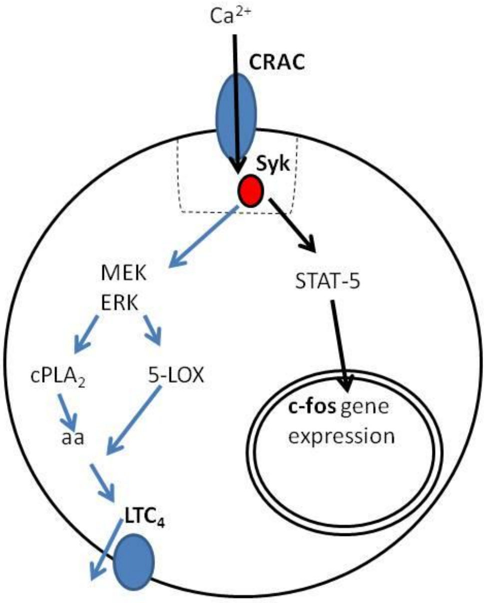

Figure 9 (adapted from Ng et al 2009) shows the activation of two temporally separate pathways by the CRAC channel dependent Ca^{2+} microdomain and the closely positioned Syk Ca^{2+} sensor. Upon CRAC channel opening the local Ca^{2+} entry is sensed by Syk to cause stimulation of the MEK/ERK pathway and subsequently activate phospholipase A_2 ($cPLA_2$) and 5-lipoxygenase (5-LOX) enzymes. This leads to the generation and secretion of leukotriene C_4 (LTC_4). At the same time, Syk activates STAT-5, (transcription factor) for nuclear c-fos expression.

Ca^{2+} sensors provide critical links to convey a local Ca^{2+} signal into long-range signalling. More on the structure and function of calmodulin and its regulation of ion channels, such as CRAC channels will be discussed later. Before we consider factors which regulate CRAC channels, we must first gain an overview of the biophysical properties, molecular determinants, and activation of CRAC channels. This is addressed in the next section (**1.6**).

1.6 Store-operated CRAC channels

The concept of store-operated Ca^{2+} entry was first proposed by Putney in 1986. Putney found that under conditions where Ca^{2+} stores were full no Ca^{2+} influx was present in parotid acinar cells, yet upon store depletion Ca^{2+} influx was recorded. The concept was termed 'capacitative calcium entry'. Consistent with this idea, Takemura et al 1989 revealed Ca^{2+} influx in response to thapsigargin. Thapsigargin is a drug which blocks the sarcoplasmic reticulum Ca^{2+} ATPase pump (SERCA) in the ER membrane, preventing Ca^{2+} uptake into the ER stores. Since the ER membrane is not tight for Ca^{2+} the ER becomes slowly depleted of Ca^{2+} via the gradual diffusion of Ca^{2+} out of the ER into the cytoplasm. Depletion of the ER Ca^{2+} stores provides the stimulus to activate the CRAC channels (please see sections **1.6.4** and **1.6.5** for details regarding the molecular determinants of the CRAC channel and the model of CRAC channel activation respectively). More direct evidence for store-operated Ca^{2+} entry was demonstrated by Hoth and Penner in 1992, who directly measured store depletion-induced Ca^{2+} release activated Ca^{2+} current, I_{CRAC} in mast cells.

Physiologically, ER store depletion and subsequent CRAC channel activation occurs in response to agonists that bind to plasma membrane receptors (seven transmembrane, G-protein coupled receptors) that are coupled to the enzyme phospholipase C (Zweifach and Lewis 1993). Activation of phospholipase C cleaves PIP_2 (phosphatidylinositol 4, 5 bisphosphate) to form IP_3 (inositol 1,4,5 trisphosphate) and DAG (diacylglycerol). IP_3 directly binds to IP_3 receptors on the ER membrane, subsequently causing the Ca^{2+} to pass out of the ER and into the cytoplasm. The fall in Ca^{2+} within the store provides the activation stimulus for CRAC channels to open. (Figure 10, illustrates the cascade of events involved). Physiological triggers for CRAC channels are therefore IP_3-inducing agonists, such as histamine, ATP and leukotriene C_4.

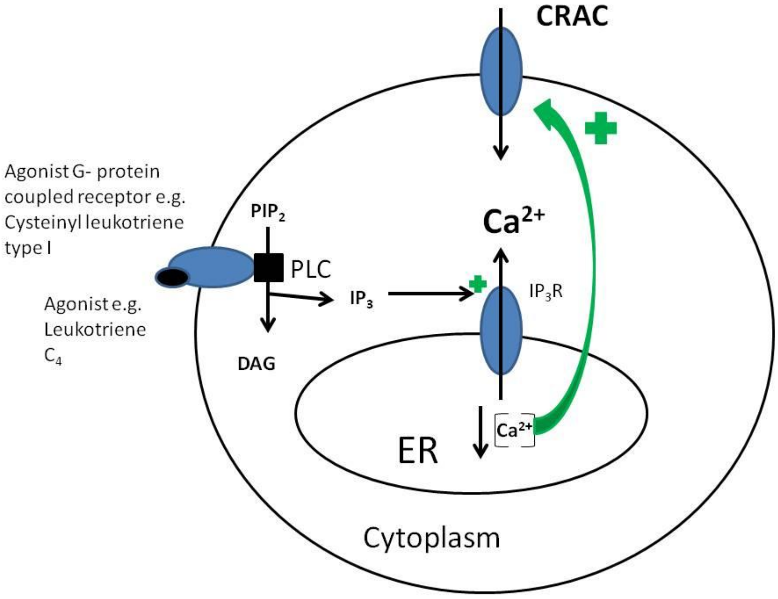
CRAC
Agonist G- protein coupled receptor e.g. Cysteinyl leukotriene type I
Agonist e.g. Leukotriene C_4
PIP_2
PLC
IP_3
DAG
Ca^{2+}
IP_3R
Ca^{2+}
ER
Cytoplasm

Figure 10 (adapted from Parekh 2010) illustrates the activation of CRAC channels upon agonist stimulation. Agonist evoked IP_3-induced Ca^{2+} release causes depletion of the intracellular ER Ca^{2+} stores, which subsequently activates and opens the CRAC channel (Ca^{2+} release activated Ca^{2+} channel) so that Ca^{2+} can enter the cell.

1.6.1 *Key features of I_{CRAC}*

Hoth and Penner 1992 used whole-cell patch clamp recordings to measure directly I_{CRAC} in mast cells, evoked when ER stores are depleted of Ca^{2+} by three independent methods. These included application of IP_3 to open IP_3-dependent Ca^{2+} release receptors on the ER membrane, ionomycin (an ionophore which permeabilizes the ER membrane) or high cytoplasmic EGTA, (which increases the Ca^{2+} gradient between the ER and cytoplasm and prevents refilling by chelating the Ca^{2+}). All three methods evoked a sustained, inwardly rectifying current at negative voltages. The current-voltage relationship is shown in figure 11. Hoth and Penner 1992 termed this current Ca^{2+} release activated current, I_{CRAC}. The current was identified to have a very positive reversal potential, which suggested a high selectivity for Ca^{2+}. Furthermore, in the presence of Ba^{2+} as the charge carrier, the current was still present but was reduced, which indicated that I_{CRAC} was the result of a Ca^{2+} selective permeation pathway. I_{CRAC} has now been evoked in many cell types.

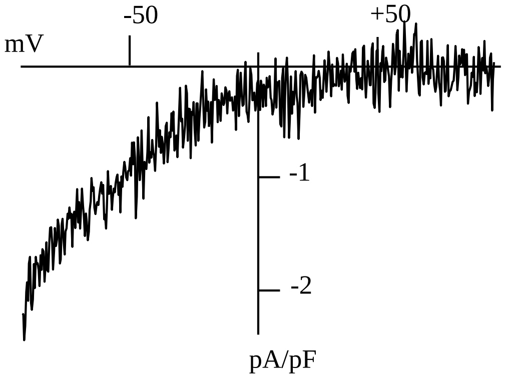

Figure 11 reveals the current-voltage relationship of I_{CRAC}, which shows the same features irrespective of how stores are emptied. The current is smooth and shows prominent inward rectification, with a very positive reversal potential > +70 mV.

The prominent inward rectification is steepened by the fast Ca^{2+}-dependent inactivation of the CRAC channels and the fact that I_{CRAC} is not supported by any detectable outward current carried by Cs^+ and K^+. The absence of any abrupt change in current with voltage indicates that the current is not activated upon membrane depolarization, as is found with VOCC channels. However, I_{CRAC} does have some slow voltage dependence, since hyperpolarizing holding potentials reduce I_{CRAC} and depolarizing holding potentials increase I_{CRAC} (Bakowski and Parekh 2000).

Evaluation of the time-course of I_{CRAC} (shown in figure 12), reveals that the current develops smoothly and slowly, taking about 100s to peak (with a half time of around 40-50s). The sizeable delay between depletion of the stores and opening of the CRAC channel is consistent with a biochemical signalling pathway being involved in CRAC channel activation.

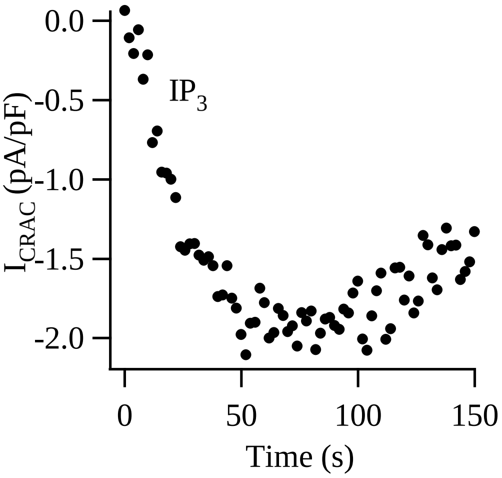

Figure 12 represents the time-course of the developing CRAC channel current, I_{CRAC}, when ER Ca^{2+} stores are depleted in an RBL-1 (rat basophilic leukemia) cell, where IP_3 is in the patch pipette.

1.6.2 *CRAC channel pore size and single channel conductance*

The selectivity of CRAC channels has been investigated through experiments which substitute an alternative ion for external Ca^{2+}. Zweifach and Lewis 1993 revealed that I_{CRAC} is selective for divalent cations over monovalent cations and that it had a selectivity ratio for divalent cations of $Ca^{2+} > Ba^{2+} \approx Sr^{2+}$. (CRAC channels can permeate Ba^{2+} and Sr^{2+} but Ba^{2+} conductance is reduced by 54% and Sr^{2+} by 44% compared with

Ca^{2+}). Additionally I_{CRAC} is fully blocked by Ni^{2+}. Experiments in divalent-free solution and ion monovalent substitution have provided important information regarding the CRAC channel pore diameter. CRAC channels lose their selectivity in divalent-free external solution where they can carry Na^+, which increases I_{CRAC} transiently. This is because in divalent-free solution, Ca^{2+} normally bound to key residues on the outer pore of the CRAC channel where it acts to block permeation to other ions and confer high Ca^{2+} selectivity of the channel, is absent. This relieves the block to other ions, allowing ions like Na^+ to pass through the channel pore (Prakriya et al 2006). More about the key residues involved in determining the high Ca^{2+} selectivity of CRAC channels shall be discussed later, in section 1.6.4. Cs^+ (0.32 nm) permeates CRAC channels weakly, trimethylamine (0.55 nm) does not. Hence the diameter of the CRAC channel pore must be between 0.32-0.55 nm. CRAC channels have a very low single channel conductance, estimated to be < 1 pS (Hoth and Penner 1993). A unitary chord conductance of about 9 fs in 2 mM external Ca^{2+} and 24 fs in 110 mM Ca^{2+} (Zweifach and Lewis 1993) is revealed in Jurkat T cells, by stationary noise analysis. This leads to the estimation that there are more than 10,000 functional CRAC channels per T lymphocyte or mast cell.

1.6.3 *Pharmacology of CRAC channels*

One major factor hindering research into the CRAC channel field is the absence of a selective CRAC channel blocker. A range of drugs is currently used such as econazole, SK&F-96365 (Franzius et al 1994), high levels of 2-aminoethoxydiphenylborane (20 µM 2-APB; Chang et al 2004), BTP2 (YM-58483) (Zitt et al 2004, Takezawa et al 2006, Quintana et al 2006), Synta (Di Sabatino et al 2009, Kar et al 2011, Ng et al 2008) and

Diethylstilbestrol (Ohana et al 2009). Although all block CRAC channels they also have secondary effects on other Ca^{2+} channels and protein targets. Therefore they are not entirely selective for CRAC channels. CRAC channels are also effectively blocked by low concentrations of trivalent cations, such as Gd^{3+} and La^{3+} (Hoth and Penner 1993, Trebak et al 2002, Ng et al 2008, Di Capite et al 2009a). However, other Ca^{2+} channels are also blocked in this way. Although these drugs are not specific to CRAC channels, experiments involving comparison of several different inhibitors is currently the best pharmacological approach. Now that the molecular identity of CRAC channels has been identified, knockdown of the pore forming subunit of the channel (Orai1) using RNA interference approaches is a specific and reliable way to impair the endogenous function of CRAC channels. However, full knockdown is rarely achieved by transfection with an RNAi construct. Establishing a selective CRAC channel blocker is therefore desperately needed.

1.6.4 *CRAC channel activation and the identification of the molecular determinants of the channel*

Several mechanisms have been proposed over the years to underlie the activation of CRAC channels. Such models include: 1) conveying of the activation signal by a diffusible messenger, 2) conformational coupling and 3) secretion like coupling, vesicular fusion and the removal of Ca^{2+} inhibition (Parekh and Putney 2005). However, landmark experiments using RNA interference based screening techniques in 2005 led to the identification of the genes that encode the CRAC channel. These experiments were carried out by Roos et al in Drosophilia S2 cells and Liou et al in HeLa cells. They revealed the required and conserved role of STIM1 (stromal interaction molecule 1) in Ca^{2+} influx through SOCCs. Confirmation of their discovery in Drosphilia S2 cells, Roos et al 2005 showed knockdown of STIM1 in Jurkat T cells or HEK cells, by transfecting cells with STIM1 RNAi, significantly impaired thapsigargin-induced Ca^{2+} influx and I_{CRAC}. STIM1 is composed of a single transmembrane domain and possesses an EF hand motif (Ca^{2+} binding domain) on the N terminus. Therefore it is a prime candidate for being the Ca^{2+} sensor involved in detecting ER Ca^{2+} store depletion. Following this, Liou et al 2005 showed that YFP (yellow fluorescent protein) tagged STIM1 colocalized with an ER marker (CFP-ER), where it had a relatively uniform distribution. Upon store depletion YFP-STIM1 redistributed into puncta (clusters), juxtaposed to the cell periphery, independently of external Ca^{2+}. Furthermore, introduction of a point mutation into the EF hand domain of STIM1 localised the mutant to puncta similar to endogenous STIM1 during store depletion. This suggests that upon store depletion, Ca^{2+} dissociates from the EF hand domain of STIM1, causing it to diffuse into puncta. Using total internal reflection fluorescence (TIRF) microscopy, redistributed STIM1 was found to maintain an ER residence but achieved a position within 100 nm of the plasma membrane. Therefore it localised close to (but not within) the plasma membrane. An investigation into the temporal profile of the process was carried out by Wu et al 2006. They monitored GFP-STIM1 movement using TIRF, whilst they simultaneously (using patch clamp experiments) measured I_{CRAC} in the same Jurkat T cell. STIM1 redistribution was found to precede CRAC channel activation, which revealed a causal relationship. They showed that STIM1 redistributed within the ER membrane into puncta close to (within 10-25 nm) but not inserted into the plasma membrane. This confirms work by Liou et al involving fluorescence quenching and electron microscopy. Furthermore, Wu et al 2006 failed to detect any corresponding bulk ER movement.

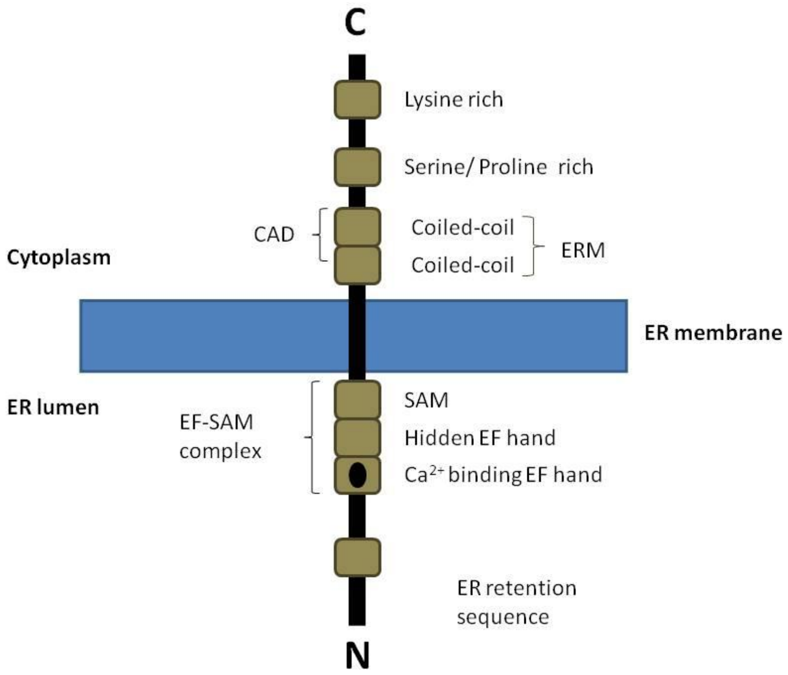
C
Lysine rich
Serine/ Proline rich
CAD
Cytoplasm
Coiled-coil
Coiled-coil
ERM
ER membrane
ER lumen
EF-SAM complex
SAM
Hidden EF hand
Ca2+ binding EF hand
ER retention sequence
N

Figure 13 (adapted from Parekh 2010) illustrates the structure of STIM1, representing the key functional domains.

STIM1 is a 77 kDa single transmembrane domain protein, which spans the ER membrane (shown in figure 13). The N terminus of STIM1 faces the ER lumen and contains: a signal peptide (an ER retention sequence), a Ca^{2+}-sensing EF hand domain, a hidden EF hand domain and a sterile α-motif domain (SAM), which interact together to form the EF-SAM domain that is important for STIM1 oligomerization (Stathopulos et al 2008). The C terminus which faces the cytosol contains two coiled-coil domains making up the ezrin-radixin-moesin (ERM) domain and serine/proline rich and lysine rich regions (Parekh 2010, Cahalan 2009). Furthermore, a CRAC activation domain, CAD, is essential for gating the CRAC channel (Park et al 2009, Parekh 2010) and is thought to be composed of the coiled-coil and part of the ERM domain of the C terminus.

In resting cells, STIM1 pairs as a dimer via connections between the C termini coiled-coil domains (Cahalan 2009). Upon store depletion dimers of STIM1 join together (oligomerize), mediated via their SAM domains (Cahalan 2009, Stathopulos et al 2008). This step precedes formation of puncta at sites juxtaposed to the plasma membrane and CRAC channel opening. Liou et al 2007 demonstrated such a finding by live FRET (Fluorescence resonance energy transfer) imagery in RBL cells following application of a physiological agonist. Furthermore, in the presence of a STIM1 mutant (with alterations to the C terminal polybasic coiled-coil domain), STIM1 oligomerized normally, yet failed to form puncta at sites close to the PM (ER-PM, endoplasmic reticulum-plasma membrane junctions). This indicates that the C terminal polybasic coiled-coil domain is essential for targeting STIM1 to the plasma membrane (to ER-PM junctions), and for CRAC channel activation (Liou et al 2007). The domain has now been assigned to be a part of CAD, the CRAC channel activation domain (Park et al 2009).

Although STIM1 is important for CRAC channel activation, it is not sufficient. Patients with inherited SCID (severe combined immunodeficiency) have impaired CRAC channel activity, yet no defective STIM1 gene (Feske et al 2005). Feske et al used two independent genetic approaches to pinpoint the gene responsible for SCID. DNA from two SCID patients and their extended families were used for genome-wide SNP analysis, to screen for target genes, by testing CRAC channel activity. They localised the defect to 74 genes on chromosome 12 (Feske et al 2006). A genome-wide RNA interference screen in Drosophila for NFAT regulators was carried out and identified the CRAC channel gene as Orai1. Knockdown of Orai1 abolished thapsigargin-induced Ca^{2+} influx in Drosophilia cells. Orai1 was mapped to the defect in chromosome 12 of the SCID patients. The defect was found to be a missense mutation (R91W) in the Orai1 gene, by sequencing genomic DNA from 23 patients. Expression of normal Orai1 (but not mutant Orai1, R91W) into SCID T cells restored CRAC channel dependent Ca^{2+}influx and I_{CRAC}. Complementary experiments by Vig et al 2006b identified the same gene. Furthermore, they localised Orai1 to the plasma membrane and the hydropathy profile predicted four transmembrane domains where the N and C termini faced the cytosol. Together, the two studies identify the importance of Orai1 for controlling CRAC channel activity. Evidence that confirmed Orai1 as the CRAC channel soon emerged. Peinelt et al 2006 showed that although overexpression of Orai1 or STIM1 individually, failed to significantly alter I_{CRAC}, overexpression of both proteins significantly amplified native I_{CRAC} (which still retained the same key features), in HEK and T cells in response to IP_3. Such enhancement suggests that STIM1 and Orai1 are necessary and sufficient to constitute the CRAC channel. If another component was to be involved, it would have to be expressed endogenously at very high amounts, which is unlikely (Parekh 2006). Mutagenesis analysis into the ion selectivity of Orai1 confirmed it was the pore of the CRAC channel, (the structure of Orai1 can be seen in figure 14). Through coimmunoprecipitation experiments, Vig et al 2006a revealed that tagged Orai1 formed multimers with itself, a key characteristic of ion channel proteins. Simultaneous tagging of Orai1 and STIM1 revealed an interaction between the ER and plasma membrane proteins. Furthermore, although expression of an Orai1 mutant (where glutamate residue E106 in transmembrane spanning region 1 had been replaced for glutamine) into HEK cells showed normal localisation to the plasma membrane and multimerization, the same mutant impaired the size of I_{CRAC} and removed its ability to permeate Na^+ in divalent-free solution (following thapsigargin stimulation). Replacement of glutamate for aspartate (at E106), another negatively charged residue, did not alter the size or time-course of I_{CRAC} but it removed its high Ca^{2+} selectivity. The usual inward rectification became outward rectification and a negative shift in the positive reversal potential was observed. Identification of human E106 as a crucial residue to confer high Ca^{2+} selectivity of CRAC channels confirms that Orai1 must be the pore subunit. Another glutamate residue in TM3 (transmembrane spanning region 3), E109 and aspartate residues (D110/112A) in TM1 and 2, were also identified as important for CRAC channel selectivity. This result was confirmed by Yeromin et al 2006 in Drosphilia and Prakriya et al 2006 in T cells and fibroblasts from SCID patients. They introduced point mutations into Orai1 and carried out ion substitution experiments to provide such evidence. Consistent with the above experiments which identify critical glutamate residues involved in establishing the high Ca^{2+} selectivity of Orai1, glutamate residues in the VOCC S5-S6 linker have been found to confer the ion selectivity of VOCC (Yang et al 1993). Therefore a similar mechanism might underlie the high Ca^{2+} selectivity of both channels, where Ca^{2+} binds to these acidic, negatively charged residues on the outer pore, blocking the permeation to other ions (Prakriya et al 2006). Although these studies identify key residues for Ca^{2+} selectivity of CRAC channels, they do not reveal whether they directly line the pore (Parekh 2010). A more powerful approach is cysteine substitution and application of thiol reagents differing in size and charge. If a residue lines the pore, the cysteine interacts with the thiol reagent which blocks the pore. Such a technique was used by McNally et al 2009, to investigate the proposed pore-lining amino acids. They found that the CRAC channel formed an outer vestibule from TM1 and TM2 that converged to form a narrow pore, which was lined by TM1 residues, starting at E106, the main Ca^{2+} binding site to confer Ca^{2+} selectivity.

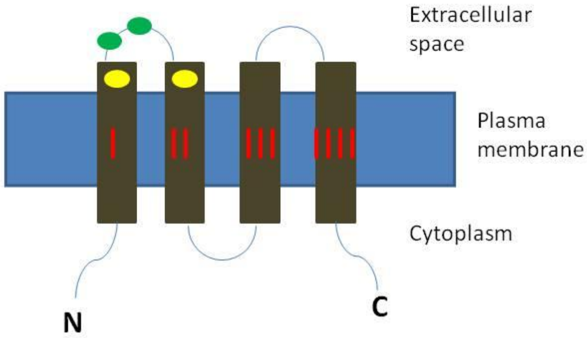

Figure 14 (adapted from Muik et al 2012) presents the predicted transmembrane structure of Orai1. It is composed of four transmembrane domains where the N and C termini reside in the cytoplasm. The yellow dots represent the glutamate residues and green dots represent the aspartate resides that are crucial for Orai1 function and are critically involved in channel selectivity.

Although I focus on Orai1 in this thesis, two additional human homologues exist, Orai2 and Orai3, which can form functional SOCCs with STIM1 (Gwack et al 2007, Lis et al 2007, DeHaven et al 2007). Orai2 is predominantly found in the kidney, lung and spleen (and brain in mouse) whilst Orai1 and Orai3 are widely distributed yet vary in levels expressed (Gwack et al 2007). Orai1 is associated with immunodeficiency disorders and overexpression of Orai2/3 fail to compensate for mutant Orai1 (Gwack et al 2007, Feske et al 2006). In mice, mast cell function was defective (notably defective degranulation and cytokine secretion) following knockdown of Orai1 and this was not compensated for by Orai2/3 (Vig et al 2008).

1.6.5 *Model of CRAC channel activation*

In resting cells, STIM1 form dimers which uniformly distribute throughout the ER membrane (Cahalan 2009). STIM1 dimers are formed via the C terminal coiled-coil domain facing the cytoplasm. The full ER Ca^{2+} store at rest maintains CRAC channels in their closed state. The CRAC channel is a multimer of four Orai1 proteins (each of which has four TM spanning domains), surrounding a central pore. Such a tetrameric structure is illustrated in figure 15.

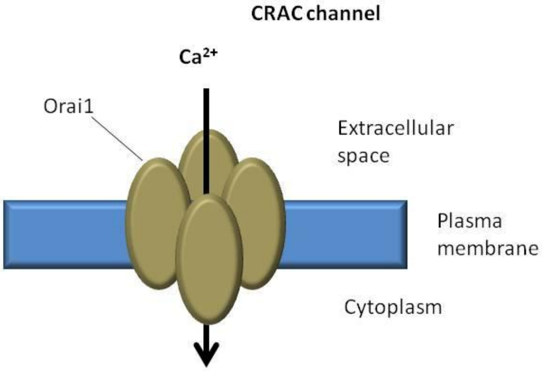

Figure 15 illustrates the predicted structure of the CRAC channel composed of four Orai1 subunits, surrounding a central pore, which is highly selective for Ca^{2+}. CRAC channels are therefore tetramers of the Orai1 protein subunit.

Upon stimulation with an IP_3-releasing agonist such as histamine or leukotriene C_4, PLC cleaves PIP_2 to generate IP_3, which subsequently binds and activates the IP_3R on the ER membrane to open and release Ca^{2+} from the ER into the cytoplasm. Ca^{2+} release causes the depletion of store Ca^{2+} and this loss is detected by dimers of STIM1 following the dissociation of Ca^{2+} from their luminal canonical Ca^{2+} binding EF hand domain, situated on the N terminus of each STIM1 (Liou et al 2005) (see figure 16). Such an action leads to 1) the destabilization of the EF-SAM complex (the interaction between the EF hand, hidden EF hand (which does not bind Ca^{2+}) and the

SAM domain, established using NMR) and 2) the partial unfolding of STIM1 which exposes the hydrophobic N terminal SAM domain (Stathopulos et al 2008). Ca^{2+}-free STIM1 dimers then join together to form larger oligomers via interactions between their SAM domains, which are now exposed. These resulting oligomers subsequently redistribute (Liou et al 2007) from their uniform positions to puncta at sites that are juxtaposed to the plasma membrane (within 10-25 nm, Wu et al 2006). What exactly targets STIM1 localisation to the plasma membrane is unclear at present, although Orai1 is not believed to be involved in this step (Parekh 2010, Xu et al 2006). Here clusters of Orai1 multimers subsequently form, following STIM1 oligomerization and migration to puncta (Luik et al 2008). The interaction between STIM1 and Orai1 stabilizes STIM1 at the plasma membrane and opens the CRAC channel.

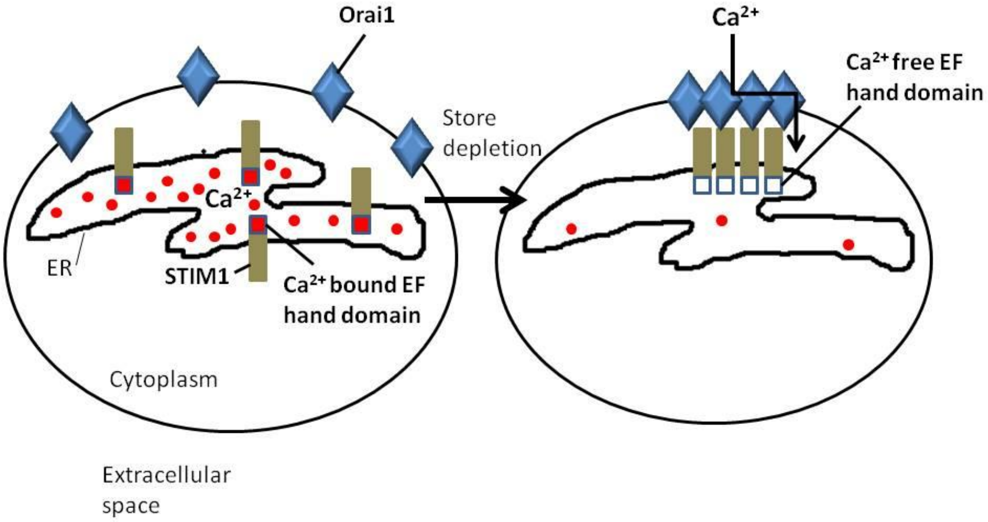

Figure 16 (adapted from Parekh 2010) illustrates the formation of ER-PM (endoplasmic reticulum-plasma membrane) junctions upon ER store depletion. In resting cells (left hand cell) STIM1 are uniformly distributed in the ER membrane bound with Ca^{2+}. Upon stimulation and ER store depletion, Ca^{2+} dissociates from the Ca^{2+} binding domain (EF hand domain) of STIM1 and STIM1 subsequently redistributes to form puncta juxtaposed to the cell periphery. Here it physically interacts with clusters of Orai1. Physical interaction between the two activates and opens the CRAC channel to allow Ca^{2+} influx.

This activation involves the CRAC channel activation domain, CAD. CAD is a highly conserved sequence of 107 amino acids. It is composed of the coiled-coil and part of the ERM domain in the C terminus of STIM1 and likely binds to the cytoplasmic facing N and C termini of Orai1 to open the channel (Park et al 2009). Park et al expressed a series of STIM1 fragments in HEK cells and monitored NFAT-dependent gene transcription (using an NFAT reporter gene) as a measure of CRAC channel activity. They showed that the fragment STIM1 342-448 was the smallest residue sufficient to cause NFAT transcription. Expression of this domain, which they called CAD in HEK cells with Orai1 caused a sustained cytosolic Ca^{2+} rise that was inhibited by 2-APB and 10 µM La^{3+} and activated I_{CRAC} immediately upon break-in. Park et al 2009 reported that CAD binds to the N and C termini of Orai1 and this is required for the recruitment of Orai1 multimers into clusters and CRAC channel activation, probably through inducing a conformational change in Orai1. It is thought that oligomerization of STIM1 exposes the CAD domain. This targets STIM1 to the ER-PM junctions, promoting the recruitment of STIM1 and Orai1 into clusters. The binding of Orai1 to the CAD of STIM1 causes the conformational alteration of Orai1 that opens the CRAC channel.

1.6.6 *Regulation of CRAC channel activity*

The activity of CRAC channels are regulated by various factors, including cytoplasmic Ca^{2+} (Zweifach and Lewis 1995a, b, Hoth and Penner 1993, Bakowski et al 2001, Parekh 1998, Fierro and Parekh 1999), cGMP and protein kinase G (PKG) (Moneer et al 2003), protein kinase C (PKC) (Parekh and Penner 1995), sphingosine (Mathes et al 1998, Lepples-Wienhues et al 1999), arachidonic acid (aa) (Luo et al 2001), calmodulin (Moreau et al 2005) and mitochondria (Gilabert and Parekh 2000, Gilabert et al 2001, Glitsch et al 2002, Quintana et al 2006). Parekh 2003b concluded that CRAC channel dependent Ca^{2+} entry indeed reflected the dynamic relationship between the ER, plasma membrane and mitochondria. Here I concentrate on the control of CRAC channels by calmodulin and mitochondria, both of which greatly influence the spatial and temporal profile of Ca^{2+} signals. In each case I will first of all discuss their structure and function and then consider their impact on CRAC channel activity.

1.7 Calmodulin

1.7.1 *Structure and targets of calmodulin*

Calmodulin (shown in figure 17), is one of the most abundant and ubiquitous Ca^{2+} binding proteins that is found in eukaryotic cells (Hoeflich et al 2002, Clapham 2007). Despite its small size, it binds to an extensive list of protein targets including calcineurin, NO synthase, IP_3R and the plasma membrane Ca^{2+} ATPase pump. This is often via the common calmodulin binding motif called the IQ domain, which has a consensus sequence of IQXXXRGXXX, although not all proteins that bind calmodulin have this motif.

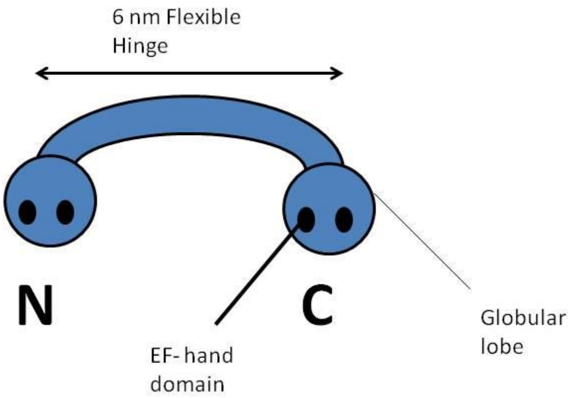

Figure 17. The cartoon illustrates the dumbbell structure of calmodulin.

Calmodulin is composed of two globular lobes called the amino (N) and carboxy (C) terminal lobes, each of which bind two Ca^{2+} ions via highly conserved EF hand domains (Hoeflich et al 2002, Johnson et al 1996, Clapham 2007) (figure 17). Calmodulin is known to activate a range of targets via several different mechanisms. Ca^{2+}-dependent enzymes such as CAM kinase I/II/IV and the phosphatase calcineurin are activated by calmodulin via displacement of an autoinhibitory domain (Clapham 2007), whilst bacterial enzyme anthrax adenylyl cyclase is activated via active site remodelling (Hoeflich et al 2002). In addition to these targets, calmodulin is known to activate the small conductance, Ca^{2+} activated potassium channel that is involved in neuronal excitability, by inducing dimerization of the membrane proteins (Hoeflich et al 2002). Furthermore, calmodulin is known to regulate a plethora of Ca^{2+} channels, where it is positioned close to or often associated with the channel itself (tethered to the channel). It is therefore likely to impact upon responses downstream of these channels.

1.7.2 *Regulation of ion channels by calmodulin*

Calmodulin has been found to bind and regulate both intracellular and plasma membrane Ca^{2+} channels. Using a range of calmodulin antagonists (W-7, W-13, CGS 9343B) and Fura 2-AM to measure cytosolic Ca^{2+}, Hill et al 1988 showed that blockade of calmodulin eliminates both thrombin-induced Ca^{2+} release in intact rat liver epithelial cells and IP_3-induced Ca^{2+} release in permeabilized cells. Consistent with this, Somogyi and Stucki 1991 found that calmodulin antagonist calmidazolium significantly suppressed phenylephrine-induced Ca^{2+} oscillations in intact hepatocytes. Therefore calmodulin appears to regulate IP_3Rs.

Unlike the majority of cases where calmodulin regulates ion channels in a Ca^{2+}-calmodulin dependent manner, calmodulin has been found to bind to the IP_3R in both a Ca^{2+}-dependent and Ca^{2+}-independent manner. Yamada et al 1995 identified the direct binding of calmodulin to IP_3R type 1 in a Ca^{2+}-dependent manner. They produced a variety of deletion mutants of IP_3R type 1 (IP_3R1) and analysed their ability to bind calmodulin-sepharose. This allowed them to reveal that amino acid sequence 1564-1585, found in the central region of the IP_3R was required for calmodulin binding. Furthermore, an antibody against peptide 1564-1585 inhibited cerebellar IP_3R1 from binding calmodulin. Finally, they measured the fluorescence of the fluorophore residue TRP which was present in the synthesised peptide 1564-1585 to investigate the direct interaction between calmodulin and this site. Fluorescence intensity of TRP increased with increased [calmodulin] proving that calmodulin directly bound to the area, an effect that was eliminated in the absence of Ca^{2+}. Similar results were revealed with IP_3R type 2 but not type 3.

Calmodulin can also bind to the IP_3R via a mechanism independent of Ca^{2+} (Patel et al 1997). Patel et al found that calmodulin could bind directly to type 1 IP_3R from rat cerebellar independently of binding Ca^{2+}. Sipma et al 1999 localised the Ca^{2+}-independent calmodulin binding site to the N terminus of the IP_3R. Binding of calmodulin to both Ca^{2+} -dependent and -independent calmodulin binding sites has been shown to inhibit IP_3R-driven Ca^{2+} release. Hirota et al 1999 investigated the regulation of IP_3R by calmodulin and provided evidence that calmodulin directly acted to suppress IP_3R type 1-driven Ca^{2+} release. They measured the flux of Ca^{2+} through a purified and reconstituted IP_3R1 in response to IP_3 whilst they varied calmodulin concentrations. The IP_3-induced Ca^{2+} flux was reduced by Ca^{2+}-calmodulin in a dose-dependent manner. Consistent with this, Michikawa et al 1999, found that even very high $[Ca^{2+}]$ could not inhibit purified, reconstituted IP_3R in the absence of calmodulin. Ca^{2+} inhibition of the IP_3R only occurred after the addition of calmodulin, so calmodulin does seem crucial for the inhibition of the IP_3R. It has been proposed that the IP_3R has multiple calmodulin binding sites. In 2000 Adkins et al proposed that calmodulin can affect the activity of the IP_3R by binding to a site within the first 159 amino acids of the N terminus, independently of Ca^{2+} binding to calmodulin, whereas Ca^{2+}-calmodulin dependent binding and subsequent inhibition of the IP_3R occurs at a central site in IP_3R1 and 2 (Sun and Taylor 2008, Yamada et al 1995). The regulation of the IP_3R by calmodulin is therefore very complex. No matter where calmodulin binds to on the IP_3R, it appears that it always acts to inhibit channel activity, but the exact mechanism involved and the importance of the different sites for binding calmodulin is unclear as yet. Difficulties with answering these questions arise from the failure of successful coimmunoprecipitation of calmodulin and the IP_3R and the indirect and unphysiological nature of experiments used to investigate IP_3R activity since it is an intracellular channel that is hard to access (much harder than plasma membrane situated channels). Different IP_3R subtypes and their relative distributions also exist, which complicates this field even further. Therapeutic importance of the regulation of the IP_3R by calmodulin was demonstrated by Gerasimenko et al 2011. They revealed that addition of calmodulin to permeabilized acinar cells or application of CALP-3 (a calmodulin activator) to intact pancreatic acinar cells impaired alcohol-induced, IP_3R-dependent Ca^{2+} release and trypsin activity. The protection of alcohol-induced pancreatitis by calmodulin could therefore help towards treating the effects of alcohol poisoning. Although Ca^{2+} is not always required to bind to calmodulin (Nadif Kasri et al 2004), Ca^{2+} is still believed to be needed for the regulation of IP_3R by calmodulin (Adkins et al 2000, Missiaen et al 1999). Missiaen et al 1999 revealed that 10 µM calmodulin inhibited IP_3-induced Ca^{2+} release only when cytosolic Ca^{2+} was 0.3 µM or higher in permeabilized A7r5 cells. Therefore Ca^{2+} does seem to be always important for calmodulin to inhibit IP_3R-driven Ca^{2+} release, even if calmodulin binds to the IP_3R independently of Ca^{2+} binding to it. The Ca^{2+} may induce changes in the conformation of the IP_3R, favouring a mode which facilitates calmodulin binding to the channel, which subsequently acts to inhibit the IP_3R (Sun and Taylor 2008).

Plasma membrane Ca^{2+} permeable ion channels have been shown to bind and be regulated by calmodulin. Several of the TRP channels (transient receptor potential channels) bind calmodulin via their C-terminus. Examples are TRPV6, where Ca^{2+}-calmodulin mediates slow Ca^{2+}-dependent channel inactivation (Niemeyer et al 2001), and TRPV5 (Strotmann et al 2003). Strotmann et al showed that calmodulin had an opposite effect on TRPV5 channel activity compared to TRPV6. Ca^{2+}-dependent potentiation of TRPV5 in response to 4α-PMA was abolished in a mutant TRPV5 which could not bind calmodulin, whereas Ca^{2+}-dependent inactivation of the channel was unaffected.

Calmodulin is also able to bind and regulate the activity of VOCC channels in excitable cells. Peterson et al 1999 showed that inactivation of L-type Ca^{2+} channels following a depolarizing pulse was eliminated by expression of a calmodulin mutant that could not bind Ca^{2+} in either the N- or C-lobes. Since the double negative calmodulin mutant completely abolished Ca^{2+}-dependent inactivation of L-type Ca^{2+} channels in the presence of endogenous calmodulin, Peterson et al concluded that calmodulin tethered to the channel must be involved. Zühlke et al 1998, 1999 revealed that a point mutation to the IQ motif in the C terminal tail of the L-type channel subunit α_{1C} eliminated Ca^{2+}-dependent inactivation (CDI, the negative feedback mechanism to prevent excessive increases in intracellular Ca^{2+}), yet potentiated Ca^{2+}-dependent facilitation (CDF, the positive feedback mechanism to enhance channel activity). Furthermore, they found that whilst calmodulin interacted with the IQ domain of the WT L-type channel in the presence of Ca^{2+}, this interaction was significantly impaired in the presence of a point mutation in the IQ motif, which had removed Ca^{2+}-dependent regulation. This demonstrated that Ca^{2+}-dependent inactivation and facilitation of L-type channels involved calmodulin binding to the IQ motif. Calmodulin has also been shown to regulate the activity of P/Q-type VOCCs, through an interaction with the IQ domain (DeMaria et al 2001). DeMaria et al showed that coexpression of P/Q-type channels and a calmodulin mutant insensitive to Ca^{2+} eliminated both CDI and CDF of these channels. The findings are consistent with those found with L-type channels and therefore suggest calmodulin is pre-bound to the channel. The pre-association of calmodulin with VOCCs was confirmed in living cells by Erickson et al 2001, using a fluorescence resonance energy transfer technique, (FRET). This involved coexpressing YFP (yellow fluorescent protein) fused to α_{1C} of the L-type channel with either camodulin fused to CFP (cyan fluorescent protein), or a calmodulin mutant unable to bind Ca^{2+} fused to CFP. Both conditions caused YFP emission to increase due to FRET, indicating the channel and calmodulin were <100Å apart in resting cells. Since a similar result was found with wild type calmodulin and a calmodulin mutant insensitive to Ca^{2+}, it confirmed that the interaction between the channel and calmodulin was Ca^{2+}-independent. DeMaria et al 2001 explain the ability for calmodulin pre-associated to the IQ domain to mediate both facilitation and inactivation of VOCC channels by assigning separate roles to the N- and C-lobes of calmodulin. They used two additional calmodulin mutant constructs, one where the N-lobe was insensitive to Ca^{2+} and another where the C-lobe was insensitive to Ca^{2+} and expressed them in HEK cells. In the presence of the N-lobe mutant, CDI was impaired yet CDF was left intact. By contrast, expression of the C-lobe mutant impaired CDF and left CDI intact. This therefore poses the question of how such lobe-specific regulation of Ca^{2+} channels can be carried out by calmodulin.

Since the two lobes of calmodulin are joined by a 6 nm flexible linker, both lobes are exposed to the same level of Ca^{2+} (Tadross et al 2008). Therefore differences in the $[Ca^{2+}]$ to which each of the lobes is exposed cannot explain the lobe-specific regulation. In order to understand the mechanism involved, one must consider the Ca^{2+} binding and unbinding kinetics of each lobe separately. Calcium binds 70 times faster to the N-lobe (1.6×10^{8} $M^{-1}s^{-1}$) than the C-lobe (2.3×10^{6} $M^{-1}s^{-1}$) and dissociates 170 times faster from the N-lobe (405± 75/s at 10°C) compared to the C-lobe (2.4± 0.2/s at 10°C) (Johnson et al 1996). This suggests that each lobe of calmodulin is sensitive to different temporal Ca^{2+} signals (Parekh 2011). In 2008 Tadross et al showed that whilst the C-lobe of calmodulin was sensitive to transient Ca^{2+} signals, the N-lobe was unable to sense such signals. Ca^{2+}-dependent facilitation is controlled by local, transient Ca^{2+} signals whilst CDI is dependent on slowly developing global

Ca^{2+} signals (Tadross et al 2008). Since Ca^{2+} dissociates rapidly from the N-lobe, it would require a maintained elevation in Ca^{2+} to have time to sense and transduce the signal. Channel microdomains responsible for CDF rapidly (over microseconds) build up and collapse. Therefore the rise in Ca^{2+} quickly returns to pre-stimulation levels upon channel closure. The N-lobe quickly unbinds Ca^{2+} upon collapse of the Ca^{2+} microdomain; this short period of elevated Ca^{2+} does not provide sufficient time for the lobe to induce CDF. However the C-lobe holds on to Ca^{2+} for much longer, maintaining its Ca^{2+}-bound state even when the channel microdomain collapses and the Ca^{2+} signal returns to pre-stimulate levels, therefore it can induce CDF (Tadross et al 2008). CDI on the other hand develops over hundreds of milliseconds. The slowly developing sustained global rise in Ca^{2+} (arising from distant sources) provides continuous exposure of high levels of Ca^{2+} to the N-lobe, allowing time for the lobe to transduce the calcium signal and induce CDI.

However, the N-lobe of calmodulin senses local Ca^{2+} signals resulting from certain open Ca^{2+} channels (Dick et al 2008). Dick et al showed that in contrast to the regulation of P/Q-type channels by calmodulin, the N-lobe of calmodulin bound to L-type channels had local Ca^{2+} sensitivity. A novel Ca^{2+}- calmodulin binding domain was identified in the N terminus of the L-type Ca^{2+} channel called NSCATE, which was not present in P/Q-type channels. Introduction of NSCATE into P/Q-type channels caused the Ca^{2+} sensitivity of the N-lobe to change from global to local. Likewise, disturbance of the NSCATE in the L-type channel caused the Ca^{2+} sensitivity of the N-lobe to shift to global (Dick et al 2008). The binding of calmodulin to the NSCATE domain must somehow change the Ca^{2+} unbinding kinetics of the N-lobe in favour of the Ca^{2+}-calmodulin bound state (Parekh 2011).

1.7.3 *Regulation of CRAC channels by calmodulin*

In non-excitable cells, evidence supports the view that calmodulin regulates CRAC channel activity too. Moreau et al 2005 measured I_{CRAC} directly using whole-cell patch clamp recordings in RBL-1 cells. I_{CRAC} was significantly impaired in the presence of a calmodulin mutant insensitive to Ca^{2+} or after expression of a calmodulin inhibitory peptide, under conditions of weak physiological buffer (where cytoplasmic Ca^{2+} could rise). More recently a calmodulin binding site (24 amino acids long) in the N terminus of Orai1 at amino acids 68-91 has been identified (Mullins et al 2009). Mullins et al coexpressed a YFP tagged Orai1 N terminus fragment with flag-calmodulin into HEK cells and using anti-flag antibodies showed that calmodulin coimmunoprecipitated with the N terminus of Orai1 in a Ca^{2+}-dependent manner. Furthermore, horseradish peroxidise-coupled calmodulin binding to an Orai1 N terminal fragment peptide and calmodulin-sepharose pull down assays using Orai1 N terminal fragments narrowed the amino acid binding site to position 68-91. Following this, mutant Orai1 constructs which could not bind calmodulin (for example A73E) caused loss of CDI of the channel. This suggested that calmodulin binding to the N terminus of Orai1 was important in CDI of the CRAC channel. Since calmodulin is found to be pre-associated with VOCCs where it regulates their activity, it is plausible that calmodulin may also be continuously tethered to Orai1 as well. Consistent with this view, whilst calmodulin inhibitors failed to affect CDI of a SOCC current (similar to I_{CRAC}) in hepatocytes, expression of a Ca^{2+}-insensitive mutant of calmodulin reduced CDI of I_{SOCC} (Litjens et al 2004). The ability of the calmodulin mutant to alter CDI despite the lack of effect with chemical inhibitors is similar to the results seen with VOCC channels, where calmodulin is found to be pre-bound. The idea is that calmodulin pre-bound to a channel is protected from chemical inhibitors, whereas free calmodulin is rapidly antagonized.

1.7.4 *Calmodulin as a local Ca^{2+} sensor*

In addition to the regulation of Ca^{2+} permeable ion channels, calmodulin has an important signalling role. Calmodulin has been shown to couple local Ca^{2+} entry through L-type Ca^{2+} channels to downstream nuclear gene expression, which has assigned a role for calmodulin in long-range signalling. Since calmodulin binds to a variety of Ca^{2+} permeable channels, including the CRAC channel, it gives rise to the idea that calmodulin is involved in sensing the local Ca^{2+} entry through these channels and relaying it to drive specific cellular responses some distance away from the membrane. Calmodulin may therefore have a dual role on CRAC channels, providing 1) a mechanism for Ca^{2+} regulation of CRAC channels whilst 2) transducing the local Ca^{2+} entry through CRAC channels to downstream effectors. The sensing of local CRAC channel dependent Ca^{2+} entry by calmodulin is postulated to underlie CRAC channel driven activation of transcription factor NFAT-1 in mast cells, Kar et al 2011. Activation of NFAT-1 involves the Ca^{2+}-calmodulin dependent protein phosphatase calcineurin.

1.8 Mitochondria

Mitochondria have long been known to be the major site for ATP synthesis inside cells, (central to cell metabolism). This occurs via the Kreb cycle, where Ca^{2+} activates three rate limiting enzymes: pyruvate dehydrogenase, NAD^{+}- isocitrate dehydrogenase and 2-oxoglutarate dehydrogenase (McCormack et al 1990). These enzymes oxidise glucose to generate ATP and energy rich reducing cofactors, NADPH and $FADH_2$. Such cofactors subsequently generate ATP by supplying electrons to fuel ATP synthesis via the ATP synthase, which is situated in the inner mitochondrial membrane (IMM). This cycle of events ensures that enough ATP is produced for energy-dependent cellular processes. Hajnóczky et al 1995 demonstrated the close coupling between mitochondrial Ca^{2+} uptake and metabolism, by monitoring the activity of the Ca^{2+}-dependent rate limiting enzymes critical for ATP synthesis. To do this they simultaneously measured free [Ca^{2+}] within mitochondria whilst monitoring the redox state of a mitochondrial pyridine nucleotide cofactor in individual hepatocyte cells. Reduction of NADP to NADPH is associated with an increase in fluorescence signal, which can be monitored to track mitochondrial metabolism. Hajnóczky et al 1995 found that the NADPH rise in fluorescence, closely matched a mitochondrial matrix Ca^{2+} rise, (the uptake of Ca^{2+} by mitochondria).

1.8.1 *Mitochondria are not simply sinks for Ca^{2+}*

For a long time mitochondria were simply considered as Ca^{2+} sinks to supply Ca^{2+} for ATP synthesis. A major role for mitochondria in shaping intracellular Ca^{2+} signals and regulating downstream Ca^{2+}-dependent cellular responses was initially discounted. This was due to findings that 1) mitochondria only release small amounts of Ca^{2+}

(mainly via the slow acting $3Na^+/Ca^{2+}$ exchanger; Sedova et al 2000, Palty et al 2010, 2012, molecularly identified by Palty et al as NCLX) compared to robust Ca^{2+} release from the ER via the fast acting IP_3R. In addition 2) the uptake of Ca^{2+} by mitochondria involves a low affinity Ca^{2+} transporter, with a Km of approximately 10-20 µM, (McCormack et al 1990, Rizzuto et al 1993, 2000, Moreau et al 2006, Parekh 2003a, Nicholls 2005, Carafoli 2003). Mitochondria were therefore thought unlikely to respond to physiological rises in bulk cytosolic $[Ca^{2+}]$ upon stimulation, which occur within the micromolar range (1-2 µM). However, Ca^{2+}-sensitive fluorescent probes (such as aequorin, Rhod 2-AM and the more recently constructed pericam) targeted to the mitochondria, both to the matrix (Moreau et al 2006, Csordás and Hajnóczky 2003) and the intermembrane space (the space between the inner and outer mitochondrial membranes) (Rizzuto et al 1998) have enabled mitochondrial matrix Ca^{2+} and Ca^{2+} at the surface of the mitochondria to be measured directly. Such probes have been used to show that mitochondria rapidly accumulate large quantities of Ca^{2+} robustly, despite their low affinity Ca^{2+} uptake transporter. This is due to exposure of the uptake transporter to high, local Ca^{2+} signals.

In 1992 Rizzuto et al introduced mitochondrial targeted apo-aequorin (formed by the fusion of cDNA for aequorin and that of a mitochondrial presequence for organelle targeting), into endothelial cells. Aequorin is a Ca^{2+}-sensitive photoprotein, which emits light when Ca^{2+} binds to it. In addition, the calcium fluorescent dye Rhod 2 has been compartmentalised within mitochondria to provide another way to measure free Ca^{2+} within the matrix. Such an approach has been used by Babcock et al 1997 in chromaffin cells, to test the response to depolarization steps or muscarine/

bradykinin application and also by Moreau et al 2006 in digitonin permeabilized RBL cells, to test the response to cytosolic Ca^{2+} loads. Simultaneous measurement of cytosolic and mitochondrial Ca^{2+} concentrations revealed that even modest cytosolic elevations in Ca^{2+} in response to IP_3 agonists, produced rapid Ca^{2+} transients in mitochondria. Rizzuto et al 1993, transfected intact HeLa cells with a mitochondrial targeted aequorin, whilst loading cells with the cytosolic Ca^{2+}-sensitive dye Fura 2. Application of histamine caused a large rise in cytosolic Ca^{2+} and at the same time caused a large, rapid increase in mitochondrial Ca^{2+} concentration. In RBL cells, Moreau et al 2006 compartmentalised Rhod 2 into the mitochondrial matrix following permeabilization of the cells with digitonin and showed that Rhod 2 fluorescence rapidly increased in response to a cytosolic Ca^{2+} load (10 µM). At rest, mitochondrial Ca^{2+} concentration is around 80-200 nM. Upon IP_3-driven stimulation, a bulk cytoplasmic Ca^{2+} rise to 1-2 µM results in increases in averaged mitochondrial Ca^{2+} concentration (from all mitochondria) to 250-1000 nM and in mitochondria close to Ca^{2+} release sites rises of tens of µM can occur. Such an effect is supported by studies into the localisation and interaction between mitochondria and the ER (Rizzuto et al 1999, Moreau et al 2006) and mitochondria and the plasma membrane (important in T cells, Quintana et al 2006).

Mitochondria are now regarded as being important in the regulation of the spatial and temporal profile of Ca^{2+} signals, such as cytosolic Ca^{2+} oscillations. Jouaville et al 1995 showed that injecting Xenopus oocytes with respiratory substrates (pyruvate, malate or succinate) to energize mitochondria increased the speed and size of IP_3-induced cytosolic Ca^{2+} oscillations. Such an effect was impaired by inhibitors of mitochondrial Ca^{2+} uptake. This highly dynamic organelle is therefore of great importance when considering intracellular Ca^{2+} signalling and the regulation of CRAC channels and CRAC channel driven downstream responses. Therefore this thesis investigates the involvement of mitochondrial Ca^{2+} buffering in such regulation.

1.8.2 *Structure and biophysical properties of mitochondria*

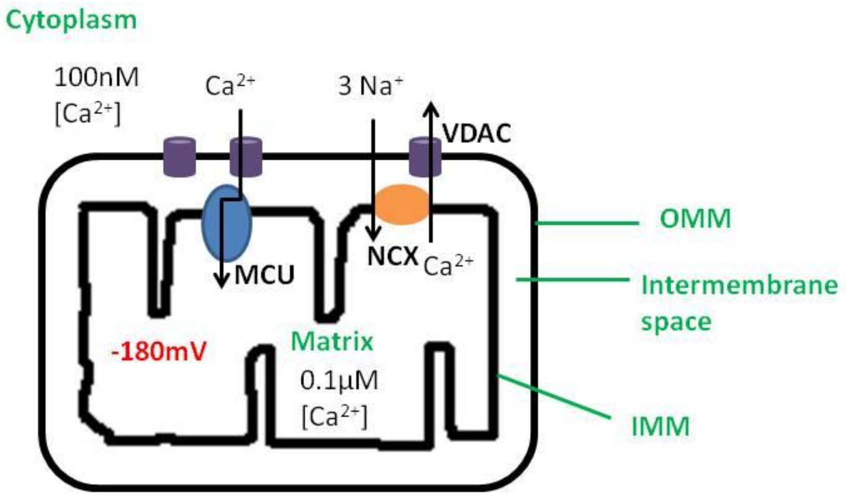

Figure 18 summarizes the structure and key Ca^{2+} transporters of a mitochondrion. Two membranes, the outer mitochondrial membrane (OMM) and the inner mitochondrial membrane (IMM) encapsulate the intermembrane space. Within the IMM is the mitochondrial Ca^{2+} uniporter (MCU). MCU takes up Ca^{2+} into the mitochondrial matrix and is juxtaposed to the voltage-dependent anion channel (VDAC), the main Ca^{2+} pathway in the OMM. Ca^{2+} is also slowly released from the mitochondrial matrix to the cytoplasm mainly via the 3Na^{+}/ Ca^{2+}exchanger, molecularly identified by Palty et al 2010, 2012 as NCLX. (Ca^{2+}/H^{+} exchangers also exist and extrude some matrix Ca^{2+}, Jiang et al 2009 identified one as Letm1, however its role in extrusion is less clear than the NCX exchanger). Across the inner mitochondrial membrane there is a large electrochemical gradient, composing of a highly hyperpolarized potential (around -180 mV) and a large Ca^{2+} gradient for driving Ca^{2+} into the matrix when cytosolic Ca^{2+} rises.

1.8.2.1 *Electrochemical gradient for driving mitochondrial Ca^{2+} uptake*

The uptake of Ca^{2+} by mitochondria is a passive process, due to the huge electrochemical gradient across the inner mitochondrial membrane. Mitochondria have two membranes. The outer mitochondrial membrane (OMM) is freely permeable to Ca^{2+} due to the presence of porins (channels freely permeable to small molecules and ions like Ca^{2+}), such as VDAC, which provides the major Ca^{2+} pathway within the OMM (Brdiczka et al 1991). The inner mitochondrial membrane does not contain porins. Ca^{2+} can cross this membrane however, via regulated Ca^{2+} channels, which before their molecular identity had already been termed the mitochondrial Ca^{2+} uniporter (MCU). Together, the two membranes enclose the intermembrane space. A huge electrochemical gradient for Ca^{2+} is maintained across the inner mitochondrial membrane. This is composed of two components, an electrical component arising from the maintenance of a highly hyperpolarized inner mitochondrial membrane potential (around -180 mV, Mitchell 1966) and a chemical component to provide a Ca^{2+} concentration gradient across the membrane to favour Ca^{2+} uptake when cytosolic Ca^{2+} is raised. The highly hyperpolarized inner mitochondrial membrane potential is achieved by the pumping of protons out of the mitochondrial matrix, across the inner mitochondrial membrane and into the intermembrane space (Mitchell 1966). This is in exchange for electrons transferred along the inner mitochondrial membrane electron transport chain. Such proton pumping creates a pH gradient between the intermembrane space and the matrix. The ability of mitochondria to keep free Ca^{2+} concentration within the matrix low, establishes the chemical component for driving Ca^{2+} uptake. The Ca^{2+} binding ratio within the matrix is estimated to be >2000 (Babcock et al 1997). This helps to maintain the matrix, low free Ca^{2+} concentration, together with the slow Ca^{2+} extrusion across the IMM mainly via the $3Na^{+}/Ca^{2+}$ exchanger (Arnaudeau et al 2001, Tang et al 1997, Parekh 2003a, Sedova et al 2000, Palty et al 2010, 2012).

The importance of a highly hyperpolarized IMM for driving mitochondrial Ca^{2+} uptake can be appreciated by measuring the effects of membrane depolarization on mitochondrial matrix Ca^{2+}. Moreau et al 2006 revealed that pre-incubation of RBL cells with the protonophore FCCP, prevented a detectable rise in mitochondrial Ca^{2+} concentration following even a very high cytosolic Ca^{2+} load of 100 µM. Similar findings were previously found by Babcock et al 1997, who revealed in chromaffin cells that mitochondrial Ca^{2+} uptake was impaired in the presence of CCCP, (another protonophore). A highly hyperpolarized inner mitochondrial membrane therefore enables the organelle to function as an efficient buffer of Ca^{2+}.

1.8.2.2 *Characteristics and molecular determination of the mitochondrial* Ca^{2+} *uniporter*

Without permeability to Ca^{2+}, a strong electrochemical gradient alone would not be sufficient to enable mitochondria to buffer Ca^{2+}. A mechanism is required to transport Ca^{2+} into the matrix. It has long been known that this involved a ruthenium red sensitive uniporter (Carafoli 1987), termed the mitochondrial Ca^{2+} uniporter (MCU, which is in fact an ion channel). Kirichok et al 2004 first recorded this highly Ca^{2+} selective, inwardly rectifying ion channel by patch clamping the inner mitochondrial membrane of single mitoplasts. MCU Ca^{2+} uptake was highly sensitive to IMM Vm (inner mitochondrial membrane potential). Single channel recordings demonstrated the dependence of the open probability of the channel on the membrane potential. Depolarization of the membrane reduced the channel open probability (Po) considerably (11% Po at -80 mV compared with 99% at -200 mV). Single channel conductance was found to be between 2.6 pS- 5.2 pS at -160 mV.

The molecular identify of MCU has recently been established. In 2010, Perocchi et al used a targeted RNA interference screen to identify genes required for mitochondrial Ca^{2+} uptake and they identified a 54 kDa subunit called MICU1 in HeLa cells. Knockdown of MICU1 abolished mitochondrial Ca^{2+} uptake following histamine stimulation or thapsigargin application. This was independent of any change to IMM Vm or respiration in intact and permeabilized HeLa cells. The response was rescued by overexpression of normal MICU1. Furthermore, a mutant MICU1 with defective EF hand domains (Ca^{2+} binding domains) failed to rescue the response seen with knockdown of MICU1, which identified a Ca^{2+}-sensing role for MICU1 in the control of mitochondrial Ca^{2+} uptake. A GFP tagged MICU1 and mitochondrial marker were shown to coimmunoprecipitate. This localised MICU1 to the mitochondria. MICU1 is unlikely to constitute the uniporter itself since it only has a single transmembrane (TM) domain. Furthermore, the requirement for functional EF hand domains in MICU1 indicates that it plays a Ca^{2+}-sensing role. Perocchi et al 2010 therefore proposed that MICU1 was a required Ca^{2+} sensor, which regulated the uniporter activity. In some ways, this is reminiscent of the regulation of Orai1 by STIM1, where STIM1 senses the fall in ER Ca^{2+} and responds by interacting with Orai1 to activate it. MICU1 might sense and respond to changes in Ca^{2+} to activate and determine the activity of MCU.

Two subsequent studies identified the uniporter, which was called the mitochondrial Ca^{2+} uniporter (MCU) (De Stefani et al and Baughman et al 2011). Similar to their work where they identified MICU1, De Stefani et al 2011 searched the MitoCarta database for proteins that demonstrated characteristics of the uniporter and narrowed their search down to a two transmembrane domain spanning, 40 kDa protein. In agreement with this work, Baughman et al pinpointed the same protein to encode MCU by ranking genes in the whole-genome, firstly for phylogenetic similarities to the required regulatory subunit MICU1, secondly for similarities in their expression (by genome-wide RNA coexpression analysis) and thirdly by scoring the similarity of protein expression between proteins functionally related to MICU1, and MICU1 itself. De Stefani et al 2011 showed that knockdown of this identified MCU protein impaired mitochondrial Ca^{2+} uptake in HeLa cells, whilst overexpression increased the IP_3-induced rise in matrix Ca^{2+}. They purified the protein and reconstituted it into planar lipid bilayers. Here it showed Ca^{2+} permeable channel activity with characteristics of the uniporter. In contrast, a MCU mutant (in which two negatively charged residues D260Q and E263Q were mutated into glutamines) failed to evoke Ca^{2+} permeable channel activity (De Stefani et al 2011). Furthermore, tagging MCU with GFP revealed that the protein localised to the IMM. Consistent with findings by De Stefani et al where MCU had been knockdown in cultured cells, Baughman et al 2011 showed that knockdown of MCU in HeLa cells abolished mitochondrial Ca^{2+} uptake independent of any effect on IMM Vm and respiration. In addition, they provided the first evidence of a role for MCU in mitochondrial Ca^{2+} uptake in mice liver mitochondria where MCU had been knocked down by an alternative approach, in vivo. This involved injecting a MCU RNAi construct into mice and later extracting the liver. Intact mitochondria from the liver of these mice showed an almost complete failure to take up Ca^{2+} compared to mice injected with a control construct which did not knockdown MCU. Furthermore, they showed that MCU could physically interact with MICU1 and oligomerized in the IMM to form large complexes. Collectively, the two studies confirmed that MCU was indeed the mitochondrial Ca^{2+} uniporter, (which is in fact a channel with unfortunate terminology).

1.8.2.3 *Mitochondria efficiently buffer Ca^{2+} when close to sources of high Ca^{2+}*

MCU has a low affinity for Ca^{2+} (Km 10-20 µM) (McCormack et al 1990, Rizzuto et al 1993, 2000, Moreau et al 2006, Parekh 2003a, Nicholls 2005, Carafoli 2003). This raises the question of how mitochondria can rapidly accumulate large quantities of cytosolic Ca^{2+}. The answer is believed to reside in the exposure of the low affinity transporter to high, local Ca^{2+} microdomains (>10 µM). These microdomains are much higher than bulk cytosolic Ca^{2+} changes (typically 1-2 µM), which would not be sufficient to induce MCU activity. Evidence for such a mechanism was provided by Rizzuto et al 1993, through their investigation into the relationship between the ER and mitochondria. They found that stimulating HeLa cells with histamine (an IP_3-inducing agonist) in Ca^{2+}-free solution (to evoke Ca^{2+} release from the ER without any Ca^{2+} influx), induced a faster rise in mitochondrial matrix Ca^{2+} compared to the rise seen upon introduction of external Ca^{2+}. Therefore Ca^{2+} release alone induced a more rapid mitochondrial Ca^{2+} uptake compared to Ca^{2+} influx. This was despite both conditions causing a similar bulk rise in cytosolic Ca^{2+}. They explained such a phenomenon by the proposal that mitochondria were exposed to high, local Ca^{2+} microdomains during IP_3-induced Ca^{2+} release. Consistent with this, Rizzuto et al 1998 showed that mitochondria were exposed to high, local concentrations of Ca^{2+} by construction of an aequorin that was targeted to the intermembrane space. Following histamine-induced Ca^{2+} release, aequorin localised to the intermembrane space recorded a larger Ca^{2+} rise than that reported in the cytoplasm. This was consistent with the mitochondrial surface being exposed to high, local Ca^{2+} concentrations, much greater than bulk cytosolic Ca^{2+}, upon agonist stimulation. Such an arrangement allows for the efficient transfer of Ca^{2+} from the ER to the mitochondria. Consistent with IP_3R-driven Ca^{2+} release underlying efficient mitochondrial Ca^{2+} uptake, Hajnóczky et al (1995) showed in permeabilized RBL cells that both mitochondrial Ca^{2+} uptake (measured by recording Rhod 2 fluorescence compartmentalised into the matrix), and metabolic activity (monitored by the redox state of flavin and pyridine nucleotide cofactors) following low concentrations of vasopressin, were suppressed in response to thapsigargin. This was despite similar levels of global cytosolic Ca^{2+} concentrations being evoked. Thapsigargin evoked a slower rise in Rhod 2 fluorescence (mitochondrial Ca^{2+} uptake) and was less effective in increasing NADPH when compared with a low concentration of vasopressin. This could be explained with regards to the presence/ absence of IP_3R-driven Ca^{2+} release. Thapsigargin is a blocker of the SERCA pump and depletes the ER Ca^{2+} stores due to the continuous leakage of Ca^{2+} across the ER membrane. The effect is independent of IP_3R-dependent Ca^{2+} release and the generation of high, local Ca^{2+} signals. By contrast, low concentrations of vasopressin generate IP_3R-driven Ca^{2+} release and hence high, local Ca^{2+} signals. Therefore in order for the mitochondrial uniporter to efficiently take up Ca^{2+} it requires exposure to signals of high, local Ca^{2+}. For such an explanation to be true, mitochondria would have to be localised close to the ER (within 100 nm). Rizzuto et al 1998 visualized a close apposition between mitochondria and the ER by co-transfecting HeLa cells with a mitochondrial targeted and ER targeted fluorescent probe, each with different spectral wavelengths. Moreau et al 2006 confirmed such close apposition between these two organelles using electron microscopy in RBL cells, where they found mitochondria were within 10-200 nm of the ER.

The notion that the precise location of mitochondria close to local, high Ca^{2+} underlies their ability to efficiently buffer Ca^{2+} by MCU is supported by findings that in certain cells mitochondria effectively buffer plasma membrane Ca^{2+} entry. Mitochondria have been shown to be close enough to plasma membrane Ca^{2+} entry sites in Jurkat T cells to allow them to efficiently buffer Ca^{2+} influx and therefore participate in the regulation of Ca^{2+} entry channels. Upon CRAC channel activation, mitochondria move to the plasma membrane. Quintana et al 2006 monitored the localisation of mitochondria using microscopy techniques involving the use of mitochondrial fluorescent probe mitotracker, before and after stimulation with thapsigargin. They found that following thapsigargin-induced Ca^{2+} entry, subplasma membrane mitotracker fluorescence increased. Such an effect was not seen when thapsigargin was applied in zero Ca^{2+} or in the presence of cytoplasmic BAPTA to chelate the Ca^{2+} influx and was impaired in the presence of 100 nM BTP2, (to achieve a partial CRAC channel block). Therefore Ca^{2+} entry through CRAC channels was required to induce such movement. Furthermore, whole-cell patch clamp experiments used to directly measure I_{CRAC} demonstrated that under conditions that prevented mitochondria from translocating to the plasma membrane (by pre-incubating cells with nocodazole, a microtubule inhibitor), I_{CRAC} inactivated faster. Therefore the localisation of mitochondria to the plasma membrane was important to sustain I_{CRAC}, by efficiently buffering the incoming Ca^{2+} that would act negatively to feedback on the CRAC channel to inactivate it. This showed that mitochondria are involved in the control of CRAC channel dependent Ca^{2+} entry via mechanisms that depended on the location of the mitochondria. The positioning of mitochondria close to the plasma membrane in T cells enables the organelle to be exposed to sufficient Ca^{2+} levels that overcome the low affinity mitochondrial uniporter. However, such a mechanism is unlikely to be important in RBL cells under physiological conditions. This is because in RBL cells most mitochondria are found 500 nm to 1 µm from the plasma membrane, both before and after stimulation (Singaravelu et al 2011).

Mitochondria are also known to partition the cell into discrete Ca^{2+} compartments. The best example of this is found in pancreatic acinar cells. Tinel et al 1999 used mitochondrial specific fluorescent dyes, mitotracker green and Rhodamine 123, to reveal a belt of mitochondria concentrated around the secretory pole. This belt prevented the diffusion of Ca^{2+} to the basal pole. Prevention of mitochondrial Ca^{2+} uptake using CCCP transformed the restricted local Ca^{2+} in the secretory pole into a global Ca^{2+} rise that spread the whole cell. Such compartmentalisation is important to keep Ca^{2+} signals in the secretory pole for efficient secretion of zymogen granules and prevent Ca^{2+} signals invading the basolateral pole. Since mitochondria regulate Ca^{2+} entry, Ca^{2+} release and create subcellular Ca^{2+} domains dependent on their location, it is possible that distinct pools of mitochondria exist to enable them to carry out specific, localised functions. It may be the case that mitochondria within each pool have slightly different characteristics that allow them to function more efficiently to achieve their precise role (Parekh 2003a). In pancreatic acinar cells, such subpopulations of mitochondria have been shown to exist (Park et al 2001). Whilst mitochondria close to the plasma membrane buffer Ca^{2+} entry, mitochondria close to the nucleus separate nuclear and cytoplasmic Ca^{2+} oscillations and mitochondria that compartmentalise at the secretory pole buffer Ca^{2+} oscillations arising within this pole.

1.8.2.4 *Physical tethering between mitochondria and the ER*

Mitochondria are motile organelles (Rizzuto et al 1998, Chen et al 2003, Mironov et al 2006). Rizzuto et al 1998 and Chen et al 2003 used time-lapse fluorescence microscopy in HeLa cells and mouse embryonic fibroblasts respectively, to reveal the constant rearrangement and movement of networks of mitochondria. How can mitochondria be reliably exposed to local Ca^{2+} signals, which are required for them to function as efficient buffers, if they have the potential to move around the cell freely? The answer involves physical attachment of mitochondria to sites that generate local Ca^{2+} signals. Exocytosis in neurons has been shown to be heavily reliant on such an association, where ER-mitochondrial disengagement reduced synaptic currents. The close interorganellar arrangement therefore optimized neuronal exocytosis (Mironov et al 2006). It is well established that mitochondria are juxtaposed to the ER at sites called mitochondrion associated membranes (MAMs) (Rizzuto et al 1998, Moreau et al 2006). Back in 1977, Shore and Tata observed close coupling between the two organelles in a typical rat hepatocyte and confirmed this with co-sedimentation experiments. They showed that >75% of mitochondria (marked with the mitochondrial localised enzyme cytochrome c oxidase) co-sedimented with > 45% of the total ER, (marked with ER compartmentalised enzyme glucose-6-phosphatase). Furthermore, they tested methods to separate such an association to investigate the underlying mechanism involved. They found that to achieve complete separation both shearing (using an ultra-turrax disintegrator) and sucrose density gradient sedimentation with KCl and EDTA were required. Although such conditions did disrupt mitochondrial morphology, absence of one of these factors failed to cause substantial separation. Therefore all three factors (shear, KCl and EDTA) represent the minimal requirements. Since such harsh conditions were needed for a complete disassociation, it led them to propose that the connection between the two organelles involved a physical attachment. Therefore the pursuit to visualize such physical contacts and establish their molecular identity and functional relevance became an interesting avenue to pursue.

Several mitochondrial bound or ER bound proteins have been proposed to be involved in ER-mitochondrial spacing and the constitution of the physical connections. These include DLP-1 / DRP-1 (Pitts et al 1999, Varadi et al 2004), tumor autocrine motility factor receptor (Wang et al 2000), PACS-2 (a multifunctional sorting protein localised to ER together with BAP31) (Simmen et al 2005), OAP1 (Cipolat et al 2004, Frezza et al 2006) and the outer mitochondrial membrane protein VDAC1 (voltage-dependent anion channel 1). It has been proposed that VDAC1 is physically linked to the IP_3R in the ER membrane via the chaperone protein grp75 and so might position the mitochondrial uniporter close to IP_3R-driven Ca^{2+} release (Rapizzi et al 2002, Szabadkai et al 2006). Visualization of such protein tethers had not been seen until Csordás et al 2006 used a precise, powerful microscopy technique. Short protein tethers of varying length (9-30 nm), were visualized both in isolation and in situ between mitochondria and the ER (Csordás et al 2006) using electron tomography. Such an approach is advantageous over previous methods, since it enables observation of very fine structural details, which would be missed with conventional micrographs. The linkages they found were independent of IP_3R physical connections, since the tethers were not affected in DT40 cells where IP_3R had been knocked down. Together with previous papers, the observations support the view that several particles may underlie the physical connection between mitochondria and the ER. Furthermore, Csordás et al 2006 investigated the physiological relevance of ER-mitochondrial spacing. They revealed that loosening the normal association between the ER and mitochondria (see figure 19) impaired the Ca^{2+} transfer between the two organelles. Permeabilized RBL cells stimulated with IP_3 showed a rapid increase in cytosolic Ca^{2+} that was mirrored by a mitochondrial Ca^{2+} rise, monitored through simultaneously measuring organelle targeted fluorescence probes. Pre-treatment with proteinase K, trypsin digestion (to cause limited proteolysis of the tethers) or a mitochondrial uncoupler, all caused normal IP_3-induced Ca^{2+} release (a normal rise in cytosolic Ca^{2+}) but IP_3-induced mitochondrial Ca^{2+} uptake was reduced. Therefore loosening normal ER-mitochondrial coupling reduces Ca^{2+} propagation between the IP_3R and mitochondria. To investigate whether tightening the ER-mitochondrial association (shown in figure 19) also impacted upon Ca^{2+} coupling between the two organelles, Csordás et al 2006 constructed and expressed a fluorescent outer mitochondrial membrane-ER linker protein (OMM-ER linker) in permeabilized RBL cells. The OMM-ER linker was roughly 5 nm in length and was composed of an OMM targeted sequence at the N terminus and an ER targeted sequence at the C terminus, to establish an ER-mitochondrial linkage. Electron tomographs identified a narrowed distance between ER-mitochondria from around 24 nm in control cells to 6 nm in OMM-ER linker expressing cells. An increased interface between the mitochondria and ER was revealed in the OMM-ER linker expressing cells. Whilst tightening had no effect on adenophostin A-induced cytoplasmic Ca^{2+} release, the mitochondrial Ca^{2+} signal was enhanced in OMM linker expressing cells. Together, the results show that Ca^{2+} propagation from the ER to the mitochondria is highly dependent on this interorganellar distance and provides a novel regulatory site for modifying Ca^{2+} signalling and subsequent cell function.

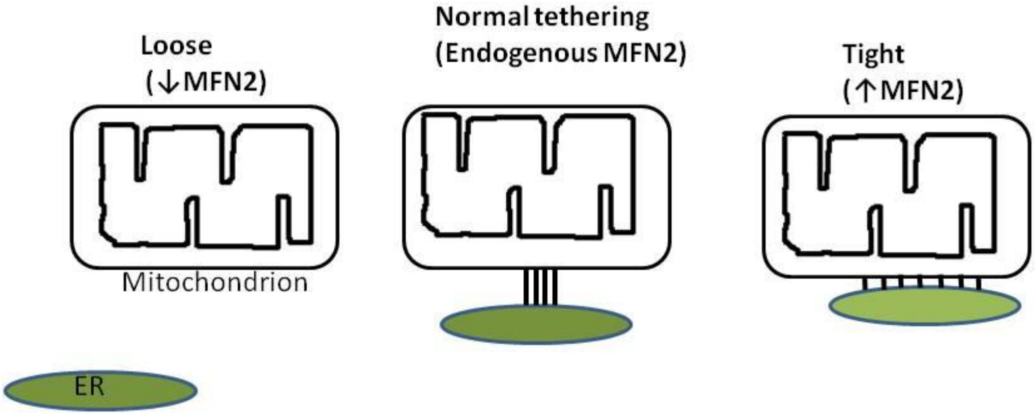

Figure 19 (adapted from Csordás et al 2006) illustrates ER-mitochondrial physical tethering. From left to right: the loose association arising from knockdown of the endogenous function of MFN2 pulls the mitochondria away from the ER. Ca^{2+} transfer between the ER and mitochondria is impaired. Normal tethering holds the ER and mitochondria within a normal distance (24 nm) for efficient Ca^{2+} transfer between the ER and mitochondria. The tight association arising from overexpressing MFN2 pulls the mitochondria closer to the ER, around 6 nm, which leads to matrix Ca^{2+} overload. The black lines between the mitochondrion and ER represent the physical tethers.

1.8.3 *Mitofusin Proteins*

In 2008, an important tethering role for the dynamin-related proteins mitofusin 1 (MFN1) and mitofusin 2 (MFN2) (each composed of a large GTPase domain and two heptad repeat domains/ coiled-coil regions; illustrated in figure 20), was established in mouse embryonic fibroblasts (MEFs) and HeLa cells (de Brito and Scorrano 2008).

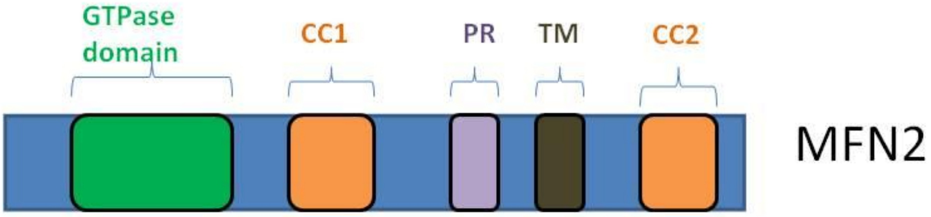

Figure 20 (adapted from Zorzano et al 2010) shows the important domains of MFN2. These include the transmembrane domain shown in brown (TM), the GTPase domain involved in mitochondrial fusion in green, two heptad repeat domains/ coiled-coil regions in orange (CC1, 2) and a proline rich domain for protein-protein interactions (purple, PR).

Knockdown of MFN1 or MFN2 in mice is embryonically lethal (Chen et al 2003). De Brito and Scorrano 2008 showed that the previously assigned mitochondrial mitofusin 2 protein had an ER localisation as well. Endogenous MFN2 was concentrated in mitochondria associated membrane sites (MAMs; points where the ER and mitochondria link) using immunofluorescence analysis. Here it was found to be crucial in the regulation of ER morphology, ER-mitochondrial tethering and Ca^{2+} propagation between the two organelles. Using electron tomography, de Brito and Scorrano found that ER-mitochondrial tethering was reduced by around 40% in mouse embryonic fibroblasts (MEFs) and HeLa cells in which MFN2 had been knocked down. This effect could be rescued by re-expression of MFN2. Investigation into the importance of ER MFN2 and mitochondrial MFN2 was achieved by the construction and use of two separate organelle targeted MFN2 mutants. These included MFN2 ActA (targeted to the mitochondria) and MFN2 IYFFT (targeted to the ER). It was revealed that expression of MFN2 IYFFT restored ER morphology and ER-mitochondrial tethering in MEFs in which MFN2 had been knocked down, whilst

MFN2 ActA only restored mitochondrial morphology. This led de Brito and Scorrano to suggest that ER MFN2 is required for interorganellar association. However, ER MFN2 alone was not able to rescue ER-mitochondrial tethering in cells doubly deficient of MFN2 and MFN1. Only coexpression of MFN2 IYFFT with MFN1, or MFN2 ActA could achieve this. Both ER and mitochondrial mitofusins are required for tethering the two organelles. The resultant hetero- or homotypic partners formed higher molecular weight complexes than each partner alone. This could be explained by the formation of multimers made up of only MFNs or, considering that a whole host of proteins have been proposed to be involved, possibly a multimer consisting of numerous proteins bound together. Furthermore, de Brito and Scorrano showed that the loosening of ER and mitochondria in MEFs in which MFN2 had been knocked down impaired the propagation of Ca^{2+} from the IP_3R to the mitochondria, (figure 19). MFN2 is therefore a crucial component of the protein complexes that determine normal ER-mitochondrial spacing and goes some way into explaining the molecular determinants of the tethers that Csordás et al 2006 find. The ability of MFN2 to control ER-mitochondrial spacing, shown in figure 19, may underlie the inherited genetic disorder Charcot- Marie- Tooth neuropathy type IIa (CMTIIa). De Brito and Scorrano 2008 found that MFN2 mutants with point mutations associated with CMTIIa failed to restore proper ER-mitochondrial spacing in MEFs in which MFN2 had been ablated. CMTIIa is an inherited, autosomal dominant genetic disorder, caused by heterogeneous MFN2 missense mutations where patients' sensory and motor neurons are degenerated (Amiott et al 2008, Züchner et al 2004). Clinically, it is characterised by sensory loss, muscle weakness, muscle atrophy and deformities in the feet (Lawson et al 2005). Since apoptosis has been linked to loosening of the ER and mitochondria (Csordás et al 2006) and overexpression of MFN2 has been shown to induce apoptosis (Guo et al 2007), it is suggested that the neurodegeneration characteristic of CMTIIa could be a consequence of impaired ER-mitochondria tethering. The work by de Brito and Scorrano raises the possibility of altering ER-mitochondrial spacing through targeting the MFN2 protein. I have taken advantage of this concept in this thesis by disrupting endogenous MFN2 which presumably alters ER-mitochondrial distance to investigate a role for this protein and ER-mitochondrial tethering in the regulation of CRAC channels and agonist-induced Ca^{2+} signals.

More recently, García-Pérez et al 2011 revealed an even more detailed view of ER/SR-mitochondrial tethering and the distribution of mitochondrial MFN2 in rat cardiac muscle, (this is illustrated in figure 21). Using transmission electron microscopy they observed more contact points (points where the outer and inner mitochondrial membrane closely associate) at SR-mitochondrial membrane junctions (sites where the SR and OMM are closely tethered), compared to SR-free outer mitochondrial membrane sites (where the SR is not close to OMM). Furthermore, they observed a higher likelihood of protein tethers between OMM-SR junctions at OMM-IMM contact sites compared to IMM-free OMM regions. Following this, the SR/ER membrane favours connection to the mitochondria via physical tethers at points where the IMM and OMM are also held close together. This would allow all three membranes (SR/ER, OMM and IMM) to be held within close association and suggests that such regions act as docking sites for protein tethers. Such an arrangement would enhance the efficiency of Ca^{2+} transfer from the IP_3R to the IMM localised uniporter, by reducing the distance needed for Ca^{2+} to travel.

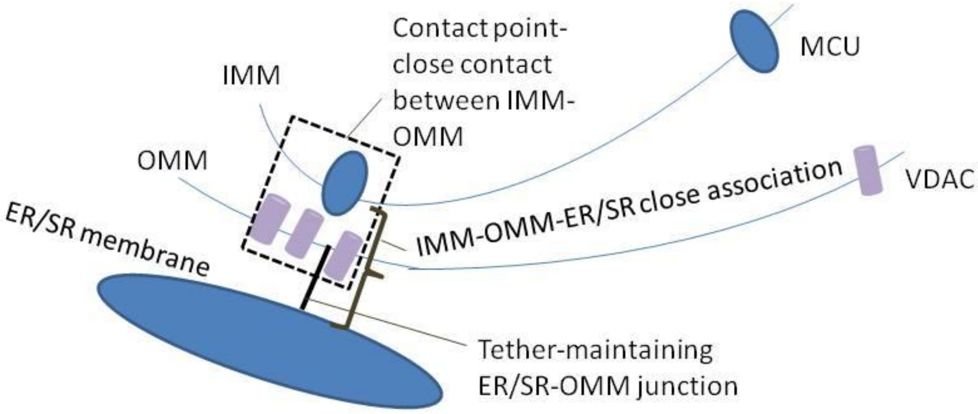
Contact point-close contact between IMM-OMM
IMM
MCU
OMM
VDAC
ER/SR membrane
IMM-OMM-ER/SR close association
Tether-maintaining ER/SR-OMM junction

Figure 21 demonstrates the proposed arrangement of the outer mitochondrial (OMM), inner mitochondrial (IMM) and ER/SR membrane by García-Pérez et al 2011. All three membranes are in close apposition for favourable Ca^{2+} transfer from the ER/SR to the mitochondrial matrix.

Whether such an arrangement between ER, OMM and IMM is present in non-excitable tissue needs to be investigated, as well as the distribution of the uniporter in relation to these sites. Since VDAC, the main route for Ca^{2+} to cross the OMM, is concentrated at these points (Brdiczka et al 1991) it is likely that the uniporter in the IMM will also be enriched at these contact regions, for efficient Ca^{2+} transfer.

Another recent study has identified a role for mitochondrial MFN2 in the control of STIM1 movement (Singaravelu et al 2011) and subsequent CRAC channel dependent Ca^{2+} entry in RBL cells, following mitochondrial depolarization. Therefore mitochondrial MFN2 is likely to be of significant relevance in the regulation of CRAC channels. Such a role for MFN2 and mitochondrial MFN2 in particular is investigated in this thesis.

1.8.4 *Regulation of the mitochondrial Ca^{2+} uniporter, MCU*

Since mitochondrial Ca^{2+} uptake occurs via MCU, factors which affect MCU activity are therefore likely to affect mitochondrial Ca^{2+} buffering and its subsequent influence on Ca^{2+} signalling and regulation of CRAC channels. MCU is highly voltage dependent whereby hyperpolarization increases its open probability (Kirichok et al 2004). MCU is also highly sensitive to cytosolic Ca^{2+} signals. Cytosolic Ca^{2+} can facilitate MCU activity (this requires calmodulin) (Csordás and Hajnóczky 2003, Moreau et al 2006) as well as inactivate MCU (Moreau et al 2006). Therefore Ca^{2+} biphasically regulates MCU. I have already mentioned that MCU is sensitive to high, local cytosolic Ca^{2+} signals in RBL cells. Hajnóczky et al 1995 revealed a faster mitochondrial Ca^{2+} uptake in response to IP_3-induced Ca^{2+} release (by low vasopressin) compared to IP_3-independent Ca^{2+} release (by thapsigargin). MCU activity is therefore facilitated by Ca^{2+} signals of higher amplitude. Hajnóczky et al 1995 further demonstrated a sensitivity of mitochondria to the frequency of the Ca^{2+} signal, (MCU activity is dependent on the temporal nature of the Ca^{2+} signal). They showed that mitochondrial Ca^{2+} uptake and subsequent mitochondrial metabolic activity responded preferentially to repetitive cytosolic Ca^{2+} oscillations (induced by low concentrations of vasopressin), compared to sustained cytosolic Ca^{2+} rises following application of thapsigargin or high agonist concentrations, in single hepatocyte cells. High agonist concentrations evoke sustained Ca^{2+} signals that do not oscillate. Repetitive Ca^{2+} oscillations caused a maintained mitochondrial metabolic response whereas sustained cytosolic Ca^{2+} signals (even those that arose from IP_3R-dependent Ca^{2+} release secondary to high agonist concentration exposure) only induced a transient mitochondrial Ca^{2+} rise and mitochondrial metabolic response. Hajnóczky et al 1995 suggest that although high concentrations of agonist sustain elevated cytosolic Ca^{2+}, the rate and degree of Ca^{2+} release from the stores is likely to be suppressed, due to Ca^{2+}-dependent inactivation (CDI) of IP_3R (Finch et al 1991, Bezprozvanny et al 1991). Inhibition of IP_3R-driven Ca^{2+} release would therefore reduce the effective transfer of Ca^{2+} from IP_3R to the mitochondrial matrix. Following this, mitochondria need to be exposed to constant active IP_3R-driven Ca^{2+} release events. Transient cytosolic Ca^{2+} rises would cause less inactivation of IP_3R-dependent Ca^{2+} release, promoting further release which would enhance mitochondrial Ca^{2+} uptake.

Further work by Csordás and Hajnóczky 2003, showed that Ca^{2+}-dependent facilitation of MCU was caused by a sustained increase in MCU permeability and required calmodulin. They used a novel technique to measure the permeability of MCU by recording the rate by which Mn^{2+}, which permeates MCU, could quench the Ca^{2+}-sensitive dye Fura 2-FF (compartmentalised to the mitochondrial matrix). They found that IP_3 caused an increase in cytosolic $[Ca^{2+}]$, which activated MCU, allowing Mn^{2+} to permeate the uniporter and quench Fura 2-FF, (trapped in the matrix). This revealed that IP_3-induced Ca^{2+} release increased the permeability of MCU. The enhanced Mn^{2+} quench rate remained even 90s after IP_3 stimulation. This was suggestive of a sustained increase in MCU permeability, which was inhibited in the presence of calmodulin antagonists calmidazolium and W-7. Therefore this demonstrated that MCU would buffer more Ca^{2+} following repetitive Ca^{2+} rises compared to a sustained Ca^{2+} rise, as the latter caused inactivation of the uniporter.

The importance of calmodulin for Ca^{2+}-dependent facilitation (CDF) of MCU was confirmed in RBL-1 cells by Moreau et al 2006, who showed that mitochondrial Ca^{2+} uptake was impaired by calmodulin antagonists calmidazolium and W-7.

Sustained Ca^{2+} signals are however important to cause CDI of MCU. Moreau et al 2006 demonstrated that MCU was inactivated by Ca^{2+} and this Ca^{2+}-dependent inactivation was sensitive to the duration of the Ca^{2+} signal. Therefore the findings by Hajnóczky et al that show oscillations result in the facilitation of mitochondrial Ca^{2+} buffering can also be explained by the fact that transient cytosolic Ca^{2+} rises would cause significantly less or no CDI of MCU, compared to sustained intracellular Ca^{2+} rises. Hence mitochondria would favour Ca^{2+} buffering by maintaining the activity of MCU. Moreau et al 2006 showed that Ca^{2+} inactivated MCU by exposing RBL cells to cytosolic Ca^{2+} loads whilst measuring mitochondrial matrix Ca^{2+} with Rhod 2, (this involved permeabilizing cells to remove dye not compartmentalised to the matrix). They found that the rise in mitochondrial matrix Ca^{2+} was significantly reduced when 100 µM Ca^{2+} was applied to cells following a pre-pulse of 10 µM Ca^{2+}, compared to the absence of this pre-pulse. Furthermore, they showed that the extent of this CDI could be reduced by reducing the duration of the pre-pulse. Pre-pulses of 10s duration failed to evoke significant MCU inactivation. Therefore transient cytosolic Ca^{2+} oscillations can be regarded as causing little CDI. The activity of MCU is therefore highly sensitive to the spatial and temporal profile of cytosolic Ca^{2+}signals, as well as the presence of calmodulin.

1.8.5 *Mitochondrial control of CRAC channels*

The ability of mitochondria to buffer Ca^{2+} efficiently means that they are key regulators of Ca^{2+} release (Jouaville et al 1995), Ca^{2+} entry (Gilabert and Parekh 2000, Glitsch et al 2002, Quintana et al 2006) and the formation of subcellular Ca^{2+} domains (Park et al 2001). The importance of mitochondrial Ca^{2+} uptake in the control of Ca^{2+} influx can be appreciated by considering its control on CRAC channel activity, which impacts upon a range of downstream cellular responses. These include the activation of Ca^{2+}-dependent transcriptional factors (NFAT) and control of interleukin-2 in T cells (Hoth et al 2000), exocytosis in pancreatic acinar cells (Park et al 2001), and arachidonic acid production and LTC_4 synthesis and secretion in mast cells (Chang et al 2004, 2006).

Mitochondria affect all stages of CRAC channel gating (for a summary see figure 22). They impact upon CRAC channel activation, inactivation and deactivation (Parekh 2008b). Respiring mitochondria act to facilitate and maintain CRAC channel dependent Ca^{2+} entry by simultaneously increasing the stimulus for CRAC channel activation and reducing the size and onset of slow CDI of CRAC channels.

How might mitochondria achieve such control? CRAC channel activity is sensitive to the extent of store depletion. If the ER is not sufficiently depleted of Ca^{2+}, CRAC channels fail to activate fully as a threshold of store depletion needs to be reached (Gilabert and Parekh 2000). This explains the puzzling observation that IP_3 does not fully activate CRAC channels under conditions of weak physiological buffer. In weak buffer, IP_3 fails to deplete the stores to the threshold required to fully activate CRAC channels. Using whole-cell patch clamp techniques, Gilabert and Parekh 2000 showed that the size of I_{CRAC} was significantly smaller in the presence of weak buffer (0.1 mM EGTA) compared to the presence of strong buffer (10 mM EGTA) when IP_3 and thapsigargin were present in the patch pipette. In the presence of weak buffer cytosolic Ca^{2+} concentrations would be increased indicating that CRAC channels would be impaired by a bulk rise in cytosolic Ca^{2+}. Gilabert and Parekh found that mitochondria were essential to enable the full development of I_{CRAC} by IP_3 under conditions of weak physiological buffer. Using whole-cell patch clamp experiments to directly measure I_{CRAC} in RBL cells, Gilabert and Parekh 2000 revealed that inclusion of a cocktail that maintained mitochondria in their energized state (to maintain mitochondrial Ca^{2+} buffering) caused a two-fold increase in I_{CRAC} (when IP_3 and thapsigargin were in the patch pipette), compared to the absence of this cocktail. This effect was abolished following depolarization of the IMM by exposure to antimycin A (to block complex III of the respiratory chain) and oligomycin (to inhibit ATP synthase) or after dialysis with ruthenium red (an antagonist of MCU). Furthermore, since the cocktail failed to alter the development of I_{CRAC} in the presence of strong buffer, mitochondrial regulation of I_{CRAC} must have been via a Ca^{2+}-dependent mechanism. An explanation of the above result is that mitochondrial buffering acts to reduce IP_3 receptor CDI, which would promote more robust Ca^{2+} release and hence more extensive store depletion. Another factor which determines store Ca^{2+} content is the activity of SERCA, which pumps Ca^{2+} back into the ER when cytosolic Ca^{2+} rises. Supporting this mechanism is the finding that mitochondria are within 10-200 nm of the ER in RBL cells (Moreau et al 2006, Rizzuto et al 1998). This positioning means that mitochondria are within a range that would enable the low affinity mitochondrial uniporter to effectively buffer the local release of Ca^{2+} through

IP_3Rs. Therefore mitochondrial Ca^{2+} buffering could also be promoting effective CRAC channel activation by enhancing Ca^{2+} store depletion through competing with the ability of SERCA to refill the stores (this would reduce ER Ca^{2+} replenishment). Mitochondrial Ca^{2+} buffering can therefore act to promote robust CRAC channel activation by enhancing the activation stimulus to favour store depletion, through simultaneously reducing IP_3R CDI and refilling of the stores by SERCA. This would enable IP_3 to fully activate I_{CRAC} under conditions of weak physiological buffer. Consistent with mitochondrial Ca^{2+} buffering acting on Ca^{2+} release, it has been shown that energized mitochondria reduce the level of IP_3 required to activate $I_{CRAC,}$ which should also act to promote store depletion (Gilabert, Bakowski and Parekh 2001).

Incoming Ca^{2+} also acts to regulate negatively CRAC channel activity through Ca^{2+}-dependent inactivation (CDI). Such CDI can occur via two mechanisms: fast CDI, which is reliant upon the local build up of Ca^{2+} surrounding the channel pore and develops rapidly within 10-100 ms (Zweifach and Lewis 1995a, Fierro and Parekh 1999, Gilabert and Parekh 2000), and slow CDI, which occurs over a much longer time scale (tens of seconds) and is a consequence of a global rise in cytosolic Ca^{2+} (Zweifach and Lewis 1995b, Parekh 1998). Most mitochondria are too far away from the CRAC channel pore to be able to capture the incoming Ca^{2+} and regulate fast CDI. BAPTA (a fast Ca^{2+} chelator) reduces fast CDI but EGTA (a slow Ca^{2+} chelator) fails to do so. This means that Ca^{2+} acts within approximately 5 nm of the channel to induce fast CDI (Zweifach and Lewis 1995a, Gilabert and Parekh 2000). It has been reported using electron microscopy that in RBL cells the majority of mitochondria before and after stimulation were at least 500 nm away from the plasma membrane (Singaravelu et al 2011). Consistent with this, mitochondrial depolarization had no effect on fast CDI in RBL cells (Gilabert and Parekh 2000). Mitochondria are therefore not involved in fast CDI of CRAC channels. Slow CDI on the other hand is sensitive to EGTA, which places the Ca^{2+} binding site for slow CDI of CRAC channels much further away from the channel pore (>100 nm). Mitochondria have been shown to reduce slow CDI (Gilabert and Parekh 2000). Once CRAC channels activate, mitochondria facilitate CRAC channel dependent Ca^{2+} entry by reducing the onset and extent of slow CDI. How such regulation occurs in RBL cells however is unclear. In Jurkat T cells mitochondria can directly reduce CDI by buffering the Ca^{2+} entering through CRAC channels. Mitochondria have been shown to translocate to the plasma membrane upon cell stimulation in T cells (Quintana et al 2006). This localises mitochondria close to the plasma membrane, allowing them to buffer effectively the incoming CRAC current and thus reduce CDI of the CRAC channel. However, mitochondria are unlikely to take part in such a mechanism in RBL cells where the majority of mitochondria remain 500 nm away, even following cell stimulation. It is important to investigate how mitochondria can reduce slow CDI of CRAC channels, in RBL cells.

In addition to Ca^{2+}-dependent regulation of CRAC channels by mitochondria, Ca^{2+}-independent pathways involving mitochondria have also been proposed. Mitochondria produce and release a variety of signals such as ATP (Landolfi et al 1998), cytochrome C (Demaurex and Diestelhorst 2003), free radicals (Duchen 2004), and metabolic intermediates (Bakowski and Parekh 2007). This raises the question of whether a messenger produced inside mitochondria can release into the cytosol to impact upon CRAC channel dependent Ca^{2+} entry. The synthesis and release of ATP from mitochondria for example has been shown to regulate directly SERCA pump activity (Landolfi et al 1998). Glitsch et al 2002 proposed a novel mechanism by which mitochondria can regulate CRAC channel dependent Ca^{2+} entry, independently of the ability of the organelle to buffer Ca^{2+} or generate ATP. They measured the rate of Ca^{2+} entry following admission of 2 mM Ca^{2+} to cells treated with thapsigargin in zero Ca^{2+}. In the presence of mitochondrial depolarizing agents, applied after thapsigargin-induced Ca^{2+} store depletion, the rate of Ca^{2+} entry was significantly impaired. This demonstrates a role for mitochondria in regulating CRAC channels independent of their ability to control IP_3R-driven Ca^{2+} release and SERCA pump activity and hence downstream of store depletion. Since depolarization suppresses the initial rate of CRAC channel dependent Ca^{2+} entry, the results argue against an effect on the slowly developing CDI process, as the latter would take a longer time to manifest and requires a rise in bulk Ca^{2+}. These results support a role for mitochondrial regulation of CRAC channel activity independent of Ca^{2+} buffering. Consistent with this view, Frieden et al 2004 showed in HeLa cells that replacing Mn^{2+} for Ca^{2+} as the charge carrier caused a significant reduction in CRAC channel dependent Ca^{2+} influx following mitochondrial depolarization with CCCP. This indicated a Ca^{2+}-independent pathway could be involved in mitochondrial regulation of CRAC channels. Indeed in excitable cells, mitochondrial inhibitors such as azide, FCCP and oligomycin are found to suppress action potential-induced twitch responses, (excitability in rat skeletal muscle fibres), via depolarization of the T-system membrane, by increasing Na^{+} permeability and Na^{+} loss from the T tubules. Ørtenblad et al 2003 suggested that a mitochondrial derived messenger (that was not ATP, since ATP concentration was maintained constant) was regulating a channel which affected Na^+ permeability (Ørtenblad et al 2003). Such a channel could be the plasma membrane Na^+ channel, voltage-dependent anion channel or a non-selective cation channel (Ørtenblad et al 2003). Bakowski and Parekh 2007 revealed a role for the intermediate metabolite pyruvic acid, (a precursor of the Krebs cycle, which is synthesised within the cytoplasm), in the regulation of fast CDI. Inclusion of physiological concentrations of pyruvic acid significantly reduced the size of fast CRAC channel CDI, an effect that was unaffected by blocking MCU with ruthenium red. This raises the possibility that metabolic intermediates produced inside mitochondria may release into the cytoplasm where they could regulate slow CDI of CRAC channels, independently of a direct Ca^{2+} buffering role.

In addition to these regulatory pathways mitochondria have also been reported to affect CRAC channel deactivation. Deactivation switches off CRAC channels as a result of Ca^{2+} refilling the stores. Bakowski et al 2001 demonstrated this with the finding that thapsigargin reduced deactivation of CRAC channels. Since mitochondrial Ca^{2+} uptake competes with SERCA pumps for Ca^{2+} removal, one would expect energized mitochondria to slow down CRAC channel deactivation. However, in HeLa cells mitochondria have been reported to facilitate CRAC channel deactivation. This is due to their ability to slowly release Ca^{2+} via the $3Na^+/Ca^{2+}$ exchanger close to the site of SERCA Ca^{2+} uptake, promoting store refilling by the SERCA pump (Arnaudeau et al 2001). Since mitochondria are involved in all stages of CRAC channel gating, an important and unresolved question concerns the mechanisms that regulate mitochondrial calcium uptake. Elucidation of these pathways will deepen our understanding of how CRAC channels are controlled under physiological conditions.

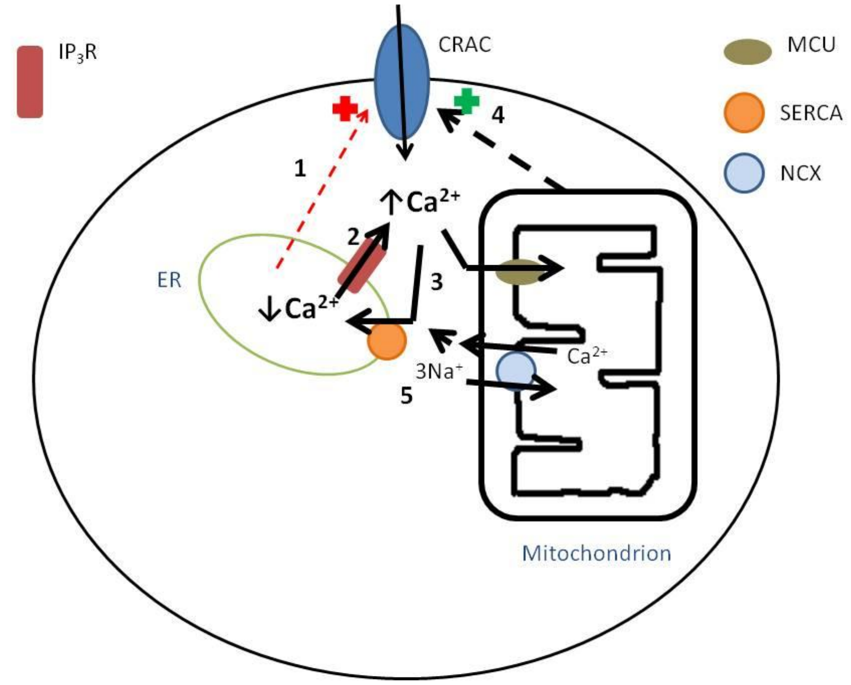

Figure 22 (adapted from Parekh 2008b) shows mitochondrial regulation of the CRAC channel. Upon agonist stimulation, the IP_3R activates and releases Ca^{2+} from the ER depleting the ER Ca^{2+} store, which subsequently activates and opens the CRAC channel, allowing Ca^{2+} to enter the cell (1.). 2) Mitochondria buffer Ca^{2+} release via the IP_3R this decreases CDI of the IP_3R, enhancing and prolonging Ca^{2+} release. This subsequently promotes CRAC channel activation by enhancing store depletion. 3) The mitochondrial Ca^{2+} uniporter (MCU) competes with the sarcoplasmic reticulum Ca^{2+} ATPase pump (SERCA) for the uptake of Ca^{2+}, which further promotes CRAC channel activation and activity by reducing Ca^{2+} replenishment of the stores. 4) Mitochondrial Ca^{2+} buffering decreases slow CDI of the CRAC channel, facilitating and prolonging CRAC channel dependent Ca^{2+} entry. Mitochondria may also release a messenger which positively feeds back on the CRAC channel. Such control would be independent of its Ca^{2+} buffering role. 5) The mitochondrial $3Na^{+}$/ Ca^{2+} exchanger (NCX) slowly releases Ca^{2+} to nearby SERCA to facilitate ER store replenishment with Ca^{2+}. This subsequently deactivates the CRAC channel, switching the channel off. Mitochondrial buffering acts through all of these pathways to exert control on the activation, inactivation and deactivation of CRAC channels.

1.9 Aims of thesis

It is clear that the entry of Ca^{2+} is crucial for driving a plethora of cell responses in virtually all cell types. CRAC channels are an abundant Ca^{2+} channel and the dominant one in non-excitable cells. Since the molecular identity of CRAC channels was only recently established, there are still some important unanswered questions with regards to how the channels are controlled. Ca^{2+} is an important regulator, providing a powerful negative feedback pathway acting through spatially and temporally distinct mechanisms. Three independent mechanisms by which Ca^{2+} can negatively act on CRAC channels are known to exist. These include fast inactivation which arises rapidly following the local accumulation of Ca^{2+} very close to the channel pore as well as the slower developing mechanisms of deactivation (due to Ca^{2+} stores refilling, switching CRAC channels off) and slow inactivation, which is dependent on a global rise of intracellular Ca^{2+}, accumulating from distant sources. Although Ca^{2+}-dependent fast inactivation and deactivation are well understood in RBL cells, the basis of slow inactivation remains unclear. Evidence suggests a role for calmodulin and for mitochondrial Ca^{2+} uptake, but whether these processes are related or independent is not known.

This thesis seeks to address both the involvement of calmodulin and mitochondria and whether the two interact.

Chapter 3: Investigates how CRAC channels and physiologically-induced Ca^{2+} oscillations are regulated by calmodulin and whether there is any lobe-specificity to this regulation. An important question which is considered is whether both the C and N lobes of calmodulin are equally effective.

Chapter 4: Examines the regulation of mitochondrial Ca^{2+} uptake by calmodulin and in particular calmodulin tethered to Orai1, directly in intact RBL cells. This is achieved by using the ratiometric Ca^{2+} sensitive, circular permutated yellow fluorescent protein, pericam, genetically targeted to the mitochondrial matrix.

Chapter 5: Addresses how the mitochondrial tethering protein MFN2 affects mitochondrial Ca^{2+} uptake, CRAC channel dependent Ca^{2+} entry and agonist-induced cytosolic Ca^{2+} oscillations.

Taken together this thesis aims to advance knowledge in the CRAC channel field.

Chapter 2.

Materials and Methods

2. Materials and Methods

2.1 Cell culture

Human embryonic kidney (HEK 293) cells and an immortalised mast cell line (rat basophilic leukemia (RBL-1)) were purchased from American Type Culture Collection (ATCC). All cells were cultured and kept incubated at 37°C, 5% CO_2 in a solution that was composed of Dulbecco's Modified Eagle's Medium (DMEM) made up with 10% fetal bovine serum, 2 mM L-glutamine and penicillin/streptomycin, (concentration 100 units/ml penicillin and 100 µg/ml streptomycin), as previously used by Moreau et al 2005. Cells for Ca^{2+} imaging and patch clamp experiments were trypsinized and put on to coverslips for use 24-48 hours later.

Note that the term WT is the abbreviation always used to represent the control cell/cells for each respective experiment.

2.2 Materials

The cDNA and RNAi constructs that were transfected into cells, the solutions that were used and the drugs that were applied in this thesis are described in Tables **1**, **2**, **3** and **4**, respectively. All chemicals were obtained from Sigma-Aldrich if not otherwise stated.

Table 1. cDNA constructs

cDNA	**Description and/or Usage.**	**Obtained from**
Pericam	Mitochondrial targeted, Ca^{2+}-sensitive, fluorescent, ratiometric protein (developed by Nagai et al 2001 and used by Malli et al 2003).	Dr. Wolfang Graier (Institute of Molecular Biology and Biochemistry, Medical University of Graz)
GFP	Green fluorescent protein to identify successfully transfected cells.	Lonza
CAM4M	A dominant negative calmodulin mutant in which all four Ca^{2+} binding sites (EF hands) were insensitive to Ca^{2+}.	Dr. James Putney (National Institute of Environmental Health Sciences, Department of Health and Human Services, USA.)
CAM2C	A mutant calmodulin where the two Ca^{2+} binding sites on the C-lobe were Ca^{2+}-insensitive.	Dr. James Putney (as above)
CAM2N	A mutant calmodulin where the two functional Ca^{2+} binding sites on the N-lobe were insensitive to Ca^{2+}.	Dr. James Putney (as above)
Orai1	Normal functioning Orai1	OriGene

STIM1-GFP	Normal functioning STIM1 tagged with GFP	Dr. Tobias Meyer (Stanford University)
A73E Orai1 mutant	A mutant Orai1 construct with a point mutation at residue A73 (A73E), generated and previously used by Mullins et al 2009. This mutant cannot bind calmodulin, but otherwise functions like normal Orai1.	Mutagenex USA.
MFN2	Normal mitofusin 2	Previously used by Singaravelu et al 2011 and obtained from Prof. Luca Scorrano (Université De Genève, Dpt PHYM, Suisse).
MFN2 ActA	A dominant negative mutant MFN2 specifically targeted to the mitochondria	Previously used by Singaravelu et al 2011 and obtained from Prof. Luca Scorrano (as above).
MFN2 IYFFT	A dominant negative mutant MFN2 specifically targeted to the ER	Previously used by Singaravelu et al 2011 and obtained from Prof. Luca Scorrano.

pNFAT-TA-EGFP	An EGFP-based reporter plasmid, used to measure NFAT-1-dependent gene expression, as previously used by Kar et al 2011.	Dr. Yuriy Usachev (University of Iowa)

Table 2. RNAi constructs

RNAi	To reduce expression of a specific protein.	
MICU1	RNAi against the mitochondrial Ca^{2+} uniporter/uptake 1 regulator (Perocchi et al 2010). RNAi sequence: GCG UCA CAG AGA UCG AAC UAC U	Invitrogen, UK
MFN2	RNAi against mitofusin 2.	Invitrogen, UK
Orai1	RNAi against Orai1. RNAi sequence: (5’ to 3’) GUCCACAACCUCAACUCCTT.	Invitrogen, UK

Table 3. Solutions used

Solution	**Composition**
Standard external solution (2 mM Ca^{2+} solution)	145 mM NaCl, 2.8 mM KCl, 2 mM $CaCl_2$, 2 mM $MgCl_2$, 10 mM D-glucose, 10 mM HEPES, pH 7.4, with NaOH.
Ca^{2+}-free external solution (zero Ca^{2+})	145 mM NaCl, 2.8 mM KCL, 2 mM $MgCl_2$, 10 mM D-glucose, 10 mM HEPES, 0.1 mM EGTA pH 7.4, with NaOH.
Low Ca^{2+} external solution (0.5 mM Ca^{2+})	145 mM NaCl, 2.8 mM KCl, 0.5 mM $CaCl_2$, 2 mM $MgCl_2$, 10 mM D-glucose, 10 mM HEPES, pH 7.4, with NaOH.
Barium external solution (5 mM Ba^{2+} solution)	145 mM NaCl, 2.8 mM KCl, 5 mM $BaCl_2$, 2 mM $MgCL_2$, 10 mM D-glucose, 10 mM HEPES, pH 7.4, with NaOH.
Internal patch pipette solution	145 mM cesium glutamate, 8 mM NaCl, 1 mM $MgCl_2$, 2 mM Mg-ATP, 0.6 or 10 mM EGTA (dependent on experiment), 0.03 mM IP_3, 10 mM HEPES, pH 7.2, with CsOH.
External bath patch solution	145 mM NaCl, 2.8 mM KCl, 10 mM $CaCl_2$, 2 mM $MgCl_2$, 10 mM CsCl, 10 mM D-glucose, 10 mM HEPES, pH 7.4 with NaOH

Table 4. Drugs applied

Drug	**Description and/ usage**	
1 µM Fura 2-AM	A Ca^{2+}-sensitive fluorescent indicator to measure the dynamic changes in cytosolic Ca^{2+} concentration ($[Ca^{2+}]$). AM moiety renders it membrane-permeable.	Invitrogen, UK
1 µM Thapsigargin	An antagonist of the sarcoplasmic reticulum Ca^{2+} ATPase (SERCA) pump on the ER membrane to cause ER store depletion and open CRAC channels.	Merck
160 nM Leukotriene C_4 (LTC_4)	Submaximal concentration of an IP_3 releasing physiological agonist used to induce cytosolic Ca^{2+} oscillations.	Cambridge Bioscience
1 mM Lanthanum (La^{3+})	Cells were pre-incubated for 5 minutes with 1 mM La^{3+} in zero Ca^{2+} to block the plasma membrane Ca^{2+} ATPase pump, PMCA, (the main extrusion pathway in RBL-1 cells) to prevent Ca^{2+} loss from the cytosol upon stimulation. Cells are exposed to an external solution completely absent of Ca^{2+}.	Sigma-Aldrich

Calmidazolium (20 μM)	Cells were pre-incubated for 15 minutes with calmidazolium, a calmodulin antagonist, to block endogenous calmodulin function.	Calbiochem
10 μM KN-62	An antagonist of Ca^{2+}-calmodulin dependent protein kinase II (CAM kinase II). Pre-incubation with KN-62 for 15 minutes was used to block the enzyme.	Sigma-Aldrich
Synta (1μM) (3-fluoropyridine-4-carboxylic acid (2’,5’-dimethoxybiphenyl-4-yl)amide)	A CRAC channel blocker previously used by Ng et al 2008. 1 μM caused partial CRAC channel blockade (approximately 50 % block).	GlaxoSmithKline, UK
FCCP (5μM) (carbonyl cyanide 4-(trifluoromethoxy) phenylhydrazone)	A protonophore to depolarize the inner mitochondrial membrane by making the membrane proton permeable. This abolishes the proton motive force and therefore the driving force for Ca^{2+} uptake into mitochondria. In FCCP (pre-incubated for 4 minutes), mitochondria can no longer buffer cytosolic Ca^{2+}.	Sigma-Aldrich

1 µM Ionomycin	Used to permeablize the inner mitochondrial membrane to Ca^{2+} (once ER stores had already been fully depleted with thapsigargin).	Toncris
2 mM EGTA-AM (Ethylene glycol tetraacetic acid)	A slow acting Ca^{2+} chelator.	Sigma-Aldrich

2.3 Cytosolic Ca^{2+} imaging

Ca^{2+} imaging experiments were carried out in the dark at room temperature (21°C) using TILL photonics, IMAGO charged-coupled device camera-based system, as was previously described by Chang and Parekh 2004. Using a Polychrome monochromator, images were acquired every 2 seconds whilst cells were excited alternatively at 356 and 380 nm, (20 ms exposures). Emitted light was collected at > 510 nm. Ca^{2+} signals were analysed offline using IGOR Pro for Windows and were plotted as R (356/380). Cells were loaded with 1 µM Fura 2-AM in the dark for 45 minutes at 21°C and then washed three times in standard external solution (2 mM Ca^{2+} solution). To allow for further de-esterification I waited 15 minutes. Each coverslip was then placed into a chamber and bathed in 1 ml of 2 mM Ca^{2+} external solution or Ca^{2+}-free solution. A water immersion objective lens of magnification x40 was used and solutions of controlled concentrations were then applied directly to the point of focused cells using appropriate pipettes. To deplete Ca^{2+} stores and activate

CRAC channels, cells are stimulated with 1 µM thapsigargin in Ca^{2+}-free solution. Thapsigargin blocks the ER (endoplasmic reticulum) resident SERCA pumps preventing Ca^{2+} re-uptake into the ER. This resulted in store depletion because the Ca^{2+} that leaked out of the ER, across the ER membrane which was not 'tight' for Ca^{2+}, can no longer get pumped back into the ER. The resultant store depletion opens CRAC channels. Stimulation with thapsigargin in Ca^{2+}-free solution leads to a transient Ca^{2+} signal. Once the signal had returned to baseline (after approximately 400s), 2 mM Ca^{2+} was applied and entered the cells through the open CRAC channels. The initial rate of rise following the addition of 2 mM Ca^{2+} or 5 mM Ba^{2+} was recorded as a measure of the CRAC channel activity. This is the most reliable measure of the rate of CRAC channel dependent Ca^{2+} influx because it better reflects the number of CRAC channels open. Steady state measurements on the other hand reflect the balance between Ca^{2+} entry and extrusion.

2.4 Mitochondrial matrix Ca^{2+} imaging

Mitochondrial matrix Ca^{2+} imaging experiments were carried out using pericam, (constructed by Nagai et al 2001 and used by Malli et al 2003). Pericam is a ratiometric, fluorescent Ca^{2+} protein that is targeted into the mitochondrial matrix in intact cells to specifically measure dynamic changes in matrix Ca^{2+} under physiological conditions. It is a circular, permutated fluorescent protein designed to sense Ca^{2+}. It contains both a GFP unit and a mitochondrial presequence, which encodes a 12-amino acid, N-terminal presequence of subunit V, mitochondrial enzyme cytochrome c oxidase. This mitochondrial presequence specifically targets it to the mitochondrial matrix in intact cells (Nagai et al 2001). The same camera and software were used as previously described for Fura 2. However this time cells were excited alternately at 488 nm and 430 nm, (20 ms exposure), and emission collected at 535 nm (Malli et al 2003). RBL-1 cells were transfected with the construct pericam using the nucleofection-based system Amaxa, described in section **2.5**. Transfected cells were imaged 48 hours after they were plated on to glass coverslips. Pericam located into puncta and regions of interest were drawn around these areas of fluorescence within the cell. Controls to verify that pericam is measuring mitochondrial Ca^{2+} are shown in section **4.2**, **b**. GFP was not required for this type of transfection because the pericam itself was a self fluorescent protein and cells which had been successfully transfected were visible upon excitation at wavelength 488 nm.

2.5 Cell transfection

Cells were transfected with a variety of cDNA constructs or RNAi molecules directed against specific proteins, all of which are identified in **Tables 1** and **2**. Such constructs were either fluorescently tagged with an enhanced green fluorescent protein GFP, (for example STIM1-GFP), or co-transfected with GFP or the ratiometric fluorescent protein pericam separately. Presence of the fluorescent marker was important to identify cells that had been successfully transfected, so that only these cells were selected for imaging. Rat basophilic leukemia (RBL-1) cells were transfected using the nucleofection-based system from Amaxa, (Cell line nucleofector Kit V) (Chang et al 2008). HEK 293 cells were transfected using the lipofectamine method (Di Capite et al 2009b), (after pre-incubation in Dulbecco’s modified Eagle’s medium with 10% fetal bovine serum and 2 mM L-glutamine). Cells were passaged onto glass coverslips for

Ca^{2+} imaging and patch clamp experiments, where cells were used 48 hours after plating. GFP alone was transfected into cells as a control. 1.6 µg was the standard amount of cDNA used for transfection, apart from with MFN2 ActA where double the quantity was required to cause significant effects (3.2 µg).

2.6 Gene reporter assay

Cells were transfected with EGFP-based reporter plasmid that contained an NFAT promoter. After 24 hours cells were stimulated in 2 mM Ca^{2+} with 160 nM LTC_4 at room temperature and were left for 40 minutes in the incubator. LTC_4 was then removed in exchange for 2mM external Ca^{2+} and the percentage of cells expressing EGFP (green cells) was recorded 24 hours later, as was previously described by Kar et al 2011.

2.7 Patch clamp experiments of I_{CRAC} undertaken together with my supervisor (Professor Anant Parekh)

Whole-cell patch clamp recordings were carried out to measure the current flowing through CRAC channels (I_{CRAC}) directly, at room temperature (21°C), as was described by Moreau et al 2005. Sylgard-coated, fire-polished pipettes with direct current resistance of 5 MΩ were filled with internal solution. The subsequent liquid junction potential that arose from this glutamate-based internal solution was taken into account by a correction of +10 mV. An external bath solution described in **Table 3** was used for measuring I_{CRAC}. Voltage ramps spanning -100 to +100mV in 50 ms intervals at 0.5 Hz from a holding potential of 0 mV, were applied to measure I_{CRAC} as was previously carried out by Ng et al 2009. An 8-pole Bessel filter at 2.5 KHz was used to filter the currents, and currents were digitized at 100 µs. The amplitudes measured from the voltage ramps at -80 mV were divided by the cell capacitance to normalize the currents to cell size. Using the automatic compensation of the EPC-9/2 amplifier, capacitative currents were compensated for before each ramp. Leak currents were subtracted by averaging three-five ramp currents obtained just before the onset of I_{CRAC} development and subtracting this value from all subsequent currents. 10 MΩ was the typical series resistance.

2.8 Fluorescence microscopy carried out with a lab colleague (Ms Charmaine Nelson)

Cell culture medium bathing the cells was removed and cells were fixed at -20°C for 10 minutes in analar methanol, (pre-chilled at -20°C). Analar methanol was washed from cells three times, (5 minutes per wash), with 10 mM PBS (phosphate-buffered saline) and was left at room temperature bathed in PBS. All subsequent washes were carried out using the same protocol, (three, 5 minute washes in 10 mM PBS). Cells were blocked with blocking agent composed of 2% bovine serum albumin (BSA) and 1% normal goat serum in PBS, and were left for one hour. After one hour's incubation, the serum mix was pipetted off the cells which were washed with PBS. A primary MFN2 antibody raised in a mouse (from Santa Cruz Biotechnology) was diluted 1:250 in carrier, (composed of blocking agent diluted by 1:10 in PBS), and was left overnight at 4°C. Cells were allowed to reach room temperature before removing the primary antibody and this was followed by washing with PBS. The secondary antibody was a mouse Alexa 594 raised in goat (Invitrogen, excitation 590 nm, emission 617 nm; red stained). It was loaded at a dilution of 1:2000 with PBS for 2 hours. The cells were then mounted in vectashield mounting medium containing DAPI, which stained for DNA, (DAPI, excitation 358 nm, emission 461 nm; blue stained). Images were visualized after mounting using a leica fluorescence microscope.

2.9 Statistical significance

To assess the statistical significance of two values I entered the mean ± SEM., (standard error of the mean), for each variable into an unpaired t-test. I considered $p<0.01$ (**) to be highly significant and $p<0.05$ (*) to be significant. A p-value greater than 0.05 was considered of no statistical significance (p=NS).

Chapter 3.

Lobe-specific modulation of CRAC channels by calmodulin

3.1 Introduction

Ca^{2+} is an extremely important intracellular messenger, activating a plethora of kinetically distinct cellular processes (Berridge et al 2003, Rizzuto and Pozzan 2006, Parekh and Putney 2005). These range from muscle contraction (Berridge 1997, Berridge et al 2000) (which occurs within milliseconds), exocytosis (Neher 1998), enzyme activation (Fagan et al 1998, Gu and Cooper 2000, Chang et al 2004, 2006) and gene expression (Dolmetsch et al 2001, Ng et al 2009, Kar et al 2011), to cell growth and proliferation (occurring over several hours to days; Greka et al 2003, Wang and Poo 2005, Li et al 2005). How such a broad second messenger activates certain Ca^{2+} -dependent cellular responses and not others at the same time is not entirely clear. It is now known that the spatial (Neher 1998, Chang et al 2008, Ng et al 2009, Rizzuto and Pozzan 2006) and temporal profile (Dolmetsch et al 1998) of the Ca^{2+} signal is critical in conveying such Ca^{2+}-dependent specificity. The spatial profile of the Ca^{2+} signal refers to changes in the intracellular calcium concentration in space, (where the Ca^{2+} rise occurs and how high and how far it spreads) (Parekh 2010). The temporal profile of Ca^{2+} on the other hand, refers to the time-course of the Ca^{2+} signal, (how long the Ca^{2+} stays high and whether the signal oscillates with time). The most basic Ca^{2+} signal is the Ca^{2+} microdomain (Neher 1998). Here Ca^{2+} builds up rapidly (microseconds), within nanometers of an open Ca^{2+} channel pore to very high concentrations, much higher than bulk cytosolic $[Ca^{2+}]$, (Neher 1998, Rizzuto and Pozzan 2006, Parekh 2008a).

The position of a target relative to the Ca^{2+} microdomain determines the speed and extent of its activation (Neher 1998, Parekh 2010). Close to the channel pore, within

20 nm, targets (even with a low affinity for Ca^{2+}) are generally activated rapidly with high fidelity. Further away from the channel, targets are exposed to much lower concentrations of Ca^{2+} and depending on their affinities for Ca^{2+} the probability for these targets to be efficiently activated can be significantly reduced. Low Ca^{2+} affinity targets will be poorly activated when located far from the microdomain. By contrast, higher affinity ones can still be activated (Neher 1998). Ca^{2+} microdomains can therefore directly and rapidly drive cellular processes (Rizzuto and Pozzan 2006) that occur within close proximity to the channel but how they activate cellular responses some hundreds of nanometers away from the channel, such as nuclear gene expression is an important question to consider. In 2001, Dolmetsch et al described a mechanism which linked the local Ca^{2+} influx through VOCCs (voltage-operated Ca^{2+} channels) to nuclear gene expression. The Ca^{2+} sensor calmodulin, which was associated with the IQ domain of the L-type Ca^{2+} channels, was found to relay this local Ca^{2+} signal. Local entry of Ca^{2+} through the VOCCs binds to calmodulin tethered to the L-type channel, forming a Ca^{2+}-calmodulin complex which subsequently dissociates from the channel into the cytoplasm. Here Ca^{2+}-calmodulin activates the Ca^{2+}-calmodulin dependent phosphatase calcineurin and the downstream ERK/MAPK pathway, to relay the signal to the nucleus, (see section **1.5**, figure 8 for an illustration of this). Experimental evidence for this novel pathway was established through the expression of mutant L-type channels that were unable to bind calmodulin, due to mutations in their IQ domain, into neuronal cells. These neurons were found to be deficient in activating ERK-1 and ERK-2 and showed impaired gene transcription in response to depolarization, measured by recording the activity of Ca^{2+}-dependent transcription factors (CREB and MEF-2).

In non-excitable cells, the major route of Ca^{2+} entry is through store-operated Ca^{2+} channels (SOCCs), of which the most important and best characterised is the CRAC channel (Ca^{2+} released activated Ca^{2+} channel) (Hoth and Penner 1992, Parekh and Putney 2005, Zweifach and Lewis 1993). The channel is composed of both the Ca^{2+} sensor, STIM1 (Roos et al 2005, Liou et al 2005) and the channel pore subunit, Orai1 (Feske et al 2006, Vig et al 2006a, b). Local entry of Ca^{2+} through CRAC channels activates an array of temporally distinct cellular processes, ranging from enzyme activation (Fagan et al 1998, Bautista and Lewis 2004, Chang et al 2004, 2006) to gene expression (Ng et al 2009, Kar et al 2011). CRAC channel microdomains are conveyed to distant targets through the involvement of Ca^{2+} sensors that are located close to or associated with the channel. For example, Ng et al 2009 demonstrated that local Ca^{2+} entry through CRAC channels was detected by the non-receptor tyrosine kinase, Syk. Syk was located to the plasma membrane and Syk activation was found to elicit two temporally distinct pathways upon local Ca^{2+} entry: firstly, Syk stimulated the cytosolic enzymes phospholipase A_2 and 5-lipoxygenase, which resulted in the synthesis and secretion of LTC_4, a process which developed within seconds; secondly, Syk led to the phosphorylation of the transcription factor STAT-5 and its translocation to the nucleus for c-fos expression, which occurred over tens of minutes. RBL-1 cells stimulated with thapsigargin and exposed to Syk inhibitors or transfected with Syk RNAi, were shown by Ng et al to have reduced STAT-5 phosphorylation and c-fos expression. This demonstrated the important role played by Syk in CRAC channel driven downstream cellular responses.

Following Ca^{2+} channel activation, the rise in local $[Ca^{2+}]$ that occurs when Ca^{2+} enters through the channel is an important regulator of its activity (Zühlke et al 1999, DeMaria et al 2001, Hirota et al 1999, Strotmann et al 2003, Sun and Taylor 2008, Moreau et al 2005, Rizzuto et al 2006, Anderson 2001). Calmodulin is an important Ca^{2+} sensor (Hoeflich et al 2002) critical for long-range signalling by VOCCs in excitable cells (Dolmetsch et al 2001) and which can detect local Ca^{2+} entry through Ca^{2+} channels. Calmodulin is a ubiquitous Ca^{2+} binding protein with four highly conserved Ca^{2+} binding domains (EF hands). It is composed of two globular lobes, the N- and C-lobe, each containing two EF hand Ca^{2+} binding sites, joined together via a 6 nm flexible hinge (Hoeflich et al 2002, Johnson et al 1996). Calmodulin can associate with a variety of Ca^{2+} channels, (e.g. TRPV4, Strotmann et al 2003, TRPV6, Niemeyer et al 2001, L-type VOCC, Peterson et al 1999 and Zühlke et al 1998, 1999, P/Q-type VOCC, DeMaria et al 2001, IP_3R type 1, Yamada et al 1995 and Patel et al 1997) and regulates channel activity. This is important in determining the size of the Ca^{2+} microdomains and the subsequent activation of downstream Ca^{2+}-dependent cellular responses. Through a series of mutagenesis experiments, DeMaria et al 2001 assigned opposing modulatory roles to each lobe of calmodulin in the regulation of VOCC activity. A Ca^{2+}-insensitive calmodulin mutant completely eliminated both calcium-dependent facilitation (CDF) and calcium-dependent inactivation (CDI) of P/Q-type channels. Two further calmodulin mutants: one where the N-lobe alone was Ca^{2+}-insensitive and another where the C-lobe alone was Ca^{2+}-insensitive, demonstrated a separate function to each lobe of calmodulin in the gating of P/Q-type channels. The N-lobe was found to drive CDI and the C-lobe was found to be critical for CDF of these channels.

For CRAC channels, incoming Ca^{2+} acts both to facilitate channel opening via positive feedback and to inactivate the channels via negative feedback (Moreau et al 2005). Both types of regulation can occur without being cancelled out because negative feedback and positive feedback have different kinetics. These feedback mechanisms impact upon the size of the microdomain that develops and the subsequent activation of downstream targets.

Inactivation of CRAC channels occurs via three independent mechanisms: (1) fast inactivation, (2) store refilling (deactivation) and (3) slow inactivation. Fast Ca^{2+}-dependent inactivation develops rapidly with time constants of 10 and 100 ms and is a consequence of the local accumulation of Ca^{2+} within 7 nm of the channel (Zweifach et al 1995a and Fierro and Parekh 1999). This type of inactivation is independent of slow Ca^{2+} chelators like EGTA and depends on calmodulin. In 2009, Mullins et al identified a Ca^{2+}-dependent calmodulin binding site within the N terminus of Orai1, composed of a 24 amino acid sequence (residues 68-91). They showed mutations in the calmodulin binding site altered fast inactivation. Store refilling occurs over a slower timescale (20-30s) and acts to deactivate the CRAC channel by switching off the activation stimulus for CRAC channels (reducing the extent of store depletion) (Bakowski et al 2001). Additionally slow, bulk Ca^{2+}-dependent inactivation (CDI) develops over a timescale of tens of seconds to minutes and requires a rise in global cytoplasmic Ca^{2+} (Zweifach et al 1995b and Parekh 1998). In contrast to fast inactivation, slow inactivation and deactivation of CRAC channels are both suppressed by slow Ca^{2+} chelators and are heavily affected by mitochondrial Ca^{2+} buffering (Gilabert and Parekh 2000, Hoth et al 2000, Arnaudeau et al 2001, Malli et al 2005). Mitochondrial Ca^{2+} uptake is regulated by Ca^{2+}-calmodulin (Csordás et al 2003 and Moreau et al 2006), suggesting a possible regulatory role for calmodulin in slow CDI of CRAC channels.

Moreau et al 2005 provided evidence for Ca^{2+}-calmodulin in the positive feedback regulation of CRAC channels. Ca^{2+}-calmodulin was shown to facilitate CRAC channel driven Ca^{2+} entry but only under conditions where bulk cytoplasmic Ca^{2+} was able to rise. Whole-cell patch clamp recordings were used to directly measure the CRAC channel current (I_{CRAC}) in RBL-1 cells. I_{CRAC} was reduced in the presence of a Ca^{2+}-insensitive calmodulin mutant when calcium stores were depleted in the presence of a weak intracellular Ca^{2+} buffer (when cytoplasmic Ca^{2+} can increase) but not in strong Ca^{2+} buffer conditions (which prevents a cytoplasmic Ca^{2+} rise). Similar findings were made following dialysis with a calmodulin inhibitory peptide. Therefore the facilitation of CRAC channels by calmodulin requires a rise in cytoplasmic Ca^{2+}. How calmodulin regulates slow inactivation of CRAC channels and whether there is any lobe-specificity to this is not clear and shall be addressed in this Chapter.

3.2 Results

a. Calmodulin Constructs

To investigate whether calmodulin regulated CRAC channels in a lobe-specific manner, I have used three different mutant calmodulin constructs. These are shown in the cartoon below, in addition to normal calmodulin endogenously expressed in the cells. The cartoon illustrates from left to right: normal, endogenous calmodulin (all four Ca^{2+} binding sites are intact), CAM4M (a dominant negative calmodulin mutant completely insensitive to Ca^{2+}), CAM2N (a calmodulin mutant where the N-lobe cannot sense Ca^{2+} but the C-lobe can) and CAM2C (a calmodulin mutant where the C-lobe cannot sense Ca^{2+} but the N-lobe can).

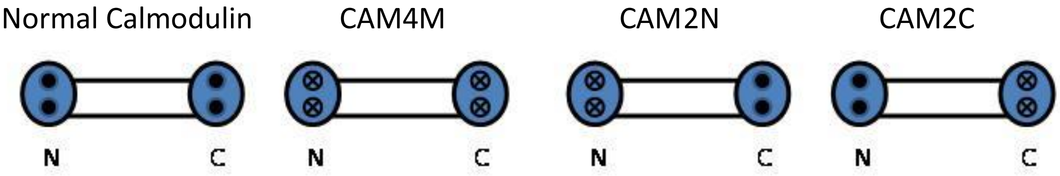

b. Calmodulin facilitates CRAC channel activity in a Ca^{2+}-dependent manner

To measure the rate of Ca^{2+} entry through store-operated Ca^{2+} channels, I stimulated cells with thapsigargin, a sarcoplasmic reticulum Ca^{2+} ATPase (SERCA) pump antagonist, in Ca^{2+}-free external solution (zero Ca^{2+}) (figure 1**A**). Inhibiting SERCA pumps with thapsigargin prevents the refilling of the endoplasmic reticulum (ER) with Ca^{2+} and subsequently causes depletion of the intracellular calcium stores, through the gradual leakage of calcium across the ER membrane. Depletion of the ER opens plasma membrane CRAC channels. Once the rise in cytosolic Ca^{2+} following ER store depletion had fallen back to resting levels, a process that occurred due to the activity of the plasma membrane Ca^{2+} ATPase pump (PMCA; Moreau et al 2005 in RBL-1 cells), 2 mM Ca^{2+} was applied to the cells. This resulted in a robust increase in intracellular Ca^{2+} because Ca^{2+} rapidly entered through the open CRAC channels (figure 1**A**). The initial rate of rise of this Ca^{2+} entry was measured because it is a better indicator of CRAC channel activity than measurements taken at steady state levels. CRAC channel dependent Ca^{2+} entry was significantly reduced when calmodulin was pharmacologically inhibited by the antagonist calmidazolium [20 µM], previously used by Moreau et al 2006 (see figure 1**B** for a typical cell trace and **C** for aggregate data). I have strengthened this finding by transfecting RBL-1 cells with the various calmodulin mutants, (these are illustrated in the cartoon above). Each calmodulin mutant construct was transfected into cells together with GFP (green fluorescent protein) cDNA to identify cells that were successfully transfected. Only GFP positive cells were selected for recordings. The transfection technique did not affect CRAC channel dependent Ca^{2+} entry since Moreau et al 2005 demonstrated that transfection of various GFP levels alone into RBL-1 cells, caused no significant change to CRAC channel dependent Ca^{2+} influx. This result I also confirmed myself. Therefore any change to CRAC channel dependent Ca^{2+} entry could be assigned to the expressed calmodulin mutant. Consistent with the pharmacological evidence, CRAC channel dependent Ca^{2+} entry was significantly reduced when cells were expressing the calmodulin mutant in which both Ca^{2+} binding EF hands were defective (CAM4M) (figure 1**D**, **E**). In figures 1**B** and **D,** cells had been pre-stimulated with thapsigargin at 100 seconds (s) in zero Ca^{2+} and then administered with 2 mM Ca^{2+} at approximately 650s and 610s respectively. Aggregate data are summarized in figures 1**C** and **E**. CAM4M reduced the initial rate of rise of the Ca^{2+} signal to a similar extent to that attained with calmidazolium (approximately 55% and 60% respectively), (figures 1**C**, **E**).

Since most regulation of Ca^{2+} channels by calmodulin is in a Ca^{2+}-dependent manner, it was interesting to investigate whether this was also the case for the regulation of CRAC channels. If so, then CAM4M should have no effect on CRAC channels when 5 mM Ba^{2+} is used as the charge carrier instead of Ca^{2+}. 5 mM Ba^{2+} readily permeates CRAC channels (Moreau et al 2005, Fierro and Parekh 2000) but activates calmodulin much less effectively than Ca^{2+} (Sun et al 2010). Consistent with a role for Ca^{2+}-calmodulin dependent regulation of CRAC channels, figure 1**F** shows no significant difference in CRAC channel activity in the presence or absence of CAM4M when Ba^{2+} is the charge carrier. This reveals that regulation of CRAC channels by calmodulin is through cytoplasmic Ca^{2+}. Cartoon model **1** below illustrates the facilitation of CRAC channel dependent Ca^{2+} entry by Ca^{2+}-calmodulin.

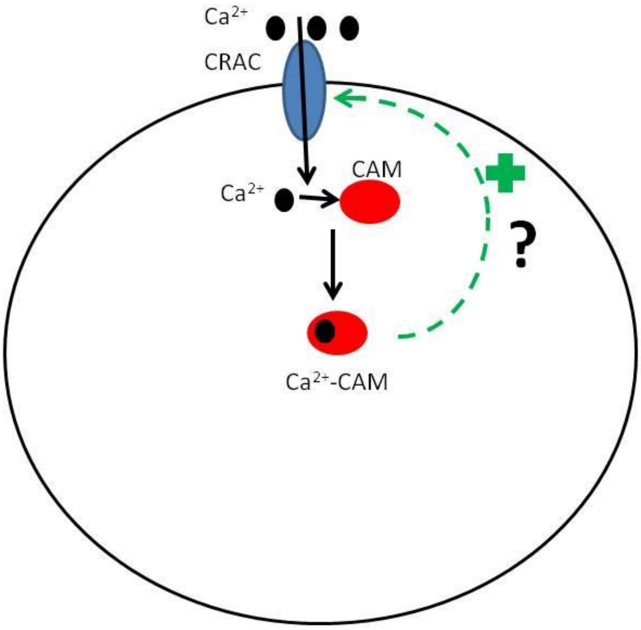

Cartoon model 1 illustrates the regulation of CRAC channels by cytoplasmic Ca^{2+}. Calmodulin is found to facilitate CRAC channel dependent Ca^{2+} entry in a Ca^{2+}-dependent manner. Upon CRAC channel activation Ca^{2+} enters the CRAC channel, binds to calmodulin (CAM) to form a Ca^{2+}-CAM complex which positively enhances CRAC channel activity.

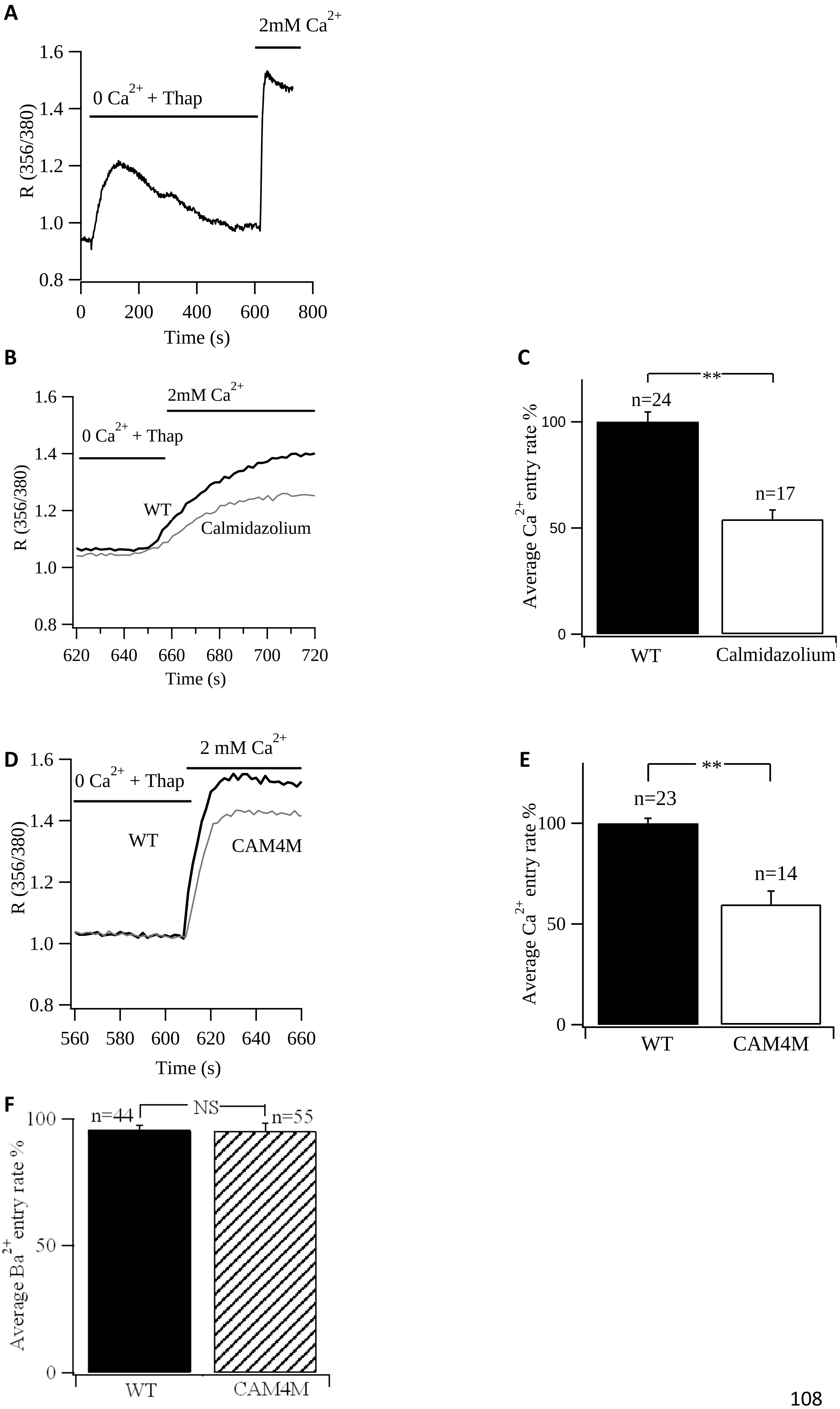
A
2mM Ca2+
0 Ca2+ + Thap
R (356/380)
1.6
1.4
1.2
1.0
0.8
0
200
400
600
800
Time (s)
B
2mM Ca2+
0 Ca2+ + Thap
WT
Calmidazolium
R (356/380)
1.6
1.4
1.2
1.0
0.8
620
640
660
680
700
720
Time (s)
C
**
n=24
n=17
Average Ca2+ entry rate %
100
50
0
WT
Calmidazolium
D
2 mM Ca2+
0 Ca2+ + Thap
WT
CAM4M
R (356/380)
1.6
1.4
1.2
1.0
0.8
560
580
600
620
640
660
Time (s)
E
**
n=23
n=14
Average Ca2+ entry rate %
100
50
0
WT
CAM4M
F
n=44
NS
n=55
Average Ba2+ entry rate %
100
50
0
WT
CAM4M

Figure 1. Calmodulin facilitates CRAC channel driven Ca^{2+} entry in a Ca^{2+}-dependent manner. **A**, the recording shows the protocol used to measure CRAC channel dependent Ca^{2+} entry. 1 µM thapsigargin was applied to RBL-1 cells bathed in Ca^{2+}-free external solution (zero Ca^{2+}) to deplete the intracellular Ca^{2+} stores (ER) and subsequently open CRAC channels. 2 mM Ca^{2+} was then added to the cells and the initial rate of rise of the Ca^{2+} signal was measured. **B**, the traces show the reduced Ca^{2+} entry through CRAC channels in HEK 293 cells in the presence of 20 µM calmidazolium compared to the absence of this drug (WT). **C**, aggregate data are compared between HEK 293 cells in the absence (WT) (n=24) and presence of 20 µM calmidazolium (n=17) ($p<0.0001$). **D**, the traces reveal that the Ca^{2+} entry through CRAC channels in RBL-1 cells is reduced in the presence of CAM4M. **E**, aggregate data from 23 untransfected (WT) and 14 CAM4M transfected RBL-1 cells are compared ($p<0.0001$). **F**, averaged data from HEK 293 cells compares the rate Ba^{2+} entry through CRAC channels in the absence (WT, n=44) or presence of CAM4M (CAM4M, n=55) (p= NS, not significant).

Note the abbreviation WT always represents the control cell/cells for each respective experiment (this is the case throughout my thesis).

c. Ca^{2+}- calmodulin modulates CRAC channels in a lobe-specific manner

Calmodulin has four distinct calcium-sensing domains: two located within the N-lobe and two within the C-lobe. The importance of each of these lobes in the modulation of CRAC channel activity however is unclear. Since I have shown that calmodulin is important in the gating of CRAC channels, I have investigated whether the two lobes of calmodulin are equally effective, using three different calmodulin mutant constructs (illustrated and described in the cartoon in section **a** of this Chapter). The same protocol was used here as in section **b**. I found that the initial rate of CRAC channel dependent Ca^{2+} entry was significantly reduced in cells expressing a calmodulin mutant in which only the C-lobe was defective (CAM2C), compared to untransfected cells (figure 2**A**, **C**). The extent of the reduction was similar to that seen with CAM4M. In contrast, cells expressing a calmodulin mutant in which only the N-lobe was defective (CAM2N) showed no significant difference in the rate of CRAC channel driven Ca^{2+} entry, compared to untransfected cells (figure 2**B**, **C**). The results reveal a lobe-specific function of calmodulin in the regulation of CRAC channels. The C-lobe is shown to play a major role and the N-lobe a minor role. This lobe-specific regulation of CRAC channels by calmodulin is not just confined to one cell type since similar results were found in HEK 293 cells. No differences in thapsigargin-induced Ca^{2+} release were seen between CAM2C (n=13, mean peak ratio 0.128 ± 0.00661 SEM.) and CAM2N (n=19, mean peak ratio 0.122 ± 0.00963 SEM., p=NS). Therefore differences in ER store Ca^{2+} content cannot explain the more effective reduction in store-operated Ca^{2+} channel dependent Ca^{2+} influx by CAM2C.

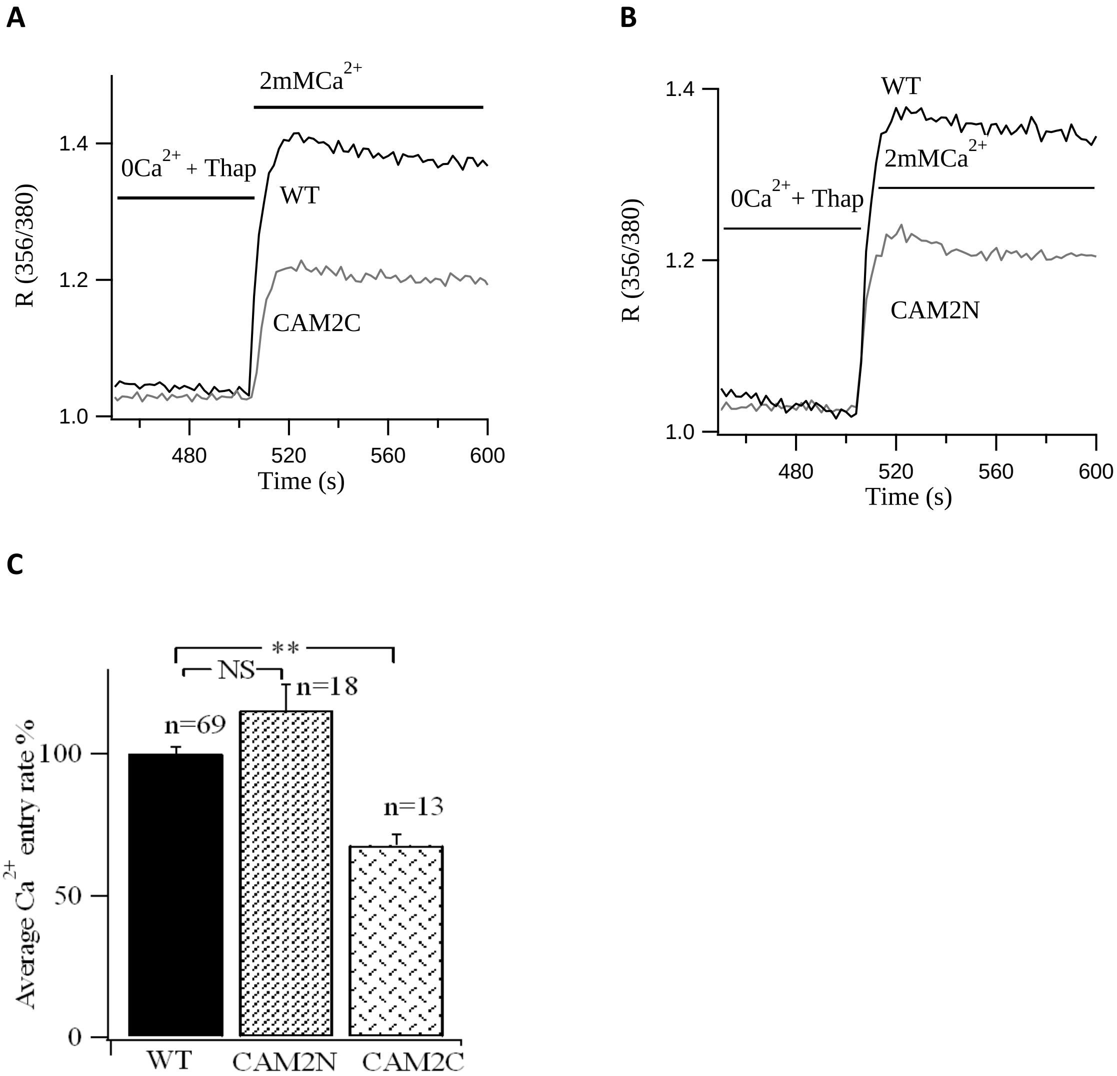

Figure 2. Calmodulin modulates CRAC channels in a lobe-specific manner. A, the traces compare Ca^{2+} entry through CRAC channels in a cell expressing CAM2C with a corresponding control (WT). **B**, the recordings compare Ca^{2+} entry signals in an untransfected RBL-1 cell (WT) and in one cell expressing CAM2N. **C**, aggregate data from 69 untransfected (WT), 18 CAM2N transfected (p=NS) and 13 CAM2C transfected RBL-1 cells (p=0.0063) compare CRAC channel driven Ca^{2+} entry rate between untransfected RBL-1 cells (WT) and cells expressing either CAM2C or CAM2N.

d. Calmodulin facilitates I_{CRAC} in a lobe-specific manner

Whole-cell patch clamp experiments (carried out with my supervisor) were used to directly measure the current flowing through CRAC channels (I_{CRAC}). In these experiments, the membrane potential is controlled and therefore cannot be altered by the calmodulin mutants. We activated I_{CRAC} by dialyzing cells with a pipette solution containing IP_3 in 0.6 mM EGTA, a moderate level of intracellular Ca^{2+} buffer, which enables a bulk cytoplasmic Ca^{2+} rise to develop upon CRAC channel activation (Glitsch and Parekh 2000). Following the onset of whole-cell recording, I_{CRAC} developed in all untransfected cells (figure 3**A**). In contrast, the size of I_{CRAC} at any given time was significantly reduced when cells were expressing CAM4M. Furthermore, the current-voltage relationship of I_{CRAC} depicted in figure 3**B** showed that at any given voltage, the size of I_{CRAC} was significantly reduced in the presence of CAM4M. Another difference was that the delay before I_{CRAC} activated was increased in the presence of CAM4M (figure 3**A**). To investigate whether I_{CRAC} was regulated by calmodulin in a lobe-specific manner, the current was recorded in cells expressing either CAM2C or CAM2N. The calmodulin mutant in which only the C-lobe was defective, CAM2C, significantly reduced I_{CRAC} in the presence of a moderate Ca^{2+} buffer. In contrast, the calmodulin mutant in which only the N-lobe was defective (CAM2N) did not significantly alter I_{CRAC} (aggregate data are summarized in figure 3**C**). These results extend the Ca^{2+} imaging results and confirm lobe-specific modulation of I_{CRAC} by Ca^{2+}-calmodulin when the current is measured directly.

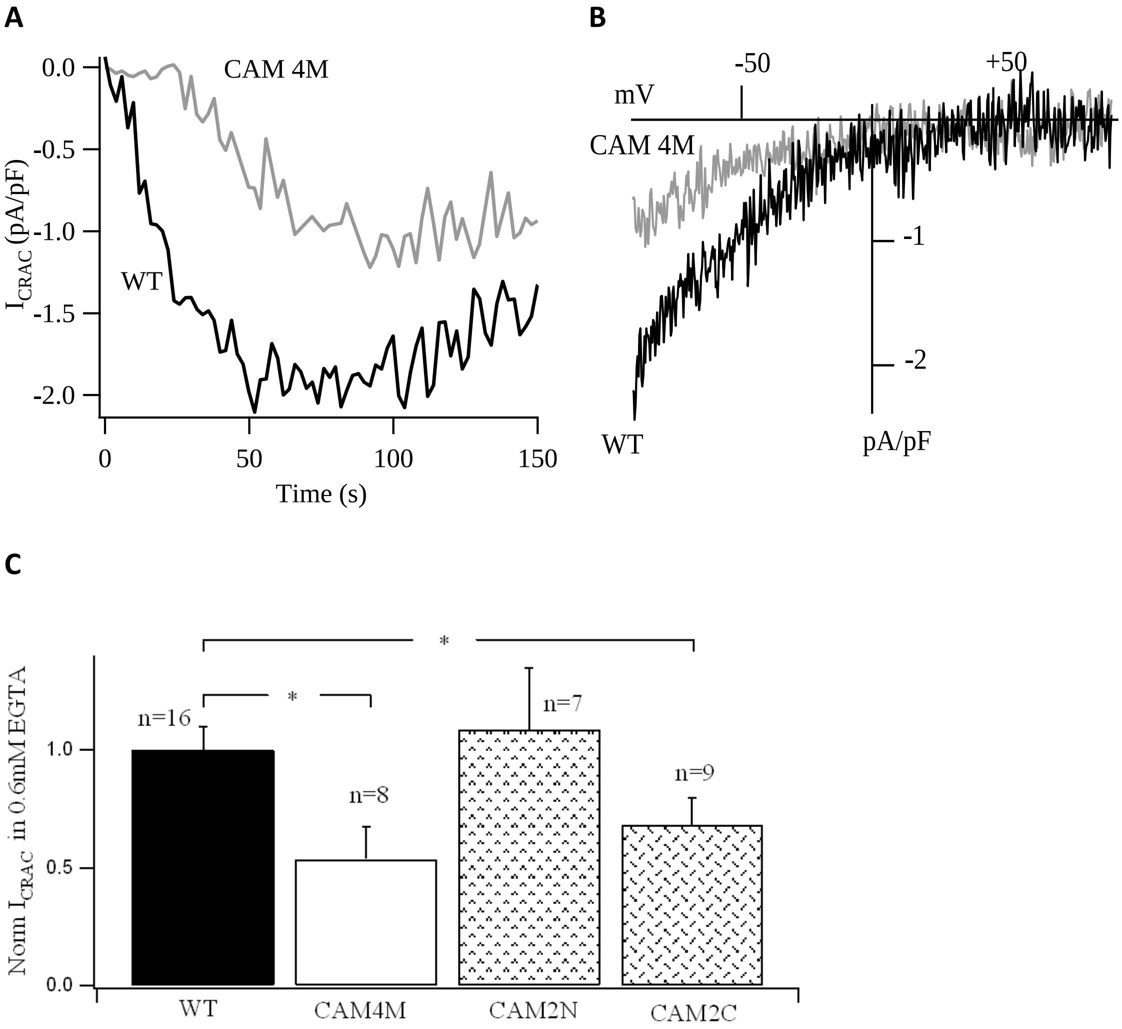

Figure 3. Whole-cell patch clamp recordings reveal a lobe-specific modulation of I_{CRAC} by calmodulin. **A**, the patch recordings compare I_{CRAC} development when cells are dialyzed with a pipette solution containing IP_3 and 0.6 mM EGTA in an untransfected cell (WT) and in one cell expressing CAM4M. **B**, the current/voltage curve shows that for any given voltage a smaller current is flowing through CRAC channels when cells are expressing CAM4M compared to untransfected cells (WT). **C**, average data from 16 untransfected (WT), 8 CAM4M transfected (p=0.0195), 7 CAM2N transfected (p=NS) and 9 CAM2C (p=0.0437) transfected RBL-1 cells demonstrate the lobe-specific modulation of I_{CRAC} by calmodulin.

e. Calmodulin modulates CRAC channels through a Ca^{2+}-dependent step.

After establishing that calmodulin regulates I_{CRAC} in a lobe-specific manner, I investigated whether this action was through a direct effect on the channel. To examine this, whole-cell patch clamp experiments (undertaken with my supervisor), were carried out to investigate whether calmodulin affected I_{CRAC} under conditions of high cytoplasmic Ca^{2+} buffering, in which a bulk cytosolic Ca^{2+} rise was prevented. Following dialysis with a pipette solution containing IP_3 and 10 mM EGTA, I_{CRAC} developed fully in all control cells and to a similar extent, although a little larger than was seen in the presence of 0.6 mM EGTA. This is because there is some refilling in the latter situation. In contrast to the results found in the presence of moderate EGTA, the size of I_{CRAC} was unaffected by CAM4M in the presence of high cytoplasmic Ca^{2+} buffering (figure 4). The regulation of CRAC channels by calmodulin is therefore not via a direct action on the channels themselves. These results reveal that in order for calmodulin to modulate I_{CRAC} a bulk rise in cytosolic $[Ca^{2+}]$ is required. Calmodulin must therefore be acting through a Ca^{2+}-dependent step to modulate CRAC channels. Cartoon model **2**, on the next page illustrates this concept.

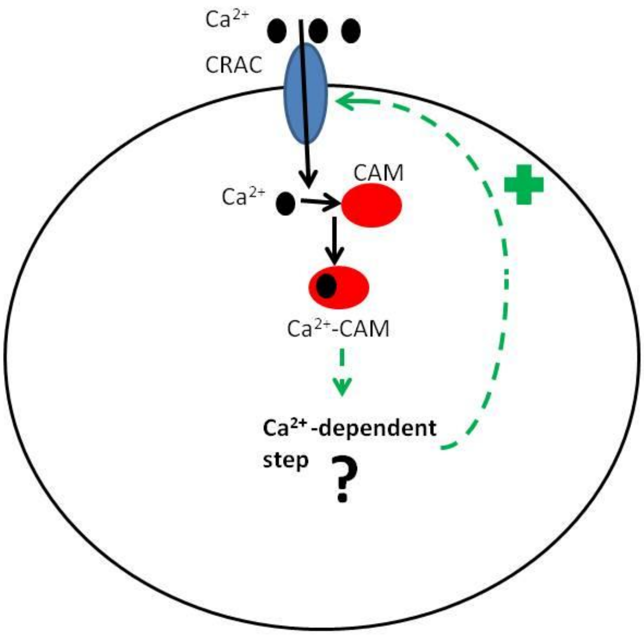

Cartoon model 2 illustrates the modulation of CRAC channels by cytoplasmic Ca^{2+} involves a Ca^{2+}-dependent step. Upon CRAC channel activation Ca^{2+} enters the CRAC channel, binds to calmodulin to form a Ca^{2+}-CAM complex which facilitates CRAC channel activity indirectly via a Ca^{2+}-dependent step since a bulk cytosolic Ca^{2+} rise is required for the lobe-specific modulation of CRAC channels by Ca^{2+}-calmodulin. This lobe-specific modulation is heavily reliant on the C-lobe of calmodulin. The C-lobe plays a major role in facilitating CRAC channel activity whilst the N-lobe plays a minor role, probably due to differences in the kinetics of Ca^{2+} unbinding from each lobe (more on this later in the Discussion, section **3.3**).

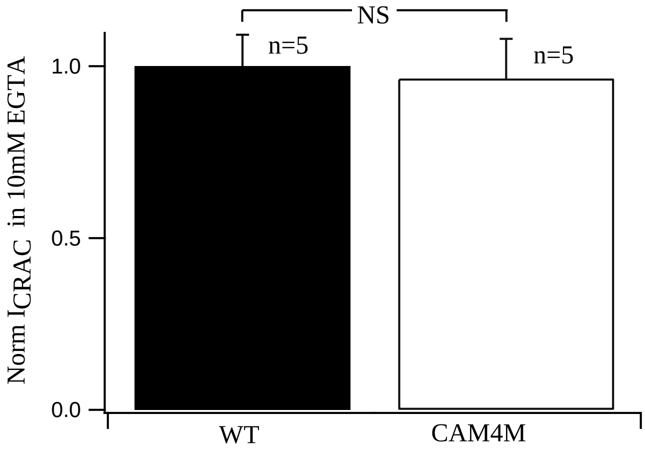

Figure 4. Calmodulin modulates I_{CRAC} through a Ca^{2+}-dependent step. Data collected from 5 untransfected (WT) and 5 CAM4M transfected RBL-1 cells (p=NS) revealed no significant difference in I_{CRAC} between the two conditions, when cells were dialyzed with a pipette solution containing IP_3 and 10 mM EGTA.

f. Calmodulin is required to maintain physiologically-induced cytosolic Ca^{2+} oscillations.

In RBL-1 cells, stimulation with low, physiological concentrations of agonist evoke cytosolic Ca^{2+} oscillations (Di Capite et al 2009a). These are maintained by CRAC channel activation. Ca^{2+} oscillations arise through regenerative Ca^{2+} release by the repetitive opening and closing of IP_3-driven Ca^{2+} release channels (IP_3R). In order for the oscillations to be sustained, entry of Ca^{2+} through CRAC channels is required to counteract loss of Ca^{2+} from the cell by the plasma membrane Ca^{2+} ATPase (PMCA). It is found that oscillations run down more quickly in zero Ca^{2+} compared to 2 mM Ca^{2+} external solution (Di Capite et al 2009a). My previous experiments used thapsigargin (an antagonist of the SERCA pump) to activate CRAC channels. Although thapsigargin reliably activates CRAC channels to their full extent, it does not provide one with an insight into the gating of CRAC channels by calmodulin under physiological conditions. I therefore investigated whether calmodulin regulated physiologically-induced Ca^{2+} signals. Low, physiological concentrations of an important proinflammatory molecule (leukotriene $C_{4,}$ (LTC_4)) (Boyce 2007), involved in asthma and allergic rhinitis (Peters-Golden et al 2006), was used to induce cytosolic Ca^{2+} oscillations in RBL-1 cells. Calmodulin modulation of these oscillations was investigated using the calmodulin mutant constructs. Application of 160 nM of LTC_4 (previously used by Di Capite et al 2009a) evoked several repetitive cytosolic Ca^{2+} oscillations in untransfected or GFP cDNA transfected RBL-1 cells (figure 5**A**) which began at a $[Ca^{2+}]$ around 68 nM and rose to 111 nM. In contrast, in cells expressing CAM4M, the LTC_4-induced cytosolic Ca^{2+} oscillations were lost. Instead, a single large Ca^{2+} spike (starting at a $[Ca^{2+}]$ around 68 nM and rising to a concentration of 161 nM) that decayed slowly was observed (figure 5**B**) with either few small or no subsequent oscillations. Figure 5**C** shows the average number of cytosolic Ca^{2+} oscillations measured per 100s bin. In the presence of CAM4M, the number of oscillations per 100s bin is significantly reduced compared to untransfected cells (WT). This demonstrates that calmodulin is required to maintain LTC_4-induced cytosolic Ca^{2+} oscillations.

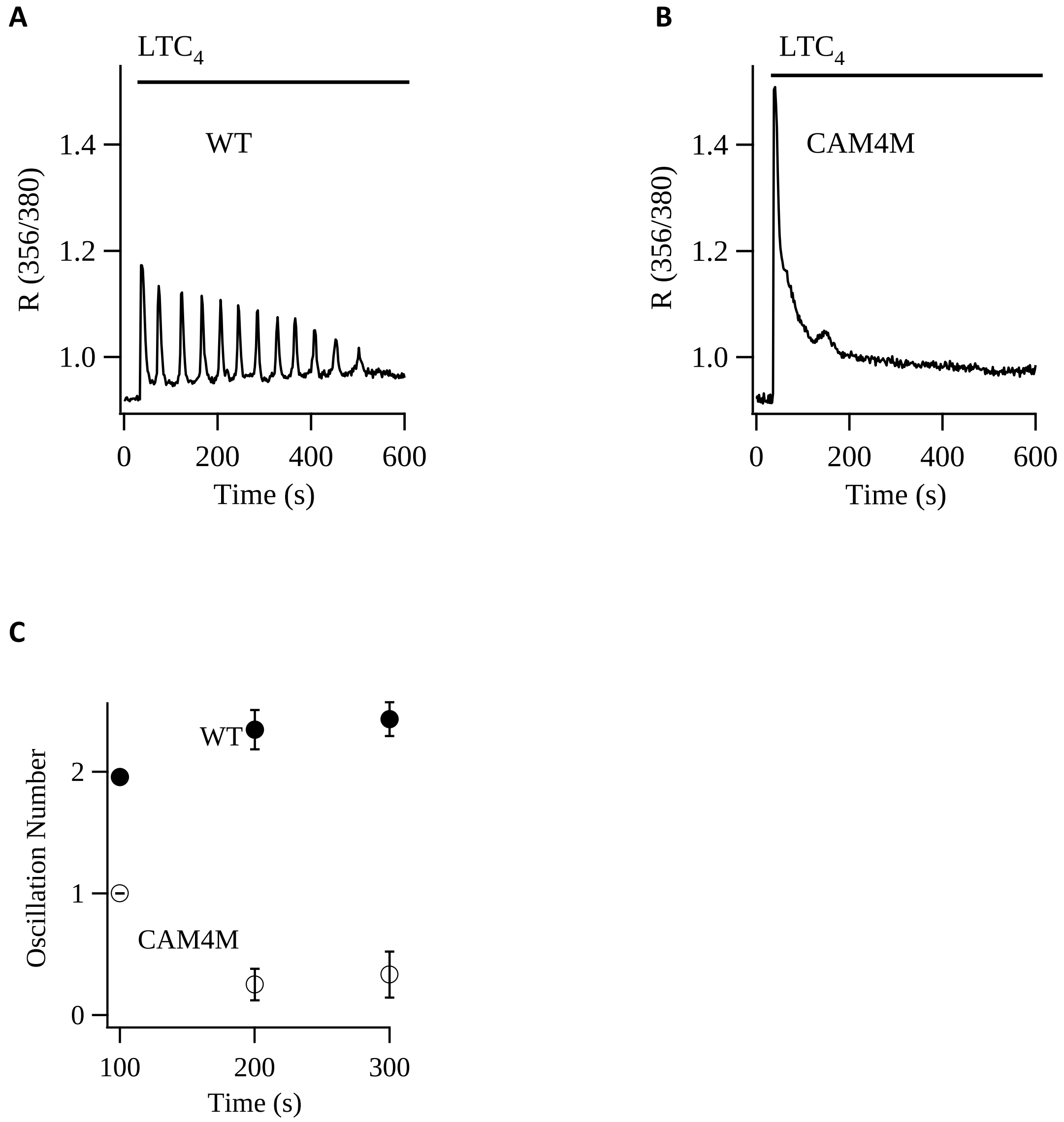

Figure 5. Calmodulin maintains physiologically-induced cytosolic Ca^{2+} oscillations. A, the trace illustrates the cytosolic Ca^{2+} oscillation pattern when an untransfected RBL-1 cell (WT) is bathed in 2 mM Ca^{2+} and stimulated with 160 nM LTC_4. The first cytosolic Ca^{2+} oscillation starts at a $[Ca^{2+}]$ around 68 nM and rises to 111 nM. **B**, the recording shows the LTC_4-induced Ca^{2+} oscillation pattern in one RBL-1 cell transfected with CAM4M. The cytosolic Ca^{2+} oscillation starts at a $[Ca^{2+}]$ around 68 nM and rises to 161 nM. **C**, presents aggregate data from 23 untransfected (WT) RBL-1 cells and 12 CAM4M transfected RBL-cells. The average number of oscillations per 100s bin is plotted and found to be significantly reduced in the presence of CAM4M.

g. The modulation of LTC_4-induced cytosolic Ca^{2+} oscillations by calmodulin does not involve CAM kinase II

One important Ca^{2+}-calmodulin dependent protein kinase is CAM Kinase II. It is possible that CAM kinase II, which is involved in Ca^{2+}-dependent facilitation of L-type calcium channels (Hudman et al 2005) and SOCCs in Xenopus oocytes (Machaca 2003), might also underlie the modulation of cytosolic Ca^{2+} oscillations by calmodulin in RBL-1 cells. However, when RBL-1 cells were pre-treated with 10 µM KN-62, an antagonist of CAM kinase II, for 15 minutes (previously used by Moreau et al 2006), LTC_4-induced cytosolic Ca^{2+} oscillations were maintained to a similar extent as was seen in the absence of KN-62 (figure 6). Therefore calmodulin is not acting through this kinase.

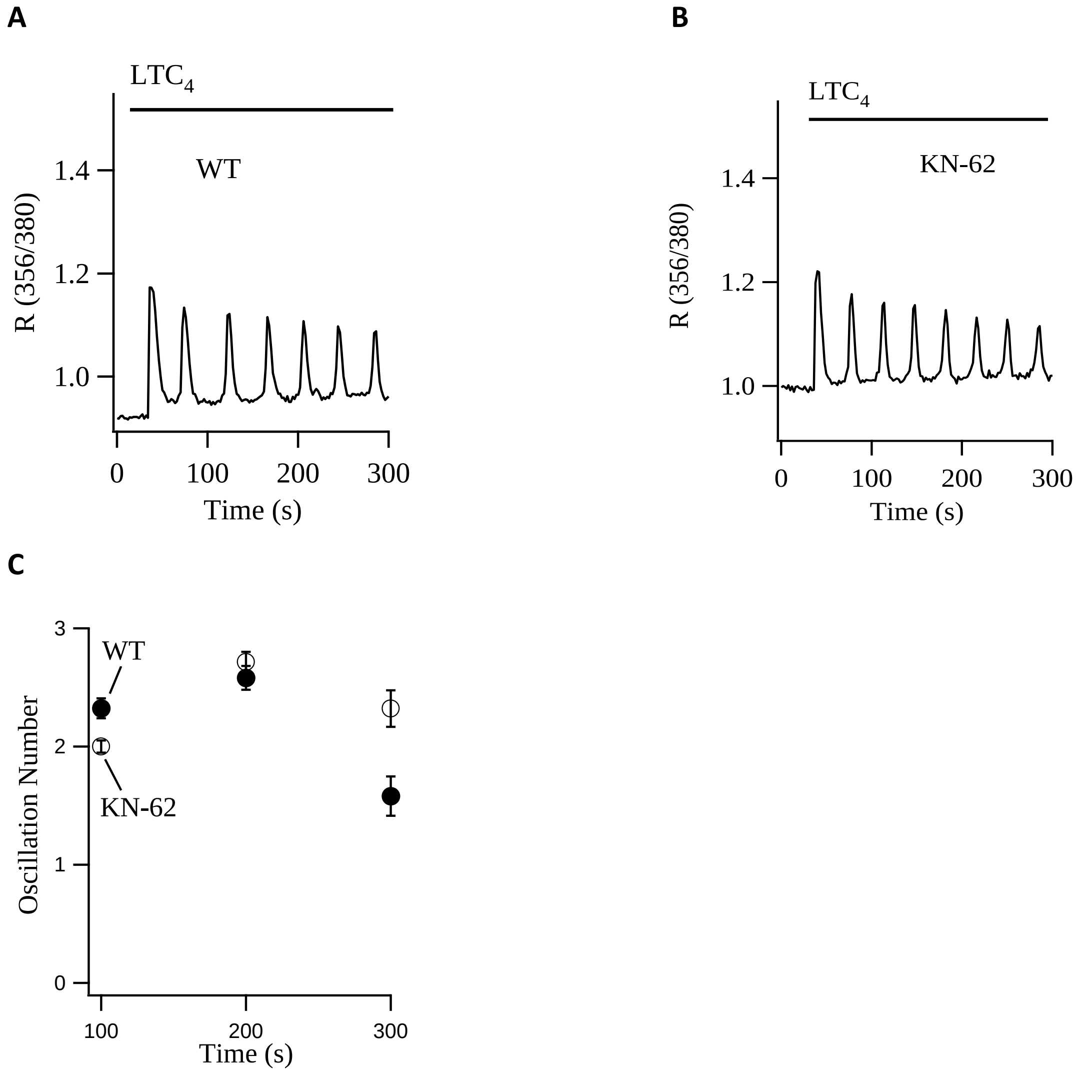

Figure 6. LTC$_4$-induced cytosolic Ca^{2+} oscillations are maintained in the presence of CAM kinase II blockade. A, the trace shows the cytosolic Ca^{2+} oscillation pattern when an untransfected RBL-1 cell (WT) is bathed in 2mM Ca^{2+} and stimulated with 160 nM LTC4. **B,** the recording illustrates the maintained pattern of cytosolic Ca^{2+} oscillations when one RBL-1 cell is pre-treated with 10 µM KN-62 in 2 mM external Ca^{2+} and stimulated with 160 nM LTC$_4$. **C**, presents aggregate data from RBL-1 cells in the absence (WT) (n=31) and the presence of 10 µM KN-62 (n=28). The time-course of the oscillations is similar in the two conditions.

h. Calmodulin modulates the maintenance of LTC$_4$-induced Ca^{2+} oscillations in a lobe-specific manner.

Since calmodulin was found to modulate CRAC channels in a lobe-specific manner, I examined the importance of each of the lobes of calmodulin in the control of LTC$_4$-induced Ca^{2+} oscillations. Consistent with the results observed in the presence of CAM4M, LTC$_4$-induced Ca^{2+} oscillations ran down more quickly in the presence of CAM2C (figure 7**A, D**). After the first oscillation, few or no further oscillations subsequently occurred. In contrast, figure 7**B** shows that oscillations were largely maintained in cells transfected with CAM2N, reminiscent of the pattern seen in untransfected RBL-1 cells. The Ca^{2+} signal remained elevated after the initial Ca^{2+} transient but the striking difference was that it then convened into the typical Ca^{2+} oscillation pattern (figure 7**B**). Figure 7**C** shows the difference in the average number of Ca^{2+} oscillations counted per 100s bin. Fewer oscillations are recorded per 100s bin in cells expressing CAM2C compared to untransfected RBL-1 cells or cells expressing CAM2N. The number of oscillations per 100s bin for CAM2C is similar to that with CAM4M (Figure 7**D**). Together the results demonstrate a greater importance of the C-lobe of calmodulin in maintaining physiologically-induced cytosolic Ca^{2+} oscillations.

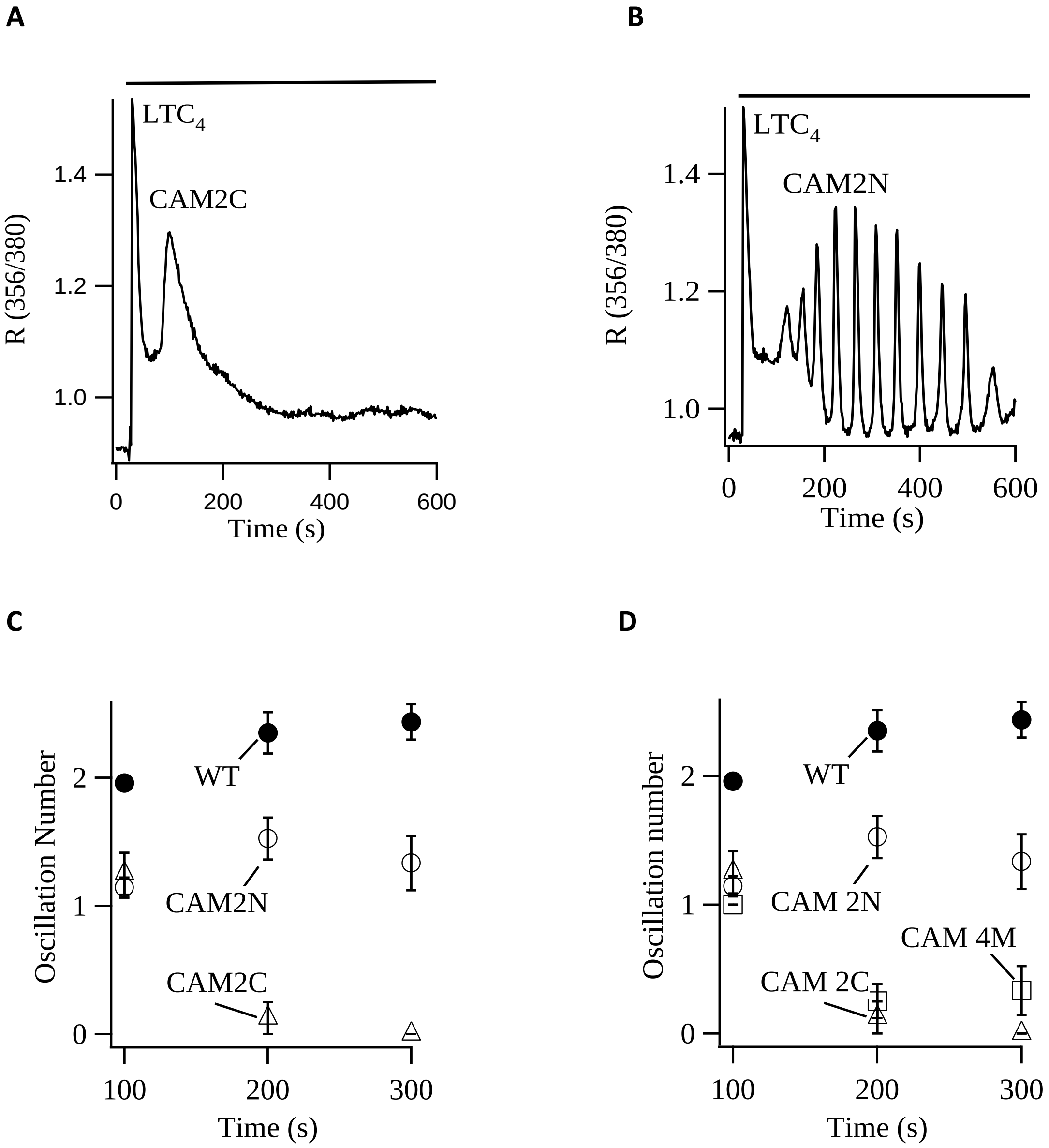

Figure 7. Calmodulin modulates LTC$_4$-induced Ca^{2+} oscillations in a lobe-specific manner. A, the trace reveals the Ca^{2+} oscillation pattern in one RBL-1 cell transfected with CAM2C and stimulated with 160 nM LTC$_4$ in 2 mM external Ca^{2+} solution. **B**, illustrates continuous LTC$_4$-induced Ca^{2+} oscillations in a single RBL-1 cell transfected with CAM2N. **C**, compares the average number of Ca^{2+} oscillations per 100s bin between untransfected RBL-1 cells (WT, n=52) and cells transfected with CAM2C (n=19) or CAM2N (n=15). **D**, shows the average number of Ca^{2+} oscillations per 100s bin for untransfected RBL-1 cells (WT) and each of the calmodulin mutants (CAM2N-open circles, CAM2C-open triangles and CAM4M-open squares).

i. Ca^{2+} influx through CRAC channels sustains cytosolic Ca^{2+} oscillations.

I have shown that calmodulin modulates CRAC channels. Can the effects of calmodulin on cytosolic oscillations be explained entirely through their effect on CRAC channels? It has been shown that CRAC channel driven Ca^{2+} entry supports LTC_4-induced Ca^{2+} oscillations (Di Capite et al 2009a). Repetitive cytosolic Ca^{2+} oscillations observed in 2 mM Ca^{2+} external solution ran down quickly in the absence of external Ca^{2+} (by 600s oscillations were lost) or after block of CRAC channels with 1 µM Gd^{3+} (Di Capite et al 2009a). I reduced Ca^{2+} entry to a level similar to that seen after expression with CAM4M, by partial block of CRAC channels with Synta (1 µM), (3-fluoropyridine-4-carboxylic acid (2’,5’-dimethoxybiphenyl-4-yl)amide), or by bathing cells in 0.5 mM (instead of 2 mM) external calcium. Both conditions reduced Ca^{2+} entry by approximately 50%, similar to the extent observed with CAM4M. Consistent with work by Di Capite et al 2009a, I found that cytosolic Ca^{2+} oscillations ran down more quickly when I reduced external calcium (to 0.5 mM) (Figure 8**A**). Furthermore I partially blocked CRAC channels by pre-treating cells for 5 minutes with 1 µM Synta, (a CRAC channel blocker identified by Ng et al 2008). 1 µM is close to the IC_{50} for I_{CRAC} inhibition. In 1 µM Synta, the cytosolic Ca^{2+} oscillations ran down more quickly compared to control cells in the absence of Synta (figure 8**B**). To strengthen this pharmacological result, I knocked down Orai1 (the plasma membrane protein that harbours the pore subunit of the CRAC channel) by transfecting RBL-1 cells with Orai1 RNAi. Orai1 RNAi was co-transfected with GFP cDNA to identify cells that had been successfully transfected. Consistent with the above findings, the Ca^{2+} oscillations were found to run down more quickly after knockdown of Orai1 and to a similar extent as was found with pharmacological blockade of CRAC channels with 1 µM Synta, compared to untransfected or GFP transfected cells (figure 8**C**). Collectively, the experiments demonstrate a role for CRAC channel dependent Ca^{2+} entry in the maintenance of cytosolic Ca^{2+} oscillations. Since calmodulin modulates CRAC channel dependent Ca^{2+} entry in a lobe-specific manner, it suggests that lobe-specific modulation of LTC_4-induced Ca^{2+} oscillations by calmodulin is mediated at least in part, through effects on CRAC channel activity.

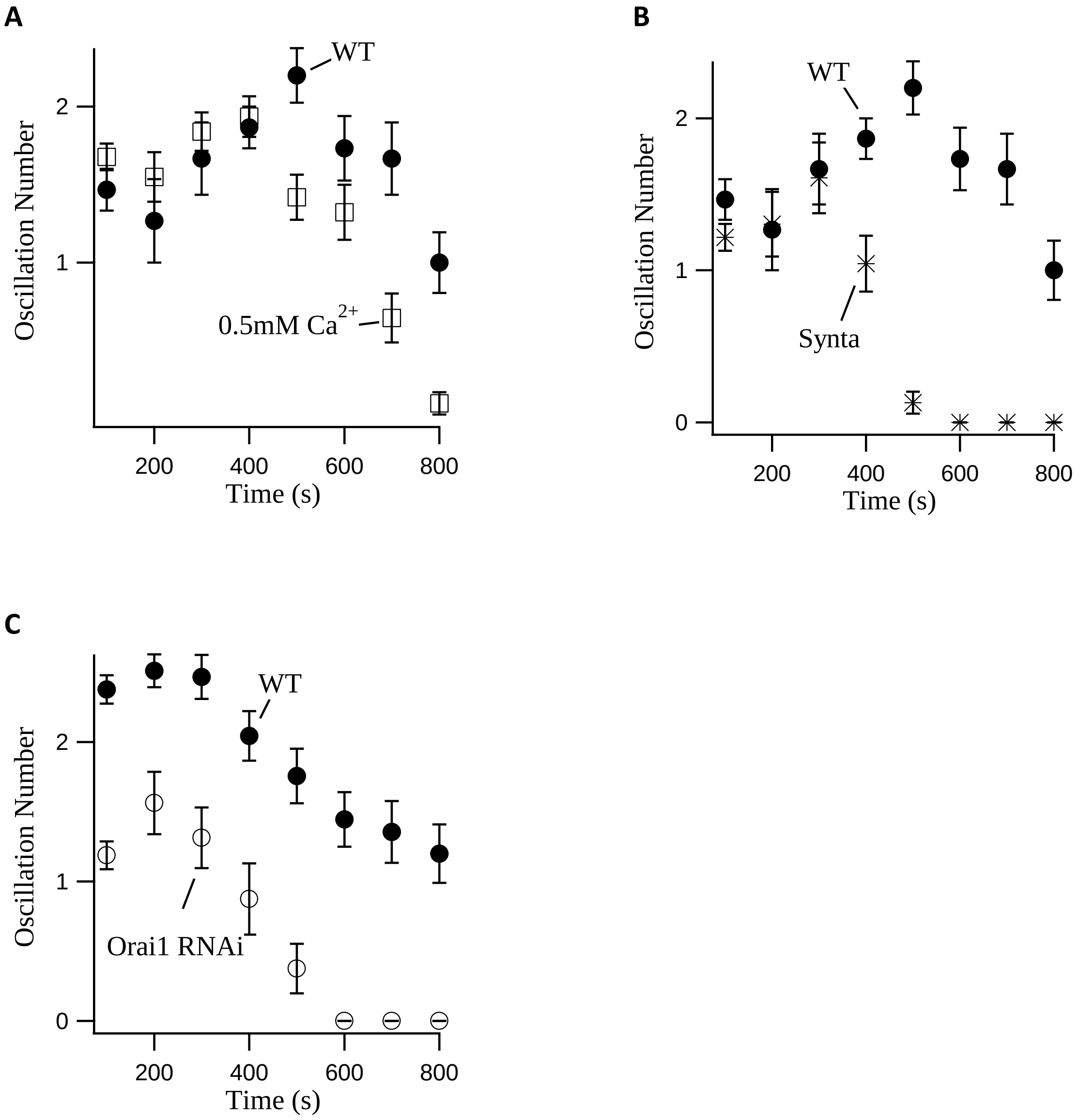

Figure 8. CRAC channel dependent Ca^{2+} entry is required to maintain LTC_4-induced Ca^{2+} oscillations. A, compares the average number of LTC_4-induced Ca^{2+} oscillations per 100s bin for RBL-1 cells that are bathed in 2 mM external Ca^{2+} (WT; n=15) or 0.5 mM external Ca^{2+} (n=31) and stimulated with 160 nM LTC_4. Oscillations ran down more quickly in low external Ca^{2+}. **B**, the average number of Ca^{2+} oscillations per 100s bin for RBL-1 cells bathed in 2 mM Ca^{2+} external solution and stimulated with 160 nM LTC_4, in the presence (n=23) or absence (WT; n=15) of 1 µM Synta are compared. **C**, presents aggregate data from 45 untransfected RBL-1 cells (WT) and 16 Orai1 RNAi transfected RBL-1 cells comparing the average number of LTC_4-induced Ca^{2+} oscillations per 100s bin.

j. Calmodulin also impacts on IP_3 receptor-driven Ca^{2+} release.

A faster run down of cytosolic Ca^{2+} oscillations is seen in the presence of 1 µM Synta, 0.5 mM external Ca^{2+} or knockdown of Orai1 (compared to their corresponding controls). However, the extent of such run down was considerably slower than that found after the expression of CAM4M (figure 5**B**, 5**C**) or CAM2C (figure 7**A**, **C**) despite a similar level of CRAC channel dependent Ca^{2+} entry in each of these conditions. The effects of calmodulin cannot therefore be attributed solely to the modulation of Ca^{2+} influx. Calmodulin likely has an action on Ca^{2+} release as well. Consistent with this idea is the finding that calmodulin affects the size of the first LTC_4-induced oscillation peak. This largely reflects IP_3 receptor (IP_3R)-driven Ca^{2+} release since the amplitude of the first Ca^{2+} oscillation peak is very similar in 2 Ca^{2+} and zero Ca^{2+} external solution, as is illustrated by Di Capite et al 2009a (see figure 2A-C of this paper).

In the presence of CAM4M, the first LTC_4-induced peak was significantly higher in amplitude compared to the response seen in untransfected RBL-1 cells (figures 9**A** and **B,** see also figure 5**B**). Cells expressing CAM2C or CAM2N also exhibited a significantly higher first oscillation peak in response to LTC_4, compared to untransfected cells (figures 9**C** and **D,** respectively, see figures 7**A** and **B f**or typical cell recordings). However, the effect seen with either of these mutants was not as dramatic as the result with CAM4M. Since both CAM2C and CAM2N significantly increase the size of the first LTC_4-induced oscillation by a similar amount, each lobe of calmodulin seems to be equally effective in the modulation of IP_3R-driven Ca^{2+} release. The effect is additive because adding the responses of both CAM2C and CAM2N together is similar to that seen with the dominant negative calmodulin mutant, CAM4M (figure 9**E**). The results provide evidence that calmodulin exerts an effect on IP_3R-driven Ca^{2+} release via an action that does not reflect a lobe-specific modulation. Since thapsigargin-evoked Ca^{2+} release (in zero Ca^{2+}) is not potentiated by the mutants (data given in section **c**), the increased Ca^{2+} release in response to LTC_4 does not reflect an increase in ER Ca^{2+} store content (more on this shall be discussed later).

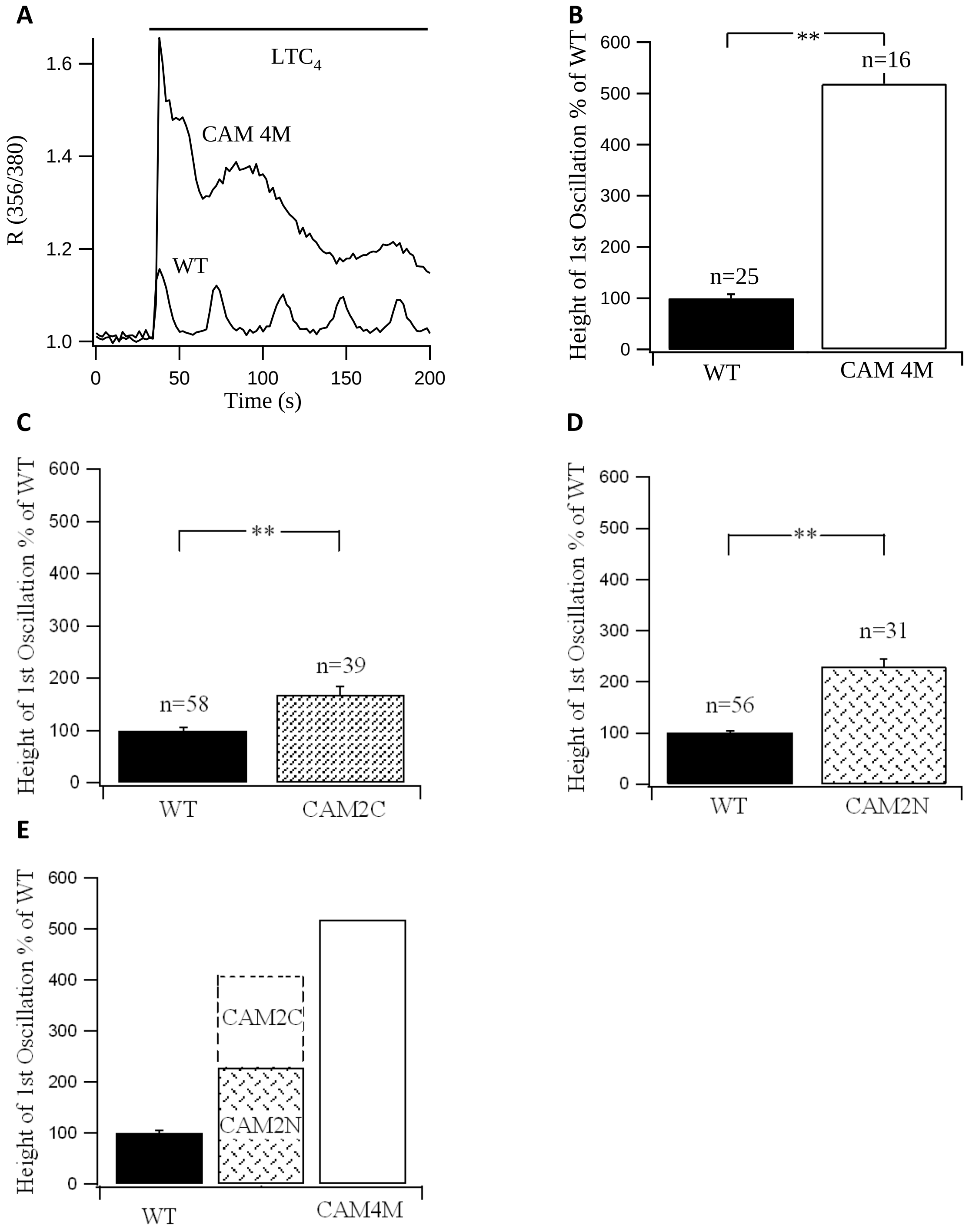

Figure 9. The effect of calmodulin on IP$_3$-mediated Ca^{2+} release. A, the traces illustrate the difference in the size of the first Ca^{2+} oscillation peak induced by 160 nM LTC$_4$ in 2 mM Ca^{2+} between an untransfected RBL-1 cell (WT) and a cell expressing CAM4M. **B**, aggregate data from 25 untransfected (WT) and 16 CAM4M transfected RBL-1 cells ($p<0.0001$) compare the average amplitude of the first oscillation peak. **C**, averaged data comparing responses from 58 untransfected (WT) and 39 CAM2C transfected RBL-1 cells ($p<0.0001$) are shown. **D**, data collected from 56 untransfected (WT) and 31 CAM2N transfected RBL-1 cells ($p<0.0001$) compare the average amplitude of the first oscillation peak. **E**, the average size of the first oscillation peak between cells expressing CAM4M and the amplitude of the response of both the CAM2C and CAM2N added together are compared.

k. Mitochondrial involvement in LTC_4-induced Ca^{2+} oscillations

Several studies have found that mitochondrial Ca^{2+} buffering regulates CRAC channels. Using whole-cell patch clamp techniques, Gilabert and Parekh 2000 revealed that increasing mitochondrial Ca^{2+} buffering, by dialyzing RBL-1 cells with a cocktail to maintain mitochondria in their energized state, enhanced I_{CRAC} in response to thapsigargin stimulation. Furthermore, Glitsch et al 2002 showed that depolarizing the inner mitochondrial membrane (preventing mitochondrial Ca^{2+} buffering) with FCCP or co-treatment with antimycin A (to block complex III of the respiratory chain) and oligomycin (to inhibit ATP synthase), impaired CRAC channel driven Ca^{2+} entry upon thapsigargin stimulation.

Following this, it has been shown that calmodulin is an important regulator of mitochondrial Ca^{2+} uptake in RBL cells. Csordás and Hajnóczky 2003 revealed that cytoplasmic calmodulin facilitated mitochondrial Ca^{2+} uptake in a Ca^{2+}-dependent manner. They used a novel method to measure the permeability of mitochondrial Ca^{2+} uptake via the mitochondrial Ca^{2+} uniporter. This involved measuring the quench rate of the Ca^{2+} sensitive dye Fura 2-FF (compartmentalised to the mitochondrial matrix), by Mn^{2+} which had passed through the uniporter upon administration of IP_3. IP_3 application caused an increase in cytosolic $[Ca^{2+}]$ which stimulated the uniporter. Mn^{2+} permeated the uniporter and quenched dye compartmentalised in the mitochondria, revealing that IP_3-driven Ca^{2+} release increased the permeability of the mitochondrial uniporter. This enhanced Mn^{2+} quench remained even 90s after IP_3 stimulation, suggestive of a sustained increase in mitochondrial uniporter permeability. Furthermore, this sustained increase in uniporter permeability was inhibited by the calmodulin antagonists calmidazolium and W-7, demonstrating Ca^{2+}-

calmodulin dependent facilitation of the mitochondrial Ca^{2+} uniporter. Ca^{2+}-calmodulin dependent facilitation of mitochondrial Ca^{2+} uptake in permeabilized RBL-1 cells was confirmed by Moreau et al 2006 using an alternate approach. This involved measuring changes in mitochondrial matrix [Ca^{2+}] in response to a high cytosolic Ca^{2+} load, using the fluorescent probe Rhod 2, located within the matrix. They showed that the calmodulin antagonists calmidazolium and W-7 significantly impaired mitochondrial Ca^{2+} uptake in response to the application of high cytosolic Ca^{2+}.

I have therefore carried out a series of experiments to investigate the hypothesis that mitochondrial Ca^{2+} buffering underlies the mechanism by which calmodulin modulates CRAC channel activity and maintains LTC_4-induced Ca^{2+} oscillations in a lobe-specific manner:

1. I administered the protonophore, FCCP (carbonyl cyanide 4-(trifluoromethoxy) phenylhydrazone), to collapse the mitochondrial membrane potential by dissipating the pH gradient. In the presence of 5 µM FCCP (previously used by Glitsch et al 2002), LTC_4-induced Ca^{2+} oscillations ran down more quickly. This was in a similar manner to that seen in the presence of CAM2C and CAM4M. A transient first oscillation spike was observed, which quickly decayed, with few or no further Ca^{2+} oscillations (figure 10**A**). Aggregate data in figure 10**B** depicts the average number of oscillations measured per 100s bin. In the presence of FCCP the number of oscillations recorded per 100s bin was significantly reduced compared to conditions where FCCP was absent. Together (and with findings by Glitsch et al 2002) the results demonstrate that the efficient uptake of Ca^{2+} by mitochondria is required to maintain CRAC channel activation and LTC_4-induced Ca^{2+} oscillations. It is unlikely

that ATP levels are significantly affected by 5 µM FCCP and that this might account for some of the effect of FCCP on LTC_4-induced Ca^{2+} oscillations since Glitsch et al 2002 found that FCCP reduced I_{CRAC} to the same extent in the presence or absence of oligomycin and dialyzing cells with IP_3 and 10 mM Mg-ATP failed to rescue impaired I_{CRAC} in cells pre-treated with antimycin A and oligomycin. Although ATP levels were not monitored in my experiment one could follow ATP levels after application of FCCP by fluorometrically monitoring the redox state of the pyridine nucleotide NADPH. Reduced NADP/ NADPH ratio causes an increase in fluorescence. Such a technique has been used by Hajnóczky et al in 1995.

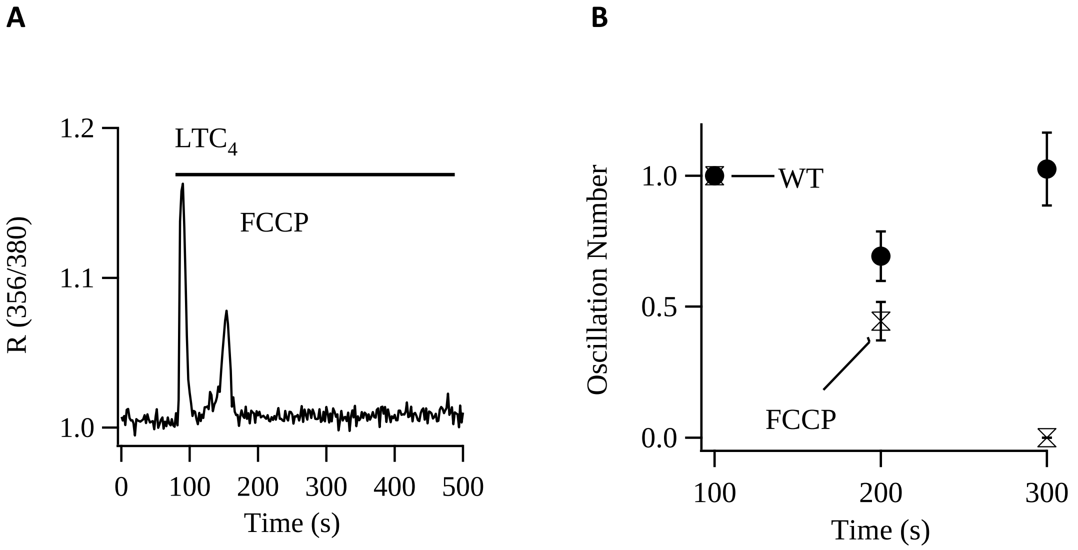

Figure 10. FCCP impairs the maintenance of LTC$_4$-induced Ca^{2+} oscillations. **A**, presents the oscillation pattern observed in one RBL-1 cell stimulated with 160 nM LTC$_4$ whilst bathed in 2 mM of external Ca^{2+}, following pre-incubation for 4 minutes with 5 µM FCCP. **B**, aggregate data reveals the number of LTC$_4$-induced Ca^{2+} oscillations that are recorded per 100s bin in the presence (n=54) or absence of FCCP (WT, n=54). Oscillations run down more quickly when cells are exposed to 5 µM FCCP for 4 minutes.

2. To strengthen the pharmacological evidence found with FCCP, I carried out a separate experiment using an alternative approach to disrupt mitochondrial Ca^{2+} buffering. Mitochondria take up Ca^{2+} passively via the mitochondrial Ca^{2+} uniporter (MCU), a highly Ca^{2+}-selective transporter (Kirichok et al 2004) that is situated within the inner mitochondrial membrane (IMM), (De Stefani et al 2011, Baughman et al 2011). A key subunit required for mitochondrial Ca^{2+} uptake has been identified by Perocchi et al 2010 using targeted RNAi screening techniques. This subunit, named the mitochondrial Ca^{2+} uniporter regulator (MICU1, mitochondrial calcium uptake 1), is a single transmembrane spanning protein, possessing two EF hand domains and localising within the IMM. Perocchi et al 2010 demonstrated that silencing MICU1 in HeLa cells abolished mitochondrial Ca^{2+} uptake.

I knocked down endogenous MICU1 by transfecting cells with MICU1 RNAi and examined the impact on CRAC channel driven Ca^{2+} entry and LTC_4-induced Ca^{2+} oscillations in RBL-1 cells. The initial rate of CRAC channel driven Ca^{2+} entry was significantly reduced in cells transfected with MICU1 RNAi (see figure 11**A** for typical cell traces and **B** for aggregate data). Furthermore, LTC_4-induced Ca^{2+} oscillations ran down more quickly in RBL-1 cells transfected with MICU1 RNAi compared to untransfected or GFP cDNA transfected RBL-1 cells (figure 11**C**, **D**). LTC_4-induced Ca^{2+} oscillations were seen to run down in a similar manner as that observed in cells expressing CAM4M, CAM2C or after pre-incubation with FCCP. A change to ATP levels cannot account for any of these effects since transfecting cells with MICU1 RNAi does not significantly alter ATP levels. This has been revealed by Perocchi et al 2010 who found that cells transfected with MICU1 RNAi had intact oxidative phosphorylation.

My results confirm that mitochondrial Ca^{2+} uptake facilitates CRAC channel dependant Ca^{2+} entry (illustrated in cartoon model **3**) and is needed to sustain cytosolic Ca^{2+} oscillations.

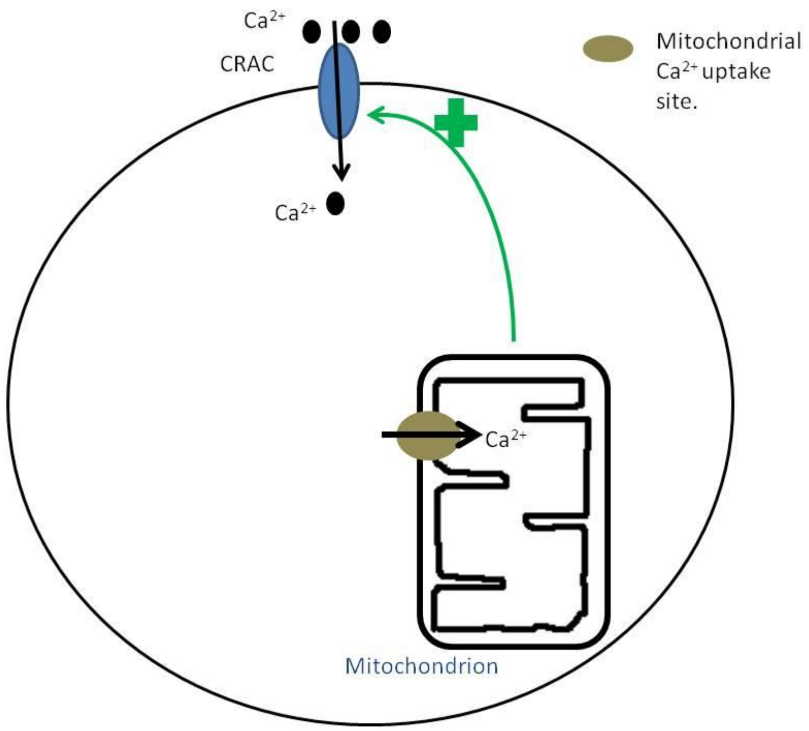
Ca2+
CRAC
Ca2+
Mitochondrial
Ca2+ uptake
site.
Ca2+
Mitochondrion

Cartoon model 3 illustrates the facilitation of CRAC channel dependent Ca^{2+} entry by mitochondrial Ca^{2+} buffering.

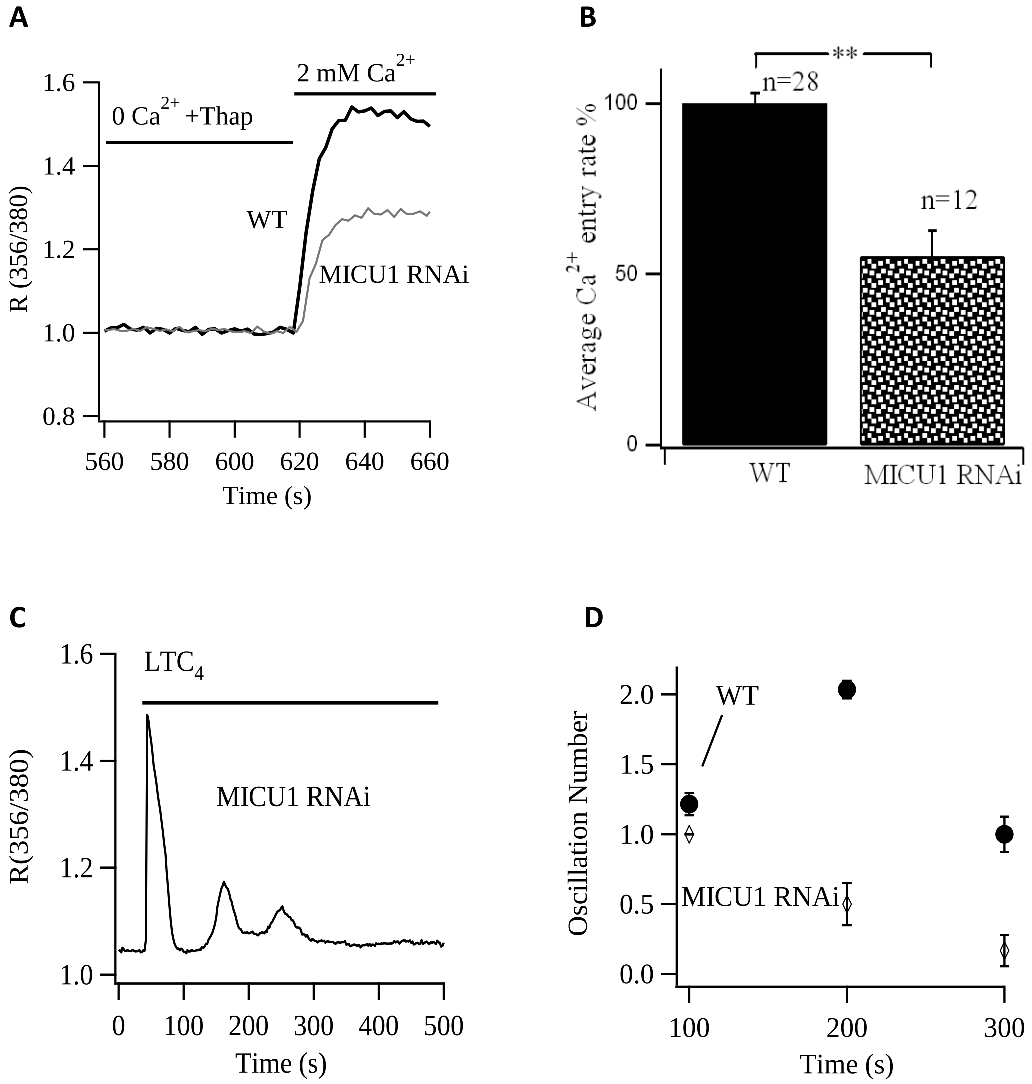

Figure 11. Knockdown of MICU1 impairs CRAC channel dependent Ca^{2+} entry and maintenance of LTC_4-induced Ca^{2+} oscillations. A, the traces reveal that the initial Ca^{2+} entry through CRAC channels is reduced in the presence of MICU1 RNAi compared to an untransfected RBL-1 cell (WT) (the same protocol is used here as in section **b**). **B**, compares CRAC channel driven Ca^{2+} entry between 23 untransfected (WT) and 12 MICU1 RNAi transfected RBL-1 cells ($p<0.0001$). **C**, the recording shows the Ca^{2+} oscillation pattern in one RBL-1 cell transfected with MICU1 RNAi and stimulated with 160 nM LTC_4 in 2 mM external Ca^{2+} solution. **D**, aggregate data from 28 untransfected RBL-1 cells (WT) and 12 MICU1 RNAi transfected RBL-1 cells, compares the average number of Ca^{2+} oscillations recorded per 100s bin following LTC4 stimulation (160 nM) in 2 mM external Ca^{2+}. Fewer oscillations are recorded per 100s bin when MICU1 is knocked down.

3. Oscillations ran down more quickly in FCCP or after knockdown of MICU1 than in zero Ca^{2+} external solution (Di Capite et al 2009a). This suggests mitochondria might affect IP_3R-driven Ca^{2+} release, as has been reported in Xenopus oocytes (Jouaville et al 1995). Therefore I designed experiments to see if mitochondrial Ca^{2+} uptake affected regenerative Ca^{2+} release in RBL-1 cells. One way to address this is to apply 1 mM lanthanum (La^{3+}) to block the plasma membrane Ca^{2+} ATPase (PMCA) pump in Ca^{2+}-free solution to impair effective Ca^{2+} clearance from the cytoplasm since PMCA is the major extrusion pathway in these cells (Carafoli 1991, Moreau et al 2005). In the presence of La^{3+} and zero Ca^{2+} external solution, no Ca^{2+} is able to enter or leave the cell. Ca^{2+} released by IP_3 receptors is therefore recycled within the cell, refilling the Ca^{2+} stores for subsequent release so that cytosolic Ca^{2+} oscillations can be maintained (Di Capite et al 2009a). Figure 12**A** shows the repetitive cytosolic Ca^{2+} oscillations that are observed when LTC_4 is applied to RBL-1 cells in the absence of external Ca^{2+} but in the presence of La^{3+}. Pre-treatment with 5 µM FCCP caused these oscillations to run down quickly. A transient first spike is observed, which quickly decays and subsequent oscillations rapidly run down (figure 12**B, C**). Since oscillations run down in the presence of 5 µM FCCP even when plasma membrane Ca^{2+} removal mechanisms are eliminated and Ca^{2+} influx is absent, the data suggest that mitochondrial Ca^{2+} buffering is required to maintain the cytosolic Ca^{2+} oscillations.

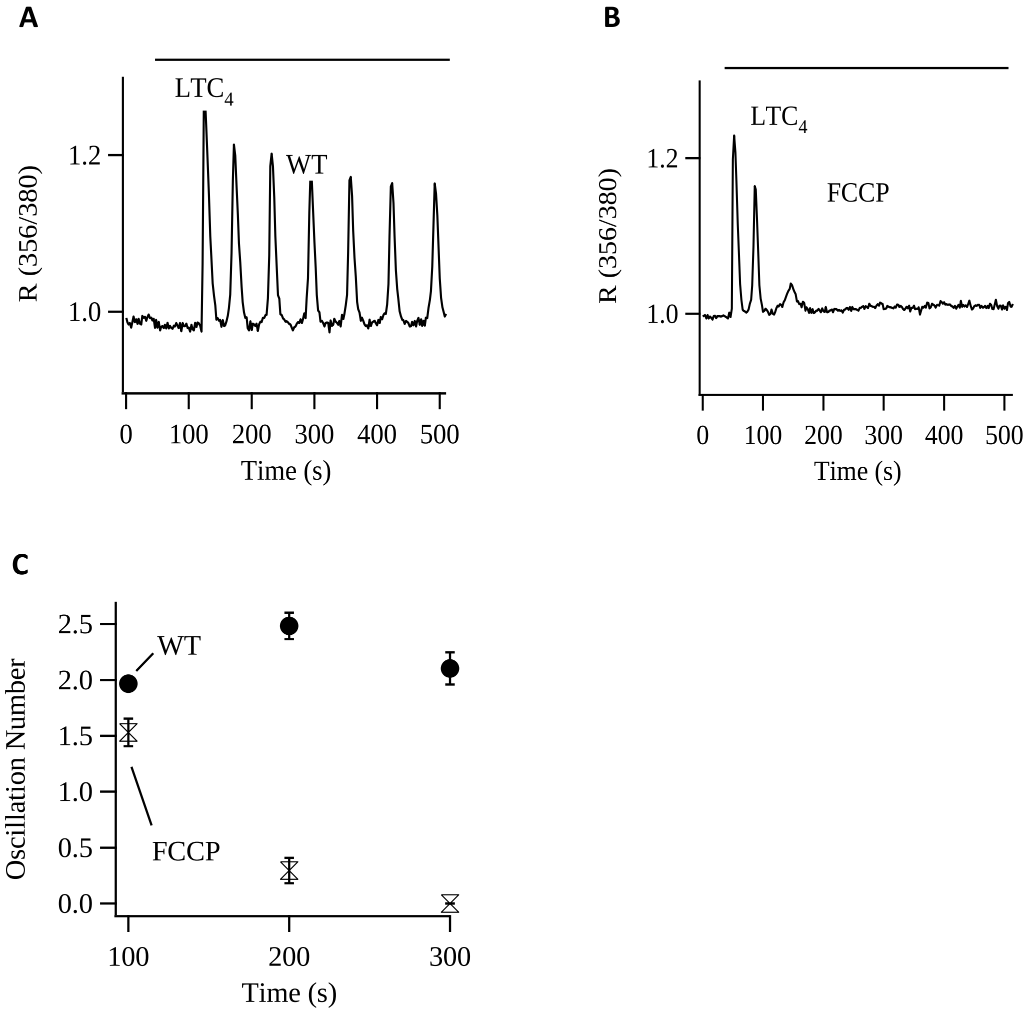

Figure 12. FCCP impairs the maintenance of LTC$_4$-induced Ca^{2+} oscillations even in the absence of external Ca^{2+} and presence of La^{3+}. **A**, presents the oscillation pattern when one RBL-1 cell is pre-incubated for 5 minutes in zero Ca^{2+} and 1 mM La^{3+} and subsequently stimulated with 160 nM LTC$_4$. In the presence of 1 mM La^{3+}, oscillations are sustained. **B**, the trace illustrates the oscillation pattern when one RBL-1 cell is pre-incubated for 5 minutes in zero Ca^{2+}, 5 µM FCCP and 1 mM La^{3+} and subsequently stimulated with 160 nM LTC$_4$. **C**, data collected from 29 RBL-1 cells in the absence of FCCP (WT) and 17 RBL-1 cells in the presence of FCCP compare the average number of LTC$_4$-induced Ca^{2+} oscillations recorded per 100s bin (in the presence of La^{3+}).

I. Addressing the mechanism underlying the increase in the first Ca^{2+} release spike induced by LTC_4 in the presence of the calmodulin mutants.

LTC_4-induced Ca^{2+} oscillations run down more quickly in low external Ca^{2+} (0.5 mM), in 1 µM Synta and after knockdown of Orai1 (figure 8) than in corresponding controls. Oscillations also run down more quickly after expression of CAM4M (figures 5**B**, **C**), CAM2C (figures 7**A**, **C**), but not CAM2N (figures 7**B**, **C**). Impairing mitochondrial uptake also leads to loss of these oscillations at a similar rate to the calmodulin mutants, CAM4M and CAM2C, (figures 10 and 11**C**, **D**). As will be shown in the next Chapter, (Chapter 4), calmodulin regulates mitochondrial Ca^{2+} uptake. The simplest explanation for calmodulin modulation of CRAC channels and LTC_4-induced Ca^{2+} oscillations is therefore through a stimulatory effect on mitochondrial Ca^{2+} uptake, reducing Ca^{2+}-dependent inactivation of the channels. However unlike with thapsigargin stimulation, agonist effects are complex and involve IP_3 production, fall in store Ca^{2+} content and IP_3R activity (which has a cytosolic Ca^{2+}dependency). The control of agonist-evoked oscillations by calmodulin is therefore unlikely to be solely by one mechanism (an action on mitochondrial Ca^{2+} uptake). I showed that the amplitude of the first LTC_4-induced Ca^{2+} release oscillation increased in the presence of the calmodulin mutants (figure 9), therefore in the following section I considered how this might occur. The increase in the first LTC_4-induced Ca^{2+} release spike in the presence of the calmodulin mutants could be due to:

1. *Increased Ca^{2+} store release*

The calmodulin mutants could increase the amount of Ca^{2+} within the intracellular Ca^{2+} stores so that upon IP_3R activation more Ca^{2+} would be released. However, only small differences (not statistically significant) in Ca^{2+} release in response to thapsigargin in Ca^{2+}-free solution (which reflects ER store content) were observed between cells transfected with CAM4M, (n=16, mean peak ratio 0.138 ± 0.00577 SEM.), CAM2C (n=13, mean peak ratio 0.128 ± 0.00661 SEM.) or CAM2N (n=19, mean peak ratio 0.122 ± 0.00963 SEM.), (p=NS between all variables). The mutants therefore have no significant effect on ER store Ca^{2+} content. Another more direct method to test this would be to genetically target a Ca^{2+} -sensitive fluorescent probe to the ER contents to measure ER [Ca^{2+}] directly in intact cells. Alternatively, cells could be loaded with a cell permeable Ca^{2+}-sensitive fluorescent dye (for example FURA 5FF-AM) and subsequently permeabilized with digitonin to remove non-compartmentalised dye.

2. *Change in IP_3R activity*

The increased Ca^{2+} release spike could be due to calmodulin affecting IP_3R activity, for example by directly acting on the IP_3R itself. Calmodulin is known to bind to type 1 and 2 IP_3Rs in a Ca^{2+}-dependent manner and regulate their activity. Yamada et al 1995 identified an amino acid sequence (Lys 1564- Arg 1585) on mouse IP_3R1 that bound calmodulin. Subsequent work by Hirota et al 1999 extended these results by showing that application of calmodulin impaired Ca^{2+} release through a purified, reconstituted IP_3R1 (Hirota et al 1999). In the absence of calmodulin, Michikawa et al 1999 showed that high [Ca^{2+}] could not inhibit purified, reconstituted IP_3R activity. Inhibition returned when calmodulin was present. Calmodulin is therefore crucial for Ca^{2+} -dependent regulation of IP_3R-driven Ca^{2+} release.

A separate Ca^{2+}-independent calmodulin binding site has also been identified within the N terminus of the IP_3R (Sipma et al 1999). Patel et al 1997 found that radioactively labelled calmodulin bound directly to the cerebellar type 1 IP_3R in the absence of calcium and this association inhibited IP_3 binding to the IP_3R. This has led Adkins et al 2000 to propose that several calmodulin binding sites probably exist on the IP_3R.

Calmodulin-dependent regulation of IP_3Rs is likely to be of clinical importance. Gerasimenko et al 2011 have found that calmodulin inhibits IP_3R-dependent Ca^{2+} release and trypsin activity in pancreatic acinar cells, in response to ethanol exposure. These results identify a potential therapy for treating alcohol-induced pancreatitis. My finding that the initial IP_3R-driven Ca^{2+} release spike is increased when calmodulin is rendered insensitive to Ca^{2+} is consistent with the concept that calmodulin inhibits IP_3R activity and that this is of physiological relevance.

3. *An effect on mitochondrial Ca^{2+} buffering*

Mitochondria are closely associated with the ER (Rizzuto et al 1998) and have been found to regulate IP_3R activity. Jouaville et al 1995 demonstrated in Xenopus oocytes that energizing mitochondria by injecting pyruvate/ malate or succinate resulted in faster and higher amplitude IP_3-driven Ca^{2+} release oscillations. They explained this effect through mitochondria buffering of IP_3R-driven Ca^{2+} release, thereby reducing Ca^{2+}-dependent inactivation of the IP_3R, which would promote further release. The calmodulin mutants may therefore increase the first LTC_4-induced Ca^{2+} release spike through affecting the ability of the mitochondria to take up Ca^{2+} released by IP_3Rs. To test this, I measured the size of the first Ca^{2+} release spike following knockdown of MICU1 (section **k.**, figure 11) or MFN2 (Chapter 5, section **d.**, figure 10). Knockdown of MICU1 increased the size of the first Ca^{2+} release spike (knockdown of MICU1 n=12, mean peak ratio 0.405 ± 0.0336 SEM., and untransfected RBL-1 cells, WT, n=28, mean peak ratio 0.265 ± 0.0173 SEM., p=0.0002). Knockdown of MFN2, which tethers ER to mitochondria, enabling effective mitochondrial Ca^{2+} uptake also significantly increased the initial IP_3-driven Ca^{2+} release spike.

In conclusion, the increase in the first LTC_4-induced Ca^{2+} release spike is probably due to enhanced IP_3R activity as well as likely effects by mitochondrial Ca^{2+} buffering. The higher amplitude of the first Ca^{2+} release spike in the presence of the calmodulin mutants cannot however explain the effects of calmodulin on CRAC channels since i) CAM2C and CAM2N lead to similar increases in LTC_4-induced Ca^{2+} release but only CAM2C leads to a decrease in thapsigargin-induced Ca^{2+} entry, and ii) the calmodulin mutants have little influence on thapsigargin-induced Ca^{2+} release, (which is independent of IP_3R-driven Ca^{2+} release). Knockdown of MICU1 or MFN2 both led to an increase in Ca^{2+} release, consistent with a contribution of mitochondria to buffering the initial Ca^{2+} release transient. Therefore both IP_3Rs and mitochondria are targets for calmodulin. Direct evidence showing that calmodulin regulates mitochondrial Ca^{2+} uptake is provided in the next Chapter, (Chapter 4).

3.3 Discussion

My findings demonstrate a lobe-specific function of calmodulin in the gating of CRAC channels and the maintenance of physiologically-induced cytosolic Ca^{2+} oscillations.

My results build upon the finding by Moreau et al 2005 that Ca^{2+}-calmodulin facilitates CRAC channel dependent Ca^{2+} entry, (cartoon model **1**). Moreau et al 2005 used the whole-cell patch clamp technique to directly measure I_{CRAC} in RBL-1 cells dialyzed with IP_3 in 0.3 mM EGTA. Under such conditions I_{CRAC} was severely reduced by overexpression of a dominant negative calmodulin mutant or after exposure to a calmodulin inhibitory peptide. Consistent with this, I found that in RBL-1 cells and HEK 293 cells transfected with a dominant negative calmodulin mutant completely insensitive to Ca^{2+} (CAM4M), or exposure to the calmodulin antagonist calmidazolium, the initial rate of Ca^{2+} entry through CRAC channels was significantly suppressed in a Ca^{2+}-dependent manner.

To investigate the possibility of lobe-specific modulation by calmodulin, I have used two additional calmodulin mutants, one where the N-lobe is insensitive to Ca^{2+} (CAM2N) and another where the C-lobe is insensitive to Ca^{2+} (CAM2C). CRAC channel activity was impaired in cells expressing CAM2C to a similar extent as that seen with CAM4M. However, CAM2N failed to alter CRAC channel activity compared to untransfected cells. These results add to the work by DeMaria et al 2001 on VOCCs in excitable cells. Through a series of mutagenesis experiments involving calmodulin mutant constructs, they established that each lobe of calmodulin exerts opposing modulatory effects on P/Q-type Ca^{2+} channels. They assigned distinct roles to both the N- and C-lobes. The C-lobe of calmodulin drove Ca^{2+}-dependent facilitation (CDF) whereas the N-lobe drove Ca^{2+}-dependent inactivation (CDI) of the P/Q-type Ca^{2+} channels. Therefore different Ca^{2+} channels in different cell types show different lobe-specific regulation by calmodulin.

In RBL-1 cells low concentrations of physiological agonists such as the proinflammatory molecule LTC_4 (Boyce 2007) induce repetitive cytosolic Ca^{2+} oscillations, (Di Capite et al 2009a). These can be observed continuously in 2 mM external Ca^{2+} but run down quickly in zero Ca^{2+} or in the presence of 1 µM Gd^{3+} to block CRAC channels (Di Capite et al 2009a). Ca^{2+} entry through CRAC channels is therefore required to support agonist-induced Ca^{2+} oscillations by supplying the Ca^{2+} needed to replenish the ER to allow for repetitive IP_3R-driven Ca^{2+} release. Consistent with this, LTC_4-induced cytosolic Ca^{2+} oscillations were shown to run down more quickly in the presence of 1 µM Synta (a submaximal concentration), after knockdown of Orai1 or by lowering the external $[Ca^{2+}]$ to 0.5 mM. All of these conditions partially impair CRAC channel driven Ca^{2+} entry and to the extent that is seen in the presence of CAM4M. To investigate the physiological relevance of CRAC channel gating by the C-lobe of calmodulin, I have tested each of the mutants' effects on LTC_4-induced Ca^{2+} oscillations. The LTC_4-induced Ca^{2+} oscillations ran down more quickly in the presence of CAM4M or CAM2C but in the presence of CAM2N the cytosolic Ca^{2+} oscillations continued. Together the results demonstrate a lobe-specific action of calmodulin on the maintenance of LTC_4-induced Ca^{2+} oscillations. However, agonist -induced Ca^{2+} oscillations are complex signals and calmodulin has many possible targets. Therefore it is unlikely that the modulation of LTC_4-induced Ca^{2+}

oscillations by calmodulin is only via a lobe-specific action of the protein on CRAC channels, (I will discuss this in more detail later on).

How might such lobe-specific modulation arise? Upon CRAC channel opening cytoplasmic Ca^{2+} concentration rises transiently. These transient signals negatively feedback to inactivate the channel. It has been found that the C-lobe of calmodulin can sense transient Ca^{2+} signals whereas the N-lobe cannot (Tadross et al 2008). This concept can be used to explain the lobe-specific gating of CRAC channels and maintenance of LTC_4-induced Ca^{2+} oscillations that I have observed. An important difference between the two lobes resides in the kinetics of Ca^{2+} binding and unbinding (Tadross et al 2008). Ca^{2+} binds to the N-lobe faster but dissociates from the N-lobe 170 times more rapidly than it does from the C-lobe (Johnson et al 1996). This means that transient Ca^{2+} signals are not long enough in duration for the N-lobe to transduce the signal to a downstream target such as the mitochondrial uniporter. Ca^{2+} that binds to the N-lobe upon CRAC channel opening would unbind rapidly upon closure of the CRAC channels due to the fast Ca^{2+} unbinding rate of the N-lobe. In this manner, the rapid on-rate and off-rate for Ca^{2+} binding to the N-lobe can be seen to be synchronized with CRAC channel opening and closure. In contrast, the C-lobe unbinds Ca^{2+} much more slowly. This means that once the C-lobe binds Ca^{2+} during CRAC channel opening it can hold on to the Ca^{2+} subsequent to the closure of the CRAC channels. This enables Ca^{2+}-calmodulin to reach downstream targets such as the mitochondrial uniporter. In conclusion, the C-lobe transduces transient signals through its ability to retain the Ca^{2+} signal even when the CRAC channels close. Following this, it is clear that the C-lobe of calmodulin is capable of facilitating CRAC channel dependent Ca^{2+} entry by cytoplasmic Ca^{2+}, whereas the N-lobe of calmodulin which is insensitive to transient cytoplasmic Ca^{2+} rises, is unable to participate in this type of modulation.

Such gating of CRAC channels by the C-lobe of calmodulin could arise from a direct action on the channel or via an indirect mechanism involving another regulatory step. Whole-cell patch clamp experiments carried out with my supervisor showed that the mechanism involved could not be directly on the channel itself. Although I_{CRAC} was significantly suppressed in cells expressing CAM4M in the presence of weak intracellular buffer, this effect was abolished in the presence of high intracellular buffer. This result is consistent with Moreau et al 2005. They showed that the presence of a calmodulin inhibitory peptide which suppressed I_{CRAC} in RBL-1 cells dialyzed in weak Ca^{2+} buffer, failed to do so in the presence of high Ca^{2+} buffer. The gating of CRAC channels by the C-lobe of calmodulin therefore requires a bulk rise in cytosolic [Ca^{2+}], (see cartoon model **2** for an illustration of this).

To identify the Ca^{2+}-dependent step involved, I have investigated a mechanism involving mitochondrial Ca^{2+} buffering. It is well known that mitochondrial Ca^{2+} uptake regulates CRAC channel development in weak physiological intracellular Ca^{2+} buffer. Gilabert and Parekh 2000 demonstrated that I_{CRAC} measured using whole-cell patch clamp techniques was significantly enhanced during dialysis with a solution that sustained mitochondrial Ca^{2+} buffering, (keeping mitochondria energized). In addition Glitsch et al 2002 revealed that elimination of mitochondrial Ca^{2+} buffering through depolarization of the inner mitochondrial membrane by administrating either FCCP, or antimycin A (to inhibit complex III of the respiratory chain) together with oligomycin (to inhibit ATP synthase), impaired CRAC channel dependent Ca^{2+} entry. They measured the initial rate of CRAC channel driven Ca^{2+} entry using Fura 2, following stimulation with thapsigargin in Ca^{2+}-free solution. Consistent with this previous work, my experiments assign physiological relevance to such control, since in the presence of FCCP, LTC_4-induced Ca^{2+} oscillations run down more quickly than in untransfected cells. Furthermore, I found that knockdown of MICU1 (an inner mitochondrial membrane EF hand containing protein identified by Perocchi et al 2010 to be a key regulatory subunit required for mitochondrial Ca^{2+} uptake), significantly impaired CRAC channel dependent Ca^{2+} entry and caused the LTC_4-induced Ca^{2+} oscillations to run down more quickly and to a similar extent as that seen in the presence of CAM4M, CAM2C or in the presence of FCCP. Together, the results confirm the physiological importance of the role played by mitochondrial Ca^{2+} buffering in the gating of CRAC channels (illustrated by cartoon model **3**) and suggests that the lobe-specific gating of CRAC channels by calmodulin might reflect a lobe-specific action on mitochondrial Ca^{2+} uptake. The C-lobe of calmodulin would facilitate CRAC channel dependent Ca^{2+} entry by facilitating mitochondrial Ca^{2+} buffering.

Since agonist-induced Ca^{2+} oscillations are complex and calmodulin is known to have many targets, the effects of calmodulin on LTC_4-induced Ca^{2+} oscillations are unlikely to be purely through one mechanism (an action on CRAC channel activity via effects on mitochondrial Ca^{2+} uptake). Furthermore, mitochondrial Ca^{2+} buffering impacts on more than just CRAC channel activity. Consistent with more than one mechanism being involved is the finding that oscillations run down less quickly in zero Ca^{2+} than in the presence of FCCP or CAM4M, so mitochondria and calmodulin must have an effect on LTC_4-induced Ca^{2+} oscillations in addition to CRAC channel modulation. There are two main sites where this action could be i) mitochondrial Ca^{2+} buffering and ii) the IP_3R itself. Reduced mitochondrial Ca^{2+} buffering causes higher local Ca^{2+} near IP_3Rs, leading to stronger Ca^{2+}-dependent inactivation of the IP_3Rs (Bezprozvanny et al 1991, Finch et al 1991) and so oscillations would disappear. Calmodulin could therefore be affecting LTC_4-induced oscillations through an action on mitochondrial Ca^{2+} buffering and thereby affecting IP_3R-driven Ca^{2+} release. The finding that knockdown of MICU1 increases the size of the first Ca^{2+} release spike (knockdown of MICU1 n=12, mean peak ratio 0.405 ± 0.0336 SEM., and untransfected RBL-1 cells, WT, n=28, mean peak ratio 0.265 ± 0.0173 SEM., p=0.0002; see also figure 11**C** and section **l.** 3.) and knockdown of MFN2 also increases release (see Chapter 5 section **d**) fits with this view. Another site for calmodulin could be ii) on the IP_3R itself, independent to mitochondrial Ca^{2+} uptake. Since calmodulin leads to Ca^{2+}-dependent inactivation of IP_3R, CAM4M, CAM2C and CAM2N would lead to less inactivation and therefore more release. More release results in stronger Ca^{2+}-dependent inactivation of the IP_3R and greater loss of Ca^{2+} due to PMCA extruding Ca^{2+}, so oscillations disappear. In 2 mM Ca^{2+}, oscillations disappear quickly for CAM4M and CAM2C because despite more release, less refilling of the Ca^{2+} stores occurs as a result of reduced influx in the presence of either of these mutants. Therefore stores do not have enough Ca^{2+} to sustain the oscillations. On the other hand in the presence of CAM2N, oscillations are largely maintained, the initial transient remains elevated at first but the oscillation pattern then restarts. This can be explained by the finding that CAM2N does not reduce Ca^{2+} influx. The delay before oscillations recover could be due to time for adequate refilling as well as recovery from Ca^{2+}-dependent inactivation of the IP_3R. In contrast, both the N- and C-lobes were found to significantly increase the amplitude of the first cytosolic Ca^{2+} release spike by a similar degree, both seemed to be equally important, and summating the N- and C-lobe responses mimicked the response seen with the dominant negative calmodulin mutant. The finding that calmodulin can affect the initial IP_3R-driven Ca^{2+} release in a manner that does not reflect a lobe-specific action is distinct from the action on Ca^{2+} entry. My results therefore suggest that a major intracellular Ca^{2+} channel (IP_3R) and a widespread Ca^{2+} influx pathway (CRAC channel dependent Ca^{2+} influx) show different lobe-specific modulation by calmodulin. The C-lobe plays a major role in the modulation of Ca^{2+} entry, whereas the N- and C- lobes seem to equally play important roles in the modulation of IP_3Rs.

Since MCU and MICU1 have recently been discovered, (De Stefani et al and Baughman et al 2011), future experiments could use bioinformatics to look for calmodulin binding sites. Following this, one could mutate these sites to see what happens to mitochondrial Ca^{2+} uptake and CRAC channel activity.

In summary my results in Chapter 3 have led me to propose a model underlying the lobe-specific modulation of CRAC channels by Ca^{2+}-calmodulin, whereby the C-lobe of calmodulin enhances CRAC channel dependent Ca^{2+} entry by facilitating mitochondrial Ca^{2+} buffering. Such a mechanism illustrated in cartoon model **4**, has been established by putting together my findings shown in cartoon model **1**, **2** and **3**.

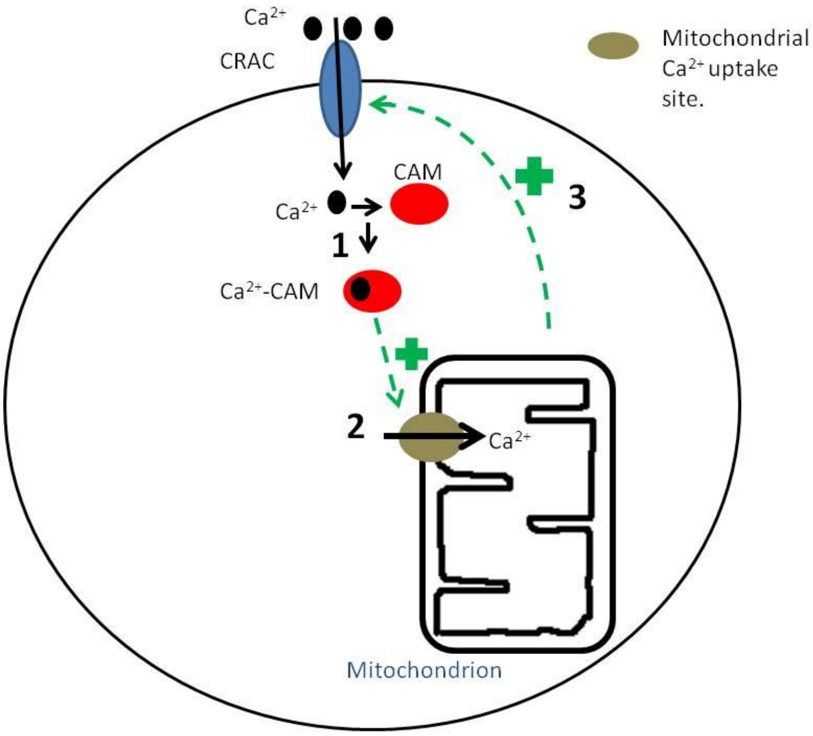

Cartoon model 4 illustrates the proposed model for the modulation of CRAC channels by cytoplasmic Ca^{2+}. Such modulation is heavily dependent on the C-lobe of calmodulin, probably due to differences in the kinetics of Ca^{2+} unbinding from the C-lobe and the N- lobe. Ca^{2+} dissociates from the C-lobe slowly whilst rapidly unbinds from the N-lobe. 1) Upon CRAC channel activation Ca^{2+} entry binds to calmodulin to form a Ca^{2+}-CAM (calmodulin) complex. 2) This complex facilitates mitochondrial Ca^{2+} buffering. 3) The enhanced mitochondrial Ca^{2+} buffering that results facilitates CRAC channel dependent Ca^{2+} entry. This is probably by reducing Ca^{2+}-dependent slow inactivation of the CRAC channels since i) Gilabert and Parekh (2000) have found Ca^{2+}-dependent slow inactivation of CRAC channels is enhanced in the presence of antimycin A and oligomycin to impair mitochondrial Ca^{2+} buffering and ii) the need for a bulk rise in cytosolic Ca^{2+} rules out Ca^{2+}-dependent fast inactivation of CRAC channels being involved. The development of slow Ca^{2+}-dependent inactivation of CRAC channels relies on a bulk rise in cytosolic Ca^{2+}.

My next results Chapter tests the idea that calmodulin regulates mitochondrial Ca^{2+} uptake by using a ratiometric, mitochondrial fluorescent protein to measure directly mitochondrial matrix [Ca^{2+}] in intact RBL-1 cells.

Chapter 4.

Regulation of mitochondrial Ca^{2+} uptake by calmodulin

4.1 Introduction

Mitochondria efficiently buffer rises in intracellular Ca^{2+}, thereby shaping cellular Ca^{2+} signals and regulating Ca^{2+}-dependent responses (Hajnóczky et al 1995, 1999, Tinel et al 1999, Jouaville et al 1995). Although the outer mitochondrial membrane (OMM) contains porins, the inner mitochondrial membrane (IMM) does not. Ca^{2+} uptake here occurs via the mitochondrial Ca^{2+} uniporter, (MCU), a 40 kDa protein channel which has only recently been established at a molecular level (De Stefani et al 2011, Baughman et al 2011). The highly Ca^{2+}-selective channel (Kirichok et al 2004), called the mitochondrial Ca^{2+} uniporter, MCU, passively takes up rises in cytosolic Ca^{2+} that are driven by the huge electrochemical gradient for Ca^{2+} across the IMM. This electrical gradient is achieved by the pumping of protons across the IMM, subsequent to the transfer of electrons (Mitchell 1966). As a result, a highly hyperpolarized potential is established across the membrane. The chemical component of the gradient is obtained through the maintenance of free Ca^{2+} within the mitochondrial matrix at low concentrations, due to a Ca^{2+}binding ratio estimated to be > 2,000 (Babcock et al 1997). In addition, matrix Ca^{2+} is maintained at low levels at rest, by the slow extrusion of Ca^{2+} out of the organelle mainly via the $3Na^{+}/Ca^{2+}$ exchanger, (Sedova et al 2000, Arnaudeau et al 2001, Tang et al 1997, Parekh 2003a, Palty et al 2010, 2012 who identified this as NCLX). As well as MCU, a required mitochondrial Ca^{2+} uniporter regulator, MICU1, has also been identified in HeLa cells by Perocchi et al 2010, using targeted RNAi screening techniques. This 53 kDa single transmembrane domain spanning protein also localises to the IMM, where it controls mitochondrial Ca^{2+} uptake probably via its ability to sense Ca^{2+} by two EF hand sensing domains. Perocchi et al 2010 showed mitochondrial Ca^{2+} uptake was impaired following knockdown of MICU1.

Evidence for the efficient buffering of cytosolic Ca^{2+} by mitochondria has been demonstrated by Csordás et al 2003, in RBL-2H3 cells. They used specifically targeted fluorescent probes to simultaneously measure changes in cytosolic and mitochondrial $[Ca^{2+}]$ upon administrating IP_3. In their experiments Fura 2-FF was compartmentalised to the mitochondrial matrix and Fluo 3 was retained in the cytoplasm. Moreau et al 2006 confirmed such a finding in RBL-1 cells, by means of an alternate approach, involving the loading of mitochondria with a membrane permeable fluorescent dye (Rhod 2-AM), and subsequently permeabilizing cells with digitonin to wash away remaining cytosolic dye. They recorded a clear mitochondrial Ca^{2+} rise in response to the application of a range of cytosolic Ca^{2+} loads. The uptake of Ca^{2+} by mitochondria under physiological conditions is important. By monitoring the redox state of flavin (the ratio of $FAD/FADH_2$) and pyridine nucleotides (the ratio of NADP/NADPH)), Hajnóczky et al 1995 showed that increased mitochondrial Ca^{2+} uptake in response to IP_3-driven cytosolic Ca^{2+} oscillations, increased the activity of mitochondrial Ca^{2+}-dependent enzymes important for ATP synthesis and metabolism.

Mitochondrial Ca^{2+} buffering is affected by a range of conditions including the state of the IMM potential, the location of mitochondria relative to high, local Ca^{2+} signals, the Ca^{2+} binding ratio within the mitochondrial matrix, the concentration of cytosolic Ca^{2+}, and the activity of the mitochondrial Ca^{2+} uniporter channel, which can be regulated by Ca^{2+}-calmodulin (Moreau et al 2006, Csordás and Hajnóczky 2003).

Depolarization of the IMM (which is normally maintained around -180 mV; Rizzuto et al 2000, Parekh 2003a, Mitchell 1966) impairs mitochondrial Ca^{2+} uptake because it removes the driving force for the passive uptake of Ca^{2+} by the uniporter. In chromaffin cells, Babcock et al 1997 found that application of CCCP (a photonophore that collapses the proton motive force) together with oligomycin (a mitochondrial ATP synthase inhibitor) depolarized the IMM. This resulted in a limited mitochondrial Ca^{2+} rise upon Ca^{2+} entry into the cytosol. Moreau et al 2006 provided evidence to support this finding in RBL-1 cells, where pre-incubation of another photonophore, FCCP, prevented a mitochondrial Ca^{2+} rise after application of even very high cytosolic Ca^{2+} loads. Collectively, the results reveal the widespread requirement for a highly hyperpolarized IMM potential for efficient mitochondrial Ca^{2+} buffering, in both excitable and non-excitable cells respectively.

Although mitochondria can buffer rises in cytosolic Ca^{2+}, they are particularly effective in taking up Ca^{2+} when located close to sites of high Ca^{2+}, typically seen near open Ca^{2+} channels (Rizzuto et al 1993, 1998, Quintana et al 2006). This is because the mitochondrial Ca^{2+} uniporter has a low affinity for Ca^{2+} (Km is ≈ 10 µM), (McCornmack et al 1990, Rizzuto et al 1993 and 2000, Nicholls 2005, Carafoli 2003, Moreau et al 2006, Parekh 2003a). Rizzuto et al 1993 and 1998 proposed that exposure of MCU to high, local concentrations of Ca^{2+} (much higher than bulk cytosolic $[Ca^{2+}]$) from Ca^{2+} release channels (IP_3R)) situated within the ER membrane, allowed for large cytosolic Ca^{2+} rises to be transmitted into the matrix by MCU. They found that histamine-induced Ca^{2+} release, in the absence of external Ca^{2+}, resulted in a larger and faster rise in mitochondrial $[Ca^{2+}]$ (measured using mitochondrial targeted aequorin), compared to the response found during Ca^{2+} influx after store depletion. Furthermore, the use of an aequorin chimera targeted to the mitochondrial intermembrane space, recorded a higher $[Ca^{2+}]$ compared to the bulk cytosolic $[Ca^{2+}]$, upon stimulation of IP_3R-dependent Ca^{2+} release (Rizzuto et al 1998). This higher $[Ca^{2+}]$ represents the IP_3R-evoked Ca^{2+} microdomains. Co-transfection of specific organelle targeted GFP tagged proteins showed that the ER and mitochondria were located within close proximity, (around 20 nm) (Rizzuto et al 1993, 1998). This underpins the effective transfer of Ca^{2+}. Disruption of this close association impairs mitochondrial Ca^{2+} uptake, which I shall discuss later in Chapter 5.

In RBL cells, MCU Ca^{2+} uptake is found to be biphasically regulated by Ca^{2+} (Ca^{2+} both activates and inactivates MCU). Moreau et al 2006 demonstrated the ability of cytosolic Ca^{2+} to inactivate MCU. They showed that the mitochondrial Ca^{2+} rise observed after application of a high cytosolic Ca^{2+} load (100 µM Ca^{2+}) was significantly reduced in the presence of a small pre-pulse of Ca^{2+}(10 µM). In addition Ca^{2+}-calmodulin dependent facilitation of MCU had previously been revealed by Csordás et al 2003 and later confirmed by Moreau et al 2006 in RBL cells. Csordás et al monitored the rate which Mn^{2+} that had passed through the uniporter quenched Fura 2-FF (compartmentalised in the mitochondrial matrix) and used this to report a sustained increase in MCU permeability upon IP_3 stimulation. Such an effect was impaired by calmodulin antagonists calmidazolium and W-7. The same antagonists impaired the mitochondrial matrix Ca^{2+} rise measured by mitochondrial trapped Rhod 2 in permeabilized RBL cells following loading of high cytosolic Ca^{2+}, confirming facilitation of MCU by Ca^{2+}-calmodulin in mast cells (Moreau et al 2006).

In Chapter 3, I showed that the C-lobe of calmodulin was critical for the modulation of CRAC channels by cytoplasmic Ca^{2+}. I provided experimental evidence that suggested the underlying mechanism could involve an action on mitochondrial Ca^{2+} buffering. Here, I have investigated the role of calmodulin in the regulation of mitochondrial Ca^{2+} uptake using the ratiometric protein, pericam. Pericam is a circular, permutated fluorescent protein developed to sense Ca^{2+} (engineered by Nagai et al 2001). It contains both a GFP unit and a mitochondrial presequence (encoding a 12 amino acid sequence of the N terminal of cytochrome c oxidase subunit IV; Nagai et al 2001) to specifically target it to the mitochondrial matrix, enabling the direct measurement of mitochondrial matrix [Ca^{2+}] in intact cells. Pericam is a very useful tool to monitor rapid mitochondrial matrix Ca^{2+} changes under physiological conditions (Malli et al 2003). This is important because previous techniques that have been used to investigate the regulation of MCU by calmodulin have involved permeabilizing cells to remove non-compartmentalised indicator. Such a method might disrupt the morphology of mitochondria. Furthermore, permeabilizing cells compromises the integrity of the plasma membrane, which is clearly not physiological. Pericam is therefore a much less invasive approach to measure mitochondrial matrix Ca^{2+}.

4.2 Results

a. A rise in mitochondrial matrix [Ca^{2+}] is evoked following ER Ca^{2+} depletion.

Csordás and Hajnóczky 2003 have demonstrated the effective transmission of Ca^{2+} from the ER to mitochondria in RBL-2H3 cells. They observe a rise in mitochondrial matrix [Ca^{2+}] in response to IP_3-induced cytosolic Ca^{2+} oscillations, through the simultaneous measurement of cytosolic and mitochondrial [Ca^{2+}] using specifically targeted fluorescent probes. Consistent with this work, Moreau et al 2006 confirm the ability of the mitochondria to effectively buffer intracellular Ca^{2+} in RBL-1 cells, using a different approach involving the permeabilization of cells. They recorded mitochondrial matrix [Ca^{2+}] in response to the application of cytoplasmic Ca^{2+} loads by a fluorescent probe trapped in the matrix, (Rhod 2). Mitochondria were loaded with the membrane permeable Ca^{2+}-sensitive fluorescent indicator, Rhod 2-AM, and permeablized with digitonin to remove cytosolic Rhod 2-AM. Another Ca^{2+}-sensitive indicator (Fura 2-AM) was targeted specifically to the cytoplasm. Here I have used an alternative approach which is less invasive to measure mitochondrial matrix [Ca^{2+}] changes (in response to stimulated Ca^{2+} release from the ER), involving the ratiometric, fluorescent protein pericam targeted to the mitochondrial matrix (Nagai et al 2001) in intact RBL-1 cells. Pericam was transfected into RBL-1 cells, where it recorded matrix Ca^{2+}, (for evidence, see section **b** of this Chapter). The pericam signal located into puncta, and regions of interest were drawn around these areas. RBL-1 cells were excited at 430 nm and 488 nm and the ratio of pericam emission reflects matrix [Ca^{2+}] (Nagai et al 2001, Malli et al 2003). After a stable baseline [Ca^{2+}] had been obtained, I stimulated cells with 1 µM thapsigargin or 160 nM of LTC_4 in 2 mM

Ca^{2+} external solution. Stimulation with thapsigargin always resulted in a slow increase in mitochondrial matrix Ca^{2+} (mean amplitude 0.0491 ± 0.00249 SEM., n=21), followed by a partial decline (figure 1**A**). On the other hand, LTC_4, which evokes high amplitude, transient release via the IP_3R in the ER membrane, resulted in a rapid, transient increase in mitochondrial matrix Ca^{2+} (mean amplitude 0.0677 ± 0.00372 SEM., n=30, p=0.0004) which settled quickly at a steady state level (figure 1**B**). After LTC_4, matrix Ca^{2+} rose quickly after a very short delay. Time-course of the matrix Ca^{2+} rise matched the onset of first cytoplasmic Ca^{2+} oscillation to LTC_4, which indicates that the pericam signal is a reflection of the first cytosolic Ca^{2+} oscillation.

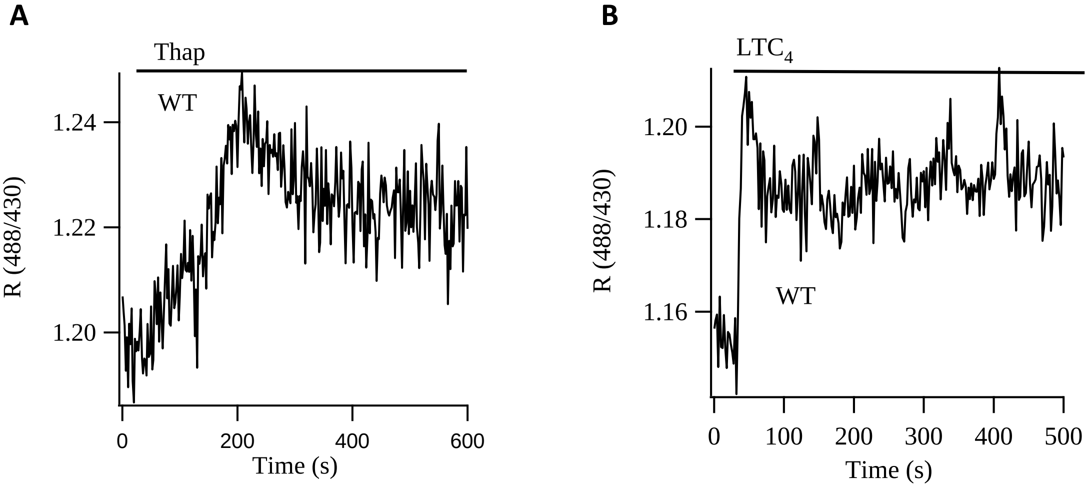

Figure 1. Ca^{2+} release from the ER induces a rise in mitochondrial matrix [Ca^{2+}]. **A**, the trace illustrates the typical mitochondrial matrix Ca^{2+} rise when one pericam transfected RBL-1 cell is bathed in 2 mM Ca^{2+} external solution and stimulated with 1 µM thapsigargin. **B**, the mitochondrial matrix Ca^{2+} rise when a pericam transfected RBL-1 cell is stimulated with 160 nM LTC_4 in 2 mM Ca^{2+} is shown.

b. It was important to confirm that the pericam was specifically targeted to the mitochondrial matrix and directly measured mitochondrial matrix [Ca^{2+}]. I therefore carried out a series of control experiments to check that the signal being measured was indeed from the mitochondrial matrix.

1. No change in the pericam signal is detected when the inner mitochondrial membrane is depolarized.

Under conditions which eliminate the highly hyperpolarized membrane potential (normally around -180 mV) of the IMM, the driving force for Ca^{2+} entry would be reduced, which would impair the uptake of Ca^{2+} by mitochondria. Therefore methods which depolarize the IMM should prevent a measurable pericam signal if pericam is specifically monitoring mitochondrial matrix Ca^{2+}. No detectable rise in the pericam signal was observed when RBL-1 cells stimulated with thapsigargin were pre-incubated for four minutes with 5 µM FCCP (figure 2**A**, **B**).

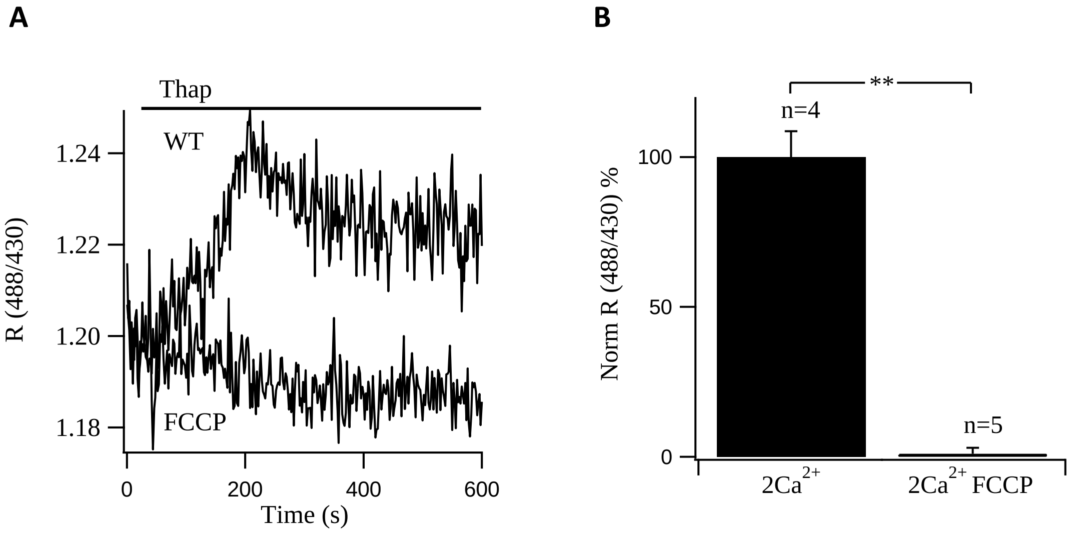

Figure 2. No measurable change is detected in the pericam signal when the IMM is depolarized. A, the recordings show the pericam response when a pericam transfected RBL-1 cell is bathed in 2 mM Ca^{2+} and stimulated with 1 µM thapsigargin in the presence (FCCP) or absence (WT) of pre-incubation for four minutes with 5 µM FCCP. In the presence of FCCP no detectable change in the pericam signal is observed. **B**, aggregate data compare the average pericam signal recorded when pericam transfected RBL-1 cells are stimulated with 1 µM thapsigargin in 2 mM Ca^{2+} external solution in the presence (n=5) or absence (WT; n=4) of 5 µM FCCP ($p<0.0001$). In the presence of FCCP the mitochondria fail to take up Ca^{2+}.

2. No change in the pericam signal is detected when the mitochondrial Ca^{2+} uniporter regulator (MICU1) is knocked down.

Knockdown of MICU1 should prevent a measurable mitochondrial matrix Ca^{2+} rise and detectable pericam signal upon stimulation with thapsigargin in 2 mM Ca^{2+}. To test this, I applied thapsigargin to RBL-1 cells transfected with MICU1 RNAi and compared the pericam signal with cells in which MICU1 had not been knocked down. No detectable rise in the pericam signal was recorded in cells in which MICU1 had been knocked down compared to pericam alone transfected cells, (see figure 3**A** for typical cell recordings and 3**B** for aggregate data). This demonstrates the requirement of MICU1 for the pericam signal, consistent with a mitochondrial localisation.

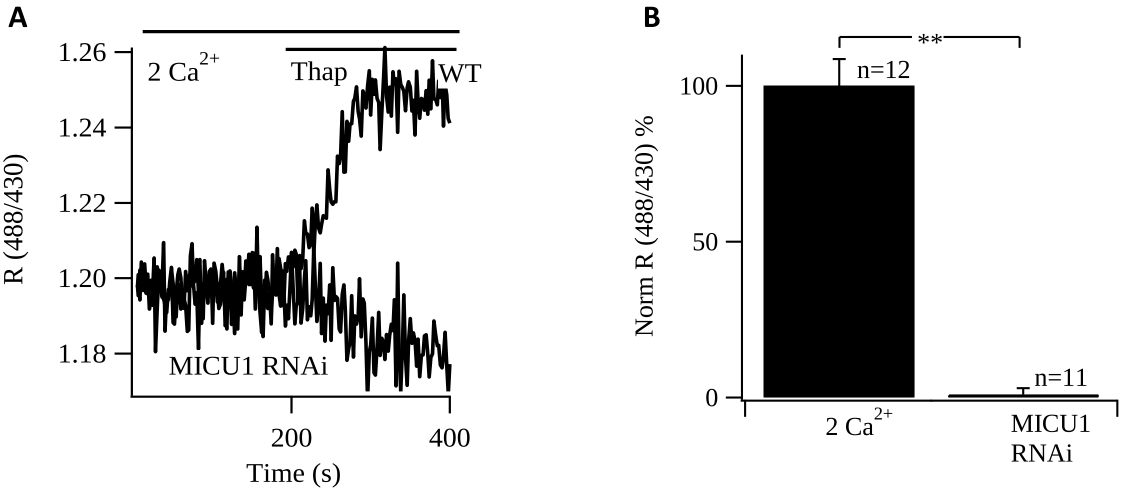

Figure 3. No detectable rise in matrix Ca^{2+} occurs when MICU1 has been knocked down. **A**, the traces reveal the pericam response when a pericam transfected RBL-1 cell (WT) is bathed in 2 mM Ca^{2+} and stimulated with 1 µM thapsigargin compared to a RBL-1 cell co-transfected with pericam and MICU1 RNAi (MICU1 RNAi). In the presence of MICU1 RNAi no detectable rise in the pericam signal is recorded following stimulation. **B**, a comparison of the average pericam signal recorded upon 1 µM thapsigargin stimulation in 2 mM Ca^{2+} for RBL-1 cells with normal endogenous MICU1 function (n=12) and cells where endogenous function of MICU1 had been knocked down (n=11) ($p<0.0001$) are presented.

3. No change in the pericam signal is detected when cells are bathed in zero Ca^{2+} external solution and stimulated with thapsigargin.

Following thapsigargin application in zero Ca^{2+} external solution, MCU is not exposed to a high, local concentration of Ca^{2+} that underpins the efficient mitochondrial Ca^{2+} buffering described by Rizzuto et al. Since MCU has a low affinity for Ca^{2+}, the small, slowly developing cytosolic Ca^{2+} signal that is evoked by thapsigargin in zero Ca^{2+} external solution (shown in figure 4**C**), should not be sufficient to activate MCU and cause a measurable mitochondrial Ca^{2+} uptake. Indeed, no detectable change in the pericam signal was recorded at 180 seconds (s) (see arrow on figure 4**B**) in RBL-1 cells that were stimulated with 1 µM thapsigargin in zero Ca^{2+} external solution, (figure 4**A** presents aggregate data and figure 4**B** shows a typical recording, the arrow represents the time point at which the matrix Ca^{2+} level was taken). In figure 4**B** cells were stimulated with 1 µM thapsigargin at 30s in zero Ca^{2+} and then administered 2 mM Ca^{2+} at 310s. A mitochondrial Ca^{2+} rise was only evident with thapsigargin stimulation when external Ca^{2+} was always present (figure 4**A**) or introduced after a period in zero Ca^{2+} (figure 4**B**). In contrast a clear cytosolic Ca^{2+} rise at 180s measured by Fura 2 in response to 1 µM thapsigargin in zero Ca^{2+} was evident in the cytosol, although this rise was significantly smaller than with addition of 2 mM external Ca^{2+} (figure 4**C**). The thapsigargin-induced cytosolic Ca^{2+} rise in zero Ca^{2+} is too small to activate MCU. The presence of CRAC channel dependent Ca^{2+} influx in addition to ER Ca^{2+} release would cause the cytosolic $[Ca^{2+}]$ to reach levels sufficient to activate MCU and drive measurable mitochondrial Ca^{2+} uptake (a rise in the pericam signal). A mitochondrial Ca^{2+} rise is however seen in zero Ca^{2+} external solution in response to a physiological level of LTC_4, which opens IP_3Rs and leads to high, local Ca^{2+}

microdomains. Such high, local Ca^{2+} signals rapidly activate MCU, even in the absence of external Ca^{2+} (figure 4**D**).

A Stimulation with thapsigargin **B** Mitochondrial matrix [Ca^{2+}]

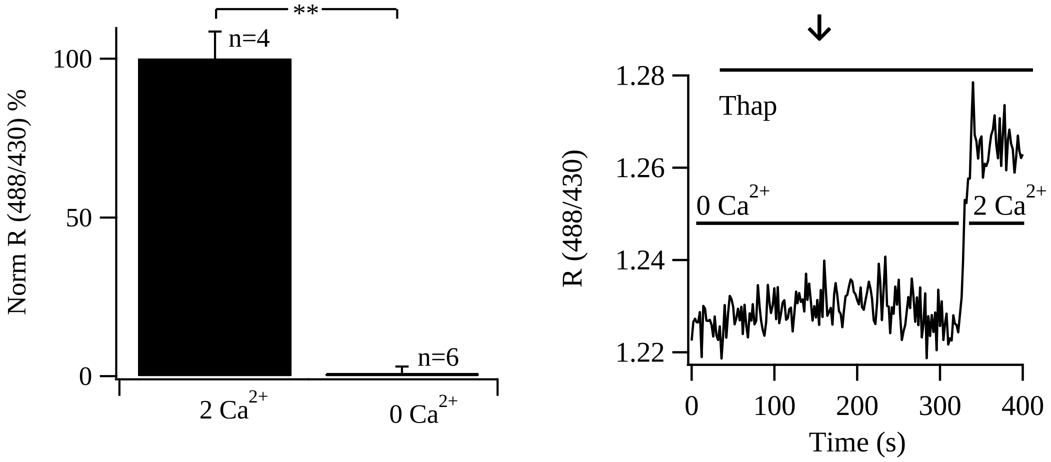

C Fura 2 measured cytosolic [Ca^{2+}] **D** Stimulation with LTC_4

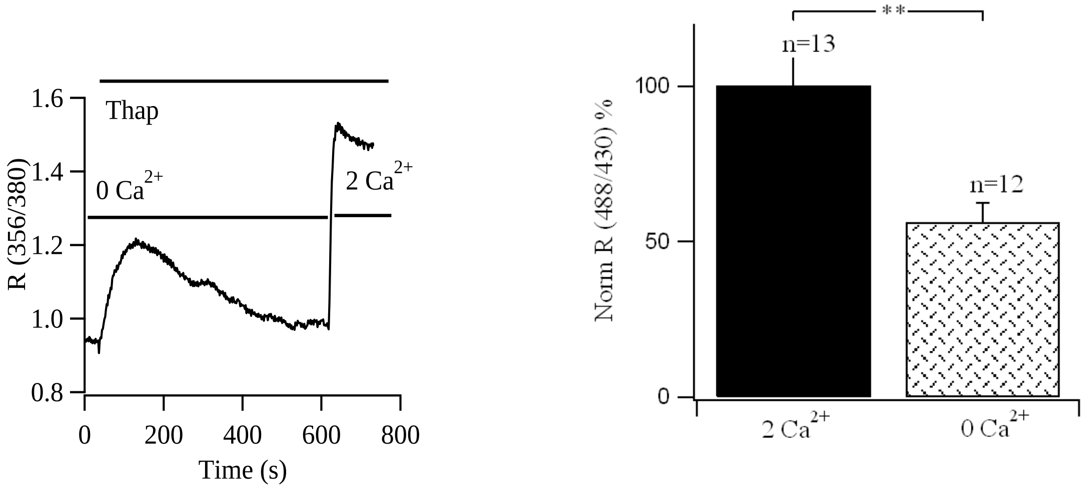

Figure 4. No detectable change in the pericam signal is observed when cells are bathed in zero Ca^{2+} and stimulated with thapsigargin. A, aggregate data shows the average amplitude of the pericam signal at 180s when cells are stimulated with 1 µM thapsigargin at 30s in the presence (n=4) or absence (n=6) ($p<0.0001$) of 2 mM external Ca^{2+} solution. Thapsigargin fails to induce a mitochondrial matrix Ca^{2+} rise in zero Ca^{2+}. **B**, the pericam signal that is recorded in response to adding 2 mM Ca^{2+} at 310s after pre-stimulation with 1 µM thapsigargin at 30s in zero Ca^{2+} is shown. Application of 2 mM Ca^{2+} at 310s enables thapsigargin to evoke a mitochondrial matrix Ca^{2+} rise (a detectable pericam signal rise). The arrow represent s the time point at which matrix [Ca^{2+}] was recorded. **C**, the trace shows the cytosolic Ca^{2+} signal measured by Fura 2 when 1 µM thapsigargin is applied to a RBL-1 cell bathed in zero Ca^{2+} external solution. 2 mM Ca^{2+} is then added. 1 µM thapsigargin evokes a clear rise in cytosolic Ca^{2+} even in zero external Ca^{2+} before 2 mM external Ca^{2+} is added. **D**, compares the averaged pericam signal induced by 160 nM LTC_4 in the presence (n=13) or absence (n=12) ($p=0.001$) of 2 mM Ca^{2+} external solution. LTC_4 induces a measurable rise in mitochondrial matrix [Ca^{2+}] even in the absence of external Ca^{2+}.

Collectively, these experiments confirm that pericam is localised to the mitochondrial matrix and specifically monitors mitochondrial matrix [Ca^{2+}]. Pericam is therefore used here to test my hypothesis that calmodulin-dependent facilitation of I_{CRAC} (found in Chapter 3) occurs through an action on mitochondrial Ca^{2+} uptake.

c. Calmodulin facilitates mitochondrial Ca^{2+} uptake

Previously, I found that the C-lobe of calmodulin gated CRAC channels and maintained LTC_4-induced cytosolic Ca^{2+} oscillations. I hypothesise that the uptake of Ca^{2+} by mitochondria is a central mechanism underlying such modulation by Ca^{2+}-calmodulin. Such a concept is illustrated in cartoon model **4** in the Discussion of Chapter 3, (section **3.3**). To test this directly in intact RBL-1 cells, I use pericam to monitor matrix Ca^{2+}. In the presence of CAM4M, the amplitude of the pericam signal was significantly reduced compared to control (pericam alone transfected, WT) cells, following stimulation with either thapsigargin (see figure 5**A** for typical cell recordings and **B** for aggregate data) or LTC_4 (figure 5**B, C**). This demonstrates directly the importance of calmodulin for the facilitation of mitochondrial Ca^{2+} uptake, see cartoon model **5** for an illustration of this.

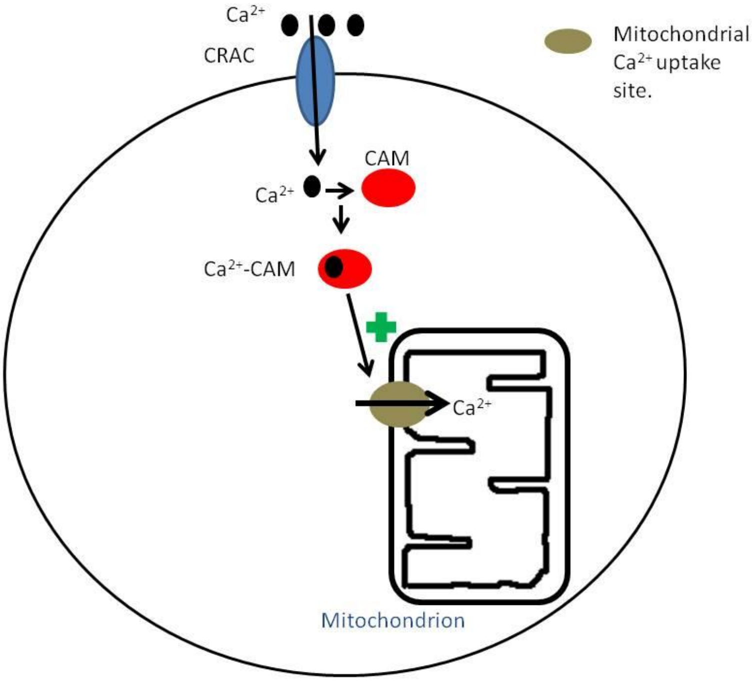
Ca^{2+}
CRAC
Mitochondrial Ca^{2+} uptake site.
CAM
Ca^{2+}
Ca^{2+}-CAM
Ca^{2+}
Mitochondrion

Cartoon model 5 illustrates Ca^{2+}-calmodulin dependent facilitation of mitochondrial Ca^{2+} uptake.

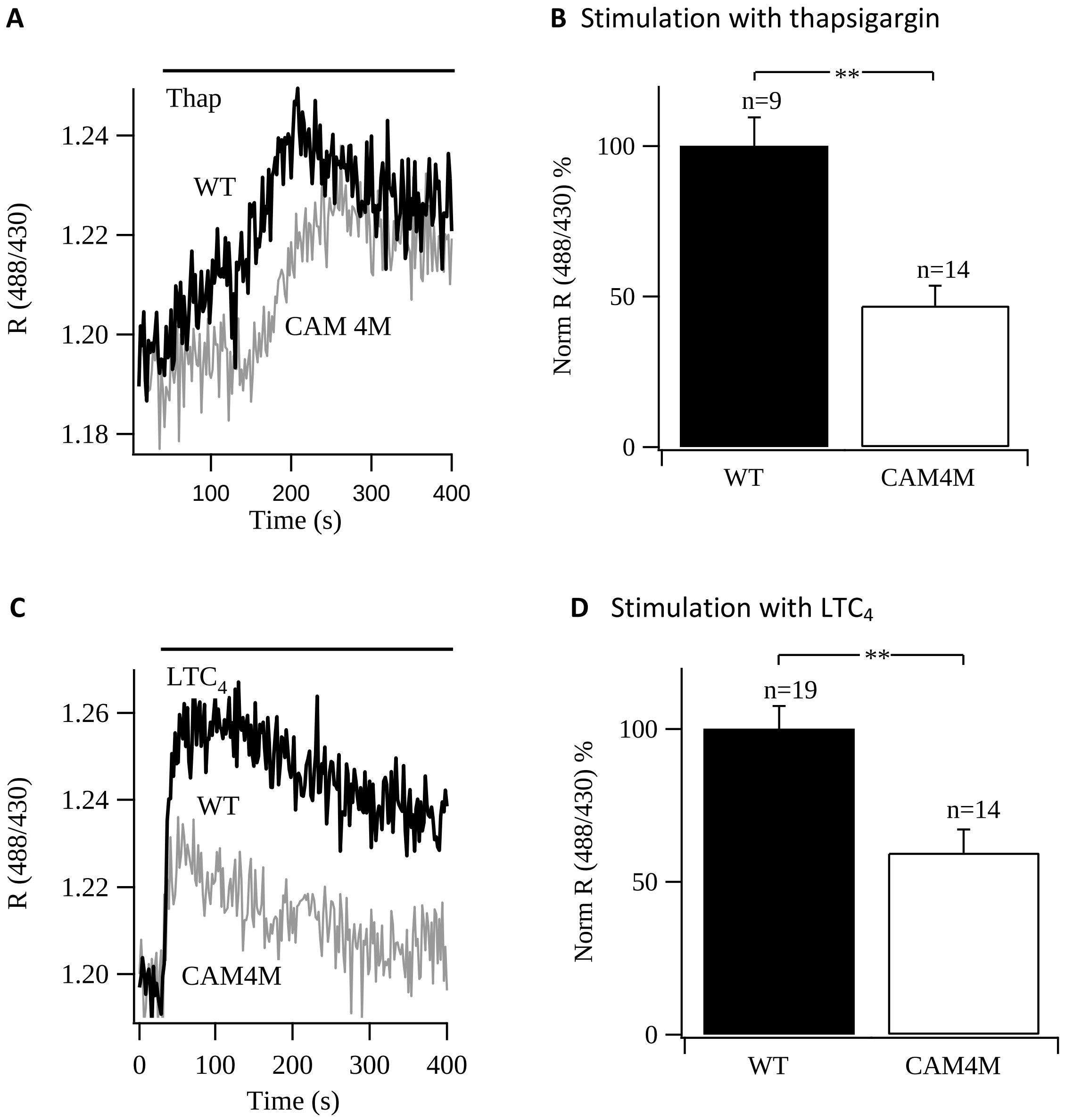

Figure 5. Calmodulin facilitates mitochondrial Ca^{2+} uptake. A, the traces illustrate that the mitochondrial matrix Ca^{2+} rise is reduced in a pericam and CAM4M co-transfected RBL-1 cell (CAM4M) compared to one where pericam alone is transfected (WT), following stimulation with 1 µM thapsigargin in 2 mM external Ca^{2+} solution. **B**, the average amplitude of the pericam signal recorded in cells transfected with pericam (WT) (n=9) and cells co-transfected with pericam and CAM4M (n=14) (p=0.0001) are shown. All RBL-1 cells were bathed in 2 mM external Ca^{2+} solution and stimulated with 1 µM thapsigargin. Expression of CAM4M significantly suppressed the pericam signal. **C**, the recordings show the reduced mitochondrial matrix Ca^{2+} rise in a single RBL-1 cell co-transfected with pericam and CAM4M (CAM4M) compared to one transfected with pericam alone (WT), in response to stimulation with 160 nM LTC_4 in 2mM external Ca^{2+}. **D**, reveals the same findings as **B** but in response to 160 nM LTC_4 (WT, pericam transfected n=19, CAM4M and pericam transfected n=10, p=0.0019) in the presence of 2 mM external Ca^{2+}.

d. Calmodulin is not essential to induce a mitochondrial matrix Ca^{2+} rise if cytosolic Ca^{2+} is very high.

To test whether a large increase in bulk Ca^{2+} can drive a mitochondrial matrix Ca^{2+} rise, I stimulated cells with thapsigargin in zero Ca^{2+} and 1 mM La^{3+}. This approach renders the cell 'tight' to Ca^{2+} since it simultaneously prevents Ca^{2+} influx and removal. La^{3+} blocks the plasma membrane Ca^{2+} ATPase (PMCA) pump, preventing Ca^{2+} extruding from the cell. Furthermore, the released Ca^{2+} is prevented from recycling back into the ER, since the SERCA pumps are blocked by thapsigargin. Therefore released Ca^{2+} cannot leave the cytoplasm and leads to a large increase in cytosolic Ca^{2+}, such a rise is much greater in size than is evoked by thapsigargin stimulation in 2 mM external Ca^{2+} alone (Chang et al 2008). I have previously shown that stimulation with thapsigargin in pericam transfected cells did not increase matrix Ca^{2+} in zero Ca^{2+} external solution (figure 4**A, B**). However, a large bulk cytosolic Ca^{2+} increase in the presence of thapsigargin, zero Ca^{2+} and La^{3+} led to an increased matrix Ca^{2+}, although this increase was unaffected by CAM4M (figure 6). This supports the view that calmodulin is not essential for a matrix Ca^{2+} rise if cytosolic Ca^{2+} is very high. Calmodulin is therefore a facilitator and not an activator of mitochondrial Ca^{2+} uptake.

Calmodulin is a ubiquitous Ca^{2+}-binding protein found throughout the cytoplasm therefore an important question is whether all of the calmodulin in the cell is important for the regulation of mitochondrial Ca^{2+} uptake or whether specific pools of calmodulin are more crucial, see cartoon model **6** to visualize this idea. The result here that CAM4M fails to affect the matrix Ca^{2+} rise in the presence of thapsigargin, zero Ca^{2+} and La^{3+} suggests that a major source of calmodulin involved in the facilitation of mitochondrial Ca^{2+} uptake is local to the CRAC channel. This proposal can be understood if you consider the effect of CAM4M on the pericam signal recorded under each of the following conditions, 1) in zero Ca^{2+} and thapsigargin where no Orai1-dependent Ca^{2+} entry or sufficient cytosolic Ca^{2+} rise to activate MCU occurs, no detectable change in pericam is recorded. 2) In 2 mM Ca^{2+} and thapsigargin, where Orai1-dependent Ca^{2+} entry is present a detectable increase in pericam is recorded and this is impaired by CAM4M. Therefore the matrix Ca^{2+} rise is calmodulin-dependent when Orai1-dependent Ca^{2+} entry is present. 3) In zero Ca^{2+}, 1 mM La^{3+} and 1 µM thapsigargin however although a larger bulk cytosolic Ca^{2+} signal is established than with 2 mM Ca^{2+} and thapsigargin no Orai1-dependent Ca^{2+} entry is present and the matrix Ca^{2+} rise is unaffected by CAM4M. Therefore in the absence of Orai1-dependent Ca^{2+} entry the matrix Ca^{2+} rise in response to even a very high cytosolic Ca^{2+} load is independent of calmodulin. Presumably the local Ca^{2+} entry through CRAC channels recruits calmodulin very close or associated with Orai1 to facilitate mitochondrial Ca^{2+} uptake (see cartoon model **6**), whilst a bulk cytosolic Ca^{2+} rise independent of Orai1-dependent Ca^{2+} entry recruits cytosolic calmodulin positioned outside the microdomain formed when CRAC channels open and Ca^{2+} enters the cell. This cytosolic calmodulin is not important for the facilitation of mitochondrial Ca^{2+} uptake. Such a proposal whereby calmodulin local to CRAC channels is a major source of calmodulin for facilitation of mitochondrial Ca^{2+} uptake is tested in the subsequent set of experiments using an Orai1 mutant construct unable to bind calmodulin.

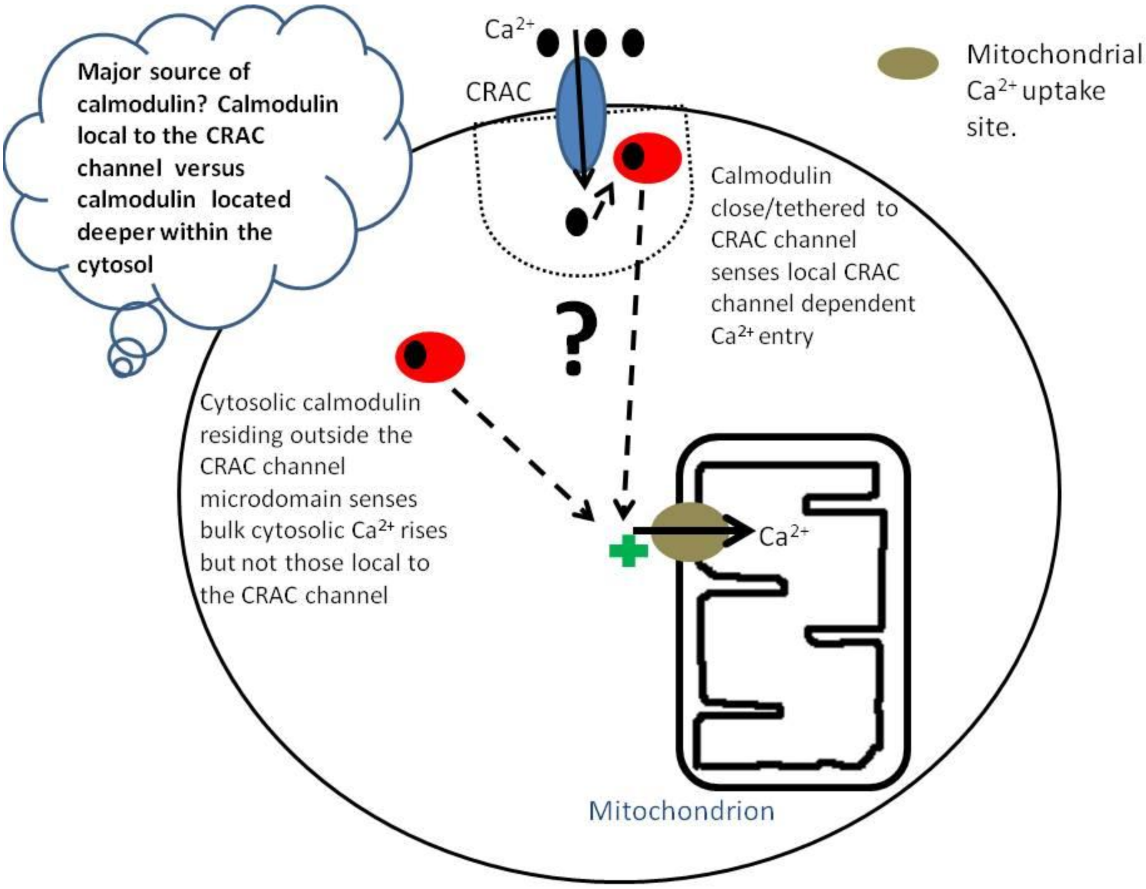
Major source of calmodulin? Calmodulin local to the CRAC channel versus calmodulin located deeper within the cytosol
Ca2+
CRAC
Mitochondrial Ca2+ uptake site.
Calmodulin close/tethered to CRAC channel senses local CRAC channel dependent Ca2+ entry
?
Cytosolic calmodulin residing outside the CRAC channel microdomain senses bulk cytosolic Ca2+ rises but not those local to the CRAC channel
Ca2+
Mitochondrion

Cartoon model 6. Calmodulin positioned local to the CRAC channel is a major source of calmodulin for the facilitation of mitochondrial Ca^{2+} uptake. This could involve calmodulin positioned very close to the CRAC channel or tethered to it directly. Cytosolic calmodulin located distant of the microdomain formed when CRAC channels open and Ca^{2+} enters the cell is not important for the facilitation of mitochondrial Ca^{2+} uptake.

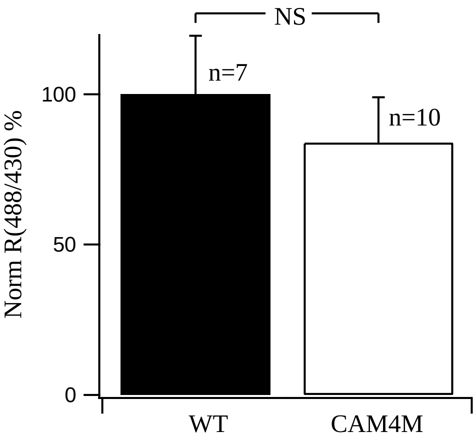

Figure 6. The mitochondrial matrix Ca^{2+} rise does not require calmodulin if cytosolic Ca^{2+} is very high. Averaged data compare the mitochondrial matrix Ca^{2+} rise for 7 pericam transfected RBL-1 cells (WT) and 10 CAM4M (and pericam) co-transfected cells (p=NS). All cells were pre-incubated for 5 minutes in zero Ca^{2+} and 1 mM La^{3+} and then stimulated with 1 µM thapsigargin.

e. Calmodulin tethered to Orai1 is a major source of calmodulin for facilitating mitochondrial Ca^{2+} uptake.

Ca^{2+} entry through CRAC channels results in the development of Ca^{2+} microdomains, regions of high, local concentrations of Ca^{2+} surrounding each open channel. The amplitude and spatial extent of these microdomains depends in part on the single CRAC channel Ca^{2+} conductance. As the latter is small, the microdomains that form do not extend very far into the cell. In order for incoming Ca^{2+} through CRAC channels to be sensed by calmodulin, calmodulin would therefore have to be located within very close proximity to the CRAC channel pore subunit (Orai1) (see cartoon model **6**). Tethered apo-calmodulin to the IQ domain of L-type Ca^{2+} channels has been shown to sense and transduce local Ca^{2+} entry through L-type channels in excitable cells (Dolmetsch et al 2001). Upon Ca^{2+} binding to calmodulin, the resultant Ca^{2+}-calmodulin complex dissociates from the channel and relays the local Ca^{2+} signal to the nucleus some hundreds of nanometres away, to activate nuclear gene expression, (see section **1.5**, figure 8). L-type channel mutants unable to bind calmodulin were shown to lack this long-range signalling (Dolmetsch et al 2001). In 2009, Mullins et al identified a Ca^{2+}-dependent calmodulin binding site within the N terminus of Orai1. This domain consisted of a 24 amino acid sequence at amino acids 68-91. Evidence that Orai1 and calmodulin interacted was revealed by coimmunoprecipitation of coexpressed Flag-myc-camodulin and GFP-myc- Orai1, using anti-flag antibodies. Coimmunoprecipitation only occurred with the N-terminus of Orai1 (not the C terminus or the II-III intracellular loop regions) and was only evident in the presence of Ca^{2+}. Furthermore, horseradish peroxidase tagged calmodulin was shown directly to interact with an Orai1 N terminal peptide (composed of amino acids 48-91). Finally, calmodulin-sepharose pull-down assays identified the site for Ca^{2+}-calmodulin binding to Orai1 at amino acids 68-91. I therefore hypothesise that the facilitation of MCU Ca^{2+} uptake by calmodulin initially involves the latter to be tethered to the N terminus of the Orai1 channel and then released into the cytosol. I have investigated this hypothesis using an Orai1 mutant construct (A73E Orai1, generated and described by Mullins et al 2009). This mutation has no effect on Orai1 function but simply renders the channel incapable of binding calmodulin (Mullins et al 2009).

1. I measured mitochondrial matrix [Ca^{2+}] using pericam in RBL-1 cells that were either overexpressing Orai1 and STIM1 or expressing A73E Orai1 and overexpressing STIM1. Whilst no significant difference in the initial rate (Orai1 and STIM1, n=9, mean 0.00419/s ± 0.00104 SEM., A73E Orai1 and STIM1 n=6, mean 0.00571/s ± 0.00149 SEM., p=NS), or initial extent (Orai1 and STIM1 mean 0.0433 ± 0.00461 SEM., A73E Orai1 and STIM1 mean 0.0523 ± 0.00471 SEM., p=NS) of mitochondrial Ca^{2+} uptake was evident, the recovery of the mitochondrial matrix Ca^{2+} signal was significantly different between these two conditions. The mitochondrial matrix Ca^{2+} signal remained elevated with little evidence of any recovery in continuous stimulation when cells overexpressed Orai1 and STIM1 (figure 7**A**). By contrast, the mitochondrial matrix Ca^{2+} signal was elevated only transiently and rapidly recovered in cells expressing A73E Orai1 and overexpressing STIM1 (figure 7**B**). Figure 7**C** compares the mitochondrial matrix Ca^{2+} signal in cells overexpressing Orai1 with cells expressing A73E Orai1, 150s after the admission of 2 mM Ca^{2+} to cells bathed in zero Ca^{2+} external solution and stimulated with thapsigargin. The smaller mitochondrial

matrix Ca^{2+} signal 150s after the admission of 2 mM external Ca^{2+} in the presence of A73E Orai1 reflects a faster recovery of the mitochondrial matrix Ca^{2+} rise. This suggests that calmodulin initially tethered to Orai1 is required to sustain calmodulin-dependent facilitation of mitochondrial Ca^{2+} uptake. Calmodulin therefore acts as an important regulator of mitochondrial Ca^{2+} uptake. It is not an activator of MCU because no difference in the initial rate or initial extent of the mitochondrial Ca^{2+} uptake is observed between the two conditions. A difference is only evident at later stages of stimulation. My result in which calmodulin sustains mitochondrial $[Ca^{2+}]$ after stimulation is consistent with work by Csordás and Hajnóczky 2003. Using permeabilized cells, they found that a second IP_3-induced cytosolic Ca^{2+} oscillation resulted in a larger rise in mitochondrial $[Ca^{2+}]$ compared to the first, and this was suppressed by calmodulin antagonists. They concluded that calmodulin was recruited by the second Ca^{2+} pulse, and this facilitated MCU permeability and thus increased mitochondrial uptake of Ca^{2+}. My results support a role for calmodulin in sustaining mitochondrial Ca^{2+} uptake in intact RBL-1 cells. Furthermore, I add to the work by Csordás and Hajnóczky by identifying calmodulin tethered to Orai1 as a major source of this calmodulin.

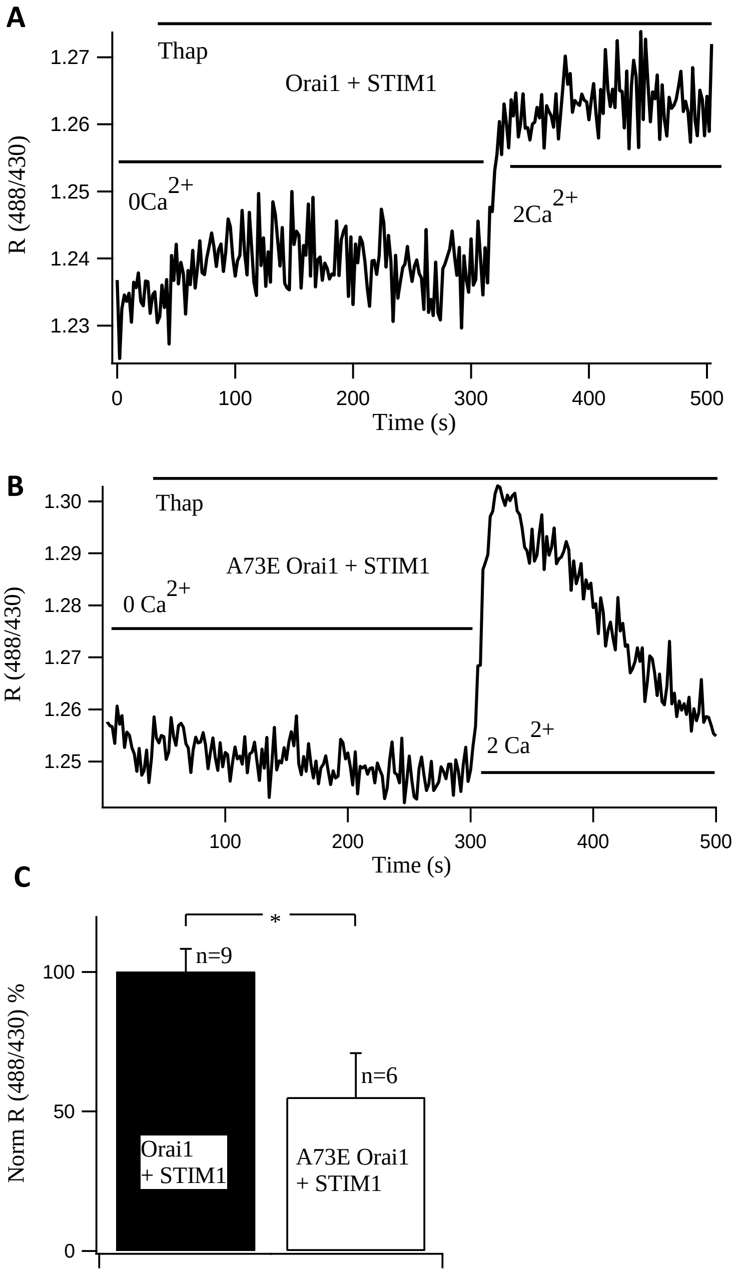

Figure 7. Calmodulin tethered to Orai1 sustains mitochondrial Ca^{2+} uptake. A, the trace presents the pericam signal when one RBL-1 cell overexpressing Orai1 and STIM1 is introduced with 2 mM external Ca^{2+} after pre-stimulation with 1µM thapsigargin in zero Ca^{2+}. Mitochondrial matrix [Ca^{2+}] remains elevated following CRAC channel dependent Ca^{2+} entry. **B**, the recording shows the pericam signal when one RBL-1 cell expressing A73E Orai1 and overexpressing STIM1 is exposed to 2 mM external Ca^{2+} following stimulation with 1 µM thapsigargin in zero Ca^{2+}. The mitochondrial matrix [Ca^{2+}] rapidly recovers following CRAC channel dependent Ca^{2+} entry in the presence of A73E Orai1. **C**, presents the comparison of the mitochondrial matrix Ca^{2+} signal 150s after admission of 2 mM external Ca^{2+} , for cells overexpressing Orai1 and STIM1 (n=9) and cells expressing A73E Orai1 and overexpressing STIM1 (n=6) ($p=0.0165$), following stimulation with 1µM thapsigargin in zero Ca^{2+}. A smaller pericam signal is observed 150s after the admission of 2 mM external Ca^{2+} in cells expressing A73E Orai1.

2. The amount of Ca^{2+} in the matrix after stimulation was measured and compared between RBL-1 cells overexpressing Orai1 and STIM1 with cells overexpressing STIM1 and expressing A73E Orai1. The amount of Ca^{2+} in the matrix should be less in the presence of A73E Orai1 compared with normal Orai1 if calmodulin tethered to Orai1 is a major source of calmodulin for facilitating mitochondrial Ca^{2+} uptake. Thapsigargin (applied at 30s in zero Ca^{2+}) was used to deplete the ER calcium stores and subsequently activate CRAC channels. Admission of 2 mM external Ca^{2+} (at 400s) evoked rapid Ca^{2+} entry and a subsequent rise in cytosolic $[Ca^{2+}]$ (recorded using Fura 2), which loaded the matrix with Ca^{2+}. External Ca^{2+} was then removed by applying 2 mM EGTA (at 600s) and consequently cytosolic $[Ca^{2+}]$ returned to pre-stimulated levels. 1 µM ionomycin was then applied to release Ca^{2+} from within the mitochondrial matrix. Fura 2 recorded the rise in cytosolic Ca^{2+} upon application of ionomycin which represented the amount of Ca^{2+} released from the mitochondrial matrix. Figures 8**A** and **B** illustrate the protocol followed and the cytosolic Ca^{2+} signal observed for a typical RBL-1 cell co-transfected with Orai1 and STIM1 (figure 8**A**) and one co-transfected with A73E Orai1 and STIM1 (figure 8**B**) respectively. Ionomycin can release Ca^{2+} from the ER as well but this is unlikely under my conditions because ER stores were already fully depleted of calcium after stimulation with thapsigargin (and application of ionomycin in zero Ca^{2+} following stimulation with thapsigargin in zero Ca^{2+} led to no clear cytosolic Ca^{2+} rise). Figure 8**C** compares the size of the cytosolic Ca^{2+} rise following exposure to ionomycin. Significantly higher Ca^{2+} signals were observed in cells overexpressing Orai1 and STIM1 (figure 8**A**, **C**) after stimulation compared to those overexpressing STIM1 and

expressing A73E Orai1 (figure 8**B**, **C**). This demonstrates that sustained mitochondrial Ca^{2+} uptake is impaired when calmodulin is prevented from binding to Orai1.

Together the experiments in section **e** allow me to identify calmodulin tethered to Orai1 as a major source of calmodulin for facilitating mitochondrial Ca^{2+} uptake, such a model is illustrated in cartoon model **7** below.

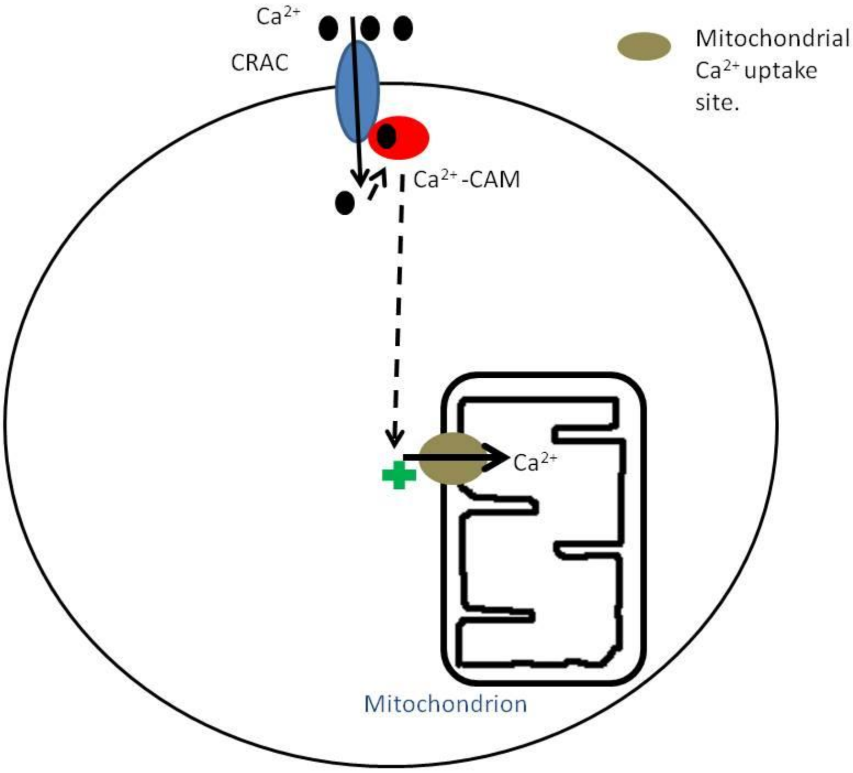
Ca^{2+}
CRAC
Mitochondrial Ca^{2+} uptake site.
Ca^{2+}-CAM
Ca^{2+}
Mitochondrion

Cartoon model 7 illustrates that calmodulin tethered to Orai1 is a major source of calmodulin for Ca^{2+}-calmodulin dependent facilitation of mitochondrial Ca^{2+} uptake.

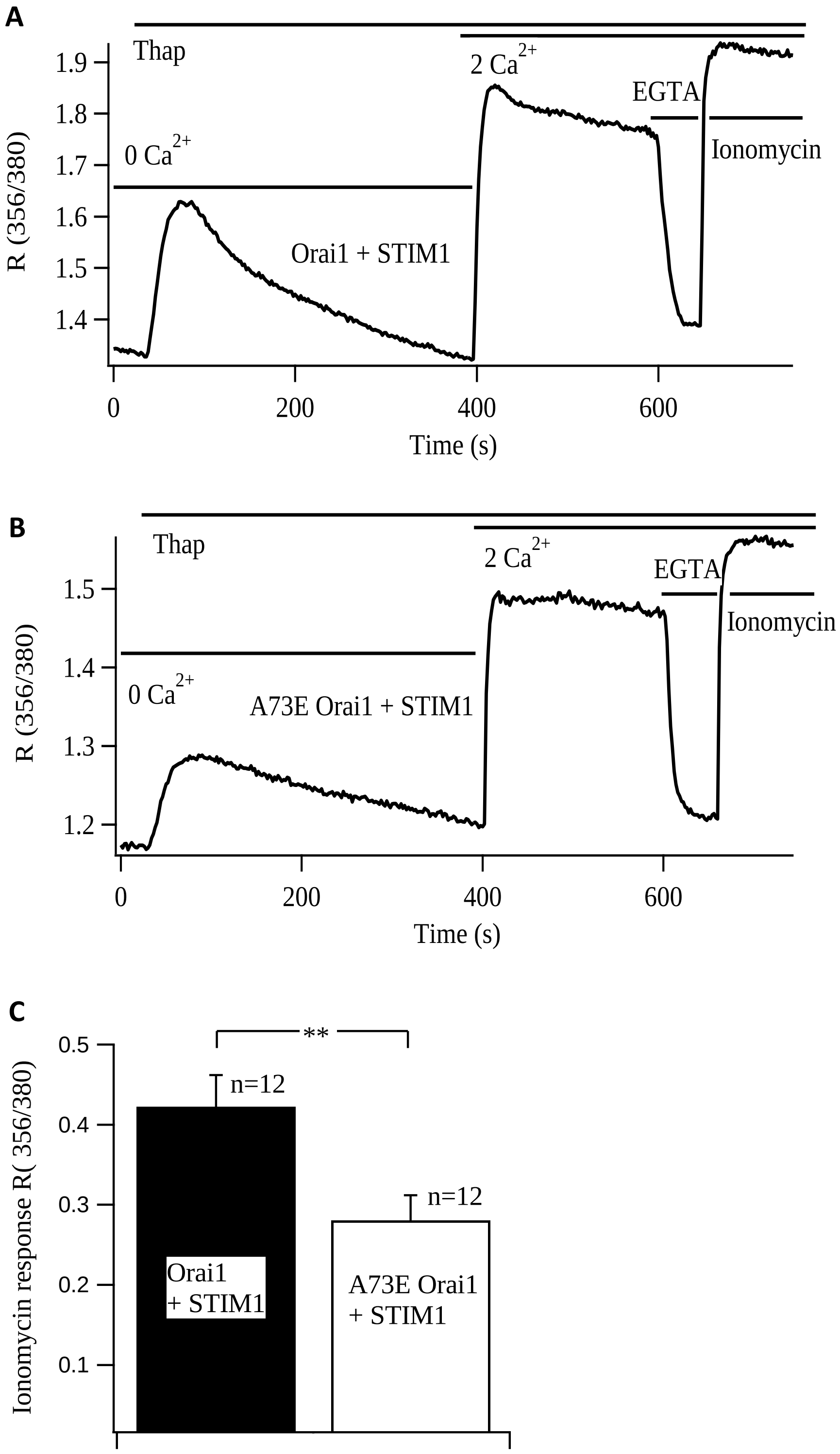

Figure 8. Calmodulin tethered to Orai1 facilitates mitochondrial Ca^{2+} uptake. A, the trace illustrates the protocol used to measure the amount of Ca^{2+} within the matrix subsequent to stimulation with 1μM thapsigargin for a cell co-transfected with normal Orai1 and STIM1. 1 μM thapsigargin was added at 30s to a cell bathed in zero Ca^{2+}. Once ER Ca^{2+} store depletion had returned to resting levels 2 mM external Ca^{2+} was added at 400s to raise cytosolic Ca^{2+} and therefore load the matrix with Ca^{2+}. After 200s in 2 mM external Ca^{2+}, the external Ca^{2+} was removed with 2 mM EGTA, at 600s, and upon recovery of the cytosolic Ca^{2+} to pre-

stimulated levels 1 µM ionomycin was added to release matrix Ca^{2+}. **B**, illustrates the same experiment but for a single cell co-transfected with A73E Orai1 and STIM1. The ionomycin-induced cytosolic Ca^{2+} rise is significantly smaller in the presence of A73E Orai1 and STIM1. **C**, The averaged data compare the amount of Ca^{2+} within the mitochondrial matrix (the size of the ionomycin-induced cytosolic Ca^{2+} rise), following stimulation with 1 µM thapsigargin between RBL-1 cells overexpressing Orai1 and STIM1 (n=12) and cells expressing A73E Orai1 and overexpressing STIM1 (n=12) (p=0.0098). In the presence of A73E Orai1, the mitochondrial matrix contained significantly less Ca^{2+}, measured by the size of the cytosolic Ca^{2+} increase (using Fura 2) after the challenge with ionomycin. This reflected a reduced mitochondrial Ca^{2+} uptake when A73E Orai1 was expressed.

f. The facilitation of mitochondrial Ca^{2+} uptake by calmodulin tethered to Orai1 cannot be explained by differences in the initial rate of CRAC channel dependent Ca^{2+} entry

The difference in the matrix Ca^{2+} between Orai1 (and STIM1) overexpressing cells and A73E Orai1 (and STIM1) expressing cells could be due to differences in the rate of CRAC channel dependent Ca^{2+} influx. To test this, I measured cytosolic Ca^{2+} signals following the admission of 1 mM external Ca^{2+} to cells pre-treated with thapsigargin in zero Ca^{2+}. 1 mM Ca^{2+} was used to prevent saturating Fura 2 in cells expressing such high levels of STIM1 and Orai1. I found no significant difference in the initial rate of CRAC channel dependent Ca^{2+} entry between the two conditions, (figure 9**A**) (Orai1 and STIM1 n=36, mean 0.0113/s ± 0.00115 SEM., A73E Orai1 and STIM1 n=34, mean 0.0102/s ± 0.000787 SEM., p=NS). This means the difference in matrix Ca^{2+} between Orai1 and A73E Orai1 (both with STIM1) is not due to a difference in the initial rate of CRAC channel dependent Ca^{2+} entry. In contrast to the initial rate of CRAC channel dependent Ca^{2+} entry, the subsequent cytosolic Ca^{2+} rise decayed slightly but significantly faster when cells expressed A73E Orai1 (and STIM1) compared with cells that overexpressed Orai1 (and STIM1) (figure 9**B**). This likely reflects increased Ca^{2+}-dependent slow inactivation of CRAC channels when mitochondrial Ca^{2+} uptake is compromised and not sustained (Gilabert and Parekh 2000). I propose that upon CRAC channel dependent Ca^{2+} entry, Ca^{2+}-calmodulin is released from Orai1 and diffuses into the cytoplasm. It then increases mitochondrial Ca^{2+} uptake via MCU (possibly through MICU1), which consequently feeds back to support CRAC channel activity by reducing Ca^{2+}-dependent slow inactivation (CDI). This mechanism that I propose has built up visually in cartoon models **1-7** with each new finding and can be seen below in cartoon model 8.

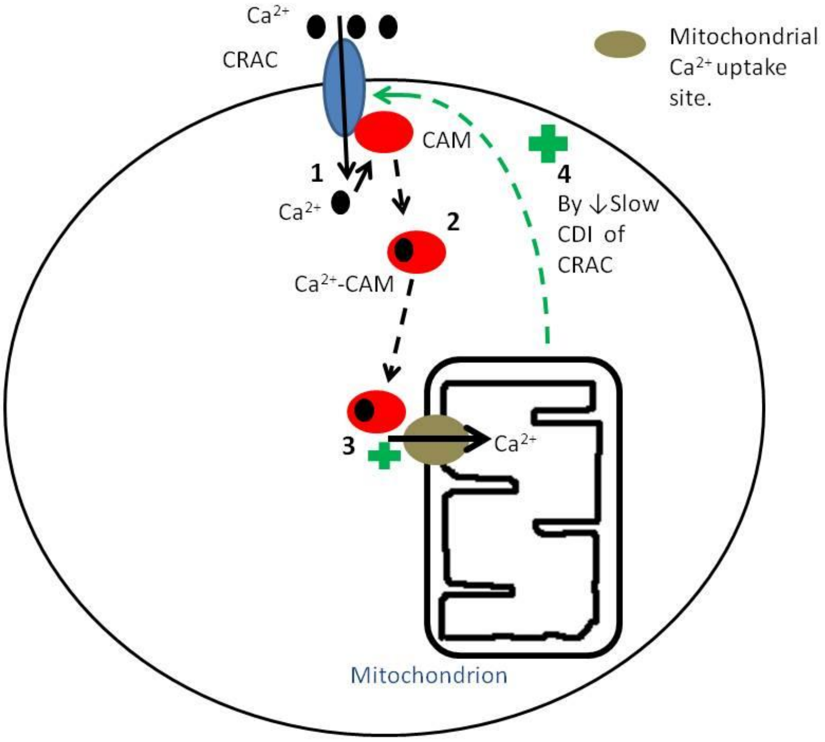

Cartoon model 8 illustrates the proposed mechanism put together from the results of Chapter's 3 and 4 for the modulation of CRAC channels by cytoplasmic Ca^{2+}. This modulation pathway is heavily reliant on the C-lobe of calmodulin. 1) Upon CRAC channel activation, local Ca^{2+} entry binds to calmodulin (CAM) that is tethered to Orai1 to form a Ca^{2+}-CAM (calmodulin) complex. 2) This complex is released from the CRAC channel and diffuses into the cytoplasm. 3) Ca^{2+}-CAM docks at a site either on MCU itself or on a closely associated protein (possibly MICU1). This leads to enhanced mitochondrial Ca^{2+} uptake. 4) Enhancing mitochondrial Ca^{2+} buffering facilitates CRAC channel dependent Ca^{2+} entry, probably by reducing Ca^{2+}-dependent slow inactivation of the channels. This view is supported by the experiment depicted in figure **9B** where the Fura 2 measured cytosolic Ca^{2+} signal 200s after admission of 1 mM Ca^{2+} is shown to decay faster in the presence of A73E Orai1 than normal Orai1. This suggests that when calmodulin cannot tether to Orai1 which prevents the sustained increase in mitochondrial Ca^{2+} uptake, Ca^{2+}-dependent slow inactivation of CRAC channels increases. Furthermore, in Chapter 3 I find that a bulk rise in cytosolic Ca^{2+} is required for Ca^{2+}-calmodulin dependent facilitation of CRAC channels. Slow CDI of CRAC channels relies on a bulk rise in cytosolic Ca^{2+}.

When calmodulin cannot bind to Orai1, Ca^{2+} influx no longer sustains mitochondrial Ca^{2+} uptake. This reduces mitochondrial Ca^{2+} buffering and therefore accelerates

Ca^{2+}-dependent slow inactivation. The latter will reduce CRAC channel activity and this will lead to a less sustained mitochondrial matrix Ca^{2+} signal.

A Initial rate of CRAC channel dependent Ca^{2+} entry

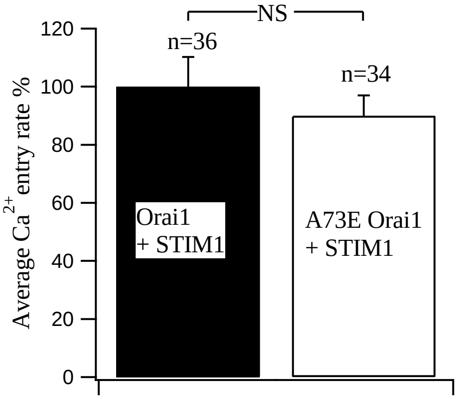

B Cytosolic [Ca^{2+}] 200s after initial CRAC channel dependent Ca^{2+} entry

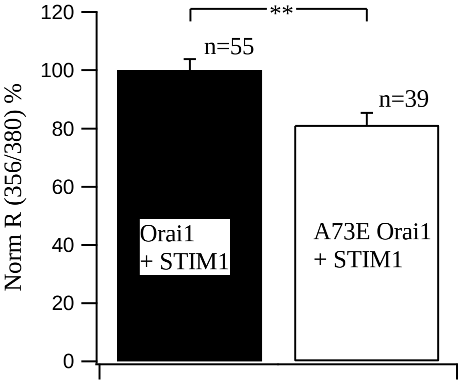

Figure 9. The effect of calmodulin tethered to Orai1 on CRAC channel activity. A, aggregate data compare the initial CRAC channel dependent Ca^{2+} entry rate between RBL-1 cells overexpressing Orai1 and STIM1 (n=36) with cells expressing A73E Orai1 and overexpressing STIM1 (n=34) (p=NS). All cells were bathed in zero Ca^{2+} external solution and stimulated with 1 µM thapsigargin. 1 mM Ca^{2+} was then introduced and the initial rate of Ca^{2+} entry was recorded. Fura 2 was the Ca^{2+}-sensitive fluorescent indicator used to monitor changes in cytosolic Ca^{2+}. No significant difference in the initial rate of CRAC channel dependent Ca^{2+} entry was observed between the two conditions. **B**, shows a comparison of the difference in the Fura 2 Ca^{2+} signal 200s after the admission of 1 mM Ca^{2+} for cells overexpressing Orai1 and STIM1 (n=55) and cells expressing A73E Orai1 and overexpressing STIM1 (n=39) (p=0.0013), (following stimulation with 1 µM thapsigargin in zero Ca^{2+}.)

g. Mitochondrial Ca^{2+} uptake facilitates NFAT-1-dependent gene expression

My work has identified a mechanism underlying the gating of CRAC channels by cytoplasmic [Ca^{2+}], (see cartoon model **8**), involving Ca^{2+}-calmodulin facilitation of mitochondrial Ca^{2+} uptake. Therefore I wanted to investigate the physiological impact of this regulatory pathway in RBL-1 cells. NFAT-1 is an important Ca^{2+}-dependent transcription factor regulating numerous genes essential for T cell activation and the generation of immune responses (Hogan et al 2003). Kar et al 2011 demonstrated a critical role for the local entry of Ca^{2+} through CRAC channels in driving NFAT-1 translocation and subsequent gene expression in both HEK and RBL-1 cell lines. They monitored the movement of a NFAT-1-GFP chimera using single cell imaging in real time. Whilst thapsigargin stimulation in 2 mM external Ca^{2+} drove NFAT-1 to the nucleus (identified through colocalization between NFAT-1-GFP and the nuclear dye DAPI), stimulation in zero Ca^{2+} failed to do so. Following this, application of the CRAC channel blocker, Synta (5 µM), markedly suppressed the migration that occurred in 2 mM external Ca^{2+}. Furthermore, cells loaded with the slow Ca^{2+} chelator EGTA, which has no effect on CRAC channel dependent Ca^{2+} microdomains but reduces bulk cytosolic Ca^{2+}, failed to impact on NFAT-1 nuclear translocation after thapsigargin stimulation in 2 mM external Ca^{2+} solution. Local CRAC channel dependent Ca^{2+} entry is therefore critical for NFAT-1 nuclear translocation. Furthermore, a role for mitochondria in the regulation of CRAC channel driven NFAT-1 movement to the nucleus has been shown. NFAT-1 migration is suppressed when mitochondrial Ca^{2+} buffering is impaired by CCCP in T cells (Hoth et al 2000) or by co-treatment with antimycin A and oligomycin in HEK cells (Kar et al 2011). Therefore I examined whether mitochondrial regulation of CRAC channels impacted on NFAT-1-dependent gene expression in RBL-1 cells, by using an EGFP-based reporter plasmid that contains an NFAT-1 promoter. Kar et al 2011 have previously used this reporter to show that local Ca^{2+} entry stimulates NFAT-1-dependent gene expression in RBL-1 cells. I transfected RBL-1 cells with an EGFP plasmid driven by the NFAT-1 promoter, alone (control cells, WT) or in conjunction with MICU1 RNAi and assessed the percentage of cells that expressed EGFP after stimulation with LTC_4. Results are summarized in Figure 10. The percentage of EGFP positive cells under basal conditions was low but increased substantially after stimulation with LTC_4. This was significantly reduced by transfection with MICU1 RNAi. The result demonstrates that mitochondrial Ca^{2+} buffering facilitates NFAT-1-dependent gene expression. Therefore the gating of CRAC channels by calmodulin through an effect on mitochondrial Ca^{2+} uptake is likely to have important physiological consequences. FCCP could be used to provide pharmacological evidence to support the findings with MICU1 RNAi. FCCP impairs mitochondrial Ca^{2+} buffering by collapsing the IMM membrane potential.

Another interesting further experiment could involve the comparison of NFAT-1-dependent gene expression between cells overexpressing normal Orai1 and STIM1 with cells expressing A73E Orai1 and overexpressing STIM1. This would enable one to establish whether calmodulin tethered to Orai1 is important in driving NFAT-1-dependent gene expression. Once calmodulin binding sites have been identified on MICU1 and, or MCU, one could mutate these sites to examine their effect on NFAT-1-dependent gene expression as well.

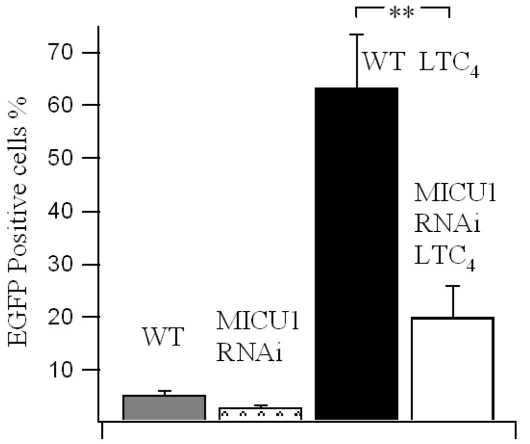

Figure 10. Mitochondrial Ca^{2+} uptake facilitates NFAT-1-dependent gene expression. Aggregate data shows the percentage of NFAT-1-EGFP positive RBL-1 cells for control non-stimulated RBL-1 cells (WT) (n=2, where n refers to the number of separate experiments carried out for each condition) or stimulated with LTC_4 (WT LTC_4) (n=2). These results are compared with RBL-1 cells transfected with MICU1 RNAi in the presence (MICU1 RNAi LTC_4) (n=2) or absence of LTC_4 (MICU1 RNAi) (n=2). Knockdown of MICU1 significantly reduced LTC_4-stimulated NFAT-1-dependent gene expression (MICU1 LTC_4) compared to control RBL-1 cells where MICU1 had not been knocked down (WT LTC_4) (p=0.0084).

4.3 Discussion

It is well known that mitochondria efficiently take up cytosolic Ca^{2+} after stimulation in RBL cells. Previous studies have observed a significant rise in mitochondrial [Ca^{2+}] following IP_3-induced Ca^{2+} release (Csordás et al 2003) and the application of cytosolic Ca^{2+} loads (Moreau et al 2006). Here I have shown that low concentrations of the physiological agonist LTC_4, which evokes cytosolic Ca^{2+} oscillations and Ca^{2+} entry through CRAC channels, also causes a detectable rise in mitochondrial matrix [Ca^{2+}] in intact RBL-1 cells. Interestingly, I did not observe mitochondrial Ca^{2+} oscillations in response to LTC_4, despite robust cytosolic Ca^{2+} oscillations. The reason for this is unclear at present but could involve partial inactivation of the mitochondrial uniporter (Moreau et al 2006) or may be due to differences in the kinetics of mitochondrial Ca^{2+} uptake and release mechanisms.

In Chapter 3, I found that Ca^{2+}-calmodulin gated CRAC channels in a lobe-specific manner and the evidence suggested that calmodulin modulated CRAC channels through an effect on mitochondrial Ca^{2+} uptake (cartoon model **4**). Therefore I have investigated Ca^{2+}-calmodulin regulation of mitochondrial Ca^{2+} uptake here.

Previous work shows that cytosolic Ca^{2+} can both facilitate and inactivate the mitochondrial Ca^{2+}uniporter (MCU) and that this facilitation requires calmodulin, (Csordás et al 2003 and Moreau et al 2006, in permeablized cells). I add to this work by first using the ratiometric, fluorescent protein, pericam to directly measure rapid rises in mitochondrial matrix [Ca^{2+}] in intact mast cells and second, by using a calmodulin mutant (CAM4M) which acts as a dominant negative analogue to reduce the function of endogenous calmodulin. Such an approach avoids concerns over the specificity of drugs that block calmodulin, which may have additional side effects. My first important finding is that the mitochondrial matrix Ca^{2+} rise that is detected through recording the pericam fluorescent signal in response to either LTC_4 or thapsigargin is significantly impaired in intact RBL-1 cells expressing CAM4M. Calmodulin is therefore required to facilitate mitochondrial Ca^{2+} uptake in intact mast cells, in response to a physiological agonist (cartoon model **5**).

I find calmodulin is not needed for mitochondrial Ca^{2+} uptake following a large cytosolic Ca^{2+} rise in the absence of any Ca^{2+} entry (evoked by 1µM thapsigargin in zero Ca^{2+} and 1 mM La^{3+}). In contrast I have shown whilst thapsigargin fails to evoke a mitochondrial Ca^{2+} rise in zero Ca^{2+} alone (which evokes only a small cytosolic Ca^{2+} rise), thapsigargin evokes a mitochondrial Ca^{2+} rise in the presence of 2 mM external Ca^{2+} and therefore in the presence of Orai1-driven Ca^{2+} entry, and this matrix Ca^{2+} rise is dependent on calmodulin. In other words, a large bulk cytosolic Ca^{2+} rise raises matrix Ca^{2+} in a calmodulin-independent manner whereas a smaller rise via Orai1 requires calmodulin for efficient mitochondrial Ca^{2+} uptake, suggesting calmodulin senses the local rise in Ca^{2+} near Orai1. Presumably, the large bulk rise in cytosolic Ca^{2+} recruits cytosolic calmodulin whilst the smaller CRAC channel dependent Ca^{2+} signals rely on local calmodulin, (see cartoon model **6** to visualize this). Therefore the calmodulin which facilitates mitochondrial Ca^{2+} uptake must be very close to, or attached to Orai1, (cartoon model **6**). Calmodulin has been found to bind constitutively to L-type Ca^{2+} channels, enabling it to sense local Ca^{2+} entry through the channel and convey the signal to distal targets, such as the nucleus (Dolmetsch et al 2001). Dolmetsch et al 2001 demonstrated the importance of calmodulin tethered to L-type Ca^{2+} channels for signalling to the nucleus through the use of L-type channel mutants that could not bind calmodulin. The mutant channels impaired gene transcription in neuronal cells. In 2009, Mullins et al identified a calmodulin binding site in the N terminus of Orai1 (at amino acid points 68-91). To see whether the calmodulin attached to Orai1 senses CRAC channel dependent Ca^{2+} influx and relays this to the mitochondria, in a similar manner as found in excitable cells (Dolmetsch et al 2001), I have compared the effect of overexpressing normal Orai1 with expressing A73E Orai1 (both with STIM1). A73E Orai1 is a mutant Orai1 construct that cannot bind calmodulin but otherwise functions as normal Orai1. RBL-1 cells expressing A73E Orai1 fail to alter the initial rate and extent of mitochondrial Ca^{2+} uptake, eliminating an essential role for calmodulin tethered to Orai1 in the activation of MCU. This is consistent with Moreau et al 2006, who found that calmodulin antagonists reduced the initial rate of MCU Ca^{2+} uptake only partially. Comparison of the time-course of the mitochondrial matrix [Ca^{2+}] following stimulation unveiled an important difference between cells expressing A73E Orai1 and overexpressing STIM1, with those overexpressing normal Orai1 (and STIM1). In the presence of A73E Orai1, the mitochondrial Ca^{2+} rise (in response to thapsigargin, after admission of 2 mM Ca^{2+}) was transient and rapidly recovered to pre-stimulation levels despite the presence of the stimulus. By contrast, cells overexpressing Orai1 and STIM1 showed a sustained elevation in mitochondrial matrix [Ca^{2+}] with little or no recovery. This demonstrates that calmodulin tethered to Orai1 is required to sustain mitochondrial Ca^{2+} uptake (as illustrated in cartoon model **7**), allowing the mitochondria to buffer larger quantities of Ca^{2+}.

I confirmed the importance of calmodulin tethered to Orai1 for sustaining mitochondrial Ca^{2+} uptake using an alternative approach. This involved measuring the amount of free Ca^{2+} remaining in the mitochondrial matrix after stimulation as an indication of the amount of Ca^{2+} taken up by the mitochondria during stimulation. I applied ionomycin to cells that had been pre-stimulated with thapsigargin, administered 2 mM Ca^{2+} for 200s (to load the mitochondria) and then exposed to low external calcium, to return cytosolic Ca^{2+} back to basal levels. Ionomycin consistently caused a rise in cytosolic Ca^{2+}, which represented the amount of Ca^{2+} within the mitochondrial matrix after stimulation, since the ER had already been depleted of Ca^{2+} (by thapsigargin). I found that expressing A73E Orai1 caused the ionomycin-induced rise in cytosolic Ca^{2+} to be significantly reduced, compared to cells overexpressing Orai1. This suggested less Ca^{2+} was buffered by the mitochondria upon stimulation under conditions where calmodulin was unable to bind to Orai1, (confirming the proposal depicted in cartoon model **7**).

Differences in the initial rate of Orai1-dependent Ca^{2+} entry cannot account for the differences in the recovery of the pericam Ca^{2+} signal or ionomycin-induced cytosolic Ca^{2+} rise between A73E Orai1 and normal Orai1. I found no significant difference in the initial rate of Orai1-dependent Ca^{2+} entry between cells expressing A73E Orai1 (and overexpressing STIM1) compared to cells overexpressing normal Orai1 (and STIM1).

Similar to the differences found for the recovery of the mitochondrial matrix Ca^{2+} signal between cells expressing A73E Orai1 and those overexpressing normal Orai1, the rate of recovery of the cytosolic Ca^{2+} rise also differed between the two conditions. The decay of the cytosolic Ca^{2+} rise after CRAC channel activation was faster but only modestly so in cells that were expressing A73E Orai1 (and STIM1). Calmodulin is therefore an important modulator (not activator) of Orai1-dependent Ca^{2+} entry and mitochondrial Ca^{2+} uptake. The calmodulin that is initially tethered to Orai1 seems to increase mitochondrial Ca^{2+} buffering and this would facilitate CRAC channel activity by reducing slow Ca^{2+}-dependent inactivation of CRAC channels (Gilabert and Parekh 2000), such a mechanism is illustrated in cartoon model **8** on the next page. Future work could test the effect of expressing A73E Orai1 (and STIM1) on slow Ca^{2+}-dependent inactivation of CRAC channels by directly measuring I_{CRAC} in RBL-1 cells using whole-cell patch clamp techniques.

My results identifying calmodulin tethered to Orai1 as a major source of calmodulin for facilitating mitochondrial Ca^{2+} buffering has led me to propose a mechanism underlying calmodulin-dependent facilitation of mitochondrial Ca^{2+} uptake. Local Ca^{2+} entry through CRAC channels binds to calmodulin tethered to Orai1, causing the protein to be released and diffuse to the mitochondrial Ca^{2+} uptake sites, where it enhances buffering of Ca^{2+} , (cartoon model **8** illustrates this mechanism and the subsequent effect on CRAC channel activity). Cartoon model's **1-7** allow one to visualize a build up of this final model which is shown in cartoon model **8** on the next page.

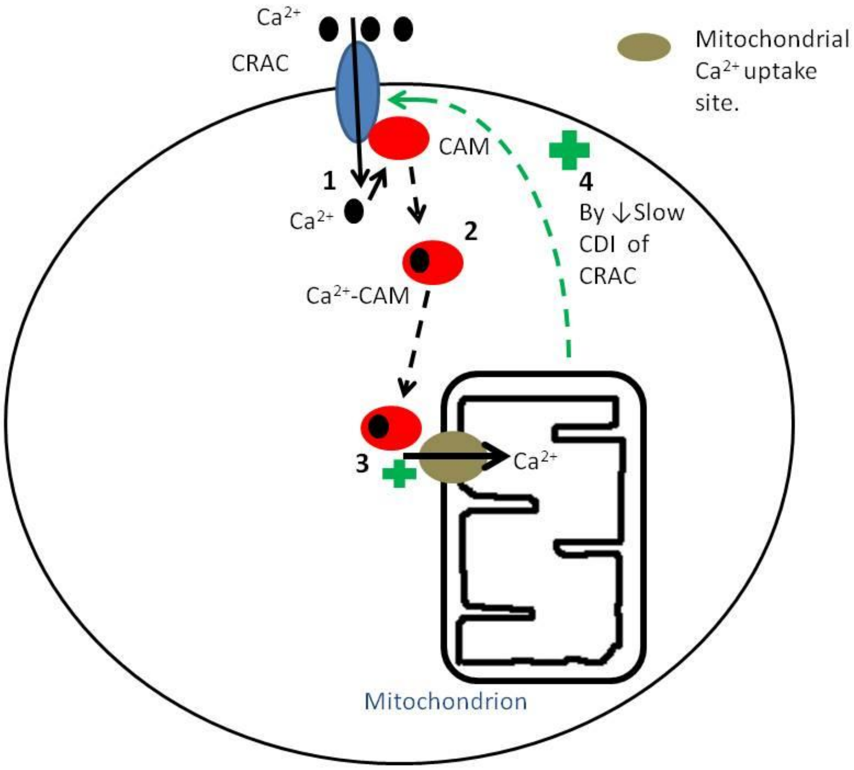

Cartoon model 8 illustrates the proposed mechanism put together from the results of Chapter's 3 and 4 for the modulation of CRAC channels by cytoplasmic Ca^{2+}. This modulation pathway is heavily reliant on the C-lobe of calmodulin. 1) Upon CRAC channel activation, local Ca^{2+} entry binds to calmodulin (CAM) that is tethered to Orai1 to form a Ca^{2+}-CAM (calmodulin) complex. 2) This complex is released from the CRAC channel and diffuses into the cytoplasm. 3) Ca^{2+}-CAM docks at a site either on MCU itself or on a closely associated protein (possibly MICU1). This leads to enhanced mitochondrial Ca^{2+} uptake. 4) Enhancing mitochondrial Ca^{2+} buffering facilitates CRAC channel dependent Ca^{2+} entry, by reducing Ca^{2+}-dependent slow inactivation of the channels. This view is supported by the experiment depicted in figure **9B** where the Fura 2 measured cytosolic Ca^{2+} signal 200s after admission of 1 mM Ca^{2+} is shown to decay faster in the presence of A73E Orai1 than normal Orai1. This suggests that when calmodulin cannot tether to Orai1 which prevents the sustained increase in mitochondrial Ca^{2+} uptake, Ca^{2+}-dependent slow inactivation of CRAC channels increases.

Only recently has the molecular identity of mitochondrial Ca^{2+} uptake been identified (De Stefani et al and Baughman et al 2011). Perocchi et al 2010 previously identified a 53 kDa, Ca^{2+}-sensing protein within the inner mitochondrial membrane (IMM) of HeLa cells using targeted RNAi screening techniques. This protein termed MICU1, although required for MCU Ca^{2+} uptake, is not the uniporter itself because it is a single transmembrane domain spanning protein. I add to this previous work by demonstrating the requirement for endogenous functioning MICU1 for mitochondrial Ca^{2+} uptake in intact RBL-1 cells. This protein could therefore be an important target for calmodulin tethered to Orai1 and underlie calmodulin-dependent facilitation of mitochondrial Ca^{2+} buffering. Recently the mitochondrial uniporter has been identified as a 40 kDa protein composed of two transmembrane spanning domains which physically interact with MICU1, (De Stefani et al and Baughman et al 2011). It is not known whether MICU1 or MCU have a calmodulin binding site. It is possible that calmodulin will bind to one or both of these proteins. In doing so, calmodulin may regulate MICU1-MCU interactions or directly bind to MCU to alter its activity by controlling the open probability of MCU by favouring a facilitatory mode.

Ca^{2+} is removed from the mitochondria in most cells mainly via the $3Na^{+}/Ca^{2+}$ exchanger (NCX) (Arnaudeau et al 2001, Sedova et al 2000 in endothelial cells, Tang et al 1997, Parekh 2003a, Palty et al 2010, 2012). The transporter has been determined molecularly in HEK 293 and SHSY-5-Y cells as NCLX by Palty et al 2010, 2012. Could calmodulin be targeting NCX to regulate mitochondrial Ca^{2+} uptake? This is unlikely because I have found that recovery of matrix Ca^{2+} following stimulation with LTC_4 or thapsigargin in 2 mM external Ca^{2+} solution to be very slow in control cells. In other words, normal mitochondrial Ca^{2+} removal is probably too slow to account for a possible facilitation of mitochondrial Ca^{2+} uptake by calmodulin.

Finally, I investigated the physiological impact of the regulation of mitochondrial Ca^{2+} uptake by calmodulin. NFAT-1 is an important Ca^{2+}-dependent transcription factor that controls the expression of numerous genes important for T cell activation and the generation of immune responses (Hogan et al 2003). Mitochondrial buffering has been shown to regulate CRAC channel driven NFAT-1 nuclear translocation in Jurkat T cells (Hoth et al 2000) and HEK cells (Kar et al 2011) through the movement of an NFAT1-GFP chimera in real time, using live single cell imaging. Inhibition of mitochondrial Ca^{2+} uptake with CCCP (Hoth et al 2000) or co-treatment with antimycin A and oligomycin (Kar et al 2011) suppressed CRAC channel driven NFAT-1-GFP migration to the nucleus. This demonstrates an important role for mitochondrial Ca^{2+} buffering of CRAC channel activity in NFAT-1 nuclear translocation. To examine whether mitochondrial regulation of CRAC channels impacts on NFAT-1-driven gene expression in RBL-1 cells, I have transfected RBL-1 cells with an EGFP-based reporter plasmid. This plasmid contained a NFAT-1 promoter and I used it to measure gene expression to LTC_4 before and after knockdown of MICU1. I found that knockdown of the mitochondrial Ca^{2+} uniporter regulator reduced NFAT-1-driven gene expression, compared with cells expressing endogenous MICU1 function. Modulation of CRAC channels by Ca^{2+}-calmodulin through an effect on mitochondrial Ca^{2+} buffering therefore influences CRAC channel driven NFAT-1-dependent gene transcription in RBL-1 cells.

The importance of this pathway was demonstrated by Feske et al 2006, who identified a single point mutation in Orai1 which suppressed CRAC channel driven NFAT-1 activation. Furthermore, they associated this mutation with patients who suffered from the hereditary condition, severe combined immune deficiency (SCID). The mechanism I have identified here (cartoon model **8**) which underlies how cytoplasmic Ca^{2+} modulates CRAC channels and subsequent NFAT-1-driven gene expression in RBL-1 cells may help towards therapies for SCID. Indeed finding a small molecule that competes with the calmodulin binding site of Orai1 might be therapeutically very useful to partially impair aberrant CRAC channel activity.

Chapter 5.

The role of MFN2 in the modulation of CRAC channels and agonist-induced Ca^{2+} signals.

5.1 Introduction

Mitochondrial Ca^{2+} uptake is crucial in determining the extent and duration of CRAC channel activity. It is required for I_{CRAC} to develop fully under physiological conditions (Gilabert and Parekh 2000) and reduces Ca^{2+}-dependent slow inactivation, leading to a prolonged Ca^{2+} rise. Consistent with this, in Chapter 3 I establish a critical role for mitochondrial Ca^{2+} buffering in the control of CRAC channels and agonist-induced cytosolic Ca^{2+} oscillations using two separate approaches to impair mitochondrial Ca^{2+} uptake. This involved depolarization of the highly hyperpolarized inner mitochondrial membrane with the protonophore FCCP (Moreau et al 2006). As well as the more specific approach involving knockdown of a required subunit for mitochondrial Ca^{2+} uptake, the mitochondrial Ca^{2+} uniporter regulator (MICU1) (Perocchi et al 2010).

Central to the Ca^{2+} buffering role played by mitochondria is the need for a close association between mitochondria and the endoplasmic reticulum (ER). Rizzuto et al 1998 visualized this close coupling in HeLa cells through co-transfection of mitochondrial targeted and ER targeted fluorescent proteins. Such an approach enabled them to observe the position of the two organelles simultaneously by use of 3D fluorescence imaging. In good agreement with this close association, Moreau et al 2006 viewed numerous mitochondria juxtaposed to the ER (within 10-200 nm) in RBL-1 cells, using electron microscopy techniques. The close coupling they observed is of paramount importance because it exposes the low affinity mitochondrial Ca^{2+} uniporter (MCU) to high, local Ca^{2+} microdomains near IP_3Rs that are required for rapid, robust, significant Ca^{2+} uptake (Rizzuto et al 1998).

However, mitochondria are motile organelles. This has been shown in HeLa cells and mouse embryonic fibroblasts through the use of time-lapse fluorescent microscopy (Rizzuto et al 1998 and Chen et al 2003). The question of how mitochondria remain localised to the ER to enable efficient transfer of Ca^{2+} therefore arises. Physical tethers between the ER and mitochondria have long been suggested (Shore and Tata 1977) to underlie the close apposition of mitochondria with the ER. Such protein tethers have been shown to exist in excitable (Boncompagni et al 2009) and non excitable cells (Csordás et al 2006) with the use of electron tomography and electron microscopy, two very powerful techniques.

The dynamin-related GTPase proteins mitofusin 1 (MFN1) and mitofusin 2 (MFN2) were known to reside in the outer mitochondrial membrane, where they were found to be important for mitochondrial docking and fusion and regulating mitochondrial morphology (Ishihara et al 2004). In 2008 de Brito and Scorrano localised MFN2 to the ER as well, where it was found to be enriched within 'mitochondria-associated membrane' patches of the ER (MAMs) and control ER morphology. MFN2 was suggested to be one important protein in the formation of ER-mitochondrial connections. De Brito and Scorrano found that the close coupling between ER and mitochondria observed in wild type mouse embryonic fibroblasts (MEFs) was significantly reduced (by around 40%) when MFN2 was ablated, an effect that was reversed upon reintroduction of MFN2. This was demonstrated by co-expression of ER-YFP (yellow fluorescent protein) and mitochondrial-RFP (red fluorescent protein) into MEFs, whilst recording the degree of colour overlap (yellow) of the two labelled organelles as a measure of organelle tethering closer than 270 nm. Furthermore, they confirmed the findings using electron tomography, which is a more advanced technique and establishes the spatial relationship between two organelles more precisely (Marsh et al 2001). Targeting MFN2 is an effective way to alter the distance between the ER and mitochondria and thus investigate the impact of this linkage on Ca^{2+} signalling. De Brito and Scorrano showed that loss of MFN2 and the consequential loss of the close ER-mitochondrial coupling decreased mitochondrial Ca^{2+} uptake in response to agonist-induced ER Ca^{2+} release. With the aid of mitochondrial specific (MFN2 ActA) and ER specific (MFN2 IYFFT) MFN2 mutants, they showed that in order for MFN2 to closely couple the ER and mitochondria, it had to form homotypic or heterotypic protein complexes. MFN2 on the ER was shown to require either MFN2 or MFN1 on the mitochondrial surface.

Through its ability to establish close associations between the ER and mitochondria, MFN2 facilitates mitochondrial Ca^{2+} buffering of ER Ca^{2+} release, (de Brito and Scorrano 2008). This is important in mitochondrial control of CRAC channels, (Gilabert and Parekh 2000). It is therefore likely that the ability of MFN2 to link the ER and mitochondria is important in the modulation of CRAC channels and agonist-induced Ca^{2+} signals following physiological levels of agonist stimulation, (which release Ca^{2+} from the ER).

Recently MFN2 has been shown to hinder CRAC channel dependent Ca^{2+} entry following mitochondrial depolarization (Singaravelu et al 2011). This pathway is likely to be of relevance under pathological conditions, where strong mitochondrial depolarization can occur (for example during neuronal excitotoxicity). It may provide a mechanism to protect cells from detrimental cytosolic Ca^{2+} overloading and necrosis (Singaravelu et al 2011). Confocal microscopy techniques were used to monitor the localisation of STIM1-eYFP after MFN2 levels were disrupted and cells were stimulated with thapsigargin. Mitochondrial depolarization resulted in less STIM1 movement to the plasma membrane and decreased CRAC channel activity. Knockdown of MFN2 rescued both responses, revealing that the inhibitory effect of mitochondrial depolarization on STIM1 trafficking is via MFN2. Furthermore, re-expression of MFN2 or expression of a MFN2 mutant specifically expressed to the mitochondria (MFN2 ActA) -but not one specifically targeted to the ER, MFN2 IYFFT-rescued the inhibitory effects of mitochondrial depolarization on Ca^{2+} entry. In other words they restored the sensitivity of STIM1 trafficking and CRAC channel entry to mitochondria depolarization. Singaravelu et al 2011 conclude that mitochondrial MFN2 is important for the control of CRAC channels in MEFs during conditions of strong mitochondrial membrane depolarization by controlling STIM1 trafficking.

De Brito et al 2008 showed that ER MFN2 is required to form tethers with MFN1 or MFN2 on the mitochondria. ER MFN2 is therefore a crucial tethering molecule in the control of Ca^{2+} signals. Any disruption to the function of mitochondrial MFN2 might however be compensated for by tethering between ER MFN2 and mitochondrial MFN1. Therefore mitochondrial MFN2 might not be such a critical protein tether. Investigating whether mitochondrial MFN2 in particular is a vitally important protein tether in the control of Ca^{2+} signals is important to consider. In addition to the ER-mitochondrial tethering function of MFN2 de Brito and Scorrano 2008 showed that loss of MFN2 also disrupted the normal shape and connectivity of the ER and endogenous morphology of mitochondria. Reintroduction of mitochondrial MFN2 but not ER MFN2 rescued mitochondrial morphology and only ER targeted MFN2 restored ER morphology. This demonstrates that MFN2 in the ER and mitochondria have separate effects on the morphology of these two organelles. Therefore mitochondrial MFN2 may have a crucial role on ER-mitochondrial tethering in RBL cells in addition to ER MFN2.

Here I use gene knockdown, overexpression of endogenous proteins and expression of mutant constructs to disrupt the endogenous function of MFN2 and in particular mitochondrial MFN2, a protein that helps link the mitochondria to the ER in RBL-1 cells. My approaches include knockdown of cellular MFN2 (found both in the ER and mitochondria) by transfecting cells with MFN2 RNAi or expression of a dominant negative MFN2 mutant specifically expressed to the mitochondria (MFN2 ActA) to impair the endogenous function of mitochondrial MFN2 exclusively, reducing its ability to link to the ER presumably by disrupting the normal mitochondrial-ER tethering distance. These molecular biological approaches are used to examine the role of MFN2 in the modulation of CRAC channels and agonist-evoked Ca^{2+} signals.

5.2 Results

a. MFN2 modulates CRAC channel dependent Ca^{2+} entry

In Chapter 3, I have shown that efficient mitochondrial Ca^{2+} buffering is important for the gating of CRAC channels as well as the maintenance of physiologically-induced cytosolic Ca^{2+} oscillations. CRAC channel dependent Ca^{2+} entry is impaired by knockdown of a key regulatory subunit of mitochondrial Ca^{2+} uptake, MICU1. In addition, LTC_4-induced cytosolic Ca^{2+} oscillations run down more quickly in the presence of protonophore, FCCP, (which depolarizes the inner mitochondrial membrane), or after knockdown of MICU1. One important feature that enables mitochondria to function as efficient buffers of intracellular Ca^{2+} is their close association with the ER (Rizzuto et al 1998, Moreau et al 2006). Since mitochondrial buffering is known to regulate CRAC channels (Gilabert and Parekh 2000), I have investigated the role of MFN2 and its ability to link the ER and mitochondria in the gating of CRAC channels. To do this I have carried out experiments using separate approaches to disrupt the endogenous function of MFN2 in RBL-1 cells.

1. First, I knocked down cellular MFN2, found in both the ER and mitochondrial membranes, by transfecting RBL-1 cells with MFN2 RNAi. Green fluorescent protein (GFP) cDNA was always co-transfected with the RNAi molecule to identify cells that had been successfully transfected with MFN2 RNAi, and only these cells were selected for single cell imaging. Transfection with MFN2 RNAi significantly reduced endogenous MFN2 (see fluorescent microscopy images in figure 1**A**). High expression of MFN2 (prominent red staining) was visualized in control cells (figure 1**A**i), whilst MFN2 protein was barely detected (little red staining) in cells in which MFN2 had

been knocked down (figure 1**A**ii). Figure 1**A** illustrated that successful knockdown of MFN2 had been achieved by transfecting cells with MFN2 RNAi. All cells were loaded with the Ca^{2+}-sensitive indicator, Fura 2, to monitor changes in cytosolic $[Ca^{2+}]$. The initial rate of CRAC channel dependent Ca^{2+} entry was measured after admission of 2 mM external Ca^{2+} following stimulation with 1 μM thapsigargin in Ca^{2+}-free external solution. Transfection with GFP cDNA alone had no effect on CRAC channel dependent Ca^{2+} entry (not shown), consistent with Moreau et al 2005. Therefore any effect seen in cells transfected with MFN2 RNAi and GFP cDNA should be regarded as a direct impact of knockdown of MFN2. Untransfected RBL-1 cells therefore provide an adequate control for my experiments.

I found CRAC channel dependent Ca^{2+} entry was significantly increased in cells in which MFN2 had been knocked down compared to untransfected cells (figure 1**B,** presents aggregate data). This confirmed a role for MFN2 in the modulation of CRAC channels in RBL-1 cells (previously revealed by Singaravelu et al 2011).

In cells in which MFN2 had been knocked down, no significant difference was found in the size of the thapsigargin-induced Ca^{2+} release in zero Ca^{2+} external solution (after transfection with MFN2 RNAi n=10 mean peak ratio 0.0724 ± 0.00976 SEM., untransfected cells n=22 mean peak ratio 0.0506 ± 0.0108 SEM., p=NS). Therefore the increased CRAC channel dependent Ca^{2+} entry observed when MFN2 had been knocked down could not be explained through variations in ER Ca^{2+} store content.

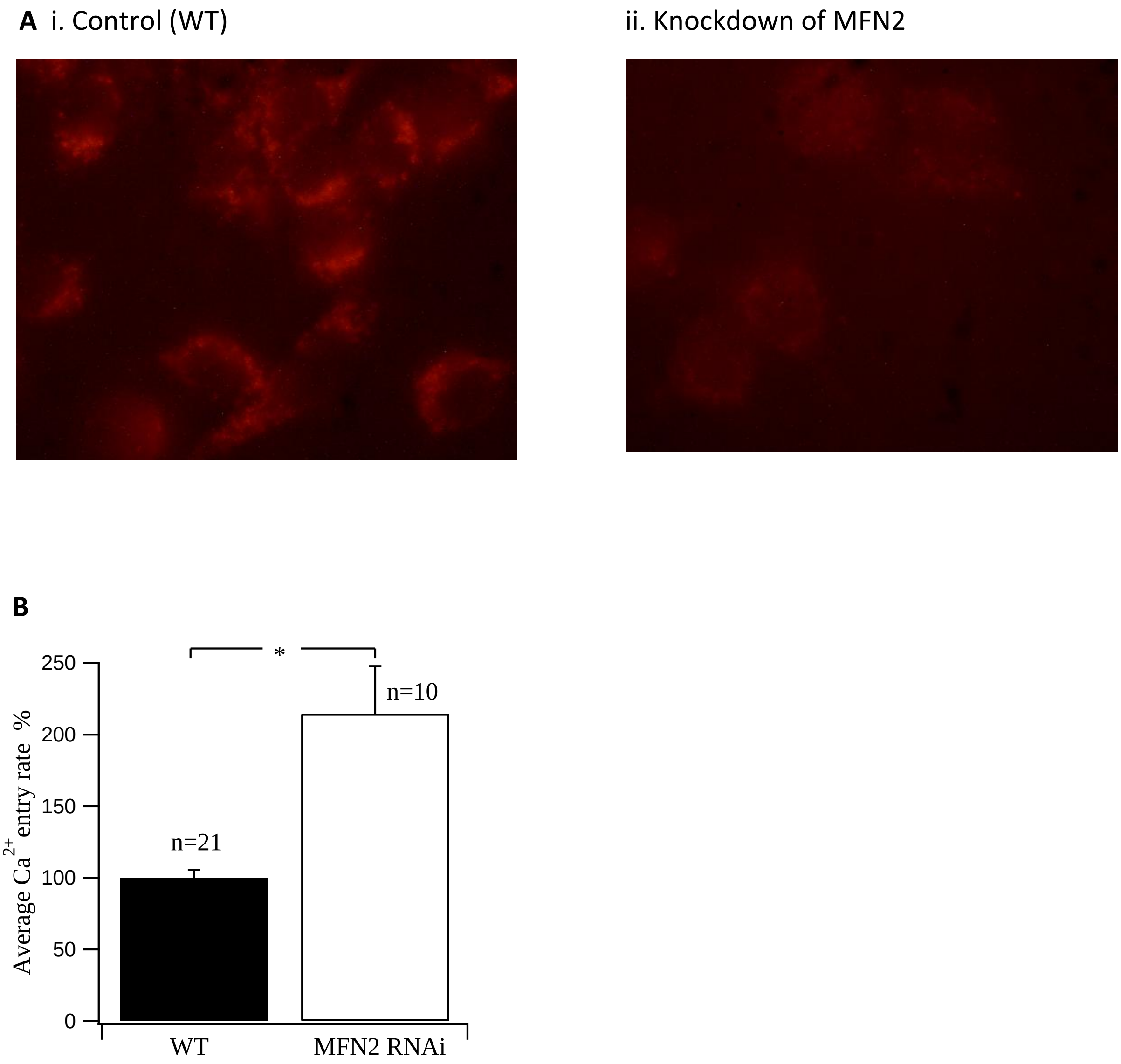

Figure 1. Knockdown of MFN2 by transfecting cells with MFN2 RNAi increased CRAC channel dependent Ca^{2+} entry. A. Fluorescence microscopy images reveal the protein distribution of MFN2, (where MFN2 is stained with a red fluorescent secondary antibody, Alexa 594), for untransfected (control; WT) RBL-1 cells (i.) and cells transfected with MFN2 RNAi (ii.). Prominent red staining of MFN2 is observed in control cells, whereas barely any red staining is seen in MFN2 RNAi transfected cells, indicating MFN2 is successfully knocked down by transfecting RBL-1 cells with MFN2 RNAi. **B**, aggregate data from 10 MFN2 RNAi transfected and 21 untransfected RBL-1 cells (WT) ($p<0.0001$) compare the average initial rate of CRAC channel dependent Ca^{2+} entry, between cells transfected with MFN2 RNAi and untransfected RBL-1 cells (WT). 1 µM thapsigargin is applied to RBL-1 cells that are bathed in Ca^{2+} -free external solution, to deplete Ca^{2+} from the intracellular Ca^{2+} stores and subsequently open CRAC channels. 2 mM Ca^{2+} is then introduced to the cells and the initial rate of rise of CRAC channel driven Ca^{2+} entry is measured using Fura 2, to monitor changes in cytosolic [Ca^{2+}].

2. To investigate the importance of mitochondrial MFN2, I transfected cells with a mutant MFN2, MFN2 ActA cDNA. This mutant is specifically expressed in the mitochondrial membrane. Expression of this mutant disrupts normal ER-mitochondrial tethering by reducing the ability of endogenous mitochondrial MFN2 to link to the ER. Presumably this disengages the close association between the ER and mitochondria, pulling the mitochondria away from the ER. Under conditions where I transfected cells with standard amounts (1.6 µg) of MFN2 ActA cDNA, I failed to detect a significant difference in CRAC channel dependent Ca^{2+} entry between untransfected and MFN2 ActA (and GFP) transfected cells. This is probably because there is still sufficient endogenous functioning mitochondrial MFN2 to keep ER-mitochondrial tethering intact. Therefore I doubled the amount (to 3.2 µg) of MFN2 ActA plasmid. Consistent with the result obtained when cellular MFN2 in both the ER and mitochondria were knocked down, CRAC channel dependent Ca^{2+} entry was significantly increased when cells were transfected with 3.2 µg of MFN2 ActA compared to untransfected RBL-1 cells, (figure 2).

Knockdown of MFN2 or expression of dominant negative MFN2 ActA both led to a similar increase in CRAC channel dependent Ca^{2+} entry rate. Therefore 3.2 µg of MFN2 ActA cDNA is sufficient to inhibit endogenous function of MFN2, to the same extent as knockdown of MFN2. I continued to transfect with 3.2 µg of MFN2 ActA cDNA for subsequent experiments to investigate the impact of reducing the endogenous function of mitochondrial MFN2 on Ca^{2+} signals.

In cells transfected with 3.2 µg of MFN2 ActA, no significant difference was found in the size of the thapsigargin-induced Ca^{2+} release compared to untransfected cells (untransfected n=29, mean peak ratio 0.0539 ± 0.00241 SEM., expression of MFN2

ActA n=14, mean peak ratio 0.0712 ± 0.0135 SEM., p=NS). Therefore the difference in CRAC channel dependent Ca^{2+} entry cannot be attributed to differences in ER Ca^{2+} store content.

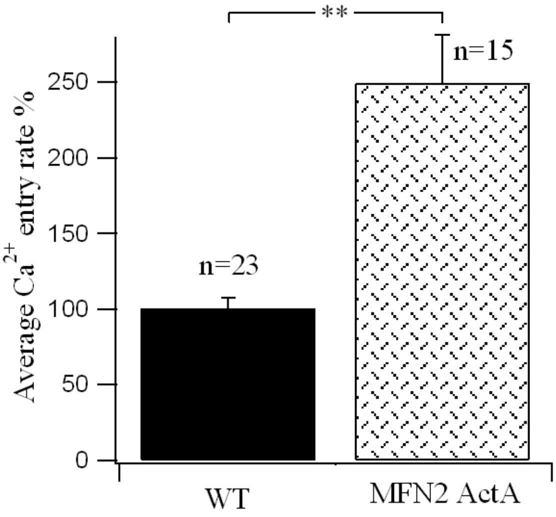

Figure 2. Expression of MFN2 ActA increases CRAC channel dependent Ca^{2+} entry. The average initial rate of CRAC channel dependent Ca^{2+} entry is compared between 15 MFN2 ActA transfected and 23 untransfected RBL-1 cells (WT) ($p<0.0001$).

3. Finally, I have overexpressed MFN2 in HEK 293 cells to investigate the impact of increasing the level of MFN2, (which would be expected to tighten ER-mitochondrial tethering, bringing the organelles closer together, although direct evidence using electron tomography is needed to confirm this), on CRAC channel dependent Ca^{2+} entry. HEK cells were used to overexpress MFN2 since it is well known that they have a higher ability to overexpress recombinant proteins and higher transfection efficiency compared to RBL-1 cells (Singaravelu et al 2011). Transfection of GFP cDNA alone had no effect on CRAC channel dependent Ca^{2+} entry in HEK 293 cells. I found that overexpression of MFN2 significantly reduced CRAC channel dependent Ca^{2+} entry compared to untransfected HEK 293 cells, (figure 3). This reveals that the modulation of CRAC channels by MFN2 is found in different cell types from different species.

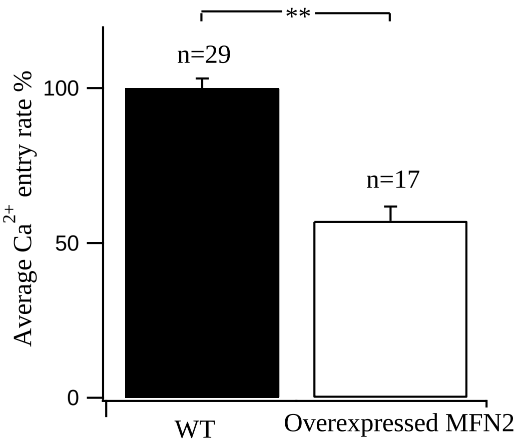

Figure 3. Overexpressing MFN2 reduces CRAC channel dependent Ca^{2+} entry in HEK 293 cells. Comparison of the average initial rate of CRAC channel dependent Ca^{2+} entry between cells overexpressing MFN2 (n=17) and untransfected HEK 293 cells (WT) (n=29) ($p<0.0001$) are presented.

b. MFN2 helps to maintain agonist-induced cytosolic Ca^{2+} signals.

Although thapsigargin reliably activates CRAC channels to their full extent, it does not provide an insight into the modulation of CRAC channels by MFN2 under physiological conditions. It was therefore important to investigate whether MFN2 modulated physiologically-induced Ca^{2+} signals. In RBL cells, submaximal concentrations of agonist evoke cytosolic Ca^{2+} oscillations, which require Ca^{2+} entry to be sustained (Di Capite et al 2009a). I used low, physiological concentrations (160 nM) of leukotriene C_4 (LTC_4) (previously used in Chapter 3 and by Di Capite et al 2009a) to induce cytosolic Ca^{2+} oscillations. I tested a role for MFN2 in the modulation of agonist-evoked cytosolic Ca^{2+} signals (following Ca^{2+} release from the ER), using two separate approaches to disrupt the endogenous function of MFN2.

1. First, I knocked down MFN2 using an RNA interference approach. Fura 2 was loaded into cells to record the dynamic changes in cytosolic [Ca^{2+}] when cells were stimulated with 160 nM LTC_4 in 2 mM external Ca^{2+}. Transfection of RBL-1 cells with GFP cDNA alone failed to have any effect on LTC_4-induced Ca^{2+} oscillations. LTC_4-induced cytosolic Ca^{2+} oscillations were found to run down more quickly when cells were transfected with MFN2 RNAi, (figure 4**B**), compared to untransfected RBL-1 cells (figure 4**A**). In contrast to untransfected RBL-1 cells where continuous oscillations were always evoked, a range of responses were observed when cells were transfected with MFN2 RNAi (figure 4**B**). Around 20% of the cells showed a big initial spike which decayed (figure 4**B**.i.) whilst around 80% of cells showed a big initial spike followed by a couple or a few subsequent oscillations (figure 4**B**. ii., iii., iv.). This is probably due to slight differences in the transfection efficiency. However in cells transfected with MFN2 RNAi a common feature was a more prolonged initial

Ca^{2+} transient followed by spikes of smaller amplitude, the number of which varied but was always significantly fewer than that found in untransfected cells. This demonstrates that MFN2, which is important for efficient mitochondrial Ca^{2+} buffering (de Brito and Scorrano 2008), helps to maintain LTC_4-induced Ca^{2+} oscillations. The result is consistent with my findings in Chapter 3 that cytosolic Ca^{2+} oscillations run down more quickly when mitochondrial Ca^{2+} buffering is impaired following pre-incubation with FCCP or after knockdown of MICU1. This suggests that MFN2 and presumably its ability to link the ER and mitochondria together helps to maintain cytosolic Ca^{2+} oscillations, probably through an effect on mitochondrial Ca^{2+} buffering.

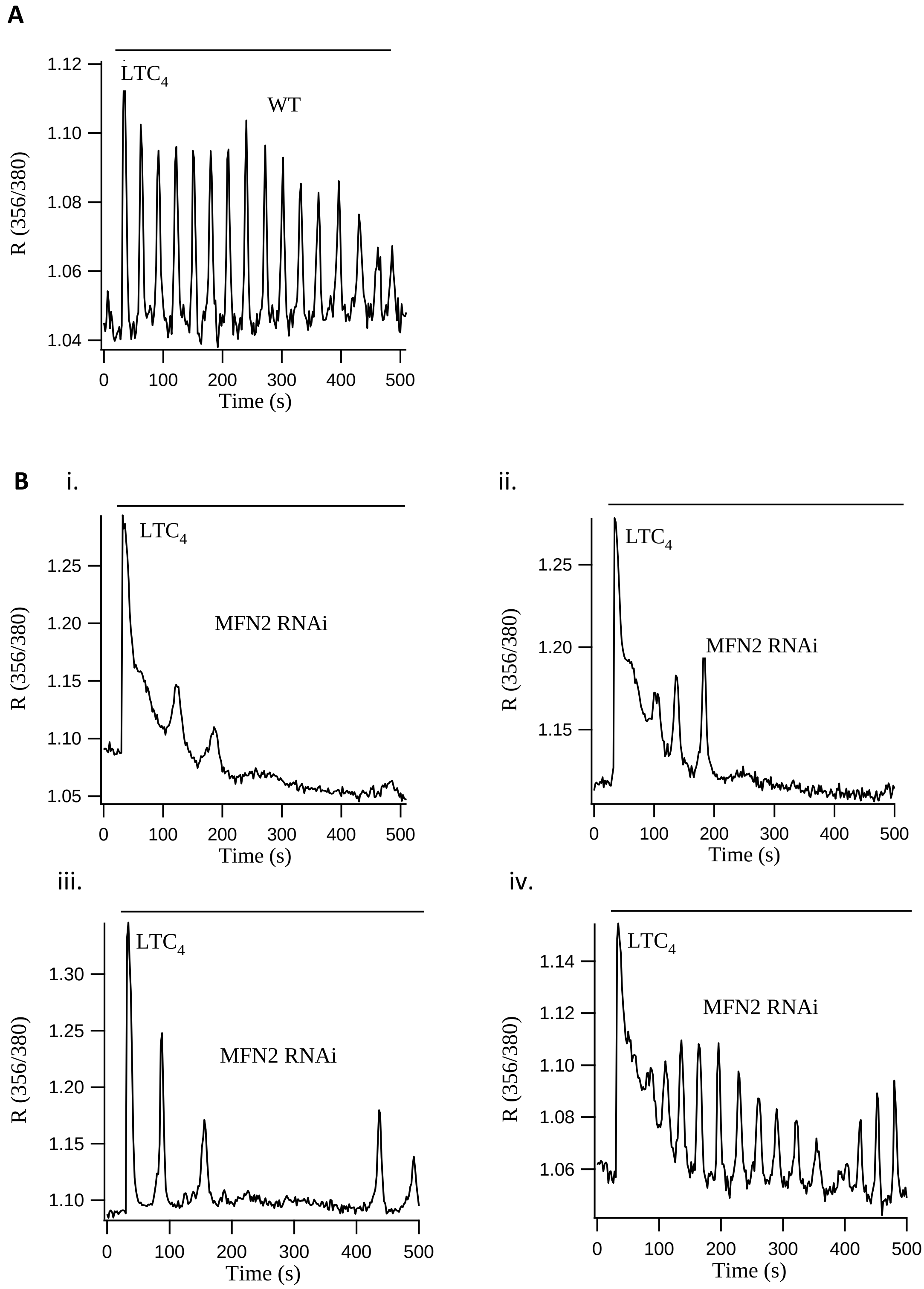

Figure 4. Knockdown of MFN2 impairs the maintenance of physiologically-induced Ca^{2+} oscillations. A, the trace presents the oscillation pattern when one untransfected RBL-1 cell (WT) is stimulated with 160 nM of LTC_4 in 2 mM external Ca^{2+}. **B**, the recordings reveal the range of oscillation patterns when RBL-1 cells are transfected with MFN2 RNAi. Approximately 20% of cells produce oscillation pattern i., whilst the remaining 80% of cells show a mixture of the patterns ii., iii. and iv.

2. In a second approach, I transfected cells with MFN2 ActA cDNA and stimulated with 160 nM LTC_4 in 2 mM Ca^{2+}. Consistent with the results obtained after knockdown of MFN2, the cytosolic Ca^{2+} oscillations ran down more quickly in cells expressing MFN2 ActA (figure 5), compared to untransfected RBL-1 cells. Figure 5 reveals the oscillation patterns in cells expressing MFN2 ActA cDNA. A large, prolonged first oscillation peak is observed with few (figure 5 ii.) or no subsequent spikes (figure 5 i.).

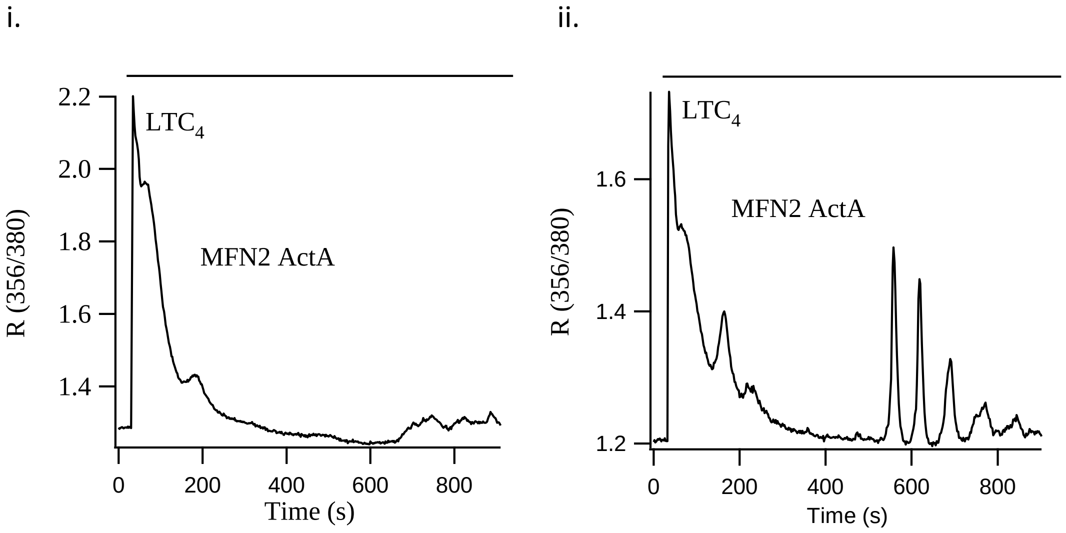

Figure 5. Expression of MFN2 ActA cDNA impairs the maintenance of cytosolic Ca^{2+} oscillations. The oscillation patterns when cells expressing MFN2 ActA are stimulated with 160 nM of LTC_4 in 2 mM external Ca^{2+} are shown by the traces. 50% of cells show pattern i., whilst the remaining 50% show an oscillation pattern similar to ii.

c. MFN2 facilitates mitochondrial Ca^{2+} uptake of IP_3-induced Ca^{2+} release

Csordás et al 2006 reported that disruption of the protein tethers between mitochondria and the ER impaired the efficient transfer of Ca^{2+} between these two organelles. Furthermore, de Brito and Scorrano 2008 showed that MEFs that were ablated of MFN2 evoked a significantly reduced ATP-driven mitochondrial Ca^{2+} uptake, under conditions where cells were permeabilized with digitonin. I find agonist-induced cytosolic Ca^{2+} oscillations run down more quickly in intact RBL-1 cells where endogenous functioning of MFN2 and notably mitochondrial MFN2 is reduced. Therefore I have hypothesised that MFN2 helps to maintain LTC_4-induced cytosolic Ca^{2+} oscillations through facilitating the transfer of Ca^{2+} from the ER to the mitochondria (presumably through maintaining the normal tethering between the ER and mitochondria). To investigate this, I have used three separate approaches to reduce endogenous MFN2 function whilst using pericam to measure directly changes in mitochondrial matrix Ca^{2+} in intact RBL-1 cells, when cells are stimulated with 160 nM LTC_4 in 2 mM external Ca^{2+} solution. RBL-1 cells were either transfected with pericam alone (control cells, WT), or co-transfected with MFN2 RNAi or with mutant MFN2 cDNA constructs specifically targeted to either the mitochondria (MFN2 ActA) or the ER (MFN2 IYFFT).

1. In cells transfected with MFN2 RNAi (and pericam), the amplitude of the pericam signal was slightly but significantly reduced compared to pericam transfected cells (control cells; WT), in response to 160 nM LTC_4 in 2 mM Ca^{2+} external solution, (figure 6). This demonstrates that MFN2 and presumably its ability to link the ER and mitochondria facilitates mitochondrial Ca^{2+} uptake of IP_3-induced Ca^{2+} release. The reduction in mitochondrial Ca^{2+} uptake provides evidence that

suggests knockdown of MFN2 probably causes a significant loosening of the association between mitochondria and the ER through the movement of mitochondria away from the ER.

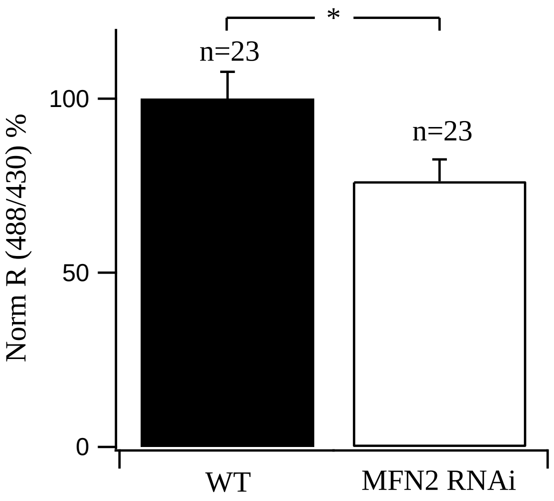

Figure 6. MFN2 facilitates mitochondrial Ca^{2+} uptake of IP_3-induced Ca^{2+} release. Aggregate data from 23 pericam transfected (WT) and 23 MFN2 RNAi (and pericam) transfected RBL-1 cells (p=0.0215) reveals that mitochondrial Ca^{2+} uptake is significantly reduced in cells where both ER and mitochondrial MFN2 are knocked down compared to pericam transfected cells (control; WT), in response to 160 nM LTC_4 in 2 mM external Ca^{2+}.

2. To investigate the role of mitochondrial MFN2 on mitochondrial Ca^{2+} buffering of IP_3-induced Ca^{2+} release, cells were co-transfected with MFN2 ActA and pericam and were compared with pericam alone transfected cells, following stimulation with LTC_4 in 2 mM Ca^{2+} external solution. In the presence of MFN2 ActA, the amplitude of the pericam signal was significantly reduced compared to pericam (alone) transfected cells (figure 7). This supports the conclusion that mitochondrial MFN2 facilitates mitochondrial Ca^{2+} uptake.

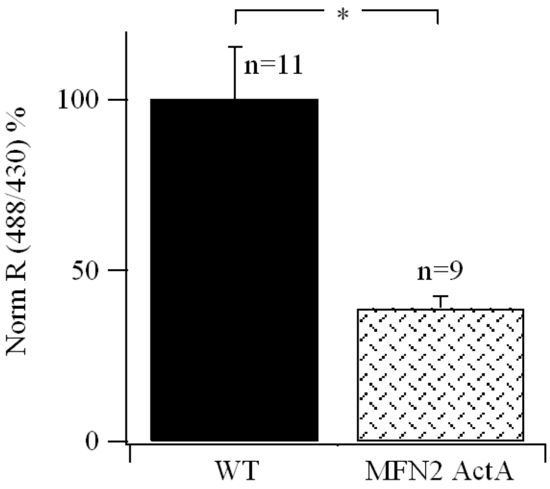

Figure 7. Mitochondrial MFN2 facilitates mitochondrial Ca^{2+} uptake. Comparison of the mitochondrial Ca^{2+} uptake between 11 pericam transfected (WT) and 9 MFN2 ActA (and pericam) transfected RBL-1 cells (p=0.0024) bathed in 2 mM external Ca^{2+} and stimulated with 160 nM LTC_4 is shown.

It is notable that transfection with 1.6 µg of MFN2 ActA failed significantly to affect the ability of the mitochondria to take up Ca^{2+} (figure 8). This suggests that 1.6 µg MFN2 ActA is not capable of significantly disengaging normal endogenous ER-mitochondrial tethering. The effects of MFN2 ActA are therefore dose-dependent. Whilst a low dose (1.6 µg) of MFN2 ActA fails to cause an effect on CRAC channel influx or agonist-induced Ca^{2+} signals, a higher dose (3.2 µg) leads to a sizeable effect on both. This indicates that a significant amount of MFN2 ActA cDNA is needed to overcome normal endogenous MFN2 function.

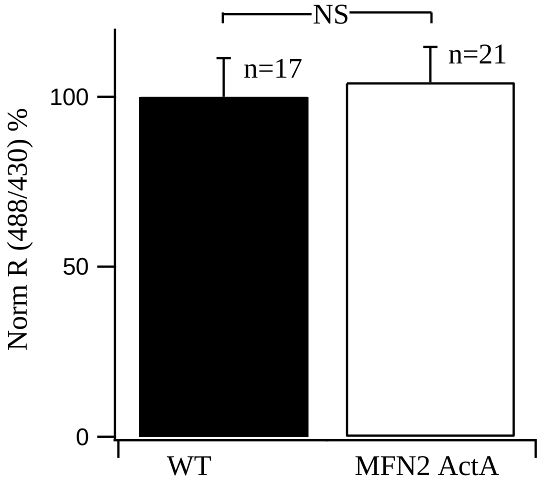

Figure 8. Transfection with 1.6 µg MFN2 ActA cDNA fails to significantly affect mitochondrial Ca^{2+} buffering. Aggregate data from 17 pericam transfected (WT) and 21 MFN2 ActA transfected RBL-1 cells (p=NS) are compared.

3. In addition to the two separate approaches used above to reduce the endogenous function of MFN2, I used another dominant negative MFN2 mutant, MFN2 IYFFT. This mutant is specifically expressed in the ER membrane and disrupts normal ER-mitochondrial tethering ((see figure 2 b) of de Brito and Scorrano 2008) presumably by reducing the ability of endogenous ER MFN2 to link to the mitochondria. I co-transfected cells with 1.6 µg of MFN2 IYFFT and pericam and compared the response to LTC_4 in 2 mM Ca^{2+} external solution, with RBL-1 cells transfected with pericam alone. In the presence of MFN2 IYFFT, the amplitude of the pericam signal was significantly reduced compared to pericam alone transfected cells (figure 9). Therefore ER MFN2 also facilitates mitochondrial Ca^{2+} uptake and suggests that the mitochondria and ER are probably further apart when the endogenous function of ER MFN2 is reduced.

This observation is to be expected since de Brito et al 2008, show that ER MFN2 is required to form tethers with MFN1 or MFN2 on the mitochondria. Under conditions where mitochondrial MFN2 has been knocked down, the ER MFN2 should still form tethers with MFN1 on the mitochondrial membrane. Therefore one might expect this interaction to compensate to maintain ER-mitochondrial coupling. The finding that knockdown of mitochondrial MFN2 does significantly affect mitochondrial Ca^{2+} uptake suggests that the protein is a crucial tethering molecule.

The reason for half the dose (1.6 µg) of MFN2 IYFFT causing similar effects on mitochondrial Ca^{2+} buffering as 3.2 µg of MFN2 ActA could be explained by the following. Some loss of endogenous mitochondrial MFN2 function is adequately compensated for by endogenous MFN1 whilst following a greater loss of endogenous mitochondrial MFN2 function further compensation cannot occur. It could be that

MFN1 is expressed in lower levels compared to mitochondrial MFN2 or its distribution is more widespread within the mitochondrial membrane and not concentrated within the MAMs like MFN2. This would cause MFN1 to establish fewer and or less important interactions with ER MFN2. Impairment of ER MFN2 by MFN2 IYFFT would not be compensated at all by MFN1 (which is found in the mitochondrial membrane), therefore lower doses of MFN2 IYFFT would reduce mitochondrial Ca^{2+} uptake to a similar extent as higher doses of MFN2 ActA. The ratio of each protein in a tethering complex may also differ. It could be that for every ER MFN2, two mitochondrial MFN2 proteins are required for effective tethering. Therefore more endogenous mitochondrial MFN2 would need to be disrupted to cause a similar impact as impairing endogenous ER MFN2 function. Further work needs to address such questions as well as directly visualizing the effect of each of the MFN2 mutants on ER-mitochondrial distance. Techniques such as electron tomography could be used.

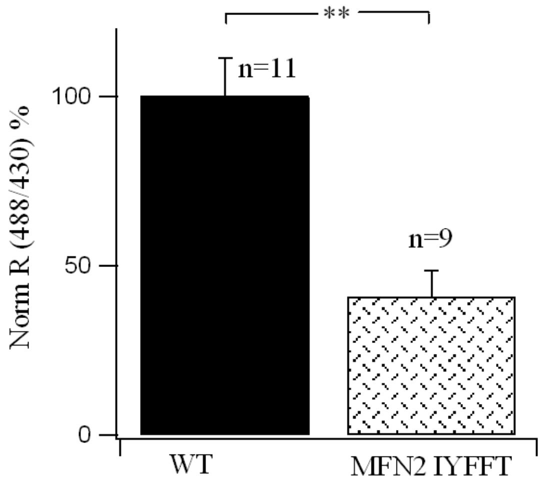

Figure 9. Expression of MFN2 IYFFT cDNA impairs mitochondrial Ca^{2+} buffering. 18 MFN2 IYFFT (and pericam) transfected and 17 pericam transfected RBL-1 cells (WT) (p=0.0001) are compared, demonstrating that expression of MFN2 IYFFT significantly reduces mitochondrial Ca^{2+} uptake to LTC_4 in 2 mM external Ca^{2+}.

d. MFN2 impacts on IP_3R-driven Ca^{2+} release

I have just shown that knockdown of MFN2 or expression of MFN2 ActA, conditions expected to impair the close coupling of the ER and mitochondria, both reduce mitochondrial Ca^{2+} uptake. Such an effect would reduce mitochondrial buffering of IP_3R-driven Ca^{2+} release events. Energizing mitochondria by applying pyruvate, malate or succinate has been shown to increase the size and speed of agonist-induced Ca^{2+} oscillations in Xenopus oocytes (Jouaville et al 1995). Furthermore, antimycin A or ruthenium red (used to impair mitochondrial Ca^{2+} buffering) have been shown to inhibit such oscillations (Jouaville et al 1995). Reducing the buffering of IP_3R-induced Ca^{2+} release events would cause the build up of cytosolic $[Ca^{2+}]$ to high levels, which would negatively feedback on IP_3Rs (Finch et al 1991, Bezprozvanny et al 1991). In doing so, IP_3R calcium-dependent inactivation (CDI) would increase. This would hinder repetitive Ca^{2+} oscillations from arising (Jouaville et al 1995) and explains why cytosolic Ca^{2+} oscillations to LTC_4 run down more quickly in cells transfected with MFN2 RNAi or expressing MFN2 ActA cDNA. Supporting this concept, I found that the peak of the first LTC_4-induced Ca^{2+} oscillation was larger and took longer to recover when both mitochondrial and ER MFN2 were knocked down following transfection with MFN2 RNAi (figure 10**A**, **B**), or when endogenous mitochondrial MFN2 function was reduced following transfection with MFN2 ActA cDNA (figure 10**C**, **D**), in comparison to control, untransfected RBL-1 cells (WT). Collectively, using these two separate approaches to disrupt the endogenous function of MFN2, the results confirm that MFN2 modulates IP_3R-driven Ca^{2+} release, (knockdown of MFN2 increases the initial IP_3R-dependent Ca^{2+} release spike). Such an effect would increase Ca^{2+}-dependent inactivation of IP_3Rs (Bezprozvanny et al

1991 and Finch et al 1991) and inhibit further Ca^{2+} release. Therefore MFN2 could promote continuous IP_3R-induced Ca^{2+} release events (cytosolic Ca^{2+} oscillations) by reducing CDI of the IP_3R.

The increased Ca^{2+}-dependent inactivation of the IP_3Rs would be exacerbated by more pronounced CRAC channel dependent Ca^{2+} entry following knockdown of MFN2 (revealed in section **a. 1.** of this Chapter). The increase in CRAC channel dependent Ca^{2+} entry would raise cytoplasmic Ca^{2+} and therefore i) enhance replenishing the ER with Ca^{2+}, supplying more Ca^{2+} for release whilst ii) contributing directly to Ca^{2+}-dependent inactivation of the IP_3R. Combined, this would increase the negative regulation of IP_3Rs and promote CDI of IP_3Rs further. As a result, cytosolic Ca^{2+} oscillations would cease quickly. My results therefore provide a potential mechanism to explain how MFN2 helps to maintain agonist-induced Ca^{2+} oscillations, through facilitating the ability of mitochondria to buffer regenerative IP_3R-induced Ca^{2+} release events by closely linking the mitochondria and ER. This presumably maintains the normal (favourable) distance between the ER and mitochondria for the efficient transfer of Ca^{2+} between these organelles.

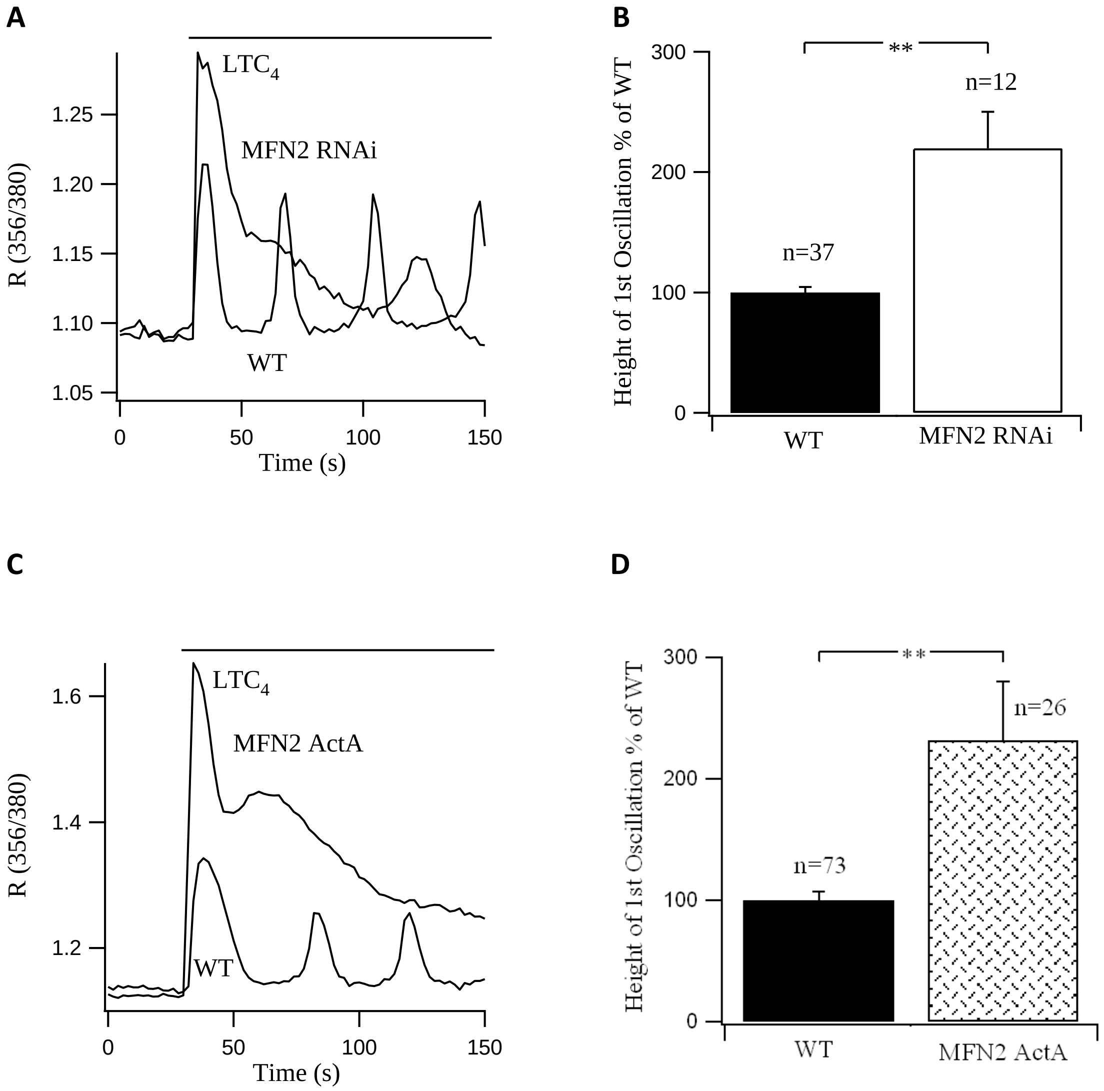

Figure 10. MFN2 modulates IP_3R-driven Ca^{2+} release. A, the traces illustrate the size of the peak of the first cytosolic Ca^{2+} oscillation for one untransfected RBL-1 cell (WT) and one transfected with MFN2 RNAi. **B**. The average height of the peak of the first cytosolic Ca^{2+} oscillation evoked in 2 mM external Ca^{2+} after 160 nM LTC_4 stimulation is shown to be significantly larger in RBL-1 cells transfected with MFN2 RNAi (n=12) compared to untransfected RBL-1 cells (n=37, WT) (p<0.0001). **C**, the recordings show the difference in the amplitude of the peak of the first cytosolic Ca^{2+} oscillation between an untransfected RBL-1 cell (WT) and one transfected with MFN2 ActA. **D**, aggregate data from 26 MFN2 ActA transfected and 73 untransfected RBL-1 cells (WT) (p<0.0001) reveals that the height of the peak of the first cytosolic Ca^{2+} oscillation evoked in 2 mM external Ca^{2+} after 160 nM LTC_4 stimulation is significantly larger in cells expressing MFN2 ActA.

5.3 Discussion

Mitochondria are known to regulate CRAC channels in a Ca^{2+}-dependent manner. An increase of mitochondrial Ca^{2+} buffering increases CRAC channel development (Gilabert and Parekh 2000). One important feature underlying the ability of mitochondria to effectively buffer Ca^{2+} from the ER stores is their close juxtaposition with the ER (Rizzuto et al 1998, Moreau et al 2006). Since mitochondria are motile organelles (Chen et al 2003, Rizzuto et al 1998), they must be held in place to achieve and maintain close contact with the ER. Many proteins have been identified to form the physical complexes that are involved. In 2008 de Brito and Scorrano used electron tomography to show that loss of MFN2 increased the distance between the ER and the mitochondria. Furthermore, MFN2 ablation reduced mitochondrial Ca^{2+} uptake of ER Ca^{2+} release in response to the agonist ATP. MFN2 is therefore one important protein that is known to constitute the physical complexes that link the mitochondria and ER together. By maintaining ER-mitochondrial tethering, it holds the two organelles at a distance that facilitates Ca^{2+} transfer from the ER to the mitochondria in response to physiological agonists. Targeting MFN2 is therefore an effective way to modify the distance between the ER and mitochondria and investigate the impact this has on cellular Ca^{2+} signals. My findings add to work by de Brito et al. Here I have used the genetically encoded fluorescent protein, pericam, to measure mitochondrial matrix Ca^{2+} changes directly in intact RBL-1 cells. Furthermore, I have used two additional approaches to reduce the endogenous function of MFN2. Firstly, I have transfected cells with RNAi against MFN2 to knockdown endogenous function of cellular MFN2. Secondly, I have expressed MFN2 mutants that are specifically targeted to either the mitochondria (MFN2 ActA) or the ER (MFN2 IYFFT). These mutants act as dominant negative proteins, reducing the endogenous function of mitochondrial MFN2 or ER MFN2, respectively. Using these approaches, I show knockdown of MFN2 significantly reduces mitochondrial Ca^{2+} uptake in response to a low dose of LTC_4 in 2 mM external Ca^{2+} solution. Furthermore, mitochondrial Ca^{2+} uptake is significantly reduced in cells expressing either MFN2 ActA, which is expected to reduce the ability of the mitochondria to link to the ER, or MFN2 IYFFT which is expected to reduce the ability of the ER to link to the mitochondria. The results reveal that both ER and mitochondrial MFN2 have important roles in the modulation of mitochondrial buffering of IP_3-induced Ca^{2+} release. This is particularly interesting because de Brito and Scorrano 2008 found that ER MFN2 was required to form tethers with MFN1 or MFN2 on the mitochondrial membrane. Therefore one might expect reducing the function of mitochondrial MFN2 to be compensated for by the intact tethering between the endogenous ER MFN2 and mitochondrial MFN1. However, since reducing the function of mitochondrial MFN2 alone significantly impairs mitochondrial Ca^{2+} buffering this provides evidence that mitochondrial MFN2 has a crucial role in the modulation of agonist-induced Ca^{2+} signals. The reduced mitochondrial Ca^{2+} uptake in response to IP_3-induced Ca^{2+} release, when the endogenous function of MFN2, and in particular mitochondrial MFN2 was reduced, provides indirect evidence that the ER and mitochondria are significantly further apart under such conditions.

Recently an additional function has been assigned to mitochondrial MFN2. Singaravelu et al 2011 identify a role for mitochondrial MFN2 in the control of STIM1 trafficking and subsequent CRAC channel dependent Ca^{2+} entry in MEFs. This regulation occurred under conditions where mitochondria were depolarized. Therefore this may provide a protective mechanism to limit CRAC channel dependent Ca^{2+} entry when normal buffering mechanisms are disrupted, during strong mitochondrial depolarization (Singaravelu et al 2011).

Since MFN2 affects mitochondrial Ca^{2+} buffering (de Brito et al 2008) and STIM1 trafficking (Singaravelu et al 2011), both of which modulate CRAC channel activity (Gilabert and Parekh 2000, Singaravelu et al 2011, Parekh 2003a, Quintana et al 2006), I have tested the role of MFN2 and mitochondrial MFN2 in the modulation of CRAC channels. To do this, I first measured the initial rate of CRAC channel dependent Ca^{2+} entry by stimulating cells with 1 µM thapsigargin in Ca^{2+}-free external solution and then admitting 2 mM external Ca^{2+}. Secondly, I monitored cytosolic Ca^{2+} oscillations induced by low physiological concentrations of LTC_4 (160 nM). Fura 2 was used in both cases to monitor the changes in cytosolic [Ca^{2+}] that occurred.

I found that reducing the endogenous function of MFN2 significantly increased CRAC channel dependent Ca^{2+} entry. Furthermore, expression of MFN2 ActA, which is expected to reduce the ability of mitochondrial MFN2 to link to the ER, also significantly increased CRAC channel dependent Ca^{2+} entry. This confirms a role for mitochondrial MFN2 in the modulation of CRAC channels in RBL-1 cells. Differences in ER store Ca^{2+} content could not account for the effect observed, since no significant difference was found in the size of the Ca^{2+} release response to thapsigargin in Ca^{2+}-free external solution between untransfected cells and those transfected with MFN2 RNAi or MFN2 ActA cDNA. Overexpression of MFN2 (which is expected to tighten the association between the ER and mitochondria) reduced CRAC channel dependent Ca^{2+} entry in HEK cells. Together the results reveal that MFN2 and in particular mitochondrial MFN2 modulates CRAC channels and in different cell types from different species.

The question of how MFN2 and mitochondrial MFN2 may achieve such control on CRAC channels shall now be addressed. Singaravelu et al 2011 demonstrated the control of STIM1 trafficking to the plasma membrane junctions and subsequent CRAC channel dependent Ca^{2+} entry by mitochondrial MFN2 under conditions in which mitochondria were depolarized. They visualized STIM1 movement by monitoring the distribution of STIM1-eYFP in MEFs using confocal microscopy techniques after thapsigargin stimulation. Following mitochondrial depolarization STIM1 movement and CRAC channel dependent Ca^{2+} influx were reduced and these effects were rescued by knockdown of MFN2. Therefore susceptibility of STIM1 movement and CRAC channel dependent Ca^{2+} entry to mitochondrial depolarization was via MFN2. Furthermore, re-expression of normal MFN2 or expression of a mutant MFN2 exclusively targeted to the mitochondria (but not one targeted to the ER) into MFN2-deficient MEFs restored the effects caused by knockdown of MFN2 on STIM1 trafficking and Ca^{2+} influx through CRAC channels. CRAC channel susceptibility to mitochondrial depolarization that was lost following knockdown of MFN2 was therefore rescued by reintroduction of MFN2 or expression of mitochondrial (but not ER) targeted MFN2. However, the inhibitory effect seen by reintroducing MFN2 was overcome by co-transfecting STIM1 with MFN2. Together the results demonstrate that mitochondrial MFN2 exerts control on STIM1 movement during conditions where the mitochondria are depolarized. This can be explained by considering the ratio of MFN2: STIM1. When MFN2:STIM1 ratio is reduced, hindrance on STIM1 movement by MFN2 is decreased and STIM1 has the freedom to move more freely upon stimulation. By contrast, increasing MFN2:STIM1 would enhance the hindrance on STIM1 movement by MFN2, reducing STIM1 trafficking. Supporting work by Singaravelu et al in MEFs, I find in RBL-1 cells that mitochondrial MFN2 (with the use of the same mutant used by Singaravelu et al, MFN2 ActA) is important in the modulation of CRAC channel dependent Ca^{2+} entry. One explanation is that this reflects an action of mitochondrial MFN2 on STIM1 trafficking. This could be tested by investigating whether mitochondrial MFN2 physically interacts with STIM1, using coimmunopreciptation experiments, to bring about such modulation of CRAC channel activity.

An alternative explanation for why Ca^{2+} influx increases after knockdown of MFN2 is that it might move mitochondria away from the ER and consequently bring pools of mitochondria closer to the plasma membrane. Here, they could buffer cytosolic Ca^{2+} rises that are induced by CRAC channel dependent Ca^{2+} entry more efficiently due to a closer association with the plasma membrane. Such regulation has been shown to be important in Jurkat T cells where mitochondria have been revealed to translocate to the plasma membrane following CRAC channel activation, (using both confocal and two-photon microscopy approaches; Quintana et al 2006). In doing so they sustain CRAC channel dependent Ca^{2+} entry by reducing slow Ca^{2+}-dependent inactivation of CRAC channels (Quintana et al 2006). Could such an action be involved in RBL-1 cells under physiological conditions, where mitochondrial movement reduces Ca^{2+}-dependent inactivation? This is unlikely since electron microscopy techniques reveal hardly any mitochondria juxtaposed to the plasma membrane before or after stimulation with thapsigargin (Singaravelu et al 2011). Most mitochondria are between 500 nm to 1 µm from the cell periphery (Singaravelu et al 2011). However, it is possible that the reduction in ER-mitochondrial tethering (secondary to disrupting the endogenous function of MFN2) releases a few mitochondria so that they are better able to approach the plasma membrane and capture incoming Ca^{2+}. Future experiments tracking mitochondrial movement in cells in which MFN2 levels have been manipulated could test this directly. This pathway may be of relevance under pathological conditions where the normal ER-mitochondrial tethering is disrupted such as found in the inherited, human disorder Charcot-Marie-Tooth neuropathy type IIa (CMTIIa), which is associated with mutations of MFN2 (Züchner et al 2004).

My second important finding is that MFN2, and in particular mitochondrial MFN2, helps to maintain agonist-induced cytosolic Ca^{2+} oscillations. This reveals an important role for mitochondrial MFN2 in the regulation of agonist-induced Ca^{2+} signals. Using two separate approaches to reduce the endogenous function of MFN2, I have investigated the role of MFN2 in the modulation of LTC_4-induced cytosolic Ca^{2+} oscillations. These oscillations were shown to rundown more quickly after reduction of the endogenous function of either cellular MFN2 (in both the ER and mitochondria) or mitochondrial MFN2, compared to untransfected or GFP transfected RBL-1 cells. In addition, the peak of the first Ca^{2+} release transient was larger after the endogenous function of MFN2 was reduced. Differences in the initial

IP_3-driven Ca^{2+} release spike between untransfected cells and cells in which endogenous MFN2 function has been reduced cannot be a consequence of differences in ER store Ca^{2+} content since I have shown that the size of the thapsigargin-induced Ca^{2+} release in zero Ca^{2+} is not significantly different between untransfected cells and cells transfected with MFN2 RNAi or MFN2 ActA cDNA.

What could be the underlying mechanism? I found that the height of the first LTC_4-induced Ca^{2+} oscillation was significantly higher and broader when presumably the ability of mitochondrial MFN2 to link to the ER was reduced. The increased initial IP_3R-driven Ca^{2+} release spike that occurred with reduction of the endogenous function of MFN2 could be explained as a consequence of the disengagement of the ER-mitochondrial tethering. Despite increasing Ca^{2+} release to LTC_4, loss of MFN2 is associated with reducing mitochondrial Ca^{2+} uptake, this supports the view of increasing the distance of mitochondria from ER and therefore less Ca^{2+} buffering. Such an effect reduces the ability of the mitochondria to buffer IP_3R-induced Ca^{2+} release leading to a larger cytosolic Ca^{2+} rise. The increase in the initial IP_3R-induced Ca^{2+} release spike should cause greater Ca^{2+}-dependent inactivation (CDI) of IP_3Rs, curtailing subsequent Ca^{2+} oscillations (Finch et al 1991, Bezprozvanny et al 1991). The larger CRAC channel dependent Ca^{2+} entry seen after knockdown of MFN2 would cause further inactivation of the IP_3Rs. Combined, this would lead to strong and sustained IP_3R inhibition and therefore the run down of the agonist-induced cytosolic oscillations.

Chapter 6.
General Discussion

6.1 General discussion

Since Ca^{2+} is known to be an important intracellular messenger activating a plethora of kinetically distinct cellular processes (Berridge et al 2003, Rizzuto et al 2006, Carafoli 2002), it is important to understand how this broad second messenger induces a specific Ca^{2+}-dependent response. Growing evidence supports the view that the spatial profile of the Ca^{2+} signal is central for Ca^{2+}-induced specificity. The most basic spatially restricted Ca^{2+} signal is the Ca^{2+} microdomain, which forms rapidly following the opening of Ca^{2+} permeable ion channels that are positioned on the plasma membrane (such as the CRAC channel), or residing on the membranes of specific intracellular organelles, (such as the IP_3R on the ER membrane) (Neher 1998, Parekh 2008a, Rizzuto et al 2006). The resultant high, local Ca^{2+} signal that forms around the channel pore impacts upon the activity of the channel and subsequent downstream responses (Neher 1998, Parekh 2008a, Chang et al 2008, Kar et al 2011, Moreau et al 2005). How local Ca^{2+} induces such effects on Ca^{2+} channels is important to understand.

Much is known about how local Ca^{2+} entry through voltage-operated Ca^{2+} channels (VOCCs) regulates channel activity (Peterson et al 1999, Zühlke et al 1998, 1999, Anderson 2001, DeMaria et al 2001) and downstream cellular responses close to the channels (such as exocytosis, Neher 1998 and the activation of Ca^{2+}-dependent K^+ channels, Roberts et al 1990, Prakriya et al 1996, Berkefeld et al 2006), as well as those further away (for example nuclear gene expression in neurons, Deisseroth et al 1996, Dolmetsch et al 2001, Kornhauser et al 2002). By contrast, little is known about the signalling effects of local Ca^{2+} entry through CRAC channels. Since the molecular identity of CRAC channels (Orai1 (Feske et al 2006, Vig et al 2006a, b) and STIM1 (Roos et al 2005, Liou et al 2005, Wu et al 2006)) has been established relatively recently compared to other Ca^{2+} channels, several important unanswered questions still remain. These include: How does the local Ca^{2+} entry through CRAC channels regulate activity of the channel? How does local Ca^{2+} drive Ca^{2+}-dependent activation of downstream cellular targets located far from the channel? Does local Ca^{2+} influx affect organelle function? My thesis has concentrated on answering such questions and my main conclusions are documented here. I propose a mechanism in the modulation of CRAC channels by cytoplasmic Ca^{2+} involving Ca^{2+} microdomains, calmodulin and prolonged stimulation of mitochondrial Ca^{2+} uptake, (illustrated in cartoon model **8** and built up visually in cartoon model's **1-7**).

Calmodulin is a ubiquitous Ca^{2+} sensor composed of two globular lobes (N- and C-) each containing two EF hand domains (Hoeflich et al 2002, Johnson et al 1996). Calmodulin associates with a range of Ca^{2+} channels (IP_3R, Yamada et al 1995, TRPV6, Niemeyer et al 2001, TRPV5, Strotmann et al 2003, L-type VOCC, Erickson et al 2001) and has been shown to both regulate VOCC activity (Zühlke et al 1998, 1999, Peterson 1999, DeMaria et al 2001) and drive subsequent nuclear gene expression (Dolmetsch et al 2001). Since a calmodulin binding site has now been identified on Orai1 (Mullins et al 2009) and most calcium-dependent facilitation of Ca^{2+} channels occurs in a calmodulin-dependent manner (Moreau et al 2005, 2006, Csordás and Hajnóczky 2003), I have investigated the modulation of CRAC channels by Ca^{2+}-calmodulin.

Chapter 3 demonstrates that CRAC channel dependent Ca^{2+} entry evoked by thapsigargin, and LTC_4-induced cytosolic Ca^{2+} oscillations in mast cells, are both modulated by calmodulin. Transfection of RBL-1 cells with a calmodulin mutant completely insensitive to Ca^{2+} (CAM4M), significantly impaired CRAC channel activity and the maintenance of LTC_4-induced cytosolic Ca^{2+} oscillations. This was not evident when Ba^{2+} was the charge carrier. Therefore I conclude that Ca^{2+}-calmodulin facilitates CRAC channel dependent Ca^{2+} entry (illustrated in cartoon model **1**), which is consistent with Moreau et al 2005 in RBL-1 cells. Furthermore, using three separate calmodulin mutant constructs each with alterations to their ability to sense and bind Ca^{2+}, I find that calmodulin controls CRAC channels and affects the maintenance of LTC_4-induced cytosolic Ca^{2+} oscillations in a lobe-specific manner. This result builds upon work by DeMaria et al 2001 in excitable cells, where they assign separate modulatory roles to each lobe of calmodulin in the control of VOCCs. Whilst the C-lobe of calmodulin drove CDF, the N-lobe drove CDI of P/Q-type Ca^{2+} channels. My work identifies a major role for the C-lobe but not the N-lobe in the modulation of CRAC channels in mast cells. This is the first time lobe-specific modulation of a Ca^{2+} channel has been reported in non-excitable cells. I show that both a dominant negative calmodulin mutant (CAM4M) and a mutant where the C-lobe cannot sense Ca^{2+} (CAM2C) significantly impair CRAC channel dependent Ca^{2+} entry and cause LTC_4-induced cytosolic Ca^{2+} oscillations to run down more quickly (than corresponding control cells). In contrast, a mutant where only the N-lobe cannot sense Ca^{2+} (CAM2N) has a minor effect on these Ca^{2+} signals.

Whole-cell patch clamp experiments carried out with my supervisor identified that Ca^{2+}-calmodulin was not acting directly on the channel pore, because the inhibitory effects of CAM4M were seen in the presence of low but not high cytosolic buffer. Therefore I established that the modulation of CRAC channels by Ca^{2+}-calmodulin involved a Ca^{2+}-dependent step, (cartoon model **2**). This led me to investigate the mechanism that was underlying the lobe-specific modulation of CRAC channels by Ca^{2+}-calmodulin.

CRAC channel dependent Ca^{2+} entry is required to support LTC_4-induced cytosolic oscillations because oscillations run down faster in zero Ca^{2+} (Di Capite et al 2009a), and under conditions which partially impair CRAC channel dependent Ca^{2+} entry, in comparison to agonist stimulation in 2 mM external Ca^{2+}. Such conditions to partially impair CRAC channels that I have used here include 1) submaximal blockade of channels with the inhibitor Synta (1 µM), 2) lowering external Ca^{2+} from 2 mM to 0.5 mM concentration or 3) knockdown of Orai1. Despite lowering Ca^{2+} entry to a level similar to that seen in the presence of CAM4M, oscillations ran down faster in the presence of the calmodulin mutant. Therefore the effects of calmodulin on cytosolic Ca^{2+} oscillations cannot be completely assigned to Ca^{2+}-calmodulin modulation of Ca^{2+} entry. Agonists induce more complex signals than thapsigargin and calmodulin is known to have many targets. I have found that calmodulin regulates these more complicated signals by more than one mechanism. Calmodulin is shown to effect IP_3R activity from the finding that all three calmodulin mutants increase the amplitude of the first IP_3-induced Ca^{2+} spike. Modulation of the initial IP_3R-driven Ca^{2+} release spike by calmodulin cannot however explain the lobe-specific modulation of CRAC channels and maintenance of LTC_4-induced Ca^{2+} oscillations by calmodulin. Calmodulin is shown to effect initial IP_3-dependent Ca^{2+} release in a manner that is not lobe-specific. Both lobes of calmodulin seem to be equally effective in the modulation of the initial IP_3R-driven Ca^{2+} release spike (since the size of the first Ca^{2+} release spike increases by similar amounts in the presence of CAM2C or CAM2N).

To establish the pathway underlying the lobe-specific modulation of Ca^{2+} signals by calmodulin, I have investigated a mechanism involving mitochondria. From the use of mitochondrial targeted fluorescent indicators (such as aequorin in endothelial cells, Rizzuto et al 1992 and Rhod 2-AM in permeablized RBL-1 cells, Moreau et al 2006), these organelles are established as being important regulators of intracellular Ca^{2+} signals (Hajnóczky et al 1999, Csordás et al 2003, Tinel et al 1999, Jouaville et al 1995). Furthermore, mitochondrial Ca^{2+} buffering has been shown to affect the development of I_{CRAC} and activity of CRAC channels (Gilabert and Parekh 2000, Glitsch et al 2002), (cartoon model **3**). I therefore hypothesised that the lobe-specific gating of CRAC channels by Ca^{2+}-calmodulin was through an action on mitochondrial Ca^{2+} buffering, as proposed by cartoon model **4** at the end of Chapter 3. Consistent with this, CRAC channel dependent Ca^{2+} entry and maintenance of LTC_4-induced oscillations are impaired to a similar extent by approaches that interfere with mitochondrial Ca^{2+} uptake, including the depolarization of the IMM by FCCP and knockdown of the required regulatory subunit, MICU1, (identified by Perocchi et al 2010). The reduced Ca^{2+} entry and run down of oscillations were similar in extent to that seen after transfection with CAM4M or CAM2C.

Chapter 4 builds upon these findings by examining Ca^{2+}-calmodulin dependent modulation of mitochondrial Ca^{2+} uptake in intact mast cells, using the ratiometric, fluorescent protein pericam that is expressed in the matrix. Consistent with previous reports, I found that Ca^{2+}-calmodulin facilitated mitochondrial Ca^{2+} uptake (Moreau et al 2006, Csordás and Hajnóczky 2003), illustrated in cartoon model **5**. The size of the pericam signal following stimulation with LTC_4 was significantly reduced in cells expressing CAM4M. Using an Orai1 mutant construct that is unable to bind calmodulin (A73E, developed and used by Mullins et al 2009), I discovered that calmodulin tethered to Orai1 was likely to be a major source of calmodulin for this modulation, as cartoon model **7** shows. Although the initial rate of mitochondrial Ca^{2+} uptake was unaffected by calmodulin tethered to Orai1, the amount of Ca^{2+} buffered by mitochondria was significantly impaired in cells expressing the Orai1 mutant (A73E Orai1) and overexpressing STIM1, compared to those overexpressing normal Orai1 and STIM1. I found whilst the matrix Ca^{2+} rise was quite sustained following Ca^{2+} influx in cells overexpressing Orai1, it recovered rapidly when A73E Orai1 was present (matrix signal was transient). Furthermore, measurement of the amount of Ca^{2+} within the matrix after stimulation with thapsigargin (by recording the rise in ionomycin-induced cytosolic Ca^{2+}) revealed that cells overexpressing Orai1 took up more Ca^{2+} following stimulation than A73E Orai1 expressing cells. Since the initial rate of MCU Ca^{2+} uptake is unchanged by A73E Orai1, calmodulin tethered to Orai1 is therefore acting as a critical regulator (but not activator) of MCU.

Collectively, Chapters 3 and 4 of my thesis have enabled me to propose a mechanism underlying the lobe-specific modulation of CRAC channels by Ca^{2+} -calmodulin.

Cartoon model **8** (on the next page) illustrates this (which reflects the build up of the findings illustrated in cartoon models **1-7**). Upon CRAC channel activation, the local entry of Ca^{2+} through CRAC channels binds to calmodulin tethered to Orai1. The resultant Ca^{2+}-calmodulin complex dissociates from the CRAC channel and reaches MCU sites, facilitating mitochondrial Ca^{2+} uptake, (cartoon model **8**). This is very dependent on the C-lobe of calmodulin. The C-lobe releases Ca^{2+} slowly (slow Ca^{2+} dissociation; Johnson et al 2003), therefore is able to diffuse far to the mitochondria from Orai1. This likely explains C-lobe dependence of mitochondrial regulation of CRAC channels. Long-range signalling involving calmodulin is already established for VOCCs, where Ca^{2+} microdomains signal to the nucleus to drive CREB-dependent gene expression (Dolmetsch et al 2001). The released Ca^{2+}-calmodulin from Orai1 reaches MCU sites, and facilitates mitochondrial Ca^{2+} uptake. Such an action feeds back to facilitate CRAC channel dependent Ca^{2+} entry, (cartoon model **8**). This is likely to be through reducing the development of slow Ca^{2+}-dependent inactivation (CDI) of CRAC channels, which relies on a bulk rise in cytosolic Ca^{2+}. This is for two reasons. Firstly, I have shown CRAC channel facilitation depends upon a bulk rise in cytosolic Ca^{2+} and secondly mitochondrial Ca^{2+} buffering is known to influence slow inactivation of CRAC channels (Gilabert and Parekh 2000). Furthermore, this concept is supported by the experiment depicted in section 4.2.**f**, figure 9**B** where Fura 2 measured cytosolic $[Ca^{2+}]$ 200s after admission of 1 mM Ca^{2+} is shown to decay faster in the presence of A73E Orai1 than normal Orai1. This suggests that when calmodulin cannot tether to Orai1, which prevents the sustained increase in mitochondrial Ca^{2+} uptake, Ca^{2+}-dependent slow inactivation of CRAC channels increases. Additionally, taking into account work by Glitsch et al 2002, I cannot rule out that calmodulin-dependent stimulation of mitochondrial Ca^{2+} uptake may also lead to the release of a diffusible messenger from mitochondria which in turn acts directly or indirectly on the CRAC channels, favouring a channel conformation under which Ca^{2+} entry is facilitated.

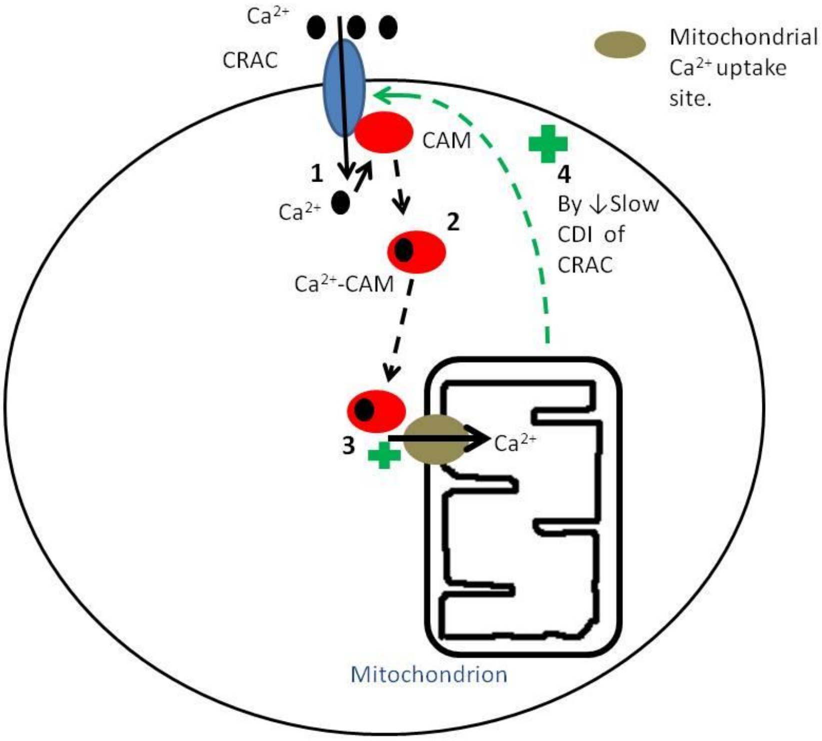

Cartoon model 8 illustrates the proposed mechanism put together from the findings of this thesis for the modulation of CRAC channels by cytoplasmic Ca^{2+}. This modulation pathway is heavily reliant on the C-lobe of calmodulin. This is probably due to differences in the kinetics of Ca^{2+} unbinding from each lobe of calmodulin. Ca^{2+} dissociates from the C-lobe slowly whilst unbinds from the N-lobe rapidly. 1) Upon CRAC channel activation, local Ca^{2+} entry binds to calmodulin (CAM) that is tethered to Orai1 to form a Ca^{2+}-CAM (calmodulin) complex. 2) This complex is released from the CRAC channel and diffuses into the cytoplasm. 3) Ca^{2+}-CAM docks at a site either on MCU itself or on a closely associated protein (possibly MICU1). This leads to enhanced mitochondrial Ca^{2+} uptake. 4) Enhancing mitochondrial Ca^{2+} buffering facilitates CRAC channel dependent Ca^{2+} entry, probably by reducing Ca^{2+}-dependent slow inactivation (CDI) of the channels. However, taking into account work by Glitsch et al 2002 one cannot rule out the possibility that a diffusible messenger released from mitochondria could be involved.

Future work should investigate the effects of each of the calmodulin mutants on MCU uptake (measured using expression of recombinant MCU with pericam in a reconstituted system). This is needed to confirm lobe-specific regulation of MCU itself by calmodulin, since my results thus far only provide indirect evidence for such a regulation. It will also be interesting to use TIRF microscopy to monitor the movement of tagged calmodulin in real-time from the plasma membrane. Now that the molecular identity of MCU has been established (De Stefani et al 2011, Baughman et al 2011), bioinformatics can also be used to identify calmodulin binding sites. One can then investigate the effect of mutating such sites on mitochondrial Ca^{2+} uptake, CRAC channel dependent Ca^{2+} entry and downstream CRAC channel driven cellular responses.

Chapter 4 concludes with an experiment using an NFAT-1 reporter gene (previously used by Kar et al 2011). This has allowed me to associate an important physiological role to mitochondrial Ca^{2+} buffering. Previous work has identified a role for local Ca^{2+} entry through CRAC channels in driving NFAT-1 nuclear translocation and NFAT-1-dependent gene expression in RBL-1 cells (Kar et al 2011). Mitochondrial Ca^{2+} buffering has also been shown to control CRAC channel driven NFAT-1 nuclear translocation in HEK (Kar et al 2011) and Jurkat T cells (Hoth et al 2000). Consistent with these findings, I provide evidence that mitochondrial Ca^{2+} uptake controls NFAT-1-driven nuclear gene expression in RBL-1 cells. I therefore suggest that the lobe-specific regulation of CRAC channels by Ca^{2+}-calmodulin involving mitochondrial Ca^{2+} buffering underlies CRAC channel driven NFAT-1-dependent gene expression in mast cells, which is vital for immune responses. This provides a mechanism by which local entry through CRAC channels can evoke a specific Ca^{2+}-dependent response in non-excitable cells located far from the channel.

Once calmodulin binding sites (which are often around 20 amino acid residues long) on MCU are identified (by methods such as calmodulin binding sepharose pull down assays and bioinformatics), further work could investigate the effect of disrupting such sites on NFAT-1-dependent gene expression. This would strengthen my hypothesis that cytoplasmic Ca^{2+}-calmodulin modulation of CRAC channels through effects of Ca^{2+}-calmodulin on MCU Ca^{2+} uptake drives gene expression. In addition, disruption of calmodulin binding sites on MCU could also be used to investigate the effect this has on other physiological responses such as ATP synthesis and metabolism, which would extend work by Hajnóczky et al 1995.

After the identification of a key role for mitochondrial Ca^{2+} uptake in the modulation of CRAC channels by calmodulin, I extended my investigation by examining whether altering factors that are known to underlie the ability of mitochondria to function as efficient buffers of Ca^{2+} also impacted on CRAC channel function and agonist-induced Ca^{2+} signals. Rizzuto et al 1998 identified a close association between the ER and mitochondria, which was crucial for robust, rapid mitochondrial Ca^{2+} uptake via the low affinity uniporter MCU. Furthermore, protein tethers have been established as being central to maintain close contact between ER and mitochondria for efficient Ca^{2+} transfer between these two organelles (Csordás et al 2006, de Brito and Scorrano 2008). One such protein is MFN2. MFN2 has been shown to regulate ER-mitochondrial tethering (de Brito and Scorrano 2008 in permeabilized MEFs) and thapsigargin-induced CRAC channel dependent Ca^{2+} entry (Singaravelu et al 2011).

Chapter 5 of this thesis supports a critical role for MFN2 and mitochondrial MFN2 in particular in the modulation of CRAC channels (possibly via effects on STIM1 trafficking and/or buffering of CDI of CRAC channels) and agonist-induced Ca^{2+} signals since I show both to be effected by disrupting endogenous cellular MFN2 or mitochondrial MFN2 function. MFN2, presumably by tethering ER to mitochondria, ensures rapid and reliable mitochondrial buffering of Ca^{2+} release. I find that in pericam transfected RBL-1 cells reducing endogenous MFN2 function impairs mitochondrial Ca^{2+} uptake. In addition since knockdown of MFN2 (by transfecting cells with MFN2 RNAi) or expression of MFN2 ActA (a mutant MFN2 construct specifically targeted to the mitochondria) significantly increased the size of the first IP_3R-dependent Ca^{2+} release spike it suggests that MFN2 acts to sustain cytosolic Ca^{2+} oscillations through reducing CDI of IP_3Rs by facilitating mitochondrial Ca^{2+} uptake of IP_3-induced Ca^{2+} release. This is presumably by maintaining a favourable distance between ER and mitochondria for efficient transfer of Ca^{2+} between these organelles. Future work could look at a role for calmodulin in MFN2 tethering and the impact of this on CRAC channel driven cellular responses.

Conclusion

Collectively, work in this thesis advances knowledge in the CRAC channel field by proposing a mechanism by which cytoplasmic Ca^{2+} can modulate CRAC channel dependent Ca^{2+} entry, involving Ca^{2+} microdomains and calmodulin stimulation of mitochondrial Ca^{2+} uptake.

Chapter 3: Identifies the modulation of CRAC channels and physiologically-induced cytosolic Ca^{2+} oscillations by Ca^{2+}-calmodulin in a lobe-specific manner, where the C-lobe of calmodulin is found to play a major role in the facilitation of CRAC channel dependent Ca^{2+} entry. The N-lobe on the other hand has a minor role. (In contrast both lobes of calmodulin seem to play an equally effective role in the modulation of a major intracellular channel, the IP_3R.)

Chapter 4: Describes a mechanism by which Ca^{2+}-calmodulin modulates CRAC channels through effects on mitochondrial Ca^{2+} uptake. Calmodulin is shown to facilitate mitochondrial Ca^{2+} uptake so that larger quantities of Ca^{2+} can be buffered. A major source of this calmodulin is found to be calmodulin tethered to Orai1.

Chapter 5: Addresses how the mitochondrial protein MFN2 affects mitochondrial Ca^{2+} uptake and CRAC channel dependent Ca^{2+} entry. It identifies a role for mitochondrial mitofusin 2 in the modulation of agonist-evoked Ca^{2+} signals and CRAC channels. Furthermore, the work in Chapter 5 proposes a mechanism to explain how mitochondrial MFN2 helps to maintain agonist-induced cytosolic Ca^{2+} oscillations, through facilitating the ability of the mitochondria to buffer regenerative IP_3R-induced Ca^{2+} release events by closely linking the mitochondria and ER.

Together, the findings of my thesis may help to advance therapeutic approaches to control CRAC channels, which play an important role in immune cell responses and allergic reactions. Search for a small molecule that competes with the calmodulin binding site of Orai1 could be therapeutically useful to partially impair aberrant CRAC channel function.

Chapter 7.
References

7.1 References

Adkins C. E. and C. W. Taylor. 1999. Lateral inhibition of $InsP_3$ receptors by cytosolic Ca^{2+}. *Curr. Biol*. 9: 1115-1118.

Adkins, C. E., S. A. Morris, H. De Smedt, K. Török and C. W. Taylor. 2000. Ca^{2+}-calmodulin inhibits Ca^{2+} release mediated by type-1, -2 and -3 inositol trisphosphate receptors. *Biochem J*. 345: 357-363.

Amiott E. A., P. Lott, J. Soto, P. B. Kang, J. Michael McCaffery, S. DiMauro, E. Dale Abel, K. M. Flanigan, V. H. Lawson and J. M. Shaw. 2008. Mitochondrial fusion and function in Charcot-Marie-Tooth Type 2A patient fibroblasts with mitofusin 2 mutations. *Exp. Neurol*. 211(1): 115-127.

Anderson M. E. 2001. Ca^{2+}-dependent regulation of cardiac L-type Ca^{2+}channels: is a unifying mechanism at hand? *J. Mol. Cell. Cardiol.* 33: 639–650.

Arnaudeau S., W. L. Kelleys, J. V. Walsch and N. Demaurex. 2001. Mitochondria recycle Ca^{2+} to the endoplasmic reticulum and prevent the depletion of neighbouring endoplasmic reticulum regions*. J. Biol. Chem*. 276(31): 29430-29439.

Babcock D. F., J. Herrington, P. C. Goodwin, Y. B. Park and B. Hille. 1997. Mitochondrial participation in the intracellular Ca^{2+} network. *J. Cell Biol*. 136(4): 833-844.

Bailey K. 1942. Myosin and adenosinetriphosphatase. *Biochem. J*. 36: 121-139.

Bakowski D. and A. B. Parekh. 2000. Voltage-dependent conductance changes in the store-operated Ca^{2+} current I_{CRAC} in rat basophilic leukaemia cells. *J. Physiol.* 529:295-306.

Bakowski D., M. D. Glitsch and A. B. Parekh. 2001. An examination of the secretion-like coupling model for the activation of the Ca^{2+} release-activated Ca^{2+} current I_{CRAC} in RBL-1 cells. *J. Physiol*. 532: 55-71.

Bakowski D. and A. B. Parekh. 2007. Regulation of store-operated calcium channels by the intermediary metabolite pyruvic acid. *Curr. Biol*. 17: 1076-1081.

Baughman J. M., F. Perocchi, H. S. Girgis, M. Plovanich, C. A. Belcher-Timme, Y. Sancak, X. R. Bao, L. Strittmatter, O. Goldberger, R. L. Bogorad, V. Koteliansky and V. K. Mootha. 2011. Integrative genomics identifies MCU as an essential component of the mitochondrial calcium uniporter. *Nature*. 476(7360): (341-345).

Bautista D. M. and R. S. Lewis. 2004. Modulation of plasma membrane calcium-ATPase activity by local calcium microdomains near CRAC channels in human T cells. *J. Physiol*. 556.3: 805-817.

Berkefeld H., C. A. Sailer, W. Bildl, V. Rhode, J. O. Thumfart, S. Eble, N. Klugbauer, E. Reisinger, J. Bischofberger, D. Oliver, H.G. Knaus, U. Schulte and B. Fakler. 2006. BK_{Ca}-Cav channel complexes mediate rapid and localized calcium-activated potassium signalling. *Science*. 314: 615-620.

Berridge M. J. 1997. Elementary and global aspects of calcium signalling. *J. Physiol*. 499(2):291-306.

Berridge M. J., P. Lipp and M. D. Bootman. 2000. The versatility and universality of calcium signalling. *Nat. Rev. Mol. Cell Biol*. 1: 11-21.

Berridge M. J., M. D. Bootman and H. L. Roderick. 2003. Calcium signalling: dynamics, homeostasis and remodelling. *Nature Rev. Mol. Cell Biol*. 4: 517-529.

Bezprozvanny I., J. Watras and B. E. Ehrlich. 1991. Bell-shaped calcium-response curves of Ins(1,4,5)P_3- and calcium-gated channels from endoplasmic reticulum of cerebellum. *Nature*. 351: 751- 754.

Boncompagni S., A. E. Rossi, M. Micaroni, G. V. Beznoussenko, R. S. Polishchuk, R. T. Dirksen and F. Protasi. 2009. Mitochondria are linked to calcium stores in striated muscle by developmentally regulated tethering structures. *Mol. Biol. Cell*. 20: 1058-1067.

Boyce, J. A. 2007. Mast cells and eicosanoid mediators: a system of reciprocal paracrine and autocrine regulation. *Immunol. Rev*. 217:168-185

Bozler E. 1954. Relaxation in extracted muscle fibres. *J. Gen. Physiol*. 38: 149-159.

Brdiczka D. G., D. B. Zorov and S.S. Sheu. 1991. Mitochondrial contact sites: their role in energy metabolism and apoptosis. *Biochim. Biophys. Acta*. 1762: 148-163.

Cahalan M. D. 2009. STIMulating store-operated Ca^{2+} entry. *Nature Cell Biol*. 11:669-676.

Carafoli E. A. 1987. Intracellular calcium homeostasis. *Rev. Biochem.* 56: 395-433.

Carafoli E. 1991. Calcium pump of the plasma membrane. *Physiol. Rev*. 71(1):129-153.

Carafoli E. 2002. Calcium signalling: a tale for all seasons. *Proc. Natl. Acad. Sci. U.S.A.* 99(3): 1115-1122.

Carafoli E. 2003. The calcium-signalling saga: tap water and protein crystals. *Nature*. 4: 326-332.

Chang W-C. and A. B. Parekh. 2004. Close functional coupling between Ca^{2+} release-activated Ca^{2+} channels, arachidonic acid release, and leukotriene C_4 secretion. *J. Biol. Chem. U.S.A*. 279(29): 29994-29999.

Chang W-C., C. Nelson and A. B. Parekh. 2006. Ca^{2+} influx through CRAC channels activates cytosolic phospholipase A_2, leukotriene C_4 secretion and expression of c-fos through ERK-dependent and independent pathways in mast cells. *FASEB. J*. 20:E1681-E1693.

Chang W-C., J. Di Capite, K. Singaravelu, C. Nelson, V. Halse and A. B. Parekh. 2008. Local Ca^{2+} influx through Ca^{2+} release-activated Ca^{2+} (CRAC) channels stimulates production of an intracellular messenger and an intercellular pro-inflammatory signal. *J. Biol. Chem*. 283: 4622-4631.

Chen H., S. A Detmer, A. J. Ewald, E. E. Griffin, S. E. Fraser and D. C. Chan. 2003. Mitofusins Mfn1 and Mfn2 coordinately regulate mitochondrial fusion and are essential for embryonic development. *J. Cell Biol*. 160(2): 189-200.

Cipolat S., O.M. de Brito, B. Dal Zilio and L. Scorrano. 2004. OAP1 requires mitofusin 1 to promote mitochondrial fusion. *Proc. Natl. Acad. Sci. U.S.A*. 101:15927-15932.

Clapham D. E. 2007. Calcium signaling. *Cell*. 131: 1047-1058.

Collins T. J., P. Lipp, M. J. Berridge, W. Li and M. D. Bootman. 2000. Inositol 1,4,5-trisphosphate-induced Ca^{2+} release is inhibited by mitochondrial depolarization. *Biochem J*. 347 (2): 593-600.

Csordás G. and G. Hajnóczky. 2003. Plasticity of mitochondrial calcium signalling. *J. Biol. Chem. U.S.A*. 278(43): 42273-42282.

Csordás G., C. Renken, P. Várnai, L. Walter, D. Weaver, K. F. Buttle, T. Balla, C. A. Mannella and G. Hajnóczky. 2006. Structural and functional features and significance of the physical linkage between ER and mitochondria. *J. Cell Biol*. 174 (7): 915-921.

de. Brito O. M. and Scorrano L. 2008. Mitofusin 2 tethers endoplasmic reticulum to mitochondria. *Nature*. 456: 605-610.

DeHaven W. I., J. T. Boyles, R. R. Boyles and J. W. Putney. 2007. Calcium inhibition and calcium potentiation of Orai1, Orai2, Orai3 calcium release-activated calcium channels. *J. Biol. Chem*. 282, 17548-17556.

Deisseroth K., Bito H. and Tsien R. W. 1996. Signaling from synapse to nucleus: postsynaptic CREB phosphorylation during multiple forms of hippocampal synaptic plasticity. *Neuron*. 16: 89–10.

De Luca H. F. and G. Engstrom. 1961. Calcium uptake by rat kidney mitochondria. *Proc. Natl. Acad. Sci. USA*. 47: 1744-1747.

DeMaria C. D., T. W. Soong, B. A. Alsikhan, R. S. Alvania and D. T. Yue. 2001. Calmodulin bifurcates the local Ca^{2+} signal that modulates P/Q-type Ca^{2+} channels. *Nature*. 411: 484- 489.

Demaurex N. and C. W. Diestelhorst. 2003. Apoptosis: the calcium connection. *Science*. 300: 65-67.

De Stefani D., A. Raffaello, E. Teardo, I. Szabò and R. Rizzuto. 2011. A forty-kilodalton protein of the inner membrane is the mitochondrial calcium uniporter. *Nature*. 476(7360): 336-340.

Di Capite J., S. W. Ng and A. B. Parekh. 2009a. Decoding of cytoplasmic Ca^{2+} oscillations through the spatial signature drives gene expression. *Curr. Biol*. 19: 853-858.

Di Capite J., A. Shirley, C. Nelson, G. Bates and A. B. Parekh. 2009b. Intercellular Ca^{2+} wave propagation involving positive feedback between CRAC channels and cysteinyl leukotrienes. *FASEB. J*. 23: 894-905.

Dick I. E., M. R. Tadross, H. Liang, L. H. Tay, W. Yang and D. Yue. 2008. A modular switch for spatial Ca^{2+} selectivity in the calmodulin regulation of Ca_V channels. *Nature*. 451: 830- 834.

Di Sabatino A., L. Rovedatti, R. Kaur, J. P. Spencer, J. T. Brown, V. D. Morisset, P. Biancheri, N. A. Leakey, J. I. Wilde, L. Scott, G. R. Corazza, K. Lee, N. Senqupta, C. H. Knowles, M. J. Gunthorpe, P. G. McLean, T. T. MacDonald and L. Kruidenier. 2009. Targeting gut T-cell Ca^{2+} release-activated Ca^{2+} channels inhibits T cell cytokine production and T-Box transcription factor T-Bet in inflammatory bowel disease. *J. Immunol*. 183: 3454-3462.

Dolmetsch R. E., R. S. Lewis, C. C. Goodnow and J. I. Healy. 1997. Differential activation of transcription factors induced by Ca^{2+} response amplitude and duration. *Nature*. 386: 855-858.

Dolmetsch R. E., K. Xu and R. S. Lewis. 1998. Calcium oscillations increase the efficiency and specificity of gene expression. *Nature*. 392: 933-936.

Dolmetsch R. E., U. Pajvani, K. Fife, J. M. Spotts and M. E. Greenberg. 2001. Signaling to the nucleus by an L-type calcium channel-calmodulin complex through the MAP kinase pathway. *Science*. 294: 333-339.

Duchen M. D. 2004. Mitochondria in health and disease: perspectives on a new mitochondrial biology. *Mol. Aspects Med*. 25: 365-451.

Ebashi, S. and F. Lipmann. 1962. Adenosine triphosphate-linked concentration of calcium ions in a particulate fraction of rabbit muscle. *J. Cell Biol*. 14: 389-400.

Erickson M. G., B. A. Alesikhan, B. Z. Peterson and D. T. Yue. 2001. Preassociation of calmodulin with voltage-gated $Ca(^{2+})$ channels revealed by FRET in single living cells. *Neuron*. 31(6): 973-985.

Fagan K. A., N Mons and D. M. F Cooper. 1998. Dependence of the Ca^{2+}-inhibitable adenyl cyclase of C6-2B glioma cells on capacitative Ca^{2+} entry. *J. Biol. Chem*. 273:9297-9305.

Feske S., M. Prakriya, A. Rao and R. S. Lewis. 2005. A severe defect in CRAC calcium channel activation and altered potassium channel gating in T cells from immunodeficient patients. *J Exp. Med*. 202:651-662.

Feske S., Y. Gwack, M. Prakriya, S. Srikanth, S-H. Puppel, B. Tanasa, P. G. Hogan, R. S. Lewis, M. Daly and A. Rao. 2006. A mutation in Orai1 causes immune deficiency by abrogating CRAC channel function. *Nature*. 44: 179-185.

Fierro L. and A. B. Parekh. 1999. Fast calcium-dependent inactivation of calcium release-activated calcium current (CRAC) in RBL-1 cells. *J. Membr*. Biol. 168: 9-17.

Fierro L. and A. B. Parekh. 2000. Substantial depletion of the intracellular Ca^{2+} stores is required for macroscopic activation of the Ca^{2+} release-activated Ca^{2+} current in rat basophilic leukaemia cells. *J. Physiol*. 522: 247-257.

Finch E. A., T. J. Turner and S. M. Goldin. 1991. Calcium as a coagonist of inositol 1,4,5-trisphosphate-induced calcium release. *Science*. 252(5004): 443-446.

Franzius D., M. Hoth and R. Penner. 1994. Non-specific effects of calcium entry antagonists in mast cells. *Pflugers Arch*. 428: 433-438.

Frezza C., S. Cipolat, O. M. de Brito, M. Micaroni, G. V. Beznoussenko, T. Rudka, D. Bartoli, R. S. Polishuck, N. N. Danial, B. De Strooper and L. Scorrano. 2006. OAP1 controls apoptotic cristae remodelling independently from mitochondrial fusion. *Cell*. 126: 177-189.

Frieden M., D. James, C. Castelbou, A. Danckaert, J. C. Martinou and N. Demaurex. 2004. Ca^{2+} homeostasis during mitochondrial fragmentation and perinuclear clustering induced by hfis1. *J. Biol. Chem*. 279: 22704-22714.

García-Pérez C., T. G. Schneider, G. Hajnóczky and G. Csordás. 2011. Alignment of sarcoplasmic reticulum-mitochondrial junctions with mitochondrial contact points. AM. J. Physiol. *Heart Circ. Physiol*. 201: H1907-H1915.

Gerasimenko J. V., L. György, P. Ferdek, M. W. Sherwood, E. Ebisui, A. V. Tepikin, K. Mikoshiba, O. H. Petersen and O. V. Gerasimenko. 2011. Calmodulin protects against alcohol-induced pancreatic trypsinogen activation elicited via Ca^{2+} release through IP_3 receptors. *Proc. Natl. Acad. Sci. U.SA*. 108(14): 5873-5878.

Gilabert J. A. and A. B. Parekh. 2000. Respiring mitochondria determine the pattern of activation and inactivation of the store-operated Ca^{2+} current I_{CRAC}. *EMBO. J*. 19(23): 6401-6407.

Gilabert J. A., D. Bakowski and A. B. Parekh. 2001. Energized mitochondria increase the dynamic range over which inositol 1,4,5-trisphosphate activates store-operated calcium influx. *EMBO. J*. 20:2672-2679.

Glitsch M. D. and A. B. Parekh. 2000. Ca^{2+} store dynamics determines the pattern of activation of the store-operated Ca^{2+} current I_{CRAC} in response to $InsP_3$ in rat basophilic leukemia cells. *J. Physiol*. 523: 283-290.

Glitsch M. D., D. Bakowski and A. B. Parekh. 2002. Store-operated Ca^{2+} entry depends on mitochondrial Ca^{2+} uptake. *EMBO. J*. 21(24): 6744-6754.

Greka A., B. Navarro, E. Oancea, A. Duggan and D. E. Clapham. 2003. TRPC5 is a regulator of hippocampal neurite length and growth cone morphology. *Nat. Neurosci*. 6:837-845.

Gu C. and D. M. F Cooper. 2000. Ca^{2+} Sr^{2+} and Ba^{2+} identify distinct regulatory sites on adenylyl cyclase (AC) types VI and VIII and consolidate the apposition of capacitative cation entry channels and Ca^{2+}- sensitive ACs. *J. Biol. Chem*. 275: 6980-6986.

Guo X., K. H. Chen, Y. Guo, H. Liao, J. Tang and R. P. Xiao. 2007. Mitofusin 2 triggers vascular smooth muscle cell apoptosis via mitochondrial death pathway. *Circ. Res*. 101: 1113-1122.

Gwack Y. S. Srikanth, S. Feske, F. Cruz-Guilloty, M. Oh-hora, D. S. Neems, P. G. Hogan, and A. Rao. 2007. Biochemical and functional characterization of Orai proteins. *J. Biol. Chem*. 282: 16232-16243.

Hajnóczky G., L. D. Robb-Gaspers, M. B. Seitz and A. P. Thomas. 1995. Decoding of cytosolic calcium oscillations in the mitochondria. *Cell*. 82: 415-424.

Hajnóczky G., R. Hager and A. P. Thomas. 1999. Mitochondria suppress local feedback activation of inositol 1,4,5-trisphosphate receptors by Ca^{2+}. *J. Biol. Chem*. U.S.A. 274(20): 14157-14162.

Hajnóczky G. and G. Csordás. 2011. Calcium signalling: fishing out molecules of mitochondrial calcium transport. *Curr. Biol*. 20(20): R888- R890.

Heilbrunn L. V. 1940. The action of calcium on muscle protoplasm. *Physiol. Zool*. 13: 88-94.

Hill T. D., R. Campos-Gonzalez, H. Kindmark and A. L. Boynton. 1988. Inhibition of inositol trisphosphate-stimulated calcium mobilization by calmodulin antagonists in rat liver epithelial cells. *J. Biol. Chem*. 263: 16479-16484.

Hirose K., S. Kadowaki, M. Tanabe, H. Takeshima and M. Lino. 1999. Spatiotemporal dynamics of inositol 1,4,5-trisphosphate that underlies complex Ca^{2+} mobilization patterns. *Science*. 284: 1527-1530.

Hirota J., T. Michikawa, T. Natsume, T. Furuichi and K. Mikoshiba. 1999. Calmodulin inhibits inositol 1,4,5-trisphosphate-induced calcium release through purified and reconstituted inositol 1,4,5-trisphosphate receptor type 1. *FEBS*. 456: 322-326.

Hoeflich K. P. and M. Ikura. 2002. Calmodulin in action: diversity in target recognition and activation mechanisms. *Cell*. 108(6):739-742.

Hofer A., C. Fasolato and T. Pozzan. 1998. Capacitative Ca^{2+} entry is closely linked to the filling state of internal Ca^{2+} stores: a study using simultaneous measurements of I_{CRAC} and intraluminal [Ca^{2+}]. *J Cell Biol*. 140:325-334.

Hogan P. G., L. Chen, J. Nardone and A. Rao. 2003. Transcriptional regulation by calcium, calcineurin, and NFAT. *Genes Dev*. 17:2205-2232.

Hoth M. and R. Penner. 1992. Depletion of intracellular calcium stores activates a calcium current in mast cells. *Nature*. 355: 353- 356.

Hoth M and R. Penner. 1993. Calcium release-activated calcium current in rat mast cells. *J Physiol*. 465:359-386.

Hoth M., D. Button and R. S. Lewis. 2000. Mitochondrial control of calcium channel gating: a mechanism for sustained signalling and transcriptional activation in T lymphocytes. *Proc. Natl. Acad. Sci. U.S.A*. 97: 10607-10612.

Hudmon A., H. Schulman, J. Kim, J. M. Maltez, R. W. Tsien and G. S. Pitt. 2005. CaMKII tethers to L-type Ca^{2+} channels, establishing a local and dedicated integrator of Ca^{2+} signals for facilitation. *J. Cell Biol*. 171(3): 537-547.

Ishihara N., Y. Eura and K. Mihara. 2004. Mitofusin 1 and 2 play distinct roles in mitochondrial fusion reactions via GTPase activity. *J. Cell Science*. 117: 6535-6546.

Isshiki M**.**, Y. S. Ying, T. Fujita and R. G. Anderson. 2002. A molecular sensor detects signal transduction from caveolae in living cells. *J. Biol. Chem*. 277:43389–43398.

Isshiki M., A. Mutoh and T. Fujita. 2004. Subcortical Ca^{2+} waves sneaking under the plasma membrane in endothelial cells. *Circ. Res*. 95: 11–21.

Jiang D., L. Zhao and D. E. Clapham. 2009. Genome-wide RNAi screen identifies Letm1 as a mitochondrial Ca^{2+}/H^{+} antiporter. *Science*. 326(5949): 144-147.

Johnson J. D., C. Synder, M. Walsh and M. Flynn. 1996. Effects of myosin light chain kinase and peptides on Ca^{2+} exchange with the N- and C-terminal Ca^{2+} binding sites of calmodulin*. J. Biol. Chem*. 271(2): 761-767.

Jouaville L. S., F. Ichas, E. L. Holmuhamedov, P. Camacho and J. D. Lechlelter. 1995. Synchronization of calcium waves by mitochondrial substrates in Xenopus Laevis oocytes. *Nature.* 377: 438-441.

Kar P., C. Nelson and A. B. Parekh. 2011. Selective activation of the transcription factor NFAT1 by calcium microdomains near Ca^{2+} release-activated Ca^{2+} (CRAC) channels. *J. Biol. Chem*. 286(17): 14795-14803.

Kawabata S., R. Tsutsumi, A. Kohara, T. Yamaguchi, S. Nakanishi and M. Okada. 1996. Control of calcium oscillations by phosphorylation of metabotropic glutamate receptors. *Nature*. 383: 89-92.

Kirichok Y, Krapivinsky and D. E. Clapham. 2004. The mitochondrial calcium uniporter is a highly selective ion channel. *Nature*. 427: 360-364.

Kornhauser J. M., C. W. Cowan, A. J. Shaywitz, R. E. Dolmetsch, E. C. Griffith, L. S. Hu, C. Haddad, Z. Xia and M. E. Greenberg. 2002. CREB transcriptional activity in neurons is regulated by multiple, calcium-specific phosphorylation events. *Neuron*. 34: 221–233.

Landolfi B., S. Curci, L. Debellis, T. Pozzan and A. M. Hofer. 1998. Ca^{2+} homeostasis in the agonist-sensitive internal store: functional interactions between mitochondria and the ER measured in situ in intact cells. *J. Cell Biol*. 142(5): 1235-1243.

Lawson V. H., B.V. Graham and K.M. Flanigan. 2005. Clinical and electrophysiologic features of CMT2A with mutations in the mitofusin 2 gene. *Neurology*. 65: 197–204

Lee Y. N., J. Tuckerman, H. Nechushtan, G. Schutz, E. Razin and P. Angel. 2004. c-fos as a regulator of degranulation and cytokine production in FCeRI-activated mast cells. *J. Immunol*. 173: 2571-2577.

Lepples- Wienhues A., C. Belka, T. Laun, A. Jekle, B. Walter, U. Wieland, M. Welz, L. Heil, J. Kun, G. Busch, M. Weller, M. Bamberg, E. Gulbins and F. Lang. 1999. Stimulation of CD95 (Fas) blocks T lymphocyte calcium channels through sphingomyelinase and sphingolipids. *Proc. Natl., Acad. Sci. USA*. 96: 13795-13800.

Lewis R. S. 2007. The molecular choreography of a store-operated calcium channel. *Nature*. 446:284-287.

Li Y., Y. C. Jia, K. Cui, N. Li, Z. Y. Zheng, Y. Z. Wang and X. B. Yuan. 2005. Essential role of TRPC channels in the guidance of nerve growth cones by brain-derived neurotrophic factor. *Nature*. 434:894-898.

Liou J., M. L. Kim, W. D. Heo, J. T. Jones, J. W. Meyers, J. E. Ferrell and T. Meyer. 2005. STIM is a Ca^{2+} sensor essential for Ca^{2+}-store-depletion-triggered Ca^{2+} influx. *Curr. Biol*. 15: 1235-1241.

Liou J., M. Fivaz, T. Inoue and T. Meyer. 2007. Live-cell imaging reveals sequential oligomerization and local plasma membrane targeting of stromal interaction molecule 1 after calcium store depletion. *Proc. Natl. Acad. Sci. USA*. 104: 9301-9306.

Lis, A., C. Peinelt, A. Beck, S. Parvez, M. Monteilh-Zoller, A. Fleig and R. Penner. 2007. CRACM1, CRACM2 and CRACM3 are store-operated Ca^{2+} channels with distinct functional properties. *Curr. Biol*. 17, 794-800.

Litjens T., M. L. Harland, M. L. Roberts, G. L. Barritt and G. Y. Rychkov. 2004. Fast $Ca(^{2+})$-dependent inactivation of the store-operated Ca^{2+} current (I_{SOC}) in liver cells: a role for calmodulin. *J. Physiol*. 558: 85-97.

Llinas R, M. Sugimori and R. B. Silver. 1992. Microdomains of high calcium concentration in a presynaptic terminal. *Science*. 256: 677–679.

Luik, R. M., B. Wang, M. Prakriya, M. M. Wu and R. S. Lewis. 2008. Oligomerization of STIM1 couples ER calcium depletion to CRAC channel activation. *Nature*. 454:538-542.

Luo D., L. M. Broad, G. S. J. Bird and J. W. Putney. 2001. Mutual antagonism of calcium entry by capacitative and arachidonic acid-mediated calcium entry pathways. *J. Biol. Chem*. 276: 20186-20189.

Machaca K. 2003. Ca^{2+} calmodulin-dependent protein kinase II potentiates store-operated Ca^{2+} current. *J. Biol. Chem*. 278(36): 33730-33737.

Malli R., M. Frieden, K. Osibow, C. Zoratti, M. Mayer, N. Demaurex and W. F. Graier. 2003. Sustained Ca^{2+} transfer across mitochondria is essential for mitochondrial Ca^{2+} buffering, store-operated Ca^{2+} entry, and Ca^{2+} store refilling. *J. Biol. Chem*. U.S.A. 278(45): 44769-44779.

Malli R., M. Frieden, M. Trenker and W. F. Graier. 2005. The role of mitochondria for Ca^{2+} refilling of the endoplasmic reticulum. *J. Biol. Chem*. 280: 12114-12122.

Marsault R, M. Murgia,T. Pozzan and R. Rizzuto. 1997. Domains of high Ca^{2+} beneath the plasma membrane of living A7r5 cells. *EMBO. J.* 16: 1575–1581.

Marsh B. J., D. N. Mastronarde, K. F. Buttle, K. E. Howell and J. R. McIntosh. 2001. Organellar relationships in the Golgi region of the pancreatic beta cell line, HIT-T15, visualized by high resolution electron tomography. *Proc. Natl. Acad. Sci. U.S.A*. 98:2399-2406.

Martin A. C. and D. M. F. Cooper. 2006. Capacitative and 1-oleyl-2-acetyl-sn-glycerol-activated Ca^{2+} entry distinguished using adenyl cyclase. *Mol Pharmacol*. 70: 769-777

Mathes C., A. Fleig and R. Penner. 1998. Calcium release-activated calcium current (I_{CRAC}) is a direct target for sphingosine. *J. Biol. Chem*. 273: 25020-25030.

McConkey D. J., P. Nicotera, P. Hartzell, G. Bellomo, A. H. Wyllie and S. Orrenius. 1989. Glucocorticoids activate a suicide process in thymocytes through an elevation of cytosolic Ca^{2+} concentration. *Arch. Biochem. Biophys*. 269: 365-370.

McCornmack J. G., A. P. Halestrap and R. M. Denton.1990. Role of calcium ions in regulation of mammalian intramitochondrial metabolism. *Physiol. Rev*. 70: 391-425.

McNally B. A., M. Yamashita, A. Engh and M. Prakriya. 2009. Structural determinants of ion permeation in CRAC channels. *Proc. Natl. Acad. Sci. USA*. 106: 22516-22521.

Michikawa T., J. Hirota, S. Kawano, M. Hiraoka, M. Yamada, T. Furuichi and K. Mikoshiba. 1999. Calmodulin mediates calcium-dependent inactivation of the cerebellar type 1 inositol 1,4,5-trisphosphate receptor. *Neuron*. 23: 799-808.

Mironov S. L. and N. Symonchuk. 2006. ER vesicles and mitochondria move and communicate at synapses. *J. Cell Science*. 119, 4926-4934.

Missiaen L., J. B. Parys, A. F. Weidema, H. Sipma, S. Vanlingen, P. De Smet, G. Callewaert and H. De Smedt. 1999. The bell-shaped Ca^{2+}- dependence of the inositol 1,4,5-trisphosphate induced Ca^{2+} release is modulated by Ca^{2+}/calmodulin. *J. Biol. Chem*. 274: 13748-13751.

Mitchell, P. 1966. Chemiosmotic coupling in oxidative and photosynthetic phosphorylation. *Biol. Rev. Camb. Philos. Soc*. 41(3):445-502.

Moneer Z., J. L. Dyer and Taylor. 2003. Nitric oxide co-ordinates the activities of the capacitative and non-capacitative Ca^{2+} entry pathways regulated by vasopressin. *Biochem J*. 370: 439-448.

Montero M, M. T. Alonso, E. Carnicero, I. Cuchillo-Ibánez, A. Albillos, A. G. Garcia, J. Garcia-Sancho and J. Alvarez. 2000. Chromaffin-cell stimulation triggers fast millimolar mitochondrial Ca^{2+} transients that modulate secretion. *Nat. Cell Biol*. 2(2): 57-61.

Moreau B., S. Straube, R. J. Fisher, J. W. Putney and A. B. Parekh. 2005. Ca^{2+}-calmodulin-dependent facilitation and Ca^{2+} inactivation of Ca^{2+} release-activated Ca^{2+} channels. *J. Biol. Chem*. 280(10): 8776-8783.

Moreau B., C. Nelson and A. B. Parekh. 2006. Biphasic regulation of mitochondrial Ca^{2+} uptake by cytosolic Ca^{2+} concentration. *Curr. Biol*. 16: 1672-1677.

Muik M., R. Schindl, M. Fahrner and C. Romanin. 2012. Ca^{2+} release-activated Ca^{2+} (CRAC) current, structure, and function. *Cell. Mol. Life Sci*. 10.1007/s00018-012-1072-8

Mullins F. M., C. Y. Park, R. E. Dolmetsch and R. S. Lewis. 2009. STIM1 and calmodulin interact with Orai1 to induce Ca^{2+}-dependent inactivation of CRAC channels. *Proc. Natl. Acad. Sci. U.S.A*. 106(36): 15495-15500.

Nadif Kasri N., G. Bultynck, J. Smyth, K. Szlufcik, J. Parys, G. Callewaert, L. Missiaen, R. A. Fissore, K. Mikoshiba and H. De Smedt. 2004. The N-terminal Ca^{2+}-independent calmodulin-binding site on the inositol 1,4,5-trisphosphate receptor is responsible for calmodulin inhibition, even though this inhibition requires Ca^{2+}. *Mol. Pharmacol*. 66: 276-284.

Nadif Kasri N., K. Török, A. Galione, C. Garnham, G. Callewaert, L. Missiaen, J. B. Parys and H. De Smedt. 2006. Endogenously bound calmodulin is essential for the function of the inositol 1,4,5-trisphosphate receptor. *J. Biol. Chem*. 281(13): 8332-8338.

Nagai T., A. Sawano, E. S. Park and A. Miyawaki. 2001. Circularly permuted green fluorescent proteins engineered to sense Ca^{2+}. *Proc. Natl. Acad. Sci. U.S.A*. 98(6): 3197-3202.

Nagai T., S. Yamada,T. Tominaga, M. Ichikawa and A. Miyawaki. 2004. Expanded dynamic range of fluorescent indicators for Ca^{2+} by circularly permuted yellow fluorescent proteins. *Proc. Natl. Acad. Sci. U.S.A*. 101: 10554–10559, 2004.

Nakahashi Y., E. Nelson, K. Fagan, E. Gonzales, J. L. Guillou and D. M. Cooper. 1997. Construction of a full-length Ca^{2+}-sensitive adenylyl cyclase/aequorin chimera. *J. Biol. Chem*. 272: 18093–18097.

Neher E. 1998. Vesicle pools and Ca^{2+} microdomains: new tools for understanding their roles in neurotransmitter release. *Neuron*. 20: 389-399.

Nelson MT., H. Cheng, M Rubart, L. F. Santana, A.D. Bonev, H. J. Knot and W. J. Lederer. 1995. Relaxation of arterial smooth muscle by calcium sparks. *Science*. 270: 633-637.

Ng S-W., J. Di Capite, K. Singaravelu and A. B. Parekh. 2008. Sustained activation of the tyrosine kinase Syk by antigen in mast cells requires local Ca^{2+} influx through Ca^{2+} release-activated Ca^{2+} channels. *J. Biol. Chem*. 283(46): 31348-31355.

Ng S-W., C. Nelson and A. B. Parekh. 2009. Coupling of Ca^{2+} microdomains to spatially and temporally distinct cellular responses by the tyrosine kinase Syk. *J. Biol. Chem.* 284(37): 24767-24772.

Nicholls D. G. 2005. Mitochondria and calcium signalling. *Cell Calcium*. 38: 311-317.

Niemeyer B., C. Bergs, U Wissenbach, V Flockerzi and C. Trost. 2001. Competitive regulation of CaT-like-mediated Ca^{2+} entry by protein kinase C and calmodulin. *Proc. Natl. Acad. Sci. U.S.A*. 98(6):3600-3605.

Ohana L., E. F. Stanley and L. C. Schlichter 2009. The Ca^{2+} release-activated Ca^{2+} current (I_{CRAC}) mediates store-operated Ca^{2+} entry in rat microglia. *Channels*. 3: 129-139.

Ørtenblad N. and D. G. Stephenson . 2003. A novel signalling pathway originating in mitochondria modulates rat skeletal muscle membrane excitability. *J. Physiol*. 548 (1): 139-145.

Palty R., W. F. Silverman, M. Hershfinkel, T. Caporale, S. L. Sensi, J. Parnis, C. Nolte, D. Fishman, V. Shoshan-Barmatz and S. Herrmann. 2010. NCLX is an essential component of mitochondrial Na^{+}/Ca^{2+} exchange. *Proc. Natl. Acad. Sci. U.S.A*. 107(1): 436-441.

Palty R. and I. Sekler. 2012. The mitochondrial Na^+/Ca^{2+} exchanger. *Cell Calcium*. 52(1): 9-15.

Parekh A. B. and R. Penner. 1995. Depletion-activated calcium current is inhibited by protein kinase in RBL-2H3 cells. *Proc. Natl. Acad. Sci. USA*. 92: 7907-7911.

Parekh A. B. 1998. Slow feedback inhibition of calcium release-activated calcium current by calcium entry. *J. Biol. Chem*. 273: 14925-14932.

Parekh A. B. 2003a. Mitochondrial regulation of intracellular Ca^{2+} signaling: more than just simple Ca^{2+} buffers. *News Physiol*. Sci. 18: 252-256.

Parekh A. B. 2003b. Store-operated Ca^{2+} entry: dynamic interplay between endoplasmic reticulum, mitochondria and plasma membrane. *J. Physiol*. 547.2: 333-348.

Parekh A. B. and J. W. Putney. 2005. Store-operated Calcium channels. *Physiol. Rev*. 85: 757-810.

Parekh A. B. 2006. A CRAC current tango. *Nat. Cell Biol*. 8(7): 655-656.

Parekh A. B. 2008a. Ca^{2+} microdomains near plasma membrane Ca^{2+} channels: impact on cell function. *J. Physiol*. 586.13: 3043-3054.

Parekh A. B. 2008b. Mitochondrial regulation of store-operated CRAC channels. *Cell Calcium*. 44: 6-13.

Parekh A. B. 2010. Store-operated CRAC channels: function in health and disease. *Nature Rev*. 9: 399-410.

Parekh A. B. 2011. Decoding cytosolic Ca^{2+} oscillations. *Trends Biochem. Sci.* 36(2): 78-87.

Park M. K., M. C. Ashby, G. Erdemli, O. H. Petersen and A. Tepikin. 2001. Perinuclear, perigranular and sub-plasmalemmal mitochondria have distinct functions in the regulation of cellular calcium transport. *EMBO. J*. 20:1863-1874.

Park C. Y., P. J. Hoover, F. M. Mullins, P. Bachhawat, E. D. Covington, S. Raunser, T. Walz, K. C. Garcia, R. E. Dolmetsch and R. S. Lewis. 2009. STIM1 clusters and activates CRAC channels via direct binding of a cytosolic domain to Orai1. *Cell*. 136:876-890.

Patel S., S. A. Morris, C. E. Adkins, G. O'Beirne and C. W. Taylor. 1997. Ca^{2+}-independent inhibition of inositol trisphosphate receptors by calmodulin: redistribution of calmodulin as a possible means of regulating Ca^{2+} mobilization. *Proc. Natl. Acad. Sci. U.S.A*. 94: 11627-11632.

Peinelt C., M. Vig, D. L. Koomoa, A. Beck, M. J. S. Nadler, M. Koblan-Huberson, A. Lis, A. Fleig, R. Penner and J-P. Kinet. 2006. Amplification of CRAC current by STIM1 and CRACM1 (Orai1). *Nat. Cell Biol*. 8(7): 771-773.

Perocchi F., V. M. Gohil, H. S. Girgis, X. R. Bao, J. E. McCombs, A. E. Palmer and V. K. Mootha. 2010. MICU1 encodes a mitochondrial EF hand protein required for Ca^{2+} uptake. *Nature*. 467: 291- 296.

Peters-Golden M., Gleason M. M. and Togias A. 2006. Cysteinyl leukotrienes: multi-functional mediators in allergic rhinitis. *Clin. Exp. Allergy.* 2006. 36(6): 689-703.

Peterson B. Z., C. D. DeMaria and D. T. Yue. 1999. Calmodulin is the Ca^{2+} sensor for Ca^{2+}-dependent inactivation of L-type calcium channels. *Neuron*. 22: 549-558.

Petkov G. V**.**, T. J. Heppner, A. D. Bonev, G. M. Herrera and M. T. Nelson. 2001. Low levels of K_{ATP} channel activation decrease excitability and contractility of urinary bladder. *Am. J. Physiol. Regul. Integr. Comp. Physiol*. 280: R1427–R1433.

Pitts K. R., Y. Yoon, E. W. Krueger and M. A. McNiven. 1999. The dynamin-like protein DLP1 is essential for normal distribution and morphology of the endoplasmic reticulum and mitochondria in mammalian cells. *Mol. Biol. Cell*. 10:4403-4417.

Prakriya M., C.R. Solaro and C. J. Lingle. 1996. $[Ca^{2+}]_i$ elevations detected by BK channels during Ca^{2+} influx and muscarine-mediated release of Ca^{2+} from intracellular Ca^{2+} stores in rat Chromaffin cells. *J. Neurosci*. 16: 4344-4359.

Prakriya M., S. Feske, Y. Gwack, S. Srikanth, A. Rao and P. G. Hogan. 2006. Orai1 is an essential pore subunit of the CRAC channel. *Nature*. 443: 230-233.

Putney J. W. 1986. A model for receptor-regulated calcium entry. *Cell Calcium*. 7:1-12.

Quintana A., E. C. Schwarz, C. Schwindling, P. Lipp, L. Kaestner and M. Hoth. 2006. Sustained activity of calcium release-activated calcium channels requires translocation of mitochondria to the plasma membrane. *J. Biol. Chem*. 281: 40302-40309.

Rapizzi E., P. Pinton, G. Szabadkai, M. R. Wieckowski, G. Vandecasteele, G. Baird, R. A. Tuft, K. E. Fogarty and R. Rizzuto. 2002. Recombinant expression of the voltage-dependent anion channel enhances the transfer of Ca^{2+} microdomains to mitochondria. *J. Cell Biol*. 159(4): 613-624.

Rizzuto R., A. W. M. Simpson, M. Brini and T. Pozzan. 1992. Rapid changes of mitochondrial Ca^{2+} revealed by specifically targeted recombinant aequorin. *Nature*. 358: 325-327.

Rizzuto R., M. Brini, M. Murgia and T. Pozzan. 1993. Microdomains with high Ca^{2+} close to IP_3-sensitive channels that are sensed by neighbouring mitochondria. *Science*. 262: 744-747.

Rizzuto R., P. Pinton, W. Carrington, F. S. Fay, K. E. Fogarty, L M. Lifshitz, R. A. Tuft and T. Pozzan. 1998. Close contacts with the endoplasmic reticulum as determinants of mitochondrial Ca^{2+} responses. *Science*. 280: 1763- 1766.

Rizzuto R., P. Bernardi and T. Pozzan. 2000. Mitochondria as all-round players of the calcium game. *J. Physiol*. 529: 37-47.

Rizzuto R., P Pinton, D. Ferrari, M. Chami, G. Szabadkai, P. J. Magalhäes, F. Di Virgillo and T. Pozzan. 2003. Calcium and apoptosis: facts and hypotheses. *Oncogene*. 22: 8819-8627.

Rizzuto R. and T. Pozzan. 2006. Microdomains of intracellular Ca^{2+}: molecular determinants and functional consequences. *Physiol. Rev*. 86: 369-408.

Roberts W. M., R. A. Jacobs and A. J. Hudspeth. 1990. Colocalization of ion channels involved in frequency selectivity and synaptic transmission of presynaptic active zones of hair cells. *J. Neurosci*. 10: 3664-3684.

Robitaille E, E. M. Adler and M. P. Charlton. 1990. Strategic location of calcium channels and transmitter release sites of frog neuromuscular synapses. *Neuron*. 5: 773-779.

Roos J., P. J. Di Gregorio, A. V. Yeromin, K. Ohlsen, M. Lioudyno, S. Zhang, O. Safrina, J. A. Kozak, S. L Wagner, M. D. Cahalan, G. Velicelebi and K. A. Stauderman. 2005. STIM1, an essential and conserved component of store-operated Ca^{2+} channel function. *J. Cell Biol*. 169(3): 435-445.

Sedova M. and L. A. Blatter. 2000. Intracellular sodium modulates mitochondrial calcium signaling in vascular endothelial cells. *J. Biol. Chem. U.S.A*. 275(45): 35402-35407.

Shore G. C. and Tata J. R. 1977. Two fractions of rough endoplasmic reticulum from rat Liver. *J. Cell Biol*. 72: 714- 725.

Simmen T., J. E. Aslan, A. D. Blagoveshchenskaya, L. Thomas, L. Wan, Y. Xiang, S. F. Feliciangeli, C. H. Hung, C. M. Crump and G. Thomas. 2005. PACS-2 controls endoplasmic reticulum-mitochondria communication and Bid-mediated apoptosis. *EMBO. J*. 24:717-729.

Singaravelu K., C. Nelson, D. Bakowski, O. M. de Brito, S. W. Ng, J. Di Capite, T. Powell, L. Scorrano and A. B. Parekh. 2011. Mitofusin 2 regulates STIM1 migration from the Ca^{2+} store to the plasma membrane in cells with depolarized mitochondria. *J. Biol. Chem*. 286 (14): 12189-12201.

Sipma H., P. De Smet, S. Vanlingen, L. Missiaen, J. Parys and H. De Smedt. 1999. Modulation of inositol 1,4,5-trisphosphate binding to the recombinant ligand-binding site of the type-1 inositol 1,4,5-trisphosphate receptor by Ca^{2+} and calmodulin. *J. Biol. Chem*. 274. 12157-12162.

Somogyi R. and J.W. Stucki. 1991. Hormone-induced calcium oscillations in liver cells can be explained by a simple one pool model*. J. Biol. Chem*. 266: 11068-11077.

Stathopulos P. B., L. Zheng, G-Y. Li, M. J. Plevin and M. Ikura. 2008. Structural and mechanistic insights into STIM1-mediated initiation of store-operated calcium entry. *Cell*. 110: 110-122.

Strotmann R., G. Schultz and T. D. Plant. 2003. Ca^{2+}-dependent potentiation of the nonselective cation channel TRPV4 is mediated by a C-terminal calmodulin binding site. *J. Biol. Chem. U.S.A*. 278 (29): 26541-26549.

Sun Y. and C. W. Taylor. 2008. A calmodulin antagonist reveals a calmodulin-independent interdomain interaction essential for activation of inositol 1,4,5-trisphosphate receptors. *Biochem. J*. 416: 243-253.

Sun T., X. S. Wu, J. Xu, B. D. McNeil, Z. P. Pang, W. Yang, L. Bai, S. Qadri, J. D. Molkentin, D. T. Yue and L. G. Wu. 2010. The role of calcium/calmodulin-activated calcineurin in rapid and slow endocytosis at central synapses. *J. Neurosci*. 30(35): 11838-11847.

Szabadkai G., K. Bianchi, P. Várnai, D. De Stefani, M. R. Wieckowski, D. Cavagna, A. I. Nagy, T. Balla and R. Rizzuto. 2006. Chaperone-mediated coupling of endoplasmic reticulum and mitochondrial Ca^{2+} channels. *J. Cell Biol*. 175(6): 901-911.

Tadross M. R., I. E. Dick and D. T. Yue. 2008. Mechanism of local and global Ca^{2+} sensing by calmodulin in complex with a Ca^{2+} channel. *Cell*. 133: 1228-1240.

Takemura H., A. R. Hughes, O. Thastrup and J. W. Putney. 1989. Activation of calcium entry by tumour promoter thapsigargin in parotid acinar cells. Evidence that an intracellular calcium pool and not an inositol phosphate regulates calcium fluxes at the plasma membrane. *J. Biol. Chem*. 264: 12266-12271.

Takezawa R., H. Cheng, A. Beck, J. Ishikawa, P. Launay, H. Kubota, J. P. Kinet, A. Fleig, T. Yamada and R. Penner. 2006. A pyrazole derivative potently inhibits lymphocyte Ca^{2+} influx and cytokine production by facilitating transient receptor potential melastatin 4 channel activity. *Mol. Pharmacol*. 69: 1413-1420.

Tang Y-g. and Zucker R. S. 1997. Mitochondrial involvement in post-tetanic potentiation of synaptic transmission. *Neuron*. 18(3): 483-491.

Thomas A. P., G. S. Bird, G. Hajnóczky, L. D. Robb-Gaspers and J. W. Putney. 1996. Spatial and temporal aspects of cellular calcium signalling. *FASEB. J*. 10:1505-1517.

Thorn P., A. M. Lawrie, P. M. Smith, D. V. Gallacher and O. H. Petersen. 1993a. Ca^{2+} oscillations in pancreatic acinar cells: spatiotemporal relationships and functional implications. *Cell Calcium*. 14: 746-757.

Thorn P., A. M. Lawrie, P. M. Smith, D. V. Gallacher and O. H. Petersen. 1993b. Local and global cytosolic Ca^{2+} oscillations in exocrine cells evoked by agonists and inositol trisphosphate. *Cell*. 74: 661-668.

Tinel H., J. M. Cancela, H. Mogami, J. V. Gerasimenko, O. V. Gerasimenko, A. V. Tepikin and O. H. Petersen. 1999. Active mitochondria surrounding the pancreatic acinar granule region prevent spreading of inositol trisphosphate-evoked local cytosolic Ca^{2+} signals. *EMBO J*. 18: 4999–5008.

Trebak M., G. S. J. Bird, R.R. McKay and J. W. Putney. 2002. Comparison of human TRPC3 channels in receptor-activated and store-operated modes. *J. Biol. Chem*. 277:21617-21623.

Tse A., F. W. Tse, W. Almers and B. Hille. 1993. Rhythmic exocytosis stimulated by GnRH-induced calcium oscillations in rat gonadotropes. *Science*. 260: 82- 84.

Tsien, R. W. and R.Y. Tsien. 1990. Calcium channels, stores, and oscillations. *Annu. Rev. Cell Bid*. 6: 715-760

Varadi A., L. I. Johnson-Cadwell, V. Cirulli, Y. Yoon, V. J. Allan and G.A. Rutter. 2004. Cytoplasmic dynein regulates the subcellular distribution of mitochondria by controlling the recruitment of the fission factor dynamin-related protein-1. *J. Cell Sci*. 117: 4389-4400.

Vasington F. D. and J. V. Murphy. 1962. Ca^{2+} uptake by rat kidney mitochondria and its dependence on respiration and phosphorylation. *J. Biol. Chem*. 237: 2670-2672.

Vig M., A. Beck, J. M. Billingsley, A. Lis, S. Parvez, C. Peinelt, D. L. Koomoa, J. Soboloff, D. L. Gill, A. Fleig, J-P. Kinet and R. Penner. 2006a. CRACM1 multimers form the ion-selective pore of the CRAC channel. *Curr. Biol*. 16: 2073-2079.

Vig M., C. Peinelt, A. Beck, D. L. Koomoa, D. Rabah, M. Koblan-Huberson, S. Kraft, H. Turner, A. Fleig, R. Penner and J-P. Kinet. 2006b. CRACM1 is a plasma membrane protein essential for store-operated Ca^{2+} entry. *Science*. 312: 1220-1223.

Vig M., W. I. DeHaven, G. S. Bird, J. M. Billingsley, H. Wang, P. E. Rao, A. B. Hutchings, M-H Jouvin, J. W. Putney and J-P. Kinet. 2008. Defective mast cell effector functions in mice lacking the CRACM1 pore subunit of store-operated calcium release-activated calcium channels. *Nat. Immunol*. 9(1): 89-96.

Wakui M., B. V. L. Potter and O. H. Peterson. 1989. Pulsatile intracellular calcium release does not depend on fluctuations in inositol trisphosphate concentration. *Nature*. 339: 317-320.

Wang H. J., G. Guay, L. Pogan, R. Sauve and I.R. Nabi. 2000. Calcium regulates the association between mitochondria and a smooth subdomain of the endoplasmic reticulum. *J. Cell Biol*. 150: 1489-1498.

Wang G.X. and M.M. Poo. 2005. Requirement of TRPC channels in netrin-1-induced chemotropic turning of nerve growth cones. *Nature*. 434: 835-838.

Weber A. 1959. On the role of calcium in the activity of adenosine 5' triphosphate hydrolysis by actomysin. *J.Biol. Chem*. 234:2764-2769.

Wu M. M., Buchanan J., R. M. Luik and R. S. Lewis. 2006. Ca^{2+} store depletion causes STIM1 to accumulate in ER regions closely associated with the plasma membrane. *J. Cell Biol*. 174(6): 803-813.

Xu P., J. Lu, Z. Li, X. Yu, L. Chen and T. Xu. 2006. Aggregation of STIM1 underneath the plasma membrane induces clustering of Orai1. *Biochem. Biophys. Res. Comm*. 350: 969-976.

Yamada M., A. Miyawaki, K. Saito, M. Yamamoto-Hino, Y. Ryo, T. Furuichi and K. Mikoshiba. 1995. The calmodulin-binding domain in the mouse type 1 inositol 1,4,5-trisphosphate receptor. *Biochem. J*. 308: 83-88.

Yang J., P. T. Ellinor, W. A. Sather, J. F. Zhang and R. W. Tsien. 1993. Molecular determinants of Ca^{2+} selectivity and ion permeation in L-type Ca^{2+} channels. *Nature*. 366: 158-161.

Yeromin A. V., S. L. Zhang, W. Jiang, Y. Yu, O. Safrina and M. D. Cahalan. 2006. Molecular identification of the CRAC channel by altered ion selectivity in a mutant of Orai. *Nature*. 443: 226- 229.

Zitt C., B. Strauss, E. C. Schwarz, N. Spaeth, G. Rast, A. Hatzelmann and M. Hoth. 2004. Potent inhibition of Ca^{2+} release-activated Ca^{2+} channels and T-lymphocyte activation by pyrazole derivative BTP2. *J. Biol. Chem*. 279: 12427-12437.

Zorzano A., M. Liesa, D. Sebastián, J. Segalés and M. Palacín. 2010. Mitochondrial fusion proteins: dual regulators of morphology and metabolism. *Semin. Cell Dev. Biol*. 21: 566-574.

Züchner S., I. V. Mersiyanova, M. Muglia, N. Bissar-Tadmouri, J. Rochelle, E. L. Dadali, M. Zappia, E. Nelis, A. Patitucci, J. Senderek, Y. Parman, O. Evgrafov, P. De Jonghe, Y. Takahashi, S. Tsuji, M. A. Pericak-Vance, A. Quattrone, E. Battologlu, A. V. Polyakov, V. Timmerman, J. Michael Schroder and J. M. Vance. 2004. Mutations in the mitochondrial GTPase mitofusin 2 cause Charot-Marie- Tooth neuropathy type 2A. *Nat. Genet*. 36(5): 449- 451.

Zühlke R. D. and Reuter. 1998. Ca^{2+}-sensitive inactivation of L-type Ca^{2+} channels depends on multiple cytoplasmic amino acid sequences of the α_{1C} subunit. *Proc. Natl. Acad. Sci. U.S.A*. 95: 3287-3294.

Zühlke R. D., G. S. Pitt, K. Deisseroth, R. W. Tsien, and H. Reuter. 1999. Calmodulin supports both inactivation and facilitation of L-type calcium channels. *Nature*. 399: 159-162.

Zweifach A. and R. S. Lewis. 1993. Mitogen-regulated Ca^{2+} current of T lymphocytes is activated by depletion of intracellular Ca^{2+} stores. *Proc. Natl. Acad. Sci. U.S.A*. 90: 6295-6299.

Zweifach A. and R. S. Lewis. 1995a. Rapid inactivation of depletion-activated calcium current (I_{CRAC}) due to local calcium feedback. *J. Gen. Physiol*. 105:209-226.

Zweifach A. and R.S. Lewis. 1995b. Slow calcium-dependent inactivation of depletion-activated calcium current. *J. Biol. Chem*. 270: 14445-14451.